Formulation and durability of metakaolin-based geopolymers

Raphaëlle Pouhet

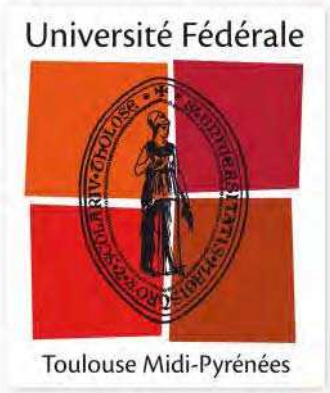

THÈSE

En vue de l'obtention du

DOCTORAT DE L'UNIVERSITÉ DE TOULOUSE

Délivré par *l'Université Toulouse III - Paul Sabatier*
Discipline ou spécialité : *Génie Civil*

Présentée et soutenue par *Raphaëlle POUHET*

Le 25 juin 2015

Titre :

Formulation and durability of metakaolin-based geopolymers

JURY

M. Frizon Fabien	*Rapporteur*
M. Habert Guillaume	*Rapporteur*
Mme. Rossignol Sylvie	*Examinateur*
Mme. Escaffit Pascale	*Examinateur*
M. Cyr Martin	*Examinateur, directeur de thèse*

Ecole doctorale : *Mécanique, Energétique, Génie Civil & Procédés*
Unité de recherche : *Laboratoire Matériaux et Durabilité des Constructions de Toulouse*
Directeur(s) de Thèse : *M. Martin Cyr*

Title : Formulation and durability of metakaolin-based geopolymers

Abstract :

The main objectives of this thesis were to assess the formulation and durability of metakaolin-based geopolymers as a binder for civil engineering materials. Geopolymers are alkali-activated materials; they are increasingly studied by the international community as they represent an alternative to traditional Portland cement. The first part of this study has been dedicated to the formulation of these materials, exclusively made from flash metakaolin and sodium silicate, which has shown performances comparable to a CEM I 52.5. A physicochemical characterization and a study of the porous network have highlighted differences between these two materials and allowed developing a database on the characteristics of the material. The achievement of concrete, up to precast plant, showed their ability to completely substitute known hydraulic binders, in terms of workability and compressive strength. Durability issues related to the high alkali content in this matrix were assessed by studies on alkali-silica reaction and carbonation. The results obtained have concluded that the alkali-silica reaction would not be detrimental in a matrix of metakaolin activated by sodium silicate, and that the very rapid reaction of the alkalis in the geopolymer pastes pore solution with atmospheric CO_2 do not lead to a significant drop of the concrete pH, which could be detrimental in cement matrix, but could lead to the appearance of efflorescence on the surfaces of geopolymer.

Key-words : Geopolymer ; Metakaolin ; Durability; Alkali-silica reaction ; Carbonation

Titre : Formulation et durabilité des géopolymères à base de métakaolin

Résumé :

Les principaux objectifs de cette thèse étaient d'évaluer la formulation et la durabilité des géopolymères à base de métakaolin utilisés comme liants dans des matériaux de construction. Les géopolymères sont des matériaux à activation alcaline faisant l'objet d'études de plus en plus nombreuses de la communauté internationale car ils représentent une alternative aux ciments Portland traditionnels. La première partie de cette étude a donc été dédiée à la formulation de ces matériaux réalisés exclusivement à partir de métakaolin flash et de silicate de sodium et a permis de mettre en évidence des performances comparables à un CEM I 52.5. Une caractérisation physico-chimique ainsi qu'une étude du réseau poreux a souligné les différences entre ces deux matériaux et a permis l'élaboration d'une base de donnée sur les caractéristiques du matériau. La réalisation de béton, allant jusqu'à la fabrication en usine de préfabrication, a montré la capacité des géopolymères à remplacer totalement les liants hydrauliques connus, en terme de mise en œuvre et de performances mécaniques. Les questions de durabilité liées au fort taux d'alcalins dans cette matrice ont été traitées par des études sur la réaction alcali-silice et sur la carbonatation. Les résultats obtenus ont permis de conclure que la réaction alcali-silice ne serait pas préjudiciable dans une matrice de métakaolin activé par du silicate de sodium, et que la réaction très rapide des alcalins de la solution interstitielle des pâtes de géopolymère avec le CO_2 atmosphérique ne conduirait pas à une chute de pH significative, préjudiciable dans les matrices cimentaires, mais faciliterait l'apparition d'efflorescences.

Mots clés : Géopolymère ; Métakaolin ; Durabilité ; Réaction alcali-silice ; Carbonatation

Remerciements

*Les travaux présentés dans ce manuscrit sont l'aboutissement de trois années de recherche effectuées en grande majorité au sein du **L**aboratoire de **M**atériaux et **D**urabilité des **C**onstructions de Toulouse, en collaboration CIFRE avec la société **SEAC** GUIRAUD FRERES. Ainsi, je tiens à adresser mes remerciements au Professeur Gilles ESCADEILLAS (directeur du LMDC), ainsi qu'à Monsieur Jacques Guiraud (directeur de SEAC), pour avoir rendu ce projet possible. Je souhaite également exprimer ma gratitude à Fabien Frizon et Guillaume Habert, qui m'ont fait l'honneur de rapporter ce travail, ainsi qu'à Sylvie Rossignol qui a accepté la présidence de mon jury de thèse.*

Il est évident que ce manuscrit n'aurait pu voir le jour sans l'aide, le soutien et l'accompagnement de nombreuses personnes, que je tiens à remercier dans ces paragraphes.

Mes premiers remerciements s'adressent à mon directeur de thèse, Martin Cyr. Je souhaite lui exprimer ma profonde gratitude pour m'avoir confié ce projet et m'avoir encadrée durant cette thèse. Sa confiance, son soutien, sa patience et son humanité m'ont apporté une autonomie de travail très appréciable, tout en maintenant un esprit d'équipe qui nous a permis d'aller si loin. Merci de m'avoir fait découvrir ce sujet passionnant que sont les géopolymères, et plus généralement merci pour tout ce que tu m'as appris durant ces trois ans, tant professionnellement qu'humainement.

Je ne saurais remercier assez mes encadrants industriels, Pascale Escaffit, Alexandre Bertrand et Jean Paul Tardy. Leur compréhension, leurs encouragements et leur gentillesse ont rendu ce premier contact dans l'entreprise, pour la jeune universitaire que j'étais, si facile. Je remercie également les personnes de chez SEAC, Argeco Développement, Demeter et Argile d'aquitaine avec qui j'ai eu le plaisir de travailler, en particulier Serge Pocher, pour m'avoir confié les rênes de son usine le temps de quelques essais, mais également Natalie Menchon, Pierre Drelon, et Mathieu Bardon.

Je souhaiterais aussi exprimer ma gratitude à l'ensemble des personnes que j'ai pu côtoyer au LMDC et qui ont, toutes à leur échelle, participé au bon déroulement de cette thèse, tant du côté administratif que technique. Un grand merci à Ghislaine, Fabienne, Vanessa, Maud, Guillaume, David, Yann, Sylvain, Frédéric, Pierre et Fred. Avec une mention spéciale pour Bernard, pour tout ce temps passé à extraire des solutions interstitielles : merci !

Bien évidement je ne peux pas oublier de remercier tous les doctorants, ATER, Post doc, (passés, présents et futurs) du LMDC, tant de belles rencontres ! En commençant par un grand merci, profondément sincère, à Raphaël, véritable frère de thèse, mon adaptation au génie civil et au LMDC n'aurait pas été aussi simple sans lui. Merci pour ton écoute et merci d'avoir répondu à mes nombreuses questions de novice que je n'osais poser à personne ! Un grand merci à Nacim, une de mes plus belles rencontres lors de la thèse, pour son réconfort et son écoute dans les meilleurs mais aussi dans les pires moments.

A mes collègues/amis qui ont ensoleillé mes pauses café et mon quotidien au labo : Célestine, Marlène, Rémi, Laila, Isabelle, Khadim, Laurent, Célimène, et j'en oublie surement… un grand merci, ces trois années n'auraient pas été les mêmes sans vous ! Je vous souhaite bonheur et réussite pour la suite !

Un grand merci également à tous ce qui ont répondu présents le jour de ma soutenance, car c'était important pour moi.

Plus personnellement, je tiens à remercier chaleureusement mes amis de longue date, et ceux rencontrés plus récemment à Toulouse (et beaucoup ont déjà été cités) pour leurs encouragements et pour avoir été là pour moi.

Je ne saurais trouver les mots pour dire à quel point je suis reconnaissante du soutien inconditionnel de ma famille. Un immense merci à vous tous, et particulièrement ma sœur Laureline, pour être toujours là pour moi, et à ma mère, qui ne m'a jamais laissée baisser les bras en 23 ans d'études et de scolarité. Je sais que c'est en grande partie grâce à toi que je suis arrivée jusque-là, merci.

Mes derniers mots et mes pensées vont à Arnaud. Pour cette année passée à tes côtés, et pour toutes celles qui suivront, merci.

Table of contents

Résumé en Français

L'évolution des connaissances sur les géopolymères et plus généralement sur les matériaux à activation alcaline, tend à montrer qu'ils pourraient représenter une alternative viable aux liants hydrauliques traditionnels pour la formulation de béton. En effet, depuis maintenant plus de trois décennies, les matériaux à activation alcaline apparaissent comme de nouveaux matériaux de construction, avec une recherche accrue ces dernières années, tant par la communauté scientifique internationale, que par les industriels du domaine du bâtiment. De nombreuses constructions dans le monde voient désormais le jour, cependant l'utilisation de géopolymères reste très minoritaire.

Le terme "Matériaux à activation alcaline" est appliqué à une classe de matériaux synthétisés par réaction d'une poudre aluminosilicatée avec une solution alcaline. Le terme "Géopolymère", inventé dans les années 1970 par le scientifique et ingénieur français, Prof. Joseph Davidovits, représente une sous-partie de cette classe de matériau, limitée à l'utilisation d'une source aluminosilicatée ayant une faible teneur en calcium, comme les cendres volantes de classe F ou le métakaolin.

Le métakaolin est un composé obtenu par calcination d'argile kaolinite, souvent très pur et donc relativement coûteux. Ainsi, malgré les nombreux avantages mis en avant dans la littérature scientifique sur les géopolymères à base de métakaolin (notamment en terme de performance mécanique, de résistance à l'acide, ou à la température), l'utilisation du métakaolin reste marginal dans les études sur les géopolymères pour la formulation de béton, et, à notre connaissance, de tels produits n'existent pas sur le marché des matériaux pour la construction.

Le groupe SEAC est une entreprise de préfabrication basée à Toulouse, commercialisant des structures en béton. Elle travaille en partenariat avec l'entreprise Argéco Développement, producteur de métakaolin dans le sud-ouest de la France. Le métakaolin produit dans cette région étant relativement impur, son coût de production est modéré, et assez proche de celui du ciment. Ainsi, cette association permettrait une réelle opportunité à la commercialisation de structure en béton de géopolymère à base de métakaolin. Cependant, comme ces matériaux sont peu représentés dans la littérature scientifique, des études approfondies du matériau, de ses applications possibles et de sa durabilité sont nécessaires.

C'est dans ce contexte que se sont inscrits ces travaux de thèse au Laboratoire Matériaux et Durabilité des Constructions (LMDC) de Toulouse, en convention CIFRE avec la société *SEAC Guiraud frère*, afin de fournir les connaissances nécessaires à une éventuelle commercialisation des géopolymères à base de métakaolin.

Les principaux objectifs de cette thèse étaient donc de formuler et de caractériser des géopolymères à base de métakaolin pour la réalisation de béton, et d'en évaluer leur durabilité. Afin d'atteindre ces objectifs, trois études consécutives ont été développées, schématiquement représentées par le logigramme suivant :

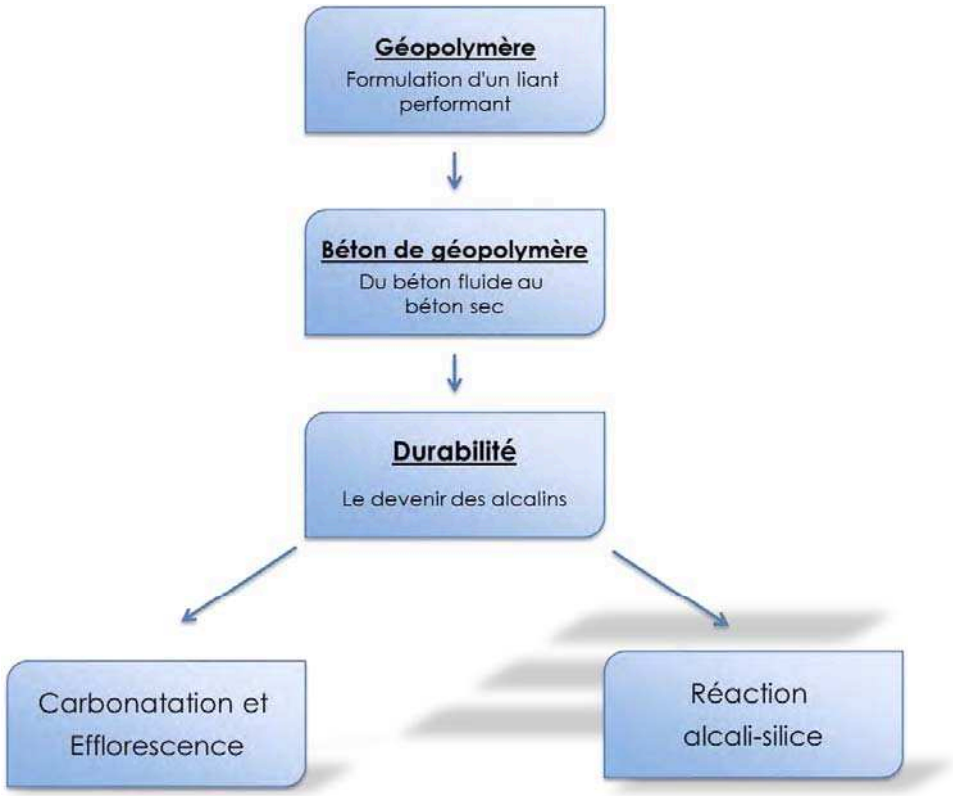

Géopolymère, formulation d'un liant performant (Chapitre I)

Dans ce premier chapitre deux études ont été menées afin de répondre aux questions suivantes :

- → Le géopolymère à base de métakaolin pourrait-il être une alternative viable au ciment Portland traditionnel ?
- → Quelles seraient les propriétés morphologiques, physiques et chimiques de ce liant alternatif ?

Ce premier chapitre a donc eu pour objectif d'étudier les propriétés mécaniques et physiques des géopolymères à base de métakaolin et de les comparer à ceux du ciment Portland afin d'évaluer la capacité de ce matériau à être utilisé comme un liant hydraulique classique.

La première partie de ce chapitre a été dédiée à l'étude performantielle des mortiers de géopolymère à base de métakaolin. L'importance des proportions molaires des quatre principaux constituant du mélange sur les performances mécaniques, souvent citée dans la littérature, a été confirmée et a conduit à la détermination d'une formulation optimale en terme de résistance à la compression: ***3,6 SiO_2 • 1 Al_2O_3 • 0,9 Na_2O • 13 H_2O***.
Il a été mesuré que la résistance à la compression obtenue pour cette formulation était au moins égale à celle d'un ciment CEM I 52,5. Ce ciment a donc été choisi comme ciment de référence pour le reste de l'étude.

Des avantages certains, comparativement au ciment, ont été mis en évidence lors de cette étude. Il a été montré une cinétique de prise beaucoup plus rapide du géopolymère, qui a atteint 80% de ces performances mécaniques finales en 3 jours, contre 28 jours pour le ciment. Il a également été observé une résistance à la flexion plus importante que pour le ciment. En revanche, il a été noté une forte tendance à la fissuration superficielle due à un retrait de dessiccation à jeune âge, et une diminution des performances mécaniques lors d'une cure sous eau.
Parallèlement, cette étude a permis de montrer que la norme utilisée pour la fabrication de mortier de ciment était applicable aux géopolymères, et a fourni des recommandations d'amélioration, notamment sur les échéances d'études (7 jours au lieu de 28 jours) et les conditions de conservation (95% d'humidité relative et non sous eau).

Dans un second temps, la caractérisation physique, chimique et morphologique des géopolymères a permis de comparer, à performance équivalente, les géopolymères aux ciments. Des études réalisées sur la réactivité et la composition chimique de cette matrice ont mis en évidence une géopolymérisation quasi-totale et moins exothermique que l'hydratation du ciment à seulement 7 jours. La caractérisation du géopolymère durci a montré la formation d'une structure amorphe homogène et stable dans le temps, identifiée comme étant le géopolymère « pur », mais également une phase cristalline, principalement composée de quartz, provenant des impuretés du métakaolin.

Une attention particulière a été portée à l'étude du réseau poreux, caractéristique primordiale d'un liant, qui a montré un volume et une organisation de pore très différente du ciment malgré des performances mécaniques similaires. Il a ainsi été mesuré pour la formulation optimale un volume poral total de 49%, avec une organisation monomodal du réseau centré sur des cols d'accès aux pores de 15nm de diamètre.

En conclusion de ces deux études, il a été noté que les données obtenues étaient en accord avec la littérature sur le sujet. Bien qu'il ait été montré un réel potentiel à l'utilisation des géopolymères à base de métakaolin comme liants, les différences fondamentales observées avec la matrice cimentaire rendent difficile l'évaluation des différentes applications possibles avec ce matériau ainsi que l'estimation de sa durabilité, particulièrement au vu de sa teneur élevée en alcalin.

Béton de géopolymère, du béton fluide au béton sec (Chapitre II)

Les études menées dans ce second chapitre ont eu pour objectif de répondre aux questions suivantes :

- → Quelles structures en béton pourraient être réalisées avec un liant géopolymère?
- → Le géopolymère pourrait-il être utilisé en usine de préfabrication de la même manière que le ciment Portland?

Dans ce deuxième chapitre consacré à l'étude des bétons de géopolymère à base de métakaolin, on a cherché à déterminer quelles applications pourraient être réalisables, et si certaines normes cimentaires pouvaient être applicables à ces matrices.

Dans un premier temps, une étude a ainsi été menée sur la formulation de ces bétons afin d'évaluer leur maniabilité, leur porosité et leur performance mécanique. L'étude de l'état frais et de l'état durci des bétons de géopolymère a permis de révéler une très large gamme d'applications possibles, allant du béton fluide adapté à la réalisation de structures armées, aux bétons très secs utilisés pour produire des unités de maçonnerie.

En effet, les formulations réalisées ont montré des classes de consistance allant de S1 à S5 (EN 206-1) et des performances mécaniques comprises entre 19 MPa et 65 MPa. Il a été noté une très forte influence de la teneur en eau du liant géopolymère sur la résistance à la compression à 7 jours, en revanche la taille ou la quantité de granulat ont un effet négligeable.

La porosité totale accessible à l'eau obtenue était de 10% à 20% en fonction des formulations, et au vu des résultats obtenus, une absence de zone de transition à l'interface géopolymère/granulat a été supposée. Une étude économique du prix du béton sans transport, a révélé que le mètre cube de béton de géopolymère pourrait être équivalent à celui du ciment, à condition de viser des performances mécaniques élevées (supérieures à 40MPa) et avec une solution d'activation ayant un prix équivalent à celui du ciment.

La gamme d'applications théoriquement réalisables selon le système normatif cimentaire a été le sujet principal de la deuxième partie de cette étude. La réalisation de deux poutres armées de 3 mètres de long avec une formulation de béton de géopolymère ayant une classe de consistance entre S3 et S4, a montré que les classes de consistance normalisées des matrices cimentaires pouvaient s'appliquer aux bétons de géopolymère à base de métakaolin activé par du silicate de sodium, en terme de réalisation de structures armées.

La réalisation d'unité de maçonnerie en usine de préfabrication a également mis en évidence l'aptitude du géopolymère à se substituer au ciment Portland traditionnel. La réalisation de blocs pleins a montré des performances similaires aux blocs de ciment commercialisés, et seul les blocs à *lame d'air* n'ont pas donné de résultat concluant et nécessiteraient une optimisation. L'utilisation de granulat biosourcé, tel que le chanvre ou le bois, a révélé une application intéressante pour les géopolymères, mais nécessiterait également des études supplémentaires de formulation et d'optimisation. Enfin cette étude, qui a nécessité l'utilisation de trois malaxeurs différents, de 10L, 200L et 1m^3, a permis de mettre en évidence une absence d'effet d'échelle pour ces matériaux.

L'observation des différentes structures réalisées, à court et moyen terme, a révélé deux problèmes liés à leur durabilité. Il a notamment été observé l'apparition de cristaux blancs en grande quantité sur les surfaces de la poutre stockée en extérieur et sur les blocs. Assimilés à des efflorescences, ces cristaux blancs indiqueraient un phénomène de carbonatation dû au CO_2 atmosphérique, ce qui a été l'objet du troisième chapitre de ce manuscrit. Enfin, il a également été observé un problème à l'interface entre le géopolymère et le granulat utilisés pour la réalisation des blocs, problème qui pourrait être associé à une réaction alcali-silice, au vu de la teneur importante en alcalin. L'évaluation de cette réaction dans la matrice géopolymérique a ainsi été l'objet du quatrième chapitre de cette thèse.

Cette étude a donc mis en évidence la capacité du géopolymère à se substituer au ciment Portland traditionnel pour la formulation de béton et à mis en évidence son aptitude à être utilisé en usine de préfabrication au même titre que le ciment. Mais l'observation des structures réalisées a également révélé deux problèmes potentiels de durabilité liés à la réaction de carbonatation et à la nature des granulats utilisés.

Durabilité, le devenir de alcalins (Chapitre III et IV)

Cette troisième partie visait à évaluer si les phénomènes connus comme préjudiciables à la durabilité de la matrice cimentaire en présence d'alcalins, pouvaient se produire dans la matrice de géopolymère. L'étude de la carbonatation et de la réaction alcali-silice ont ainsi été choisies, sur la base des résultats obtenus dans le chapitre II.

- *Carbonatation et efflorescence*

La carbonatation dans les matériaux à base de ciment Portland implique la réaction entre le dioxyde de carbone atmosphérique et les ions calcium présents dans la solution interstitielle. La formation de carbonate de calcium est alors responsable de la diminution du pH de cette solution à une valeur inférieur à 9. Cette diminution de la basicité conduit à la dépassivation des aciers de renfort, rendant ainsi possible leur corrosion. Cette formation de carbonate est également connue pour être responsable de l'apparition d'efflorescence à la surface des structures. Dans les géopolymères à base de métakaolin activé par une solution de silicate de sodium, où la teneur en calcium est négligeable, la présence de CO_2 dissous conduit à la formation de carbonate de sodium. Cette différence de produit formé dans les matrices cimentaires et géopolymériques a rendu les normes existantes pour les ciments, soit inutilisables, soit questionnables. Une étude basée sur l'analyse de la solution interstitielle a ainsi dû être développée dans cette étude afin de pouvoir évaluer les risques liés à la corrosion par carbonatation.

L'analyse de la solution interstitielle du géopolymère en fonction du temps a montré une réaction de carbonatation très rapide comparée aux matrices cimentaires, avec une carbonatation presque totale en seulement 14 jours en condition naturelle (à 20°C et 95% d'humidité relative). L'impact de cette carbonatation sur la valeur de pH de cette solution a

été évalué à un an, et a montré une stabilisation à une valeur de 10.5. Ce pH étant nettement supérieur à 9, il limiterait donc fortement les risques de corrosion dus à la dépassivation des aciers de renfort. En revanche l'étude réalisée en conditions accélérées sous atmosphère concentrée à 50% de CO_2, a mis en évidence une différence de phase entre les carbonates et les bicarbonates de sodium formés, aboutissant à un pH plus faible, susceptible d'induire des problèmes de corrosion par carbonatation. Ces résultats soulignent une utilité limitée de l'application d'essais accélérés pour l'étude de la carbonatation dans les géopolymères, étant donné la rapidité de la réaction dans ces systèmes et le fait qu'ils aboutissent à un produit de réaction non représentatif de la réaction en condition naturelle.

Des études menées sur l'efflorescence des géopolymères, via des essais en semi-immersion en conditions naturelles et accélérées, ont confirmé cette différence de phase cristalline des carbonates formés en fonction du taux de CO_2 dans l'air, mais n'ont pas montré d'influence significative sur la croissance ni la quantité de ces cristaux. Une étude des paramètres influençant cette croissance cristalline en condition naturelle a révélé l'importance de la nature de l'alcalin utilisé pour formuler les géopolymères, en montrant que l'utilisation de potassium à la place de sodium permet d'éliminer la formation d'efflorescence. Le coût des silicates de potassium est par contre jusqu'à trois fois plus élevé que celui des silicates de sodium. Il a également été montré que l'état de surface du géopolymère avait une influence significative sur l'apparition des cristaux et pouvait conduire à d'importants dommages superficiels. Enfin, aucun des agents réducteurs d'efflorescence testés dans cette étude n'ont permis de réduire la croissance des cristaux dans les systèmes à base de sodium. Cette étude des efflorescences dans les géopolymères nécessiterait d'être poursuivie afin de mieux comprendre les mécanismes d'apparition et de trouver le moyen de les éviter.

Cette étude a donc permis de conclure que, contrairement à la matrice cimentaire, la réaction de carbonatation ne représenterait pas un problème de durabilité dans les systèmes géopolymères à base de métakaolin, en ce qui concerne la corrosion par carbonatation. En revanche, il a été observé que les efflorescences induites à la suite de la carbonatation de la solution interstitielle des géopolymères pouvaient conduire, en plus des problèmes esthétiques, à d'importants dommages de surface. Cette étude a également fourni une approche expérimentale nouvelle pour évaluer l'impact de la carbonatation dans les géopolymères à base de métakaolin, qu'il serait intéressant de poursuivre et d'étendre à d'autres matériaux alcali-activés.

- *Réaction alcali-silice*

Ce chapitre a évalué le comportement des géopolymères à base de métakaolin en présence de granulats réactifs à la réaction alcali-silice (RAS). Des mortiers de géopolymère ont ainsi été réalisés avec du métakaolin flash et une solution de silicate de sodium en présence de sept sables différents, chacun ayant un niveau de réactivité à la RAS variable.

Dans un premier temps, le comportement du géopolymère réalisé avec six sables, allant d'une réactivité nulle à très élevée, a été évalué à l'aide de normes existantes, en mesurant régulièrement la variation dimensionnelle et le module d'Young dynamique de mortiers placés dans des conditions de test accéléré à 60°C et 95% d'humidité relative jusqu'à 250 jours. Des analyses MEB et EDS ont également été effectuées à 170 jours pour visualiser les produits de réaction formés. Une comparaison avec un ciment Portland ordinaire a été faite pour tous les sables utilisés afin de s'assurer de leur réactivité et de comparer la façon dont la RAS affecte ces deux systèmes. Les résultats ont montré que les géopolymères, en dépit de leur concentration en alcalin très élevée, étaient plus à même de résister à la RAS que les matrices cimentaires, et qu'aucun gonflement caractéristique ou perte significative de rigidité n'ont été observés pour ces matrices. Une exception a cependant été notée pour le mortier à base de sable de verre concassé, où une baisse significative de la rigidité a été observée, ainsi que la formation d'une couche de gel à la surface des grains de verre, mais sans entrainer de gonflement.

Dans un second temps, des mesures de variation dimensionnelle ont été effectuées sur des mortiers de géopolymère contenant du sable très réactif (opale, connu comme l'un des granulats les plus réactifs face à la RAS), dans diverses conditions de test accéléré (condition de cure, température, et dimension des mortiers). Ces mesures ont assuré la fiabilité des résultats précédents en montrant que, quelles que soient les conditions appliquées, aucun gonflement n'est observé. Il a tout de même été noté une expansion non-négligeable (> 0,1%) lorsque les mortiers sont immergés dans une solution de 1M de NaOH. Cependant, l'apparition de ces gonflements n'ayant eu lieu qu'à partir de 150 jours contre moins de 7 jours pour le ciment, cela a encore confirmé la meilleure résistance des géopolymères face à la RAS.

Enfin, un essai en condition non-accélérée a permis de conclure que malgré la sévérité plus ou moins importante des tests utilisés, les géopolymères résistent mieux que les ciments à la RAS et que la réaction ayant lieu entre un géopolymère à base de métakaolin et un sable réactif n'est pas dommageable pour la structure.

Ce dernier chapitre a ainsi montré que la réaction alcali-silice ne représenterait pas un problème de durabilité pour les structures faites en géopolymère à base de métakaolin. Ce résultat met en avant une application particulièrement intéressante pour ce liant alternatif, qui pourrait donc être utilisé avec des granulats réactifs à la RAS sans causer de dommage. Cependant, les différentes hypothèses présentées pour tenter d'expliquer l'absence de dommage dû à la RAS dans les géopolymères nécessiteraient d'être validées par des études complémentaires.

Les objectifs concernant les études de formulation et de durabilité des géopolymères à base de métakaolin flash, fixés dans ce travail de thèse, ont ainsi été remplis et mènent à de nombreuses perspectives d'études supplémentaires. Entre autre :

- Il serait intéressant d'étendre l'étude de formulation réalisée dans le premier chapitre, a d'autres sources de métakaolin, ou d'autres solutions d'activation, comme l'utilisation du potassium qui permettrait de réduire l'apparition d'efflorescences.

- Etant donné l'avantage certain que représenterait un liant qui ne serait ni sujet à la réaction alcali-silice, ni sujet à la corrosion des armatures par carbonatation, il serait utile de poursuivre ces deux études, qui pourraient aboutir à des applications avantageuses pour ce nouveau liant alternatif.

General introduction

The evolution of knowledge on geopolymers (GP), and more generally on alkali activated materials (AAM), tends to show that they could potentially offer an efficient alternative to ordinary Portland cement (OPC) in particular applications. Alkali-activated materials began to emerge as a new material for civil engineering more than three decades ago, and recent years have seen an increase in research by the international scientific community and also by industrial firms. However, in the many constructions currently under way in the world, the use of activation of metakaolin alone remains marginal.

The term "alkali-activated materials" are applied to a class of solid materials synthesised by the reaction of an aluminosilicate powder with an alkaline solution. The term "geopolymer", coined in the 1970s by the French scientist and engineer Prof. Joseph Davidovits, represents a sub-part of this class of materials, limited to the use of aluminosilicate powder having low calcium content, e.g. coal fly ash or metakaolin.

Metakaolin is obtained by calcination of kaolin clay, often very pure and therefore generally relatively expensive. So despite the many advantages cited in the literature (mechanical properties, resistance against temperature, acid or external sulfate attack), metakaolin remains marginal in the study of geopolymer binder for the realization of concrete, and to our knowledge, none of such products has been yet commercialized in the construction field. For these reasons, significant deficiencies appear in the scientific literature on the achievable applications with this binder and on the behavior of these materials over time. The question of the durability of the metakaolin-based geopolymer appears as a major issue.

It is in this context that this thesis works was conducted, in CIFRE convention with the company SEAC *Guiraud frères*. SEAC group is a prefabrication company, which works in partnership with the company Argeco Développement, producer of metakaolin in the South West of France. The metakaolin produced in this region has two advantages: relatively impure, its cost is moderate and quite similar to that of cement and also its calcination process called “flash”, which makes it a low environmental impact product. Thus, this partnership could allow the production of geopolymer-based on metakaolin as an alternative binder for concrete. However, no production would be possible without prior scientific study on the material, its formulation and its durability.

The main purposes of this thesis were thus to assess the formulation and durability of metakaolin-based geopolymers as a binder for civil engineering materials, with the aim to answer the following questions:

→ Could the metakaolin-based geopolymer binder be an efficient alternative to ordinary Portland cement? And what would be its characteristics and properties?

→ Which concrete structures could be achieved with this binder? And could it be used in precast plant in the same way as Portland cement?

→ What durability for these structures in view of their high alkaline content? Knowing the problems of carbonation and alkali-silica reaction sometimes found in Portland cement concrete, how these pathologies can affect geopolymer concretes?

In order to achieve these objectives, three consecutive parts are developed, schematically represented by the following diagram:

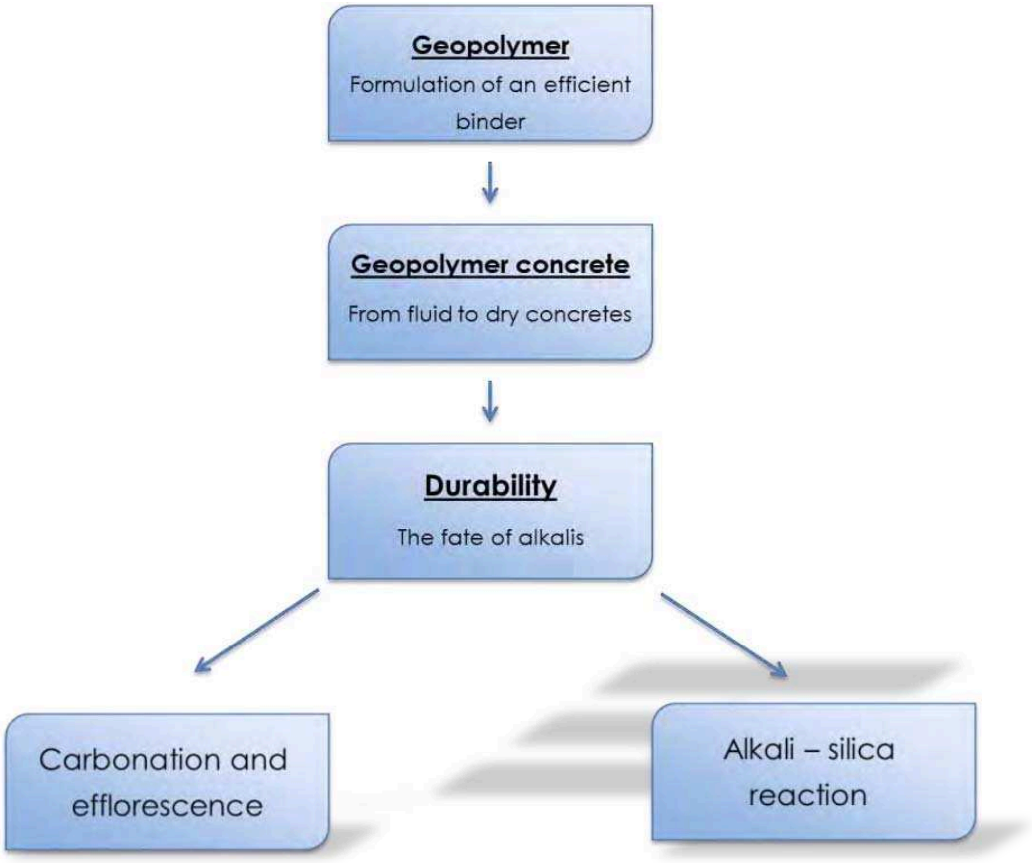

Geopolymer, formulation of an efficient binder (Chapter I)

In the purpose of determining the mechanical performances achievable with the metakaolin-based geopolymer binder, a formulation study based on the performances of mortars is carried out in this first part, in order to obtain an optimal formulation with the raw material considered. In a second time, physical, chemical and morphological characterisations of the geopolymer are used to determine the binder properties, and make comparisons, at equivalent strengths, between geopolymers and cement.

Geopolymer concrete, from fluid to dry concretes (Chapter II)

Using the knowledge acquired in the *Chapter I* on the geopolymer binder, a concrete formulation plan focused on workability, porosity and compressive strength, is carried out in order to view what applications could be achievable, and to see whether some cement standards could be applied to these matrices. The range of theoretically feasible applications is validated by the manufacture of reinforced structures and masonry units with proper equipment, up to realisation of tests in a precast plant.

Durability, the fate of alkalis (Chapter III and IV)

This third part aims to assess whether the conditions known to be detrimental to the durability of cementitious matrix, in the presence of alkalis, could occur in geopolymer system. Based on the results obtained in *Chapter II*, the study of carbonation and alkali-silica reaction was chosen.

- *Carbonation and efflorescence*

The carbonation of Portland-cement-based materials involves the reaction between atmospheric CO_2 and calcium ions in the pore solution, leading to the depassivation of steel reinforcements and their possible corrosion, and also to efflorescence. In metakaolin-based geopolymer activated by sodium silicate, in which calcium is almost non-existent, the presence of CO_2 will lead to the formation of sodium carbonates.

An experimental approach developed on pH study of geopolymer pore solution, at various time and curing conditions, could assess the impact of this carbonate formation on the risk of corrosion and efflorescence formation in these systems, highlighting the potential durability issues.

- *Alkali–silica reaction*

The alkali-silica reaction (ASR) behaviour of geopolymer is investigated in this fourth part. This widely studied reaction involving, in Portland cement concrete, the presence of soluble alkalis, a moist environment and the presence of alkali-reactive aggregates, causes significant and irreversible damages in structures due to swelling of the concrete.
A study carried out on the dimension changes and the dynamic modulus of metakaolin-based geopolymer mortars placed in favorable conditions, in presence of sand having various level of reactivity to ASR, allow the assessment of the risks associated to this reaction in geopolymer systems. A comparison with an ordinary Portland cement (OPC) for all aggregates is necessary to ensure their alkali-silica reactivity and compare how the ASR affects these two matrices.

The conclusion recalls the main results of the investigations and proposes some perspectives, which could be used for industrial applications or for a better evaluation of the durability risks in metakaolin-based geopolymer system.

Chapter I.

Formulation and Characterisation of Metakaolin based-geopolymer

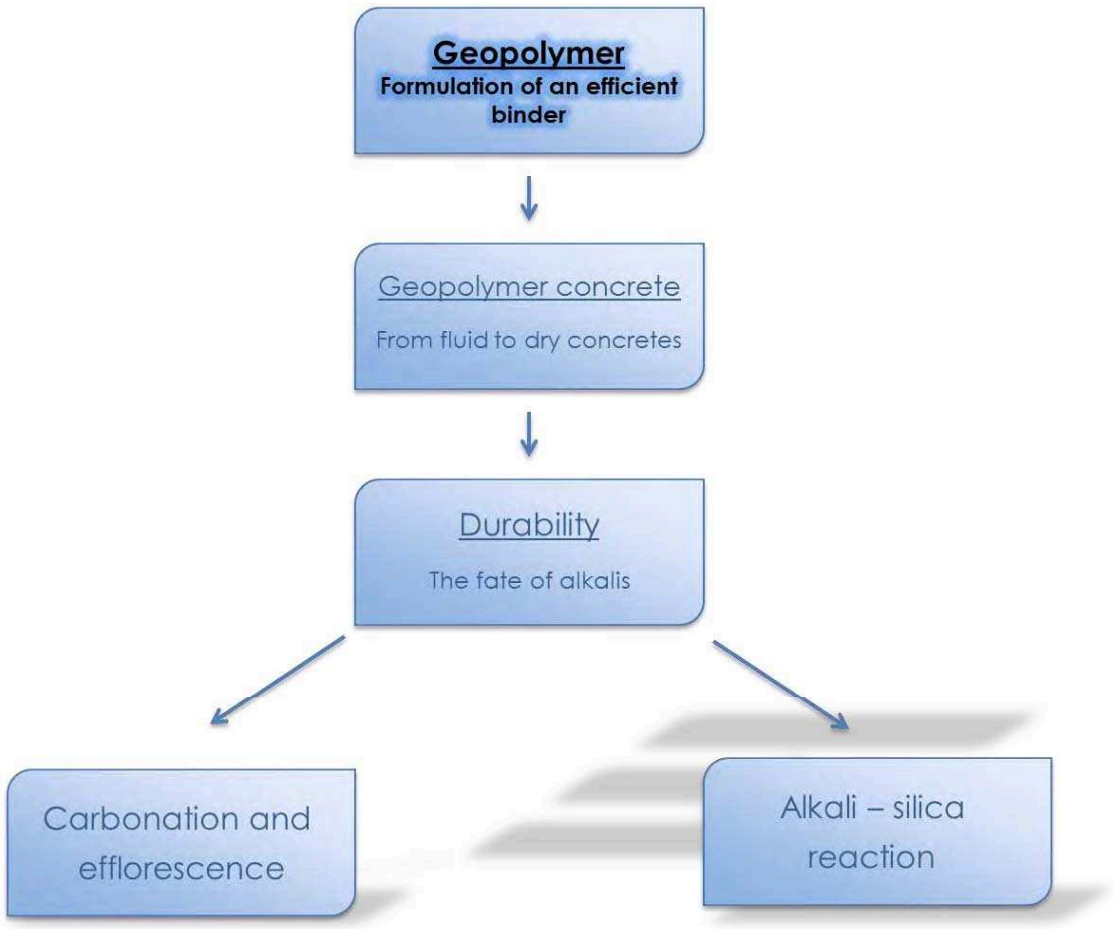

Table of contents

I. Introduction

Geopolymers are aluminosilicate materials belonging to the family of alkali-activated materials. Although the geopolymerisation reaction is still not fully understood, many studies have shown that the activation of an aluminosilicate source, such as metakaolin or fly ash, by a highly basic alkaline solution results in the formation of amorphous materials showing similar compressive strength to that of a traditional binder made with ordinary Portland cement (OPC). Given the current environmental requirements aimed at reducing the CO_2 impact of the construction industry, which is mainly due to the production of cement, the alternative of a binder having the same strength but containing no cement is a major issue. However, despite its mechanical similarities, this material presents many chemical and morphological differences which make it difficult to compare to OPC, especially considering the existing standards.

Therefore the first part of this study was designed to assess the possibility of using the geopolymer in mortar as a binder. Based on the mortar performance, the mechanical strengths in flexion and compression, the kinetics of strength development, the curing conditions, the proportion of sand and the modulus of industrial sodium silicate will be assessed in order to compare geopolymer with a CEM I of the same strength class and evaluate the application of existing standards. In a second part, this study will focus on the characterisation of optimal geopolymer formulations, in order to visualize the major differences between OPC and geopolymer at similar levels of performance. Studies of the reactivity, the free water, the porous networks, the impurities present and the stability of the geopolymer will be carried out over time to better understand metakaolin-based geopolymers and their geopolymerisation mechanisms.

This study will enable the possible applications of a metakaolin-based geopolymer binder to be defined, allow us to anticipate the mechanical performance levels and physical characteristics depending on the formulation, and finally provide recommendations on the modifications to be applied to existing standards for OPC.

II. Geopolymer: what is it?

1. Geopolymer and geopolymerisation

Geopolymers belong to the family of alkali-activated materials, which, unlike cementitious materials, require alkalis to harden. The term 'geopolymer' was coined in the 1970s by the French scientist and engineer Prof. Joseph Davidovits (Davidovits, 1976) and denotes alumino-silicate inorganic polymers obtained by activation of an alumino-silicate source having a low calcium content by an alkaline hydroxide solution at room temperature (Duxson et al., 2007a). These materials are made up of tetrahedral units that are alternately linked to polymeric precursors by sharing oxygen atoms (Figure 1) and for which a chemical nomenclature, proposed by Davidovits has been established under the term poly(sialate), where sialate is an abbreviation of silico-oxo-aluminate.

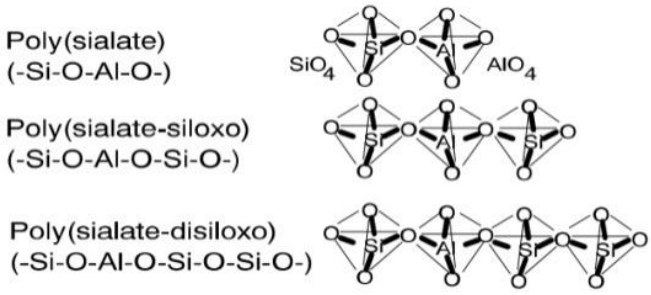

Figure 1. *Geopolymer terminology proposed by J. Davidovits (Davidovits, 1994)*

To balance the negative charge, positive ions such as K^+ or Na^+ are present in framework cavities (Davidovits, 1994; Duxson et al., 2007a), leading to a final structure like that proposed by Barbosa et al (2000), as represented in Figure 2, and corresponding to the following chemical formula:

$$M_n[-(SiO_2)_z-AlO_2]_n,wH_2O$$

where z is the Si/Al molar ratio, M the monovalent cation, n the degree of polymerisation and w the amount of bound water.

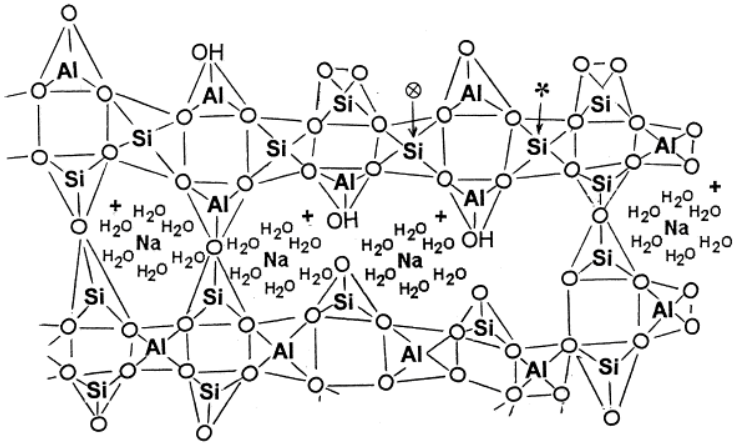

Figure 2. *Semi-schematic structure for Na–polysialate polymer proposed by Barbosa, Mackenzie, and Thaumaturgo (Barbosa et al., 2000)*

The mechanisms of geopolymerisation are not fully understood at present. The first researcher to propose a general mechanism for the alkali activation of materials primarily comprising silica and reactive alumina was Glukhovsky in the 1950s (Glukhovsky, 1956). His model divides the process into three stages: (a) destruction–coagulation; (b) coagulation–condensation; (c) condensation–crystallization. More recently, different authors (Fernández-Jiménez et al., 2005; Van Deventer et al., 2007) have extended Glukhovsky's theories in order to explain the geopolymerisation process as a whole, leading Duxson et al. to publish a highly simplified reaction mechanism for geopolymerisation (Duxson et al., 2007a). This reaction mechanism, shown in Figure 3, outlines the key processes occurring in the transformation of a solid aluminosilicate source into a synthetic alkali aluminosilicate.

This model has been divided into three reaction stages that are concurrent and partially reversible, by Xu and Van Deventer (Xu et al., 2000):

- **The dissolution** of the aluminosilicate source to form reactive precursors $Si(OH)_4$ and $Al(OH)^{4-}$.
- **Restructuring** and rearrangement of aluminosilicate precursors to a more stable state.
- **Gelation**/**Polycondensation**: polymerisation and precipitation of the system, i.e. the condensation of mono silicates and mono aluminates to form Si-O-Si and Si-O-Al.

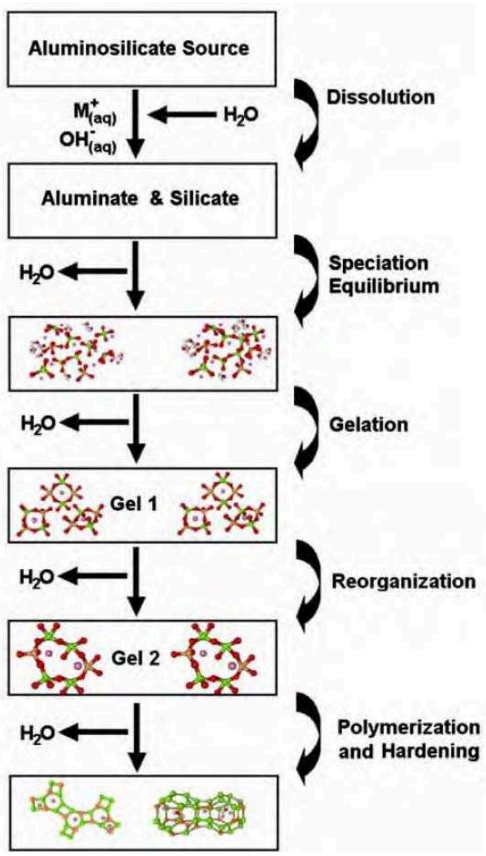

Figure 3. *Highly simplified reaction mechanism for geopolymerisation according to Duxson, , Fernández-Jiménez, Provis, , Lukey, Palomo and Deventer. (Duxson et al, 2007a)*

2. Raw materials and activating solutions

Any source of silica and alumina that can be dissolved in an alkaline solution can act as a geopolymer precursor but the most commonly used alumino-silicate sources are: class F fly ash or metakaolin (Provis and Van Deventer, 2009), each one having different SiO_2 and Al_2O_3 mass contents and a very low rate of CaO as shown in Figure 4. Many publications have referred to "slag-based geopolymer" but, as shown in this diagram, the slag has a non-negligible calcium content, so it will not be considered as a raw material for making geopolymer in the context of this study.

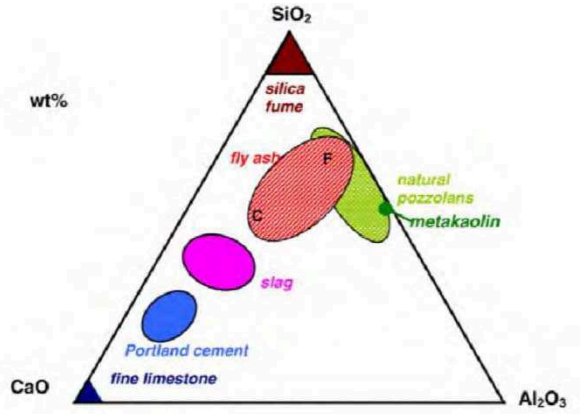

Figure 4. *$CaO–Al_2O_3–SiO_2$ ternary diagram of cementitious materials (from Lothenbach et al., 2011)*

In addition to the aluminosilicate source, a chemical activator is required to initiate the geopolymerisation reaction. The activating solution is an essential element in the geopolymerisation process because it is this solution that, depending on its quantity and its concentration, will provide the mixture with the alkalis (and in some cases the reactive silica) required to initiate the reaction and determine the final structure of the cured material (Duxson et al., 2007b). In most cases, the aluminosilicate materials are activated by a solution of alkali hydroxides or silicates under high-pH. Some rare studies cite activation by sulfate or carbonate, but these activators are generally related to alkali-activated slags (Shi et al, 2006). Several characteristics of the activating solution have been largely studied in the literature, such as the nature and concentration of the alkali, or the amount of silica, but the results obtained for metakaolin or fly ash can be generalised by the study of Duxson et al. in 2007, as presented on Figure 5 (Duxson et al., 2007b).

The authors observed that the strength increased as the Si/Al molar ratio increased, regardless of the alkali ratio, from 1.15 to 1.90 and then a small decrease was observed in compressive strength in all series of specimens beyond Si/Al = 1.90. This shows that the geopolymer develops better mechanical properties when some silicates are provided by the activating solution, the lowest strengths being obtained for the 1.15 Si/Al molar ratio corresponding to geopolymers activated by alkali hydroxide only. However, the amount of silica provided should not be too high. For example, in this study, it was set at Si/Al = 1.90. Regarding the different alkali contents, specimens exhibit similar compressive strengths for a given Si/Al ratio, suggesting that the difference in mechanical properties between specimens of different alkali mixtures is of the order of 10–20%.

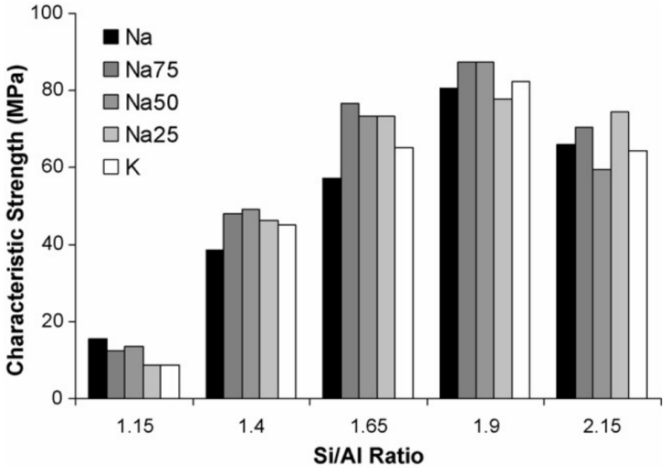

Figure 5. *Compressive strengths of geopolymer specimens synthesised at five different Si/Al ratios from alkali solutions with five different alkali cation ratios Na/[Na + K]= 0.00, 0.25, 0.50, 0.75 and 1.00, (Duxson et al., 2007b)*

3. Formulations and mechanical performance

The silica, aluminium, alkali and water brought to the mixture by the raw materials are mentioned in the literature in the form of three molar ratios, which allowed the total formulation of a geopolymer to be fixed:

- → SiO_2/Al_2O_3
- → Na_2O/Al_2O_3
- → H_2O/Na_2O

In order to see the influence of each ratio on the mechanical properties of the geopolymer, some authors, e.g. Kamalloo et al. or Roweles et al. (Kamalloo et al., 2010; Roweles et al., 2003), have correlated (artificial neural network in this case) data gathered in the literature to highlight the formulations leading to the highest performances.

Figure 6 presents the filled contour plot made by Kamalloo et al. (2010) using more than forty data items from the literature which indicate the effect of R_2O/Al_2O (where R=Na or K), SiO_2/Al_2O_3, and H_2O/R_2O molar ratios on the compressive strength of metakaolin-based geopolymers. The results show that the optimised SiO_2/Al_2O_3, R_2O/Al_2O, and H_2O/R_2O ratios to achieve high compressive strength (up to 80 MPa) should be 3.6-3.8, 1.0-1.2, and 10-11, respectively. Figure 6b clearly reveals that increasing the H_2O/R_2O ratios, which corresponds to increasing the amount of water, drastically lowers mechanical performance.

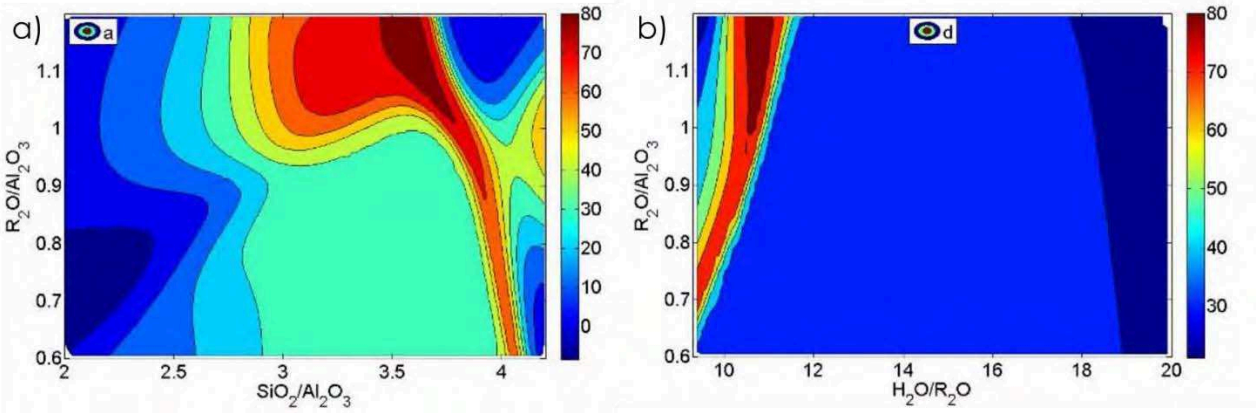

Figure 6. *Filled contour plot of compressive strength showing the effect of SiO_2/Al_2O_3, R_2O/Al_2O, and H_2O/R_2O ratios. The unit used for the contours is the MPa. (Kamalloo et al, 2010).*

4. Microstructures and porous network

The formulation parameter affects the mechanical performance of a geopolymer and also other properties, such as the microstructure or the porous network. Duxson et al. (2005) have published SEM micrographs of geopolymers exhibiting significant changes in their microstructure with variations of the Si/Al ratio. The authors state that, below an Si/Al molar ratio of 1.4, some unreacted solid aluminosilicate remains and the more the molar ratio increases, the more homogeneous the structure becomes, with a major change between 1.45 and 1.60, as can be seen on Figure 7a which shows four SEM micrographs of geopolymer having an Si/Al molar ratio of (a) 1.45, (b) 1.50, (c) 1.55 and (d) 1.60.

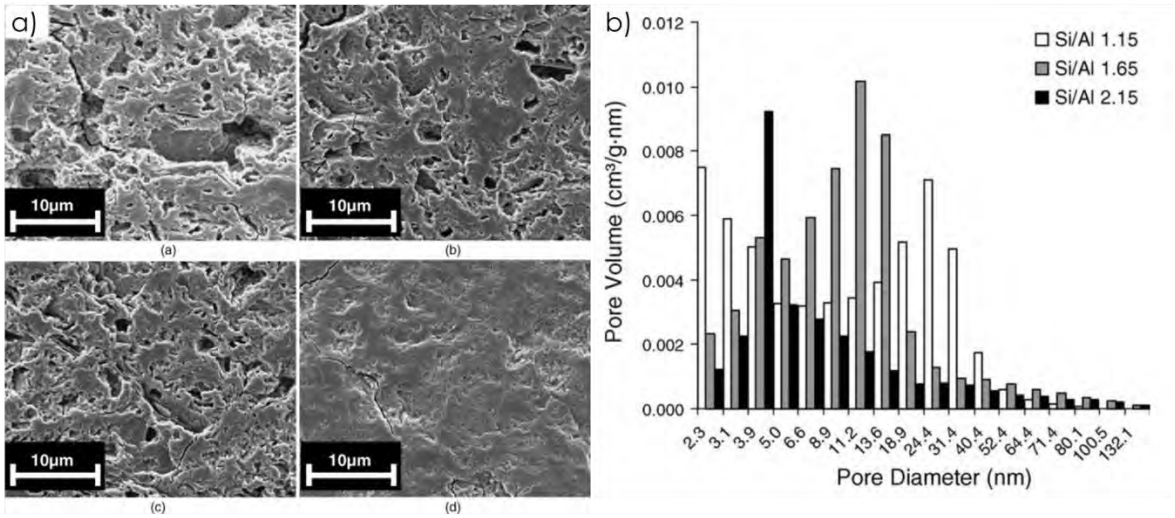

Figure 7*. a) SEM micrographs of geopolymers with Si/Al = (a) 1.45, (b) 1.50, (c) 1.55 and (d) 1.60; b) Pore volume distribution of sodium geopolymers (Duxson et al., 2005).*

The microstructures comprised both homogeneous and porous regions and the more the Si/Al molar ratio increased, the more the homogeneous portion increased. Conversely, when the molar ratio increased, the measured pore diameter become smaller, falling from an average pore diameter of 24 nm for a ratio of 1.15 to a diameter of around 5 nm for a ratio of 2.15, as can be seen in Figure 7b.

This study shows, however, that, regardless of the amount of silica introduced into the mixture, the pore distribution remains monomodal. Other authors have also shown that the

average pore diameters of geopolymers are always centred on a single value (monomodal organisation) and the change of a parameter, such as the curing temperature (Figure 8 Rovnaník, 2010) or the nature of the alkali (K or Na, Boher , 2012) merely move the average value of the pore diameter but not its monomodal distribution. Thus the geopolymer porous system appears to be quite different from that of traditional cement, which could imply differences in performance or durability between these two materials.

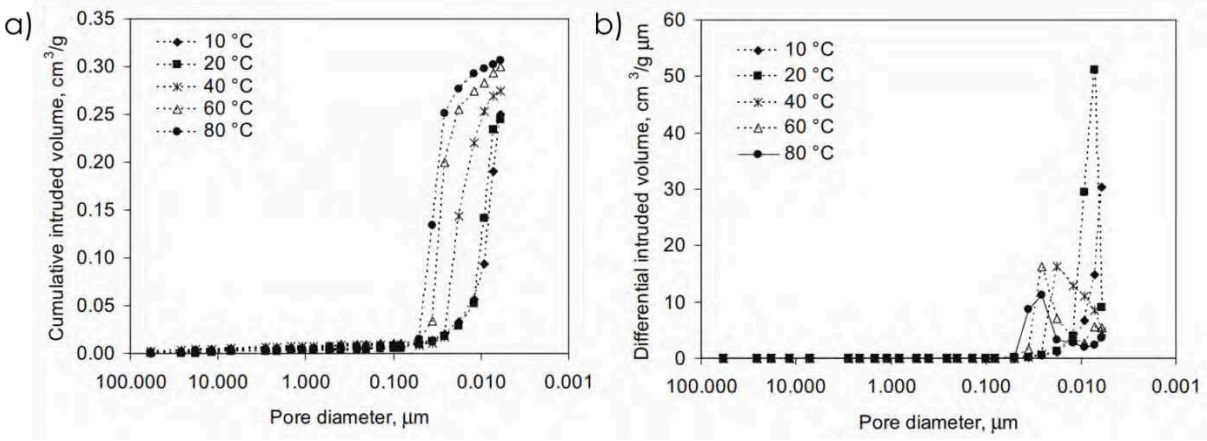

***Figure 8**. Comparison of pore distribution of geopolymers cured at 10, 20, 40, 60, and 80°C at the age of 28 days. Curing at 40, 60 and 80°C was carried out for an initial 4 h (Rovnaník, 2010).*

In short

Geopolymer definition	Aluminosilicate materials having poor calcium content
Geopolymer formation	According to three molar ratios : SiO_2/Al_2O_3, R_2O/Al_2O, and H_2O/R_2O (R= Na or K)
Strength and properties	Strongly related to the formulation
Microstructure and pore networks	Monomodal Strongly related to alkali used and this concentration
Porous network	Monomodal access pore size around 10nm to 50nm
Interrogations	The diversity of the raw materials and the geopolymerisation not fully understood wondered about the reproducibility and the possible comparison of the results presented in literature The reaction and the formulation of geopolymer being very different from those of cement, questioned about the civil engineering codes and no solutions oriented towards standardization appeared from literature

The aims of this first study will therefore be to formulate and physicochemically characterise a geopolymer based on metakaolin and sodium silicate in order to build up a knowledge database that is as exhaustive as possible, on this new material. Results will be compared with the literature data and a traditional hydraulic binder having equal strength. The possibility of applying existing standards to geopolymer matrix will also be assessed.

III. Materials and Methods

1. Material

1.1 Flash metakaolin

It was decided to use only industrial raw materials for this study. The source of aluminosilicate used in all the formulations presented here was a metakaolin obtained by flash calcination and produced in the south west of France by ARGECO Développement. The first particularity of this product is its calcination, called "Flash calcination" in reference to the combustion process (temperature around 700°C) where the particles of kaolinite are transformed into metakaolin by passing near a flame for a few tenths of a second. This process is faster and consumes less energy than other methods for the production of metakaolin (e.g. rotary kiln). Moreover, it consumes nearly 80% less energy than cement production (San Nicolas, 2011). The second specificity concerned the relatively high level of impurity in the kaolin used for the calcination (San Nicolas, 2013), which was identified by XRD (Figure 9). The results of this mineralogical analysis showed the presence of quartz (SiO_2, Powder Diffraction File (PDF) # 46-1045), anatase (TiO_2, (PDF) # 21-1272), mullite ($Al_6Si_2O_{13}$, (PDF) # 84-1205), calcite (CaO, (PDF) # 47-1743) and kaolinite ($Al_2Si_2O_5(OH)_4$, (PDF) # 83-0971) in addition to the amorphous phase corresponding to metakaolin. The proportion of each phase presented in the legend of Figure 9 was calculated by Rietveld refinement, using the free license software Maud.

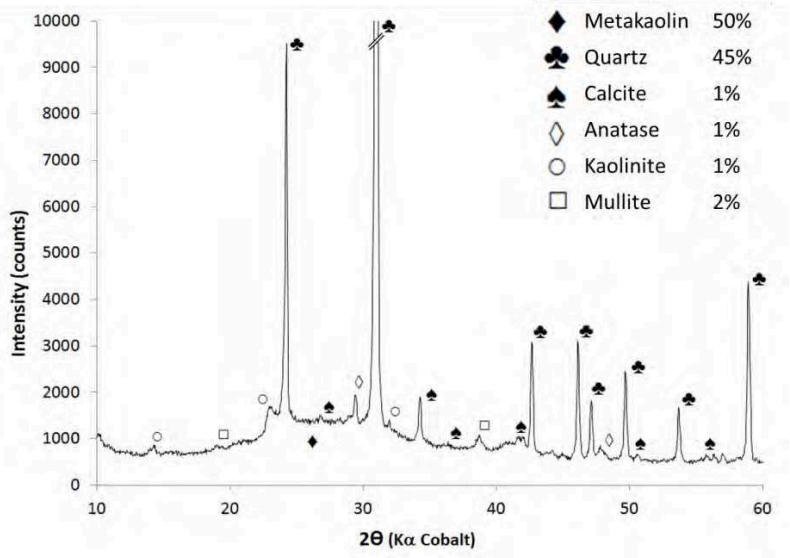

Figure 9. *XRD pattern of flash-calcined metakaolin with Rietveld quantification of phases*

The images obtained by scanning electron microscopy (SEM) and presented in Figure 10 at two different scales (a) x 2,000 and b) x 45,000) show this large amount of quartz identified by a "□" on Figure 14a and having sizes ranging from 10 to 100 µm. The presence of some spherical particles (○ on Figure 10a), having diameters of around 10 µm, previously identified as a mixture of mullite and amorphous phase due to over-calcination of the kaolinite (San Nicolas, 2013), was also noted. The "pure" metakaolin particles (Figure 10b) were found throughout the sample as very fine hexagonal particles a few nanometres thick and between 10 and 100 nm in diameter.

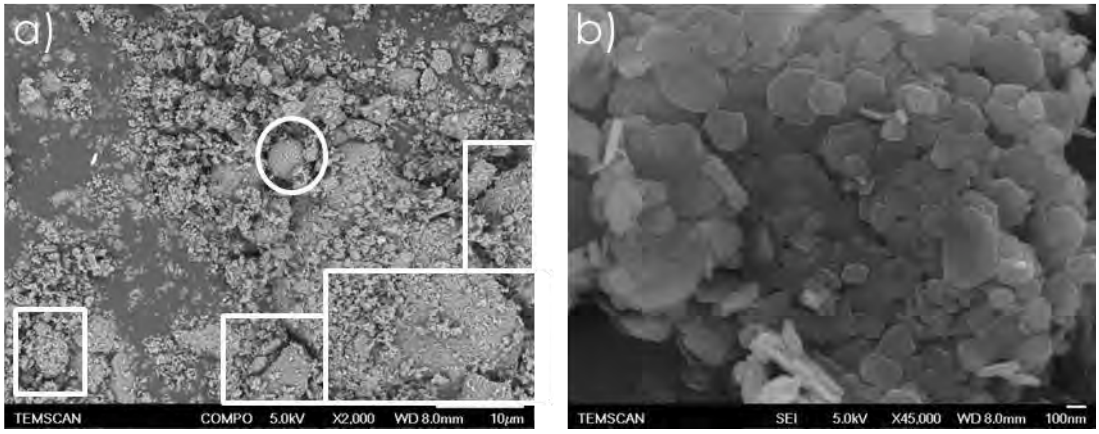

Figure 10. *Photomicrograph of flash-metakaolin obtained at two different scales a) x 2,000 and b) x 45,000. □ corresponds to the quartz and ○ to the spherical particles.*

The chemical composition obtained by ICP analysis (Table 1) presents the mass content of oxides in the metakaolin. These results showed a very large silica content, relative to the aluminium, as it exceeded 60% of the total mass of the metakaolin, which corresponds to an SiO_2/Al_2O_3 molar ratio of 4.8. This value was higher than that of kaolinite (AS_2: SiO_2/Al_2O_3=2) because of the presence of large amounts of impurities such as quartz.

Table 1. Chemical composition of the raw materials (% by weight)

	SiO_2	Al_2O_3	CaO	MgO	MnO	Fe_2O_3	K_2O	Na_2O	TiO_2	SO_3	fire loss
Metakaolin	68.10	24.10	0.91	0.22	-	3.73	0.35	0.08	1.14	0.03	1.83

All the above results allowed the amount of amorphous silica and aluminium in the metakaolin to be determined. This will be considered in the formulation of the geopolymer: SiO_2 = 29% and Al_2O_3 = 24%.

1.2 Sodium silicates

In this work, only sodium silicate solutions were studied. The activating solutions were industrial waterglass solutions containing 8 % to 17% of Na_2O by mass, corresponding to an SiO_2/Na_2O molar ratio ranging from 1.7 to 3.4 (Table 2).

Table 2. Molar ratio, mass composition and specific gravity of the industrial silicate solutions.

Waterglass solution	SiO_2/Na_2O molar ratio	$\%SiO_2$ (mass%)	$\%Na_2O$ (mass%)	$\%H_2O$ (mass%)	Specific gravity ($kg.m^{-3}$)
Wg1.7	1.7	27.5%	16.9%	55.6%	1550
Wg2.2	2.2	30.8%	14.6%	54.6%	1540
Wg3.4	3.4	26.5%	8.0%	65.5%	1370

The production of alkali silicate requires a fusion of the quartz particles (Figure 15), followed by cooling and filtration. This step has a particularly strong environmental impact, especially in terms of in CO_2 emissions and water pollution. However, the companies involved in this production (in the case of our study, Woellner®) try to minimise the harmful effects by implementing alternatives such as the hydrothermal process (second process on Figure 11 and used in our study) which, according to the manufacturer, should be less harmful for the environment.

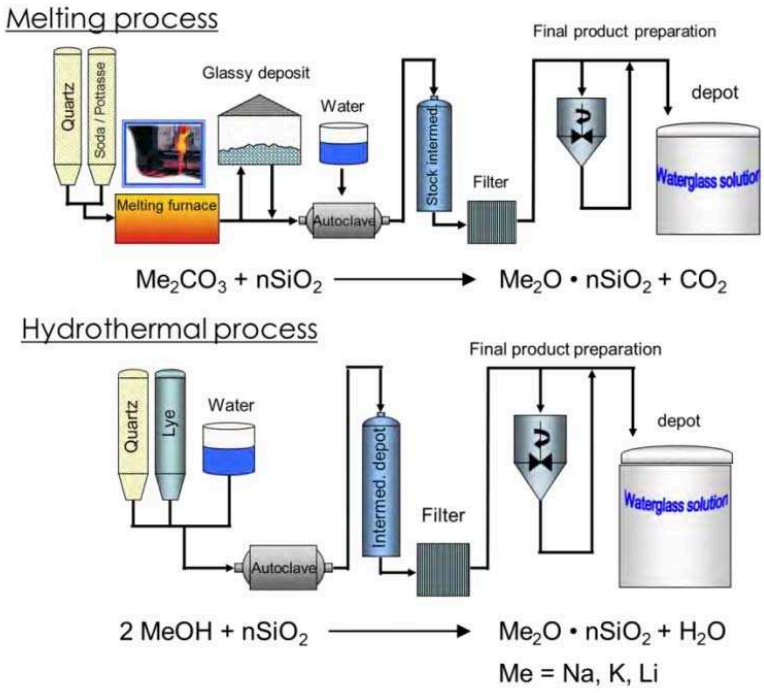

Figure 11. *Schematic representation of alkali-silicate manufacture using a melting and a hydrothermal process (Woellner®).*

2. Sample preparation and test methods

2.1 Sample preparation

The geopolymer paste was prepared in two steps. First, pure NaOH and water were added to the industrial waterglass solution to obtain the desired SiO_2/ Na_2O and H_2O/Na_2O molar ratios. After the total dissolution of the sodium hydroxide, the solution was cooled to 20°C for 24 h and then mixed with the metakaolin until a homogeneous mixture was obtained.

The geopolymer mortars were mixed and made according to French standard EN 196-1 in a 5L mixer (Automix, Controls®, Figure 12a), using the activation solution instead of the mixing water. Standard sand (EN 196-1 and ISO 679: 2009 standards) composed of well crystallised quartz and having a controlled particle size between 0 and 2 mm was used. The mortar specimens were cast in 4 x 4 x 16 cm moulds (Figure 12b) using a shock table, and pastes were cast in 7 x 4.3 x 2.2 cm plastic prisms. All specimens were cured at 20°C and 95% R.H. for 24 hours and then demoulded and stored under the same conditions until testing (except for the studies of curing conditions or for beams).

Figure 12. *5L mixer a) and b) 4 x 4 x 16 cm moulds used to cast geopolymer mortar.*

2.2 Mechanical test methods

For the mortars, the mechanical tests in flexion and compression were performed on 3 prismatic specimens of dimensions 4x4x16 cm according to EN 196-1 (Automatic mortar press, Class A - 3R® RP30/200FP). The tests were initially performed in 3-point bending and each half-prism was then tested in compression. The average confidence interval ($\alpha = 0.05$) on the compression test was 1 MPa.

2.3 Chemical and physical analysis

The chemical compositions were measured by **inductively coupled plasma and optical emission spectroscopy** (ICP-OES) using an Optima™ 7000 DV ICP-OES (PerkinElmer) equipped with a CCD sensor. Each analysis composition was subjected to an acid dilution of at least 2% in pure nitric acid (more if necessary to obtain a pH lower than 3).

Electron microscopy observations were made using a **scanning electron microscope** (JEOL JSM-6700F) and were carried out on freshly broken pieces (after platinum metallization). An analysis by **electron microprobe** (EMP) provided the quantification of each element in the volume analysed as a percentage by weight of oxides. The equipment used was a CAMECA SX Five (Centre de MicroCaractérisation Raimond Castaing, CMCR - UMS 3623) with an accelerating voltage of 15 kV and a current of 10 nA. The volume probed during each analysis was 2x2x2 μm^3. The following elements were analysed: Ca, Si, Al, Fe, Mg, S, K, Na, Ti, and Mn (10s/element + 5s for the continuous background). This analysis used polished sections of geopolymer paste. Polishing was performed dry using, first, abrasive discs and then polishing discs having silicon carbide coatings. The polished sections were then covered with a carbon film for the conduction electrons. The points of analysis were chosen carefully in order not to include the crystalline impurities in the quantification.

2.4 Mineralogical characterisation

A mineralogical study was made by **X-ray diffraction** (XRD) using a Siemens D5000 diffractometer, having Bragg-Brentano configuration and cobalt radiation (Co Kα, λ = 1,789Å). The anode voltage was 40 kV and the electric current intensity was 30 mA. The analyses were all carried out on powder previously ground to a maximum particle size of 40μm, then placed on a rotary sample holder. The acquisitions were made between 4° and 70° 2θ, with a step size of 0.04° and an acquisition time of 20 seconds per step in order to obtain acceptable resolution for a quantitative study. They were exploitated using EVA software provided with the Powder diffraction data file (PDF) of ICDD (The International Centre for Diffraction Data) allowing identification by comparison of the of the analysed compound. The quantifications using the Rietveld method were performed using the free license software Maud (Lutterotti et al., 1999).

Thermogravimetric analysis (TGA) is a technique of measurement that allows the mass variation of a sample to be followed when increasing the temperature. The results represented on weight loss curves or the derivative of the weight loss versus temperature provides information on the composition of the sample. The experimental conditions were:

Device Type: NETZSCH STA 449F3 (left on Figure 13)
Sample mass: around 1g
Maximum size of particles: less than 80 µm
Temperature rise rate: 10°C/min
Maximum test temperature: 950°C or 1000°C
Test atmosphere: air or argon

Figure 13. *NETZSCH STA 449F3 TGA and DSC (left) and NETZSCH QMS 403C (right).*

The thermal analysis was coupled with **mass spectrometry** (MS) which is an analytical chemistry technique that can identify the amount and type of chemical compounds present in a sample by measuring the mass-to-charge ratio and abundance of gas-phase ions. This coupling thus provided the nature of the evaporated compounds corresponding to the different weight losses measured by TGA. The mass spectrometer used in this study was a NETZSCH QMS 403C (right on Figure 17).

Differential scanning calorimetry (DSC) is a thermal technique used to measure the differences of heat exchange between a sample and a reference (e.g. alumina, but may also be air). The resulting curve showing the heat emitted or absorbed by the material versus the

temperature provides information on the phase transitions: glass transition temperature, the melting and crystallization temperatures and enthalpies of reaction. This is the case, in particular, for the formation of mullite precursor when metakaolin is heated to over 950°C. The experimental conditions were:

- Device Type: NETZSCH STA 449F3 (left on Figure 13)
- Sample mass: 10 to 30 mg
- Maximum size of particles: less than 80 µm
- Temperature rise rate: 10°C/min
- Test temperature: 30°C to 1100 ° C
- Test atmosphere: argon

2.5 Porous network characterisation test methods

The total pore volume noted ε (%) was determined in this study by measuring the porosity accessible to water via the French standard NF P18-459 (2010). The principle of the method was to saturate the porous network of the material with a liquid having a known density, here water, and then measure three weights M_{wate} M_{air} and M_{dry}, which allowed the porosity accessible to water (ε) and the bulk density (ρ) to be calculated using equations (1) and (2):

$$\varepsilon = \frac{M_{air} - M_{dry}}{M_{air} - M_{water}} \times 100 \qquad (1)$$

$$\rho = \frac{M_{dry}}{M_{air} - M_{water}} \times \rho_{water} \qquad (2)$$

With:

- ε: Porosity accessible to water (in %)
- ρ: Bulk density of dry sample (kg/m^3)
- M_{water}: Mass of the saturated sample in water (kg)
- M_{air}: Mass of the saturated sample in air (kg)
- M_{dry}: Mass of sample dried at 105°C (kg). Each sample was dried in an oven at 105°C until it reached a stable weight (a difference of less than 0.1% between 2 weighings 24 hours apart)
- ρ_{water}: Specific gravity of water at the test temperature (kg/m^3)

Tests were carried out on at least three prisms of geopolymer paste having dimensions 7 x 4.3 x 2.2 cm. The balance accuracy for the mass measurements was 0.001g.

X-ray microtomography images were obtained with a Nanotom 180 from Phoenix / GE (CIRIMAT - UMR 5085, INPT/UPS/CNRS). The acquisition parameters used were a voltage of 80 kV and an intensity of 100 µA. The resolution obtained for this type of sample was a 5.4 micron voxel. The volumes were rebuilt using the Datos X software (Phoenix) and VG Studio Max (Volume Graphic) to obtain an image of the porosity of the material.

To obtain information on the size of the pores in the porous network, the **mercury intrusion porosimetry (MIP)** technique was used in this study. The principle of this technique is to force the mercury into the sample by applying increasing pressure. The higher the pressure is, the more the mercury fills the small pores. If the pores are assumed to be cylindrical, the relationship between the applied pressure and the pore radius is inversely proportional (Galle 2001; Moro et al 2002). The apparatus used for this study was a 140 Pascal coupled with 240 Pascal (Fusion Instrument) and the samples analysed were pieces of paste of around 1g obtained by fresh fracture at 7 days.

The last method applied for the characterisation of the porous system was **absorption/desorption of gas** (CIRIMAT - UMR 5085, INPT/UPS/CNRS). Based on gas absorption and capillary condensation in the solid surface, this technique determined various characteristics of the microstructure of materials, such as the specific surface area, the total pore volume accessible to the gas or the pore size distribution. However, experimentally, only adsorption and desorption isotherms were determined. The specific surface area and pore size distribution were obtained by calculation using models and assumptions. For example, in this study, the surface area was calculated from the BET model, while the pore size distribution was calculated from the BJH model, two models described in the literature by Rouquerol et al. (2008). This analysis was performed using a Tristar 3020 apparatus (Micromeritics), with a degassing temperature of 100°C, on a geopolymer paste piece prepared in the same way as those studied by mercury porosimetry.

2.6 Reactivity test methods

A s**emi-adiabatic calorimetry** test, using a Langavant calorimeter according to the French standard NF P15-436 was performed on fresh geopolymer mortar to measure the heat released by the geopolymerisation reaction. In this apparatus, the mortar (≈1.6 kg) was put into a well, but not perfectly, thermally insulated bottle placed in an air-conditioned room at 20 ± 1 °C. The temperature rise of the mortar was measured with a platinum resistance thermometer (PRT) and compared with the temperature of an inert sample located in a reference calorimeter. The heat released by the reaction contained in the mortar box was equal to the sum of the heat accumulated in the sample and of two parasitic terms: the heat accumulated in the calorimeter and the heat lost into the ambient atmosphere throughout the period of the test.

The amount of **free water** in the geopolymer paste was studied. To do this, geopolymer samples (of dimensions 4.3 x 7 x 2.2 cm), were made and each component was weighed (±0.003g). Then the prisms were hermetically sealed and cured for 7 days at 20°C. The samples were then weighed again and placed in a climate chamber with controlled temperatures of 50°C, 80°C and 105°C. The mass loss was followed over time by weighing until the mass was stable (difference of less than 0.1% of the mass measured between 2 weighings 24 hours apart). Knowing the amount of water initially introduced, a simple subtraction of the weight lost depending on the temperature gave the amount of water remaining in the material and thus also the free water.

To evaluate the **shrinkage**, 4x4x16cm GP14.5 geopolymer prisms having shrinkage bolts at both ends were made for paste and mortar according EN 196-1. Immediately after demoulding, half the specimens were covered with waterproof paper to protect them from exchanges with the environment, and then all were measured using the scale micrometer method. Each measurement was the mean of three values from three replicate specimens. The specimens were therefore placed in a controlled room at a temperature of 20°C and 50% R.H. Shrinkage measurements were then performed at 2, 3, 5, 7, 14 and 28 days.

IV. Mechanical performance of geopolymer binder

The aim of the first study was to determine the optimal compressive and flexural strengths that could be achieved with the geopolymer binder depending on its formulation, cure condition, waterglass solution, or sand proportion. Thus, tests were carried out on mortar, based on the same standard (EN 196-1) used to classify different types of cement. This comparison indicated whether the standard used was appropriate for geopolymer, and also the class of cement having equivalent performance for comparison.

1. Formulation of geopolymer

1.1 Formulation principle

To formulate the geopolymer, four raw materials were required. The metakaolin provided silica and aluminium with a fixed SiO_2/Al_2O_3 ratio. The sodium silicate solution provided silica, sodium and water in fixed proportions. Only soda and water allowed the content of a single constituent, Na_2O or H_2O, respectively, to be varied (Figure 14).

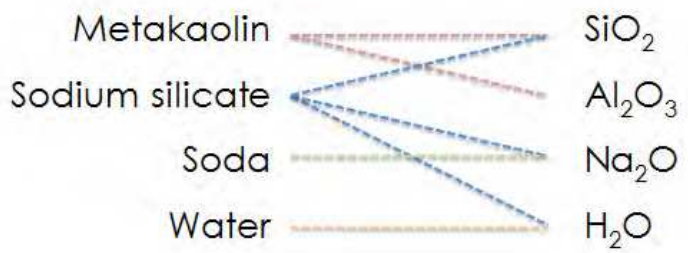

Figure 14. *Origin of the element composing the geopolymer.*

The silica, aluminium, sodium and water brought to the mixture by the raw materials were fixed in the present study in the form of three molar ratios, plus the mass ratio of the water versus solid fraction (metakaolin, solid part of sodium silicate solution and soda):

- *SiO_2/Al_2O_3* quantified the supplementary amount of silica which should be provided by the activating solution, knowing that the SiO_2/Al_2O_3 of the metakaolin was already

fixed. This ratio is known to be important regarding the strength performance of geopolymers (Duxson et al., 2007b).

- Na_2O/Al_2O_3 sets the quantity of alkali that will be supplied to the aluminosilicate source (as aluminium is provided solely by metakaolin). This ratio is often taken to be around 1 since positive ions such as Na^+ can balance the negative charge of Al^{3+} in IV-fold coordination (Kamalloo et al, 2010).
- H_2O/Na_2O corresponds to the alkali concentration in the activating solution, and could be an indicator of the total amount of water in the mixture when the other ratios are fixed.
- The *water-binder ratio* is also an important parameter that must be taken into account. It is strongly linked to the three precedent molar ratios, and cannot be modified alone while keeping all the other ratios at a constant value.

The formulations made in this study tried to assess the effect of each ratio on the compressive strength of mortars.

1.2 Formulations studied

Standard mortars according to EN 196-1 were composed of 450 g of cement, 225 g of water and 1350 g of standardised sand. For the geopolymer formulation, it was decided to keep the solid proportions, but the cement was replaced by metakaolin and the amounts of waterglass solution, soda and water were chosen according to the required molar ratio.

Table 3 shows the proportion of each component used to make 12 geopolymer mortars, presented per gram of compounds introduced or by liquid and solid fraction, together with the compressive and flexural strengths measured at 7 days. Formulations M1 to M3 differed by the amount of silica provided by the waterglass solution using three SiO_2/Al_2O_3 molar ratios from 3 to 4. Mortars named M4 to M8 had Na_2O/Al_2O_3 molar ratios ranging from 0.8 to 1.75, implying a constant sodium concentration but a variable proportion of alkalis versus silica. The last four formulations, M9 to M12 had SiO_2/Al_2O_3, and Na_2O/Al_2O_3 ratios fixed, and only the total amount of water and the sodium concentration varied.

However, it should be noted that the use of industrial raw materials severely limited the formulation possibilities. Given that the waterglass solution provided silica, water and sodium in fixed quantities, two formulations, M4 and M9, required an additional step during their preparation. In those cases, the significant water contribution of the activation solution (65.5%) made it impossible to obtain formulations having molar ratios as low as Na_2O/Al_2O_3 = 0.8 for M4 and H_2O/Na_2O = 13.5 for M9. Excess water was therefore removed from the waterglass solution by evaporation 24h before the mortar preparation, by heating at 50°C under agitation until a loss of mass equal to the required amount of water was achieved. No visual modification was observed on the remaining solution.

Moreover, it can be said that the use of the three molar ratios (two maintained constant and one modified) did not allow the water/binder ratio to be kept constant, due to the interdependence of the parameters. The only way to avoid the variation of the water content would be to modify two ratios at the same time (discussed in section 1.3).

Table 3. Geopolymer mortar formulations and mechanical strengths at 7 days.

	M1	M2	M3	M4	M5*	M6	M7	M8	M9	M10	M11	M12
SiO_2/Al_2O_3 molar ratio	**3**	**3.5**	**4**	3.6	3.6	3.6	3.6	3.6	3.6	3.6	3.6	3.6
Na_2O/Al_2O_3 molar ratio	1	1	1	**0.8**	**0.9**	**1.15**	**1.45**	**1.75**	0.9	0.9	0.9	0.9
H_2O/Na_2O molar ratio	16.5	16.5	16.5	14.5	14.5	14.5	14.5	14.5	**13.5**	**18**	**21.5**	**25**
Na_2O/Si_2O molar ratio	0.33	0.29	0.25	0.22	0.25	0.32	0.40	0.49	0.25	0.25	0.25	0.25
Formulation (g)												
Metakaolin		450				450				450		
Liquid Wg3.4	227.9	348	468.1	372	372	372	372	372	372	372	372	372
Solid NaOH	61.2	48.8	36.4	29.4	37.8	59.0	84.4	109.8	37.8	37.8	37.8	37.8
Added water	165.2	86.5	7.9	-22.6[+]	5.0	74.1	157.0	239.9	-12.1[+]	65.1	125.1	185.1
Sand		1350				1350				1350		
Formulation (kg/m^3)												
Solid binder (Mk + $silicate_{solid}$ + NaOH)	716	866	1015	991	959	888	816	754	976	904	855	812
Total water	297	297	296	230	251	297	344	384	238	294	332	366
Aggregates	1277	1273	1270	1407	1362	1262	1159	1071	1386	1284	1215	1153
Water/binder	0.41	0.34	0.29	0.23	0.26	0.33	0.42	0.51	0.24	0.33	0.39	0.45
$[NaOH]_{total}$ (mol/L)	6.7	6.7	6.7	7.7	7.7	7.7	7.7	7.7	8.2	6.2	5.2	4.4
Mechanical results at 7 days												
Compressive strength (MPa)	28.3	43.1	42.3	49.0	62.0	43.5	23.8	11.0	65.6	44.9	14.7	< 3
standard deviation	2.1	1.0	2.6	3.2	1.7	1.7	1.4	0.9	2.3	1.0	0.8	0.0
Flexural strength (MPa)	5.2	5.6	5.8	7.4	8.5	6.1	4.0	< 3	8.5	6.1	< 3	< 3
standard deviation	0.2	0.3	0.3	0.4	0.8	0.2	0.1	0.0	0.6	0.7	0.0	0.0

* Corresponds to the formulation selected for the rest of the study.
[+] Negative value due to the evaporation of water from the alkali silicate solution.

1.3 Influence of the formulation ratios on the compressive strength

SiO_2/Al_2O_3

The SiO_2/Al_2O_3 molar ratio is known to be determining for the mechanical strength of geopolymers (Duxson et al., 2005). Figure 15 shows the compressive strength of geopolymer mortar at 7 days for three different SiO_2/Al_2O_3 molar ratios ranging from 3 to 4 and corresponding to the formulations M1 to M3. A significant increase, of about 60%, of the compressive strength was measured between the formulations M1 and M2, followed by a stagnation of the values. This plateau was obtained even if the water-binder ratio continued to decrease, thus confirming the importance of the SiO_2/Al_2O_3 ratio. The maximum strength was obtained for the median value of 3.5 (at 7 days), which also showed the lowest dispersion. The M3 formulation achieved an equal strength but a non-negligible increment was observed in the setting time of the mortar for this ratio. This demonstrated the importance of active silica in the system. When it was too low, the compressive strength decreased and, when it was too high relative to the amount of aluminium, it had a detrimental effect on the setting time.

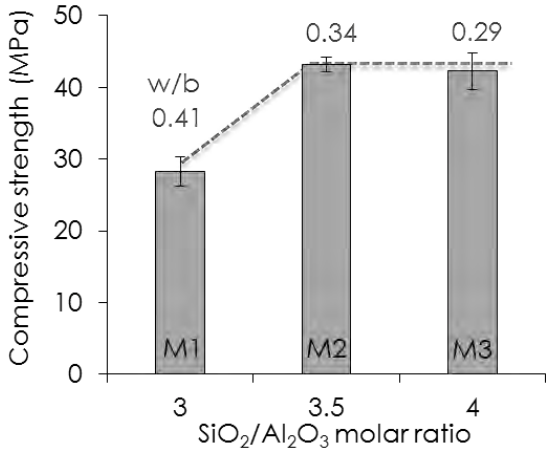

Figure 15. *Compressive strength of geopolymer mortars with different SiO_2/Al_2O_3 molar ratios at 7 days, with the water/binder ratios.*

Alkali and water proportions

The amount of alkali (sodium in this study) plays an important role in the geopolymer formulation, as a sufficient amount must be given to the system to start the geopolymerisation, but an excess can have detrimental consequences such as release of alkali gel at the surface, efflorescence, etc. Figure 16 presents the compressive strength of geopolymer mortars for Na_2O/Al_2O_3 molar ratios of 0.8 to 1.75 (formulation given in Table 3

- M4 to M8). The maximum value was obtained for the molar ratio of 0.9. For any other ratios, lower or higher, a decrease of strength was observed. The low strength at Na_2O/Al_2O_3 of 0.8 could be due either to the dry consistency of the mortar or to a possible modification of the waterglass solution caused by the heating at 50°C. The decrease in strength for higher ratios was probably strongly affected by the water content (w/b from 0.26 to 0.51). However, it cannot be excluded that the amount of alkalis had an effect on the strength evolution, since the amount of NaOH was almost tripled between ratios 0.9 and 1.75.

As seen on Figure 17, the excess of alkalis in the systems led to the production of a gel at the surface of the samples, meaning that there was too much Na+ compared to aluminium.

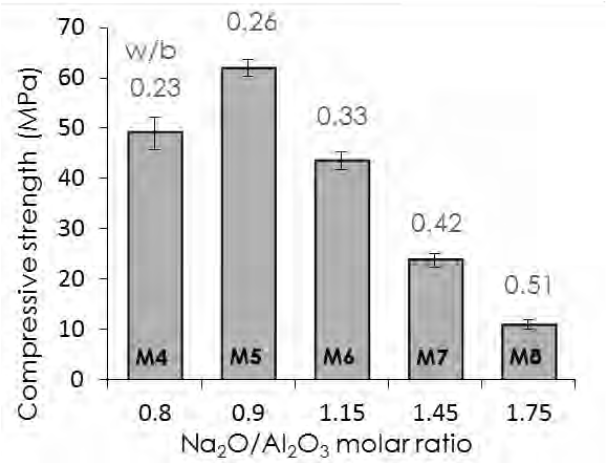

Figure 16. *Compressive strength of geopolymer mortars at 7 days with different Na_2O/Al_2O_3 molar ratios (SiO_2/Al_2O3 = 3.6 and Mk/sand = 0.33)*

Figure 17. *Paste sample of a geopolymer made with high Na_2O/Al_2O_3.*

Observation of the strength evolution in Figure 18, which presents the compressive strength for variable H_2O/Na_2O ratios (M5 and M9 to M12), led to the same conclusion as for OPC binders, i.e. the more water there is in the system, the greater the decrease in strength. In that case, only the water content varied, thus involving a decrease in the sodium concentration (dilution due to the presence of more water).

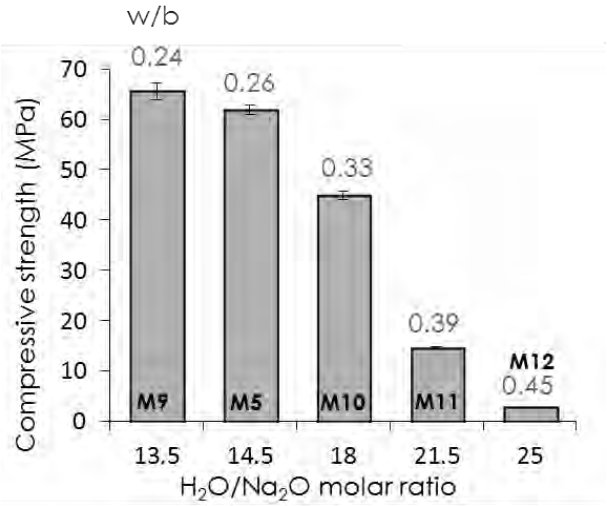

Figure 18. *Compressive strength of geopolymer mortars at 7 days with different H_2O/Na_2O molar ratios (SiO_2/Al_2O3 = 3.6 and Mk/sand = 0.33)*

In this study, the choice to modify only one of the three molar ratios at a time may have had the drawback of systematically modifying the water content of the mixtures. To increase the amount of sodium versus aluminium (Na_2O/Al_2O_3), while its concentration was maintained constant by the ratio H_2O/Na_2O, the amount of water had to be increased as well. Thus, as can be seen in Figure 19, the formulations M4 to M8 and M9 to M12 had very similar water contents, although their sodium concentrations were quite different. The actual impact of the amount of sodium may not have been properly studied because the decrease of the strength when the Na_2O/Al_2O_3 ratio increased may have been caused by the increment of the water content alone.

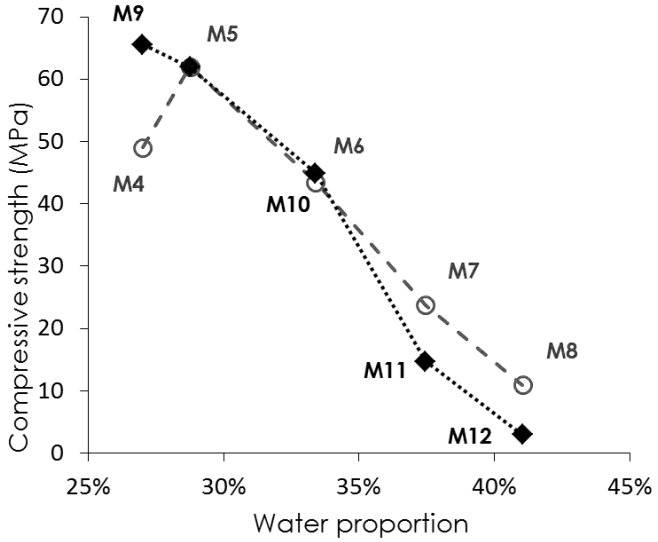

Figure 19. *M4 to M12 compressive strengths mortars depending on the water content.*

1.4 Choice of the geopolymer formulation

On the basis of the different tests reported in this section, the following formulation was chosen for the rest of the study:

$$\frac{SiO_2}{Al_2O_3} = 3.6 \quad ; \quad \frac{Na_2O}{Al_2O_3} = 0.9 \quad ; \quad \frac{H_2O}{Na_2O} = 14.5 \qquad (M5)$$

Which corresponds to the general formulation:

$$3.6\ SiO_2 \bullet\ 1\ Al_2O_3 \bullet\ 0.9\ Na_2O \bullet 13\ H_2O$$

This formulation will be used for the rest of the study and only the amount of water will be variable. Thus, for the sake of simplicity, the notation GPX will be applied, where X corresponds to the variable molar ratio H_2O/Na_2O and the two other ratios remain fixed at 3.6 and 0.9. Finally, as this material had a strength class comparable to CEM I 52.5 cement, this cement was chosen for the comparative study.

2. Hardening kinetics of geopolymer

The curing rate is an important factor for OPC specimens in order to anticipate the strength over time. Although it may vary depending on the type of cement, composition or even additives used, it is generally known that it takes 28 days of cure to make sure of having at least 80% of the final mechanical properties. In order to evaluate the cure rate of the geopolymer binder, the mortar formulation M5 (GP14.5), previously determined as the optimal formulation based on performance at 7 days, was used and tested for compressive strength at various maturities up to 2 years (Figure 20). The graph of the cure rate presented on a logarithmic scale (Figure 20a) shows two distinct phases. The first shows very fast evolution of the strength up to 60 MPa at only 3 days then, in the second, kinetics are very slow up to 730 days as the strength increases by only 10 MPa during this period. If it is considered that the strength measured at 2 years corresponds to the final performance of the mortar (Figure 20b), 80% of the geopolymer specimen's final strength was obtained in 3 days of curing.

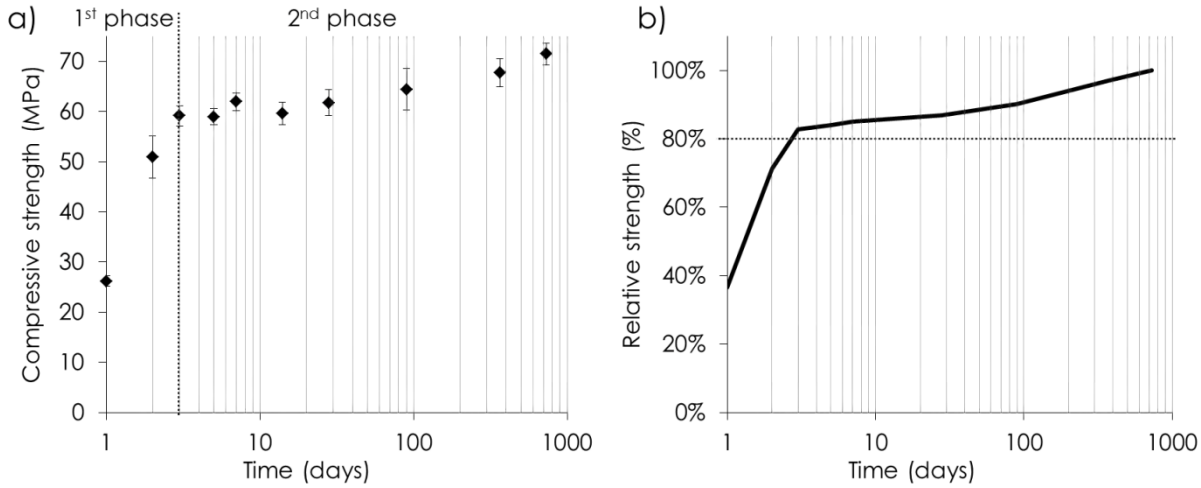

Figure 20. *Cure rate graphs of geopolymer mortar M5 on logarithmic scale presenteing the compressive strengths versus time (a) and the relative strength versus time where 100% corresponds to the final strength (b).*

This value of 80% of the final strength is an important factor as it is this strength that fixed the conventional age of testing at 28 days for all OPC standards. The results obtained for geopolymer mortars showed that this curing period is not necessary since 80% of the final strength was already obtained at 3 days. However, to ensure a sufficient reaction and facilitate the measurements (multiples of 7 are commonly used for maturity testing in civil engineering), a testing time of 7 days was chosen for this study.

3. Sand proportion

The impact of the sand content of the geopolymer mortar regarding the compressive strength was studied and the results are presented in Figure 21. It was observed that the compressive strength of the geopolymer alone after 7 days of curing was 48 MPa, a strength quite similar to those obtained for mortar having less than 40% of sand by mass. Mortars containing between 50 and 80% sand presented a strength of around 60 MPa, which is in agreement with the previous measurement of compressive strength made on geopolymer mortar having the same formulation (M5 in 1.3). Finally, beyond 80% of sand, the compressive strength dropped sharply due to a lack of workability of the mortar, which was too dry to be set up correctly because there was not enough binder in the mix to link the sand grains together.

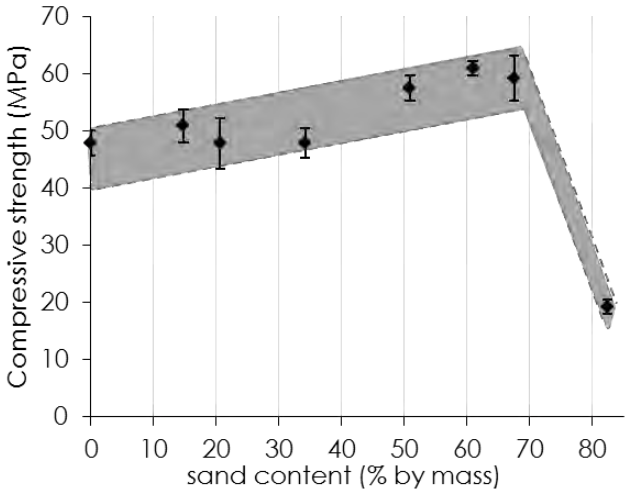

Figure 21. *Compressive strengths of GP14.5 mortars (7 days at 20°C and 95% R.H.) for different sand contents.*

4. Sodium silicate

A study was also conducted on the influence of the waterglass solution used on the mechanical performance of geopolymer. For this purpose, three mortars having similar compositions (SiO_2/Al_2O_3 of 3.6, Na_2O/Al_2O_3 of 0.9 and H_2O/Na_2O of 14.5) were prepared using the three industrial solutions presented in Table 2. To have similar sodium proportions, solid soda had to be added to the Wg3.4 and Wg2.2 solutions. Figure 22, which presents the compressive strengths measured at 7 days, shows very close values for the three solutions tested.

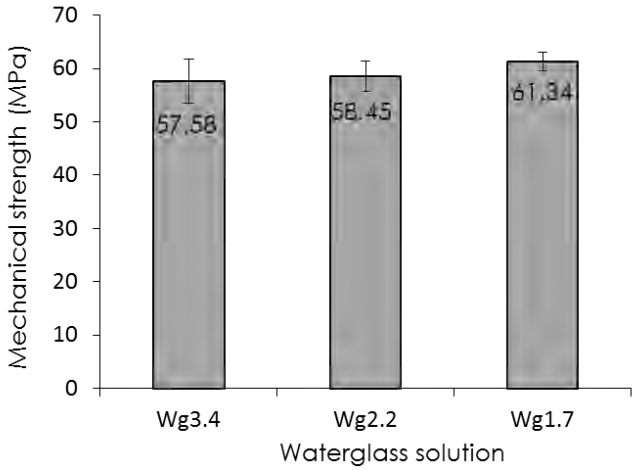

Figure 22. *Compressive strengths of GP14.5 geopolymer mortars (7 days at 20°C and 95 R.H) prepared with waterglass solutions having 3.4, 2.0 and 1.7 SiO_2/Na_2O molar ratios.*

It was simply noted that, the higher the sodium concentration of the initial activation solution, the smaller the standard deviation of the measured values. It was concluded that the addition

of sodium hydroxide for the preparation of the activation solution led to greater dispersions of the strength values. Thus solution Wg1.7 was chosen for the rest of the study. Furthermore, the use of this waterglass solution presented the advantage of eliminating the addition of sodium hydroxide during the preparation, which can be a long and dangerous step.

5. Curing conditions

In order to improve the hydration of Portland cement, it is recommended to immerse the mortars in water during the cure. As there is no standard recommending the conservation of geopolymer specimens, the impact of the curing conditions on the performance of the metakaolin-based geopolymer was assessed. Three storage conditions were imposed on geopolymer mortars from 24h to 21 days: dry atmosphere (20°C, 50 R.H.), moist atmosphere (20°C, 95 R.H.), and under water. Figure 23 shows the results of compressive strength obtained after the 21 days of curing. It was first observed that, unlike cement, geopolymer mortars did not benefit from storage under water as they lost nearly 15 MPa in these conditions compared to the maximum strength measured in a moist atmosphere (20°C and 95% R.H.). This poor development of the compressive strength under water could be attributed to leaching of the alkali and silica still present in the pore solution at 24 h and necessary for the proper structuring of the geopolymer network.

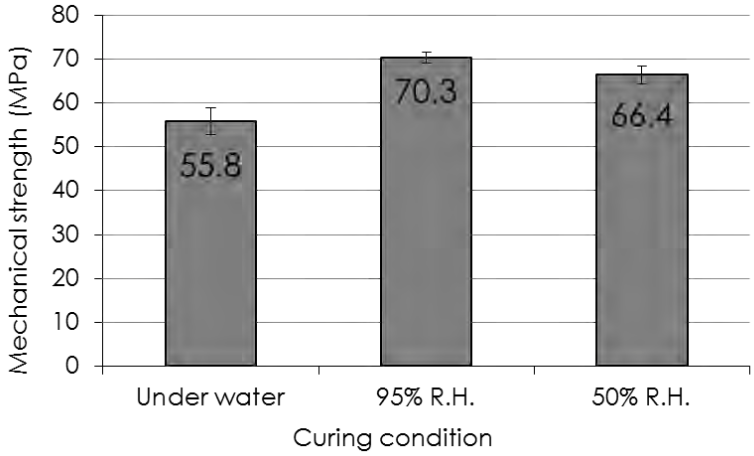

Figure 23. *Compressive strengths of GP14.5 mortars at 21 days, cured under water, at 95% R.H., or at 50% R.H. at 20°C.*

It was also highlighted that a moist environment was preferable for curing since, although exposure to average relative humidity, here 50% R.H., at 24h did not significantly impact the mechanical performance, it led to considerable surface cracking similar to that seen in Figure

24. This marked surface cracking due to drying shrinkage shows that, at 24h, the matrix was not strong enough to limit the shrinkage effect. Given the evolution of the geopolymer strength, it is probable that, if exposure to the relative humidity of 50% started after three days, cracking would be greatly reduced. This assumption was verified for other formulations. It was also noted that such cracking was greater in the case of pure paste than for mortars.
These results thus suggest that a curing condition of 95% of relative humidity should be applied during the first week after casting.

Figure 24. *Marked surface cracking on geopolymer mortar due to drying shrinkage*

6. Flexural strength

Figure 25 gives the flexural strengths measured in this study versus compressive strengths. These results highlight a behaviour common to all the 26 formulations represented on the graph, with proportionality between flexural and compressive strengths. The average Fs/Cs ratio reaches nearly 14%, which is significantly higher than the Fs/Cs ratio of 10% generally found for OPC.

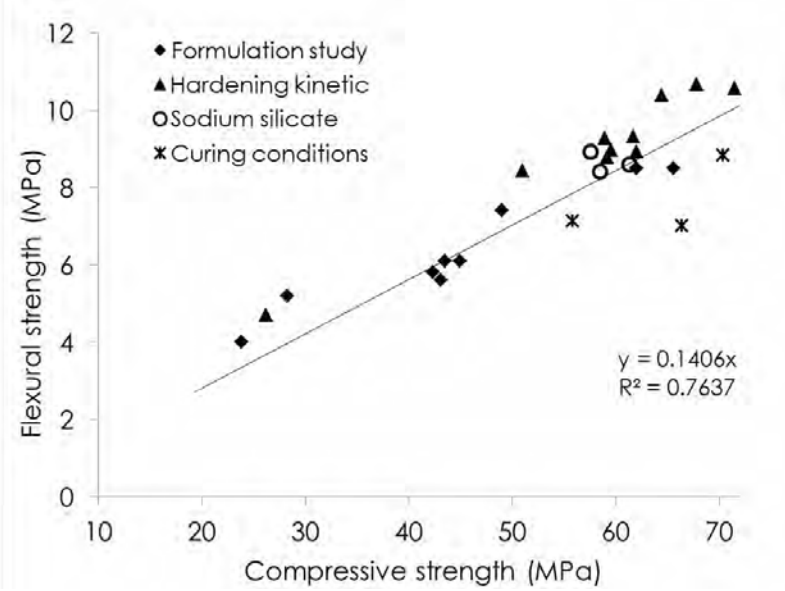

Figure 25. *Flexural versus compressive strength of all the geopolymer mortars.*

In short

Optimal formulation for the Mk of this study	3.6 SiO_2 • 1 Al_2O_3 • 0.9 Na_2O • 13 H_2O
Compressive strength	Equivalent to a CEM I 52.5
Flexural strength	Fs/Cs > 10% obtained for cement
Testing time (80% of the final Cs)	7 days
Optimal curing conditions	20°C, 95 R.H.
Activating solution	SiO_2/Na_2O modulus of 1.7 Avoid addition of sodium hydroxide
Recommendation for standard testing (based on EN 196-1)	- Insert waterglass solution instead of the added water - Test at 7 days instead of 28 days - Curing condition in moist atmosphere (20°C, 95 R.H.) instead of immersion in water

This first part has determined the optimal formulation in terms of compressive strength and raw materials used, and led to the choice of CEM I 52.5 as the cement of reference because its strength class is similar to that of the geopolymer. The results showed that the standard used to make and test the cement mortar was applicable to geopolymer, with a few modifications, mainly concerning a reduction of the testing time and the curing conditions. This optimal formulation will be used in the next section in order to characterize the geopolymer physically and chemically and compare the results with those of a CEM I 52.5 cement paste.

V. Characterisation of the geopolymer

The first part of this study highlighted similarities between the compressive strength of the optimal formulation of the metakaolin-based geopolymer binder and CEM I 52.5 cement, and the viability of geopolymer as a binder. However, the chemical and physical characteristics of the geopolymer must be assessed in order to see if the knowledge acquired on OPC over time can be applied to the geopolymer binder.

1. Morphological observation

First of all, as can be seen on Figure 26, visual observation of the geopolymer revealed a homogeneous structure that was orange-coloured due to the presence of iron in the metakaolin. Some small cavities were also observed, corresponding to air bubbles trapped during the preparation of the binder because of the viscosity of the paste, which was mostly related to the water glass solution.

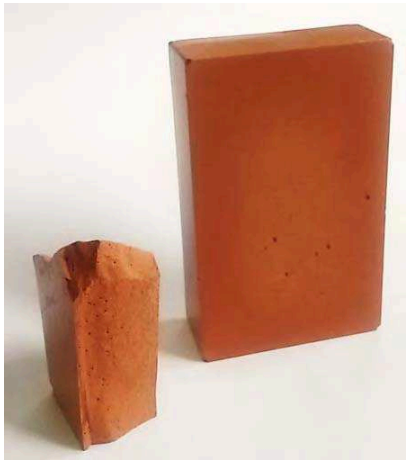

Figure 26. *Metakaolin-based geopolymer prism and piece of prism after breaking (GP14.5).*

Microscopic observation was carried out using a scanning electron microscope, and the images obtained are presented in Figure 27 at two different scales (a) x150 and (b) x350. Disregarding the large number of cracks due to sample preparation (Figure 27a), three distinct phases can be seen: crystals (identified by *) ranging from 10 to 100 µm, and most likely corresponding to the quartz brought by the metakaolin, are surrounded by a homogeneous rigid structure, identified as the "pure" geopolymer, and spherical cavities (indicated by # on Figure 27) identified as the air bubbles observed previously.

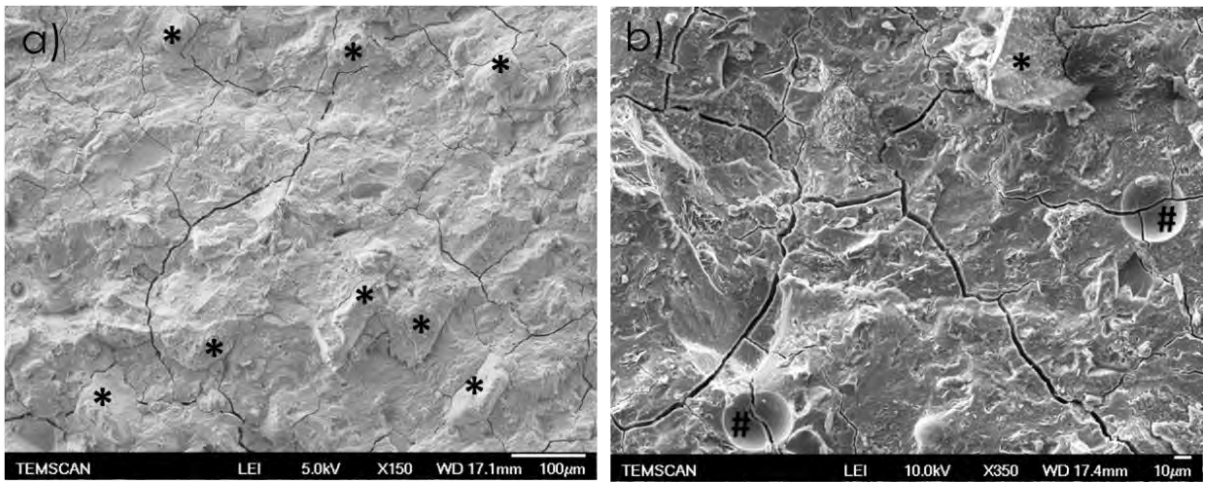

Figure 27. *Photomicrograph of metakaolin-based geopolymer (GP 14.5) obtained at two different scales (a) x150 and (b) x350. (* Quartz particles and # Air bubble cavities)*

In order to fully characterise the geopolymer paste, a study was first dedicated to the "pure" geopolymer phase and concerned its reaction, its organisation and its composition. Then, characterisation and quantification studies were performed on the crystalline impurities of the geopolymer. A complementary investigation was made on the fate of the water introduced in the composition of the geopolymer. Finally, the total porosity of the geopolymer and the organisation of its porous networks were evaluated. Whenever possible, the results obtained were compared to those for CEM I 52.5.

2. Characterisation of the four phases of the geopolymer

2.1 Pure geopolymer paste

The exothermicity of the hydration of cement is an important factor for studying the reactivity of the reaction and is known to be a potentially problematic phenomenon (especially for massive structures). It is thus important to assess the thermal impact of the geopolymerisation reaction. Figure 28 presents the results obtained by semi-adiabatic calorimetry measurement performed on GP14.5 and CEM I 52.5 mortars. The first graph (Figure 28 a), presenting the difference of temperature of the two mortars versus time, showed that the exothermicity of the geopolymerisation reaction was much lower than that of the cement hydration. However the geopolymer seemed to hold the heat more as its return to the initial temperature was slower (nearly 20h). These results, converted into heat releases (expressed in $J.g^{-1}$ of binder solid fraction), show that the heat release was more than twice as high for cement as for the geopolymer (Figure 28b).

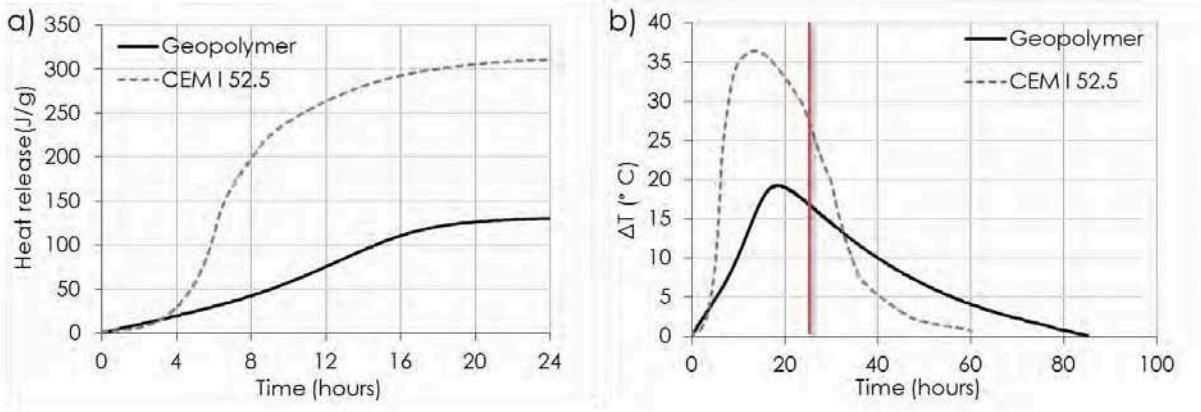

Figure 28. *Semi-adiabatic calorimetry analysis showing a) the cumulative heat release in the first 24 hours and b) the difference of temperature noted during the geopolymerisation of a GP14.5 mortar and the hydration of a CEMI 52.5 mortar.*

The fact that less heat was generated by the geopolymerisation reaction than by cement can be a clear advantage as temperature rises are sometimes harmful for cement-based materials. However, this could call the reactivity of this reaction into question. So, in order to be sure that the reaction of the metakaolin in the geopolymer was complete, differential scanning calorimetry was conducted on the metakaolin and the GP14.5 (Figure 29).

The metakaolin analysis shows three endothermic peaks. The first one, at 142°C, could be due to the presence of residual water in the metakaolin (probably because of the relative humidity of the air). The second, small endothermic peak, at 573°C, corresponds to changes in the quartz structure, which passes from α to β, and the third, at 678°C, was identified as carbonate (calcite). Finally, a relatively large exothermic peak was highlighted around 980°C due to the structural reorganization of the metakaolin when it was transformed into mullite precursor (San Nicolas, 2011).

On the geopolymer paste analysis, the same three endothermic peaks were found, with the same intensities, except for the one associated with water, which appeared much more intense, showing a greater amount of water in the geopolymer. The peaks associated with quartz and calcite had similar intensities in both analyses, suggesting that the impurity of the metakaolin was still present in the geopolymer. Finally, the most important information was given by the evolution of the peak at 980°C between the metakaolin and the geopolymer. This endothermic peak was still present in the geopolymer, but much more flared than in the initial metakaolin powder. The presence of this peak meant that not all the metakaolin in the geopolymer paste had reacted after 7 days.

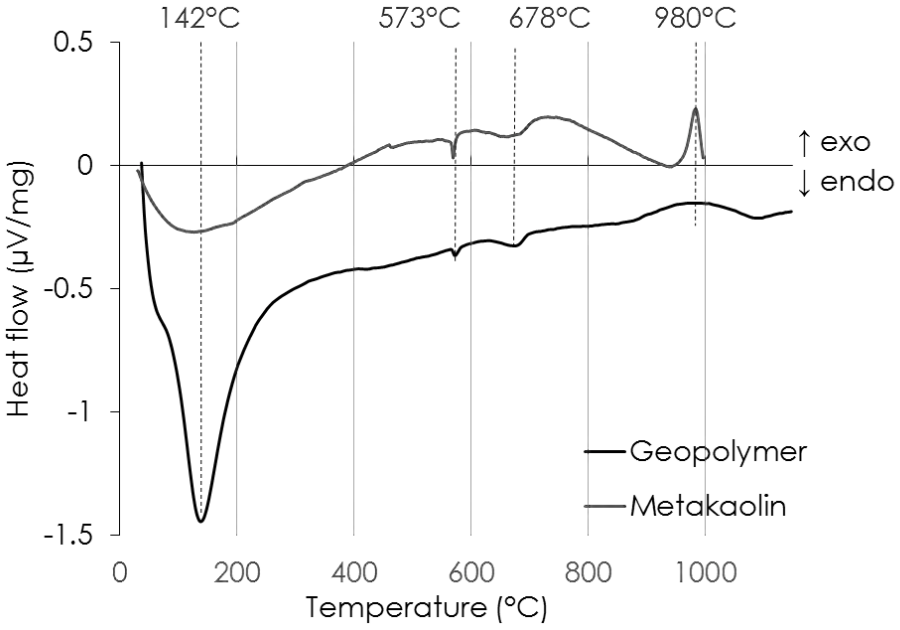

Figure 29. *Differential scanning calorimetry performed at 20°C/min up to 1000°C on flash metakaolin and geopolymer GP14.5 at 7 days.*

An X-ray diffraction analysis was performed on both metakaolin and geopolymer to see the impact of the geopolymerisation reaction on the organisation of the material. Observation of the XRD patterns presented in Figure 30 revealed information on the two previously observed phases. Regarding the amorphous phase, identified previously as the metakaolin, a shift of the diffraction halo towards higher diffraction angles was observed for the geopolymer and the intensity of the halo appeared greater. This shift was attributed to the reorganisation of the aluminosilicate precursors to form the geopolymer structure, thus highlighting the reaction of the metakaolin and the amorphous structure of the "pure" geopolymer.

It was also noted that all crystalline compounds that had been previously identified in the metakaolin were still present in the geopolymer paste, but with lower intensity. No new compounds were observed. This result confirms the coexistence of amorphous and crystalline phases in the geopolymer paste, as observed by SEM, with the amorphous phase corresponding to the "pure" geopolymer and the crystalline phase presenting exactly the same impurities as in metakaolin.

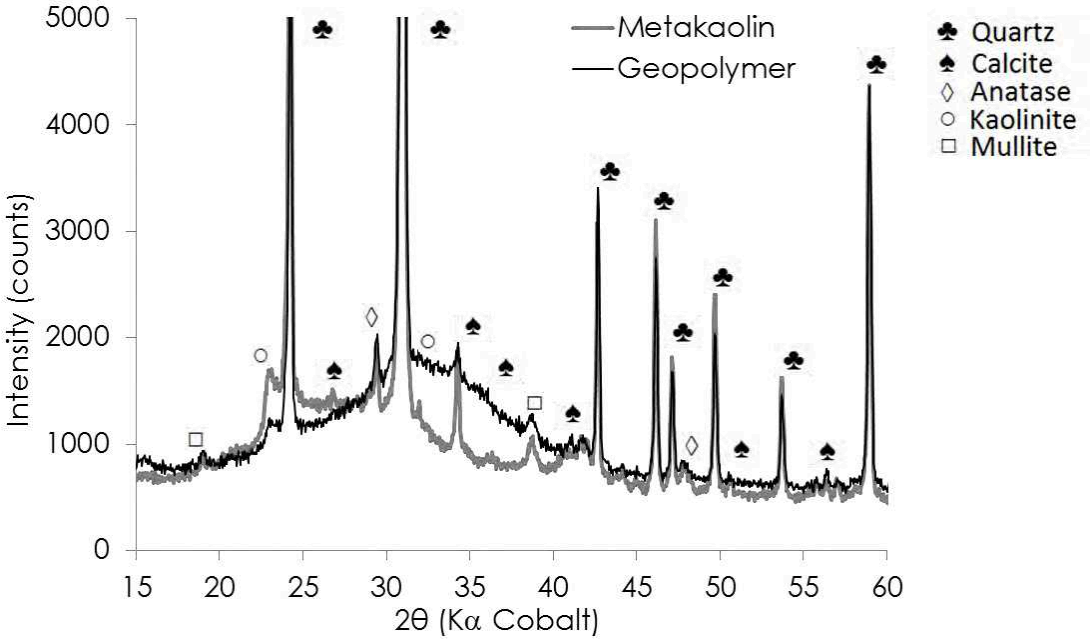

Figure 30. *XRD pattern of flash-calcined metakaolin and pure geopolymer GP14.5.*

In order to identify the potentially different phases of the "pure" geopolymer, thermogravimetric analysis was carried out. This analysis of the mass loss for a cement sample depending on the temperature allows the different hydrates present to be identified through different water losses, as, for example, in the dehydration of the C-S-H and ettringite around 100-200°C (♣ on Figure 33a), the dehydroxylation of portlandite between 450-500°C (□ on Figure 33a), and the decarbonation of calcium carbonate coming from the clinker and/or calcite at 750°C (♠ on Figure 31a).

The evolution of the mass of a GP14.5 geopolymer sample subjected to a temperature rise of 20°C/min up to 950°C is also presented in Figure 31 a. It shows only one significant loss of mass between 100° and 200°C, which was very probably due to dehydration of the structure as water was measured by mass spectroscopy (Figure 31b) at this temperature. Between 100°C and 700°C some very small mass losses were measured and were identified by MS as three different releases of carbon dioxide (Figure 31b). It can be concluded from this analysis that, unlike cement, geopolymers showed only one type of structure incorporating weakly bound water and also the presence of carbonates, which may have come from calcite or a rapid carbonation of the material.

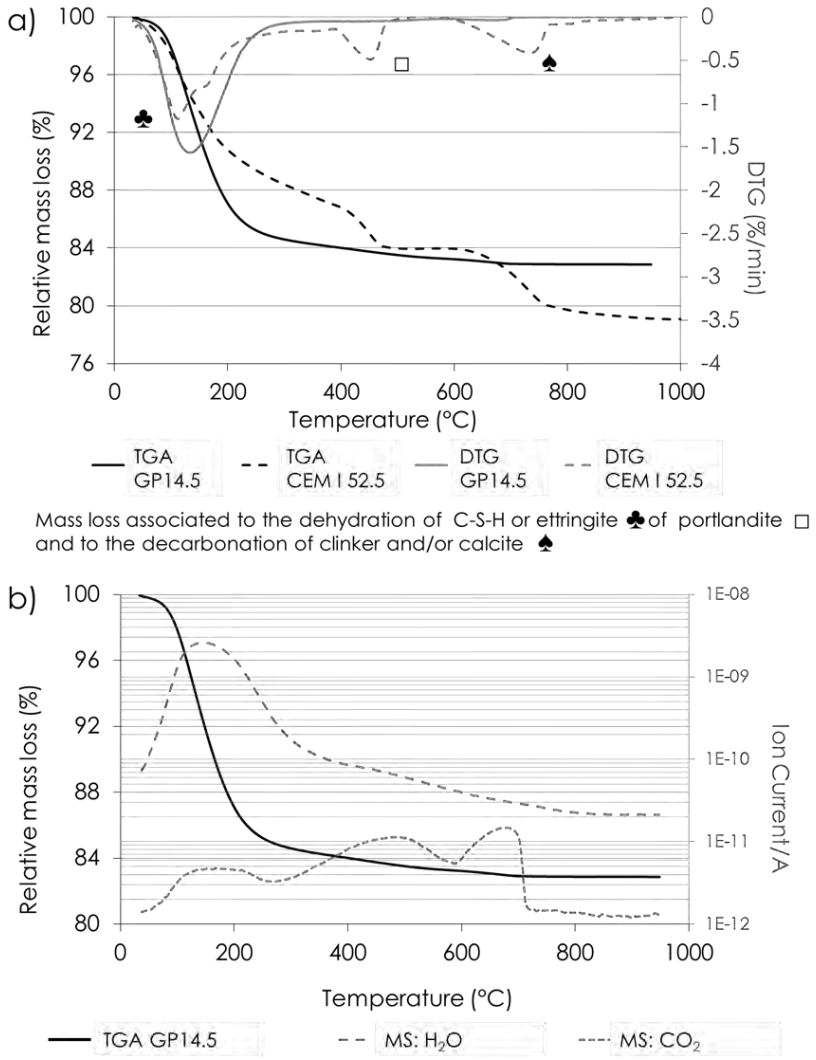

Figure 31. *Thermogravimetric analysis of geopolymer paste at 7 days performed at 20.0 °C/min up to 950°C with a) differential thermal analysis and b) H_2O and CO_2 mass spectroscopy spectrum. TGA and DTG of CEM I 52.5 cement paste (w/c=0.5) at 28 days is also presented.*

Finally, in order to obtain the chemical composition of the "pure" geopolymer, electron microprobe analysis was conducted. Two pieces of GP14.5 7 x 4.3 x 2.2 cm prisms kept for 7 days without external exchanges were thus carefully chosen, one from the centre and one closer to the surface, then placed in a resin and polished in order to have an analysis surface of around 0.5 x 0.5 cm. The observation of these matrices with this device revealed a certain heterogeneity and led to the identification of the quartz and titanium oxides, and also of iron oxides which had not been seen by XRD, and rare minerals like zircon. However, the phase corresponding to geopolymer was easily identifiable and was the subject of quantitative analysis (50 points of analysis per sample).

Figure 32 presents these two analyses on a ternary diagram representing the mass percentage of SiO_2, Al_2O_3 and Na_2O (91 measurements, after removal of the outlier values). This representation highlights an identical chemical composition for both the centre and the surface sample.

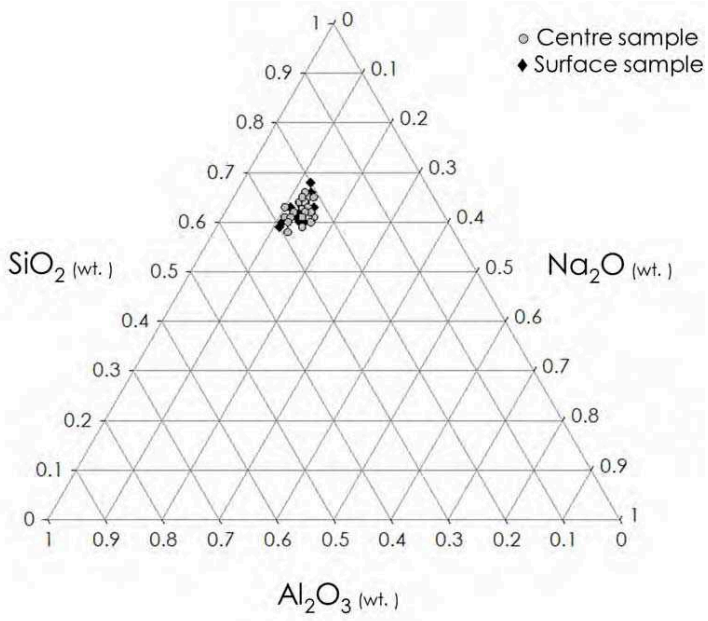

Figure 32. *Ternary diagram by mass of SiO_2, Al_2O_3 and Na_2O measured by electron microprobe on GP14.5 at 7 days (91 measurements).*

The mass contents of these oxides measured by microprobe and expressed as a percentage of the solid fraction are presented in Table 4. In this table, the theoretical oxides content calculated from the amount of raw materials introduced (expressed in percentage of the solid fraction) are also presented, together with the corresponding molar ratios. Concerning the measured silica content, the mass percentage appears to be very close to the theoretical value introduced in the mixture. However, observation of the molar ratios SiO_2/Al_2O_3 and SiO_2/Na_2O showed a larger amount of silica (versus aluminium and sodium) compared to the calculated value. It has been calculated that an SiO_2/Al_2O_3 molar ratio of 4.21 would correspond to the incorporation of 40% of the silica of the metakaolin, whereas it was previously estimated that only 29% was available for the geopolymerisation. Two hypotheses can be put forward to explain this excess: it is possible that the amount of available silica in the metakaolin was underestimated or, although this is unlikely given the very high crystallinity of quartz, the very basic activation solution may have led to dissolution of part of this silica. This showed the necessity for an accurate assessment of the crystalline phase, before and after geopolymerisation.

But the most likely hypothesis that could explain this ratio would be that the microprobe analysis was not able to analyse the "pure" geopolymer alone because some quartz was present as nanoscale particles and so would have been considered during the quantification without being visibly detected. The analysis having a measurement area of 2 x 2 x 2 µm, this would mean that around 11% of the silica in the geopolymer (corresponding to 40% measured - 29% assumed) would be in the form of micro or nanoscale quartz particles.

Table 4. SiO_2 Al_2O_3 and Na_2O mass content measured by microprobe and calculated from the amount of raw materials introduced (expressed in percentage of the solid fraction) and the corresponding molar ratios.

	Mass content (%)			Molar ration		
	SiO_2	Al_2O_3	Na_2O	SiO_2/Al_2O_3	Na_2O/Al_2O_3	SiO_2/Na_2O
Electron microprobe results	59.0 %	23.8 %	11.9 %	4.21	0.82	5.12
Results calculated from the amount introduced	57.6 %	27.1 %	15.3 %	3.61	0.93	3.89

Concerning the aluminium and sodium contents measured, in view of the molar ratios, there appears to be an alkaline deficiency, the value of 0.82 obtained being below the target value of 0.93. This lower alkali content can be explained by the fact that, at this time, the geopolymerisation reaction was not completed (as identified by DSC) and therefore the alkali introduced may not yet have been completely integrated into the structure. Another explanation for this alkali deficiency, relative to the silica and aluminium, could be given by observing the schematic representation of the geopolymeric network made by Barbosa (Figure 33). In this illustration, the sodium does not appear to be bonded to the structure, but rather inserted in the holes between the silicon-aluminium chains. Alkali could therefore have significant mobility in the hardened geopolymer, which could be responsible for the deficiency measured by microprobe. It could be assumed that, during the sample preparation (polishing, drying, and placing in a vacuum), part of the sodium was expelled from the material, explaining why the measured molar ratio was lower than the theoretical one.

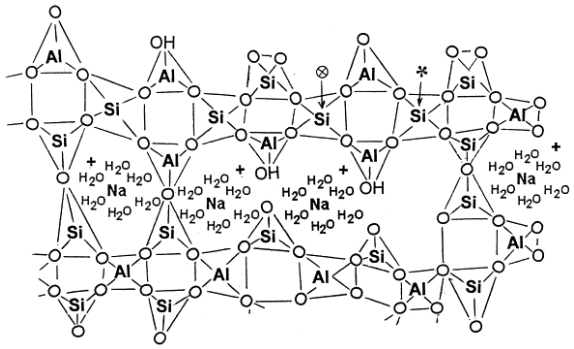

Figure 33. *Semi-schematic structure for Na–polysialate polymer proposed by Barbosa, Mackenzie, and Thaumaturgo (Barbosa et al., 2000)*

2.2 Quantification of the crystalline part

The crystalline phase of the geopolymer has been previously identified as originating exclusively from the metakaolin. The study of this phase was therefore oriented towards its quantification in both metakaolin and geopolymer, using two different methods, to assess whether the geopolymerisation reaction altered these crystals.

First, quantifications by the Rietveld method were performed on the XRD patterns of the metakaolin and the geopolymer paste GP14.5. The Rietveld method is a full-pattern analysis that minimizes the difference between experimental and calculated XRD diagrams by a least-squares procedure. To calculate an XRD diagram, some parameters have to be known and adjusted in the least squares refinement (Mahieux et al, 2010). Practically, existing text files, named CIF files, grouping together all these data for each mineral, are available online in the American Mineralogist Crystal Structure Database (*http://rruff.geo.arizona.edu/).* Several efficient Rietveld programs are also available for structure refinement and quantitative analysis and, for this study, the software used was the Rietveld-based Maud software system developed by Lutterotti (MAUD, 2012; Lutterotti et al., 1999). The Rietveld refinement was performed after identifying the crystallised minerals (ICDD cards) and finding the basic crystal structures (CIF files). In the case of the amorphous phase, the approach suggested by Lutterotti et al. (1998) based on previous work by Le Bail (1995) was used, in which the amorphous phase is modeled as a nanocrystalline solid where the long-range order is lost. The CIF files used for the amorphous phase were found in the database of the "Silica Al Glass, Amorph, cubic" software and was used to refine both metakaolin and geopolymer.

Figure 34, which represents experimental X-ray diffraction patterns of the metakaolin (a) and the geopolymer (b) with the calculated amorphous contribution, shows good superposition of the amorphous halo in both cases, resulting in a linear difference pattern (except for the crystal peak not refined). In the case where all components were considered in the computed diagram (Figure 34 c and d) only slight differences were observed in the intensity of some major peaks. Otherwise, the patterns overlapped well, thus confirming the reliability of the method.

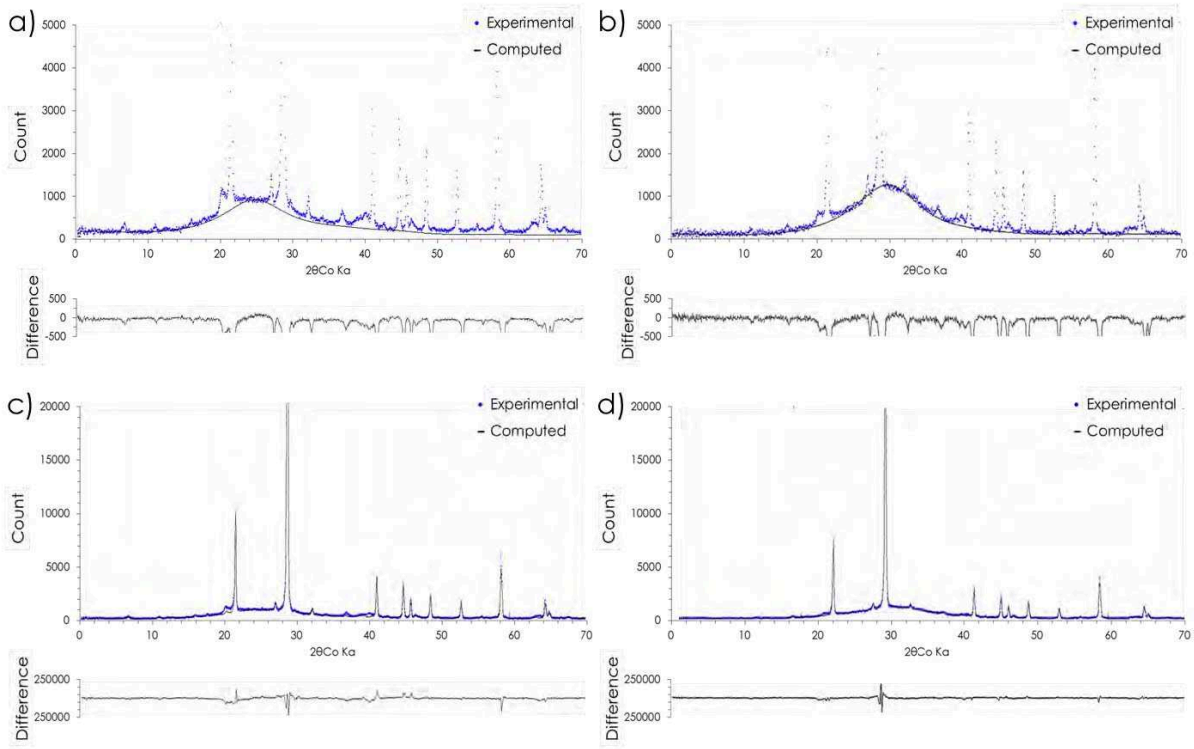

Figure 34. *Metakaolin (a and c) and the geopolymer (b and d) Rietveld refinement presenting only the amorphous contribution (a and b) and the overall quantification (c and d).*

The results obtained from Rietveld quantification for the metakaolin (Mk) and the geopolymer (GP) are presented in Table 5. A decrease was observed in the quantity of each of the crystallised components in the geopolymer analysis compared to the metakaolin, e.g. the quantity of quartz fell from 45% to 32%. This decrease was due to the dilution effect that occurred during the preparation with the addition of sodium silicate. However, since all the quantities introduced were known, it was possible to calculate the theoretical amount of quartz in the geopolymer if all the 45% found in the metakaolin was present.

Table 5. Rietveld quantification of the crystalline compounds of Mk and GP 14.5 presented in mass %.

Compounds	Quartz	Mullite	Calcite	Anatase	Kaolinite
MK	45 %	2 %	1 %	1 %	1 %
GP	32 %	1 %	0.8 %	0.5 %	0.3 %

To perform the calculation, the previous result indicating that the water introduced did not form any hydrates in the structure was exploited. If the water was not present in crystalline form it could not be considered during the quantification using the XRD pattern.

Equation (1) shows the mass content of the two solid sources: the metakaolin and also the silica and sodium provided by the activating solution. Thus, as it was assumed that the water was not considered for the quantification, metakaolin would represent 74% of the final mass of the geopolymer (equation 2). Now, considering the 45% of quartz found in the 74% of metakaolin, the theoretical quartz content in the geopolymer would be 33% (equation 3). The content found in the geopolymer by the Rietveld method, giving a close value of 32%, would mean that the hypothesis of the water not being in the form of hydrates could be consistent and that quartz was most likely not altered by the geopolymerisation reaction.

$$\text{Geopolymer content} = 52\%_{MK} + 18\%_{\text{solid } SiO_2 \text{ and } Na_2O} + 30\%_{\text{water}} \quad (1)$$

$$\text{Geopolymer solids part} = 74\%_{Mk}\ \left(\frac{52\%}{52\%+18\%}\right) + 26\%_{\text{solid } SiO_2 \text{ and } Na_2O} \quad (2)$$

$$\text{45\% quartz in the Mk} = 33\%_{Quartz\ (74\% \times 45\%)} + 67\%_{\text{amorphous phase}} \quad (3)$$

An X-ray tomography study was also performed on a sample of geopolymer having the same formulation (GP14.5), allowing both the quantification of the quartz crystals, and the visualization of their distribution. The image of a cross section presented in Figure 35a highlights the various components. The black circles inside the material were previously identified as occluded air bubbles, the many lighter grey spots having random forms were assigned to the crystalline phase, while the dark grey represents the amorphous part. On the 3D section of the sample presented in Figure 35b, all the dark grey has been removed in order to isolate the crystalline part of the sample so as to be able to quantify it.

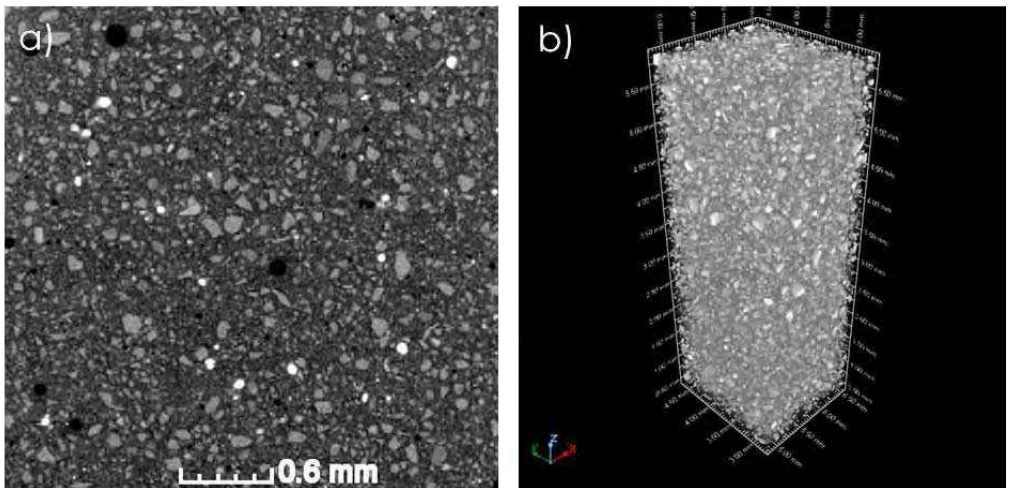

Figure 35. *X-ray tomography visualization of geopolymer paste showing: a) a cross section and b) a 3D section where the "pure" geopolymer has been removed.*

First, this analysis showed a very homogeneous distribution of the crystals through the sample, with sizes ranging from the resolution limit of some µm up to about 600µm. The quantification calculation also revealed that the crystalline phase represented 17% by volume in the sample. Knowing the density of the geopolymer paste (1.34), and given that the majority of the crystalline phase was composed of quartz having a density of 2.65, it was then possible to calculate the mass fraction of this crystalline phase via the calculation below:

$$17\% \frac{2.65}{1.34} = 34\%$$

Thus the methods used to quantify the crystal phase of the geopolymer, each involving different parameters, both led to the conclusion that the mass proportion of impurity in the sample was around 1/3. These results also imply that the impurities were not altered by the geopolymerisation reaction.

2.3 Water in the geopolymer

The results of the previous sections have shown that the water, in the hardened geopolymer, would not be bound in the network in hydrate form as suggested in the schematic representation of Barbosa et al. (2000, Figure 33). Thus, determining the fate of the water in the hardened geopolymer paste is an important aspect of its characterisation. It was therefore decided to study the amount of water that could be removed by drying the specimens at relatively moderate temperature.

To do this, three formulations were chosen, having initial water contents of 30.3%, 33.0% and 37.0%, corresponding to formulations GP14.5, GP17 and GP20, respectively, and the drying temperatures applied were 50°C, 80°C and 105°C. During the preparation of the geopolymer pastes, special attention was paid to the accuracy of the weighing of the raw materials, in order to know the exact amount of each component introduced. Then the preparation was cast in plastic moulds, which were hermetically sealed during the entire curing time of seven days at 20°C. At the end of this period, the samples were demoulded, weighed and then placed in climatic chambers at 50°C, 80°C and 105°C. The mass loss of the geopolymer pastes was then regularly monitored by weighing, until stabilisation was achieved. Knowing the mass of

water initially introduced into the sample, the value of the mass loss, corresponding to the amount of water evaporated, allowed the percentage of water evaporated to be calculated for each drying temperature. For each formulation and each temperature, three identical specimens were followed to obtain the average values of the measurements presented in Table 6.

Table 6. Initial amount of water for three geopolymer formulations and amount of water remaining after stabilisation of the mass loss at three different drying temperatures: 50°C, 80°C and 105°C.

Formulation		GP14.5	GP 17	GP 20
Initial amount of water (mass%)		30.3%	33.0%	37.0%
Final amount of water (mass%) after stabilisation of the mass loss at	$T_{driying}$ = 50°C	7.9%	7.3%	6.9%
	$T_{driying}$ = 80°C	4.5%	4.2%	4.0%
	$T_{driying}$ = 105°C	2.9%	2.9%	2.8%
Relative mass loss of water (%) after stabilisation of the mass loss at	$T_{driying}$ = 50°C	72.6%	77.4%	80.7%
	$T_{driying}$ = 80°C	84.8%	87.1%	89.2%
	$T_{driying}$ = 105°C	90.1%	91.2%	92.3%

It was thus observed that, whatever the initial water content in the geopolymer paste, after drying at 105°C, this content was reduced to about 3% for all the formulations, corresponding to a relative water mass loss of around 90%. It was also observed that the evolution of the relative mass loss of water in GP14.5, GP17 and GP20 tended to an asymptotic value above 105°C (Figure 36), suggesting a slower evolution for the loss of the 10% of remaining water. It would have been interesting to see which drying temperature would lead to the evaporation of all of the water introduced but, according the TGA previously presented, evaporation of the remaining water would be a long process, as traces of water were still measured at 700°C.

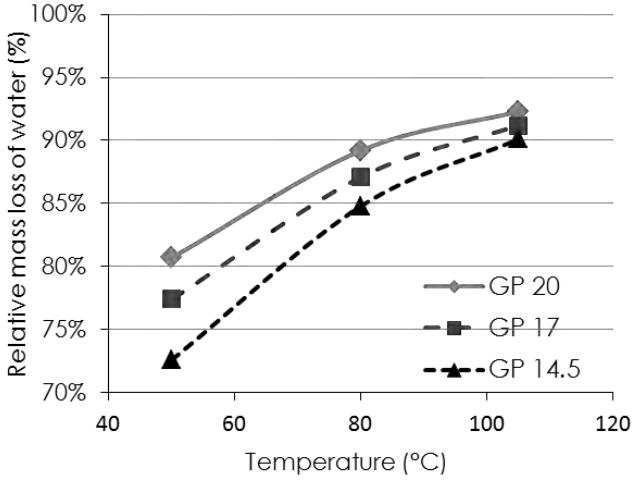

Figure 36. *Evolution of the relative mass loss of water in GP14.5, GP17 and GP20 depending on the drying temperature.*

Several conclusions can be drawn from these results:

- At only 105°C, more than 90% of the water initially introduced had evaporated, resulting in a water content of less than 3% in the geopolymers regardless of the initial water content. This would mean that the water introduced into the geopolymer mixture does not react with the materials to form hydrates as is the case for cement.
- As the water introduced could be removed easily, it is highly probable that it has a crucial effect on the final porosity of the material. Also, it appears that the 50°C drying temperature is not sufficient to evaporate the water from the smaller pores of the GP14.5 formulation compared to GP20, which could indicate a finer porosity of the formulation with the lower initial water content.
- In view of these results, it seems that the schematic illustrations of the geopolymer structure represented by Barbosa (2000: Figure 33), where water is not linked to the structure, are reasonable.

2.4 Total porosity and pore microstructure

It is very important to know the distribution and organization of the porous network in the cement matrix because it is not only linked to the compressive strength of materials but also provides a durability indicator. Thus, obtaining such information for the geopolymer was essential. To do this, X-ray tomography, total porosity accessible to water, mercury intrusion porosimetry (MIP) and porosity by gas absorption, via the BET and BJH theory, were used in this study on geopolymer pastes having different water contents and, in some cases, on cement paste having a w/c ratio of 0.5.

Total porosity

The first observations of the porosity of the geopolymer were made visually and with SEM images, and were attributed to a macroporosity due to the trapping of air bubbles during the sample preparation. This kind of porosity is strongly linked to the method of preparation and the viscosity of the mixture and is thus very variable. However, knowing the proportion of air entrapped during the preparation of a geopolymer paste provides an indicative value.

Thus a GP14.5 geopolymer paste prepared without any shock or vibration was analysed by X-ray tomography to visualize the air occlusions, assess their size distributions and quantify their cumulative volume. A 3D section of the sample of dimensions 2 x 2 x 5 mm was isolated and analysed. Figure 37 a presents this 3D section, showing the overall sample and where the air occlusions are easily identified by their dark coloration. Using this strong contrast between the air and the matrix allowed the software to isolate this volume and to represent it separately. Figure 37 b, which isolates the entrapped air fraction, shows significant numbers of spheres with diameters ranging from 40 µm up to nearly 300 µm. It was calculated that this cumulative volume represents 2% of the sample. The distribution of the sphere sizes is illustrated by different colours: the blue corresponds to diameters lower than 200 µm with decreasing diameters shown in darker shades of blue, while all other colour corresponds to diameters ranging from 200 µm to 300 µm. The spheres seem to have a homogeneous distribution in the sample and have no privileged organization. This representation did not allow us to see whether the macroporosity was interconnected.

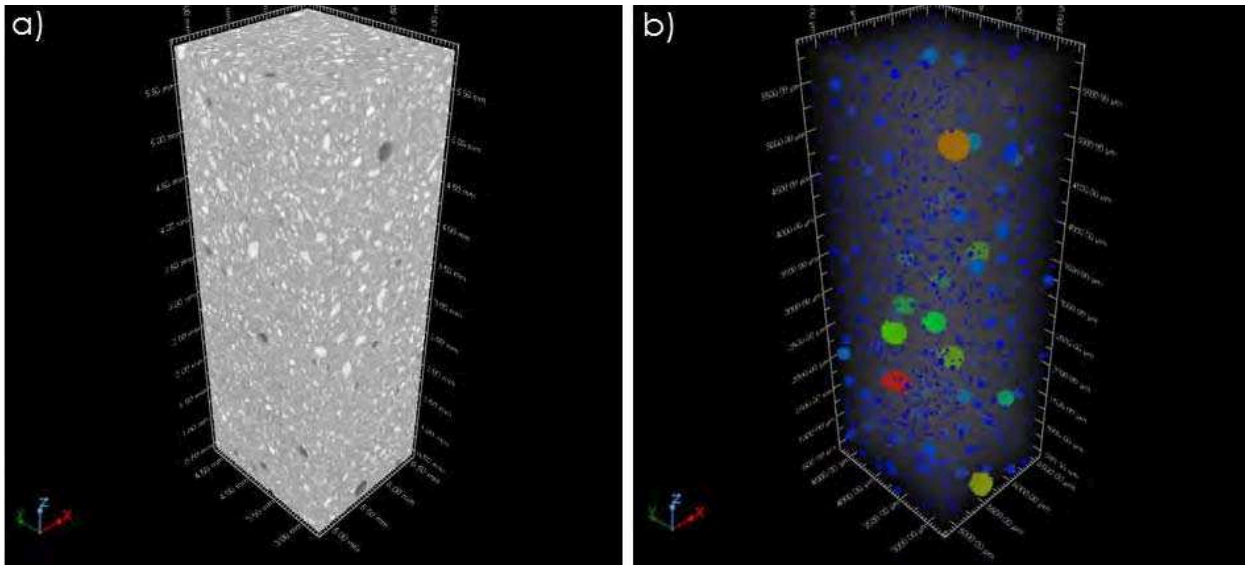

Figure 37. *X-ray tomography visualisation of GP14.5 paste showing: a) 3D section of the sample and b) the same 3D presenting only the air occlusion.*

Total porosity accessible to water (NF P18-459) and mercury intrusion porosimetry (MIP) were performed on three geopolymer formulations and on CEM I 52.5 paste in order to calculate their total pore volumes. Table 7 shows the porosity accessible to water measured using the same three drying temperatures as those used for the study of water. The porosities accessible to water (Φ_w) and the mercury porosity value obtained by MIP (Φ_{Hg}) are given in volume %. Nevertheless, it should be emphasised that the pore volume measured by MIP

underestimates the value of the total porosity (Galle, 2001). The use of mercury limits the range of accessible pores to between 100 µm and around 7 nm (with the apparatus used), all porosities below and above these limits not being detected. In contrast, the water penetration pore access range is much wider and goes down to around 0.5 nm. Thus, subtracting the volume measured by mercury from that measured by water (Φ_w - Φ_{Hg}) at the same drying temperature (50°C in this case) gives the pore volume located outside the MIP pore access limits.

Table 7. Total porosities measured by water intrusion (Φ_w) and by MIP (Φ_{Hg}) measurement.

	GP14.5	GP17	GP 20	CEM I 52.5 (w/c = 0.5)
Φ_w (%) $T_{driying}$ = 50°C	41.1%	45.9%	49.8%	35.7%
Φ_w (%) $T_{driying}$ = 80°C	46.6%	50.9%	54.4%	40.6%
Φ_w (%) $T_{driying}$ = 105°C	49.0%	53.0%	56.4%	43.5%
Φ_{Hg} (%) [7nm-100µm]	28.5%	35.5%	39.6%	27.4%*
$\Phi_{w\ at\ 50°C}$ -Φ_{Hg} (%)	12.6%	10.4%	10.2%	8.3%

* Data from Galle, 2001: CEMI, w/c = 0.5, Oven-drying 60°C.

The water porosity data obtained show that the total porosity of the geopolymers is always higher than for CEM I paste for a given drying temperature. It was logically observed that, the higher the drying temperature, the higher the porosity obtained. Moreover, it appears that the amount of water in the geopolymer formulation has a significant impact on the total porosity, since increasing the initial quantity of water leads to an increase of the porous network volume.

Given that the same formulations and the same drying temperatures were used for the measurement of the total porosity and the amount of water evaporated (previous section), it was possible to compare these results. A graph of these measured data (Figure 31), showing the total volume measured by water intrusion versus the volume of water evaporation for the same formulation at the same drying temperature, shows a clear correlation. This linearity would imply that the total pore volume that was measured would correspond to the amount of water introduced into the material. These results thus suggest that the total pore volume may be determined as soon as the amount of water introduced is known.

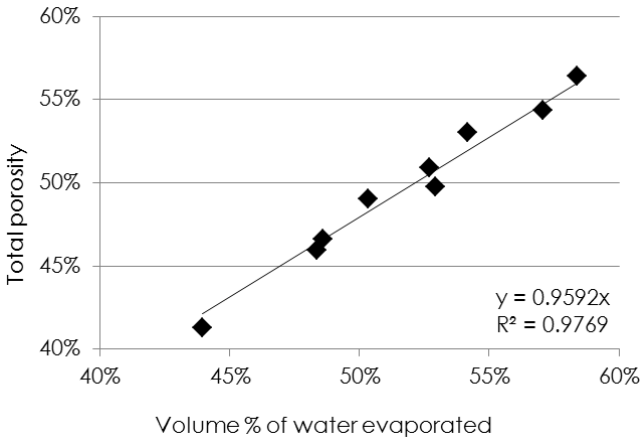

Figure 38. *Total porosity accessible to water versus volume of evaporated water for GP14.5, GP17 and GP20 for a given drying temperature.*

Regarding the value of the total pore volume of the geopolymer, and based on the results of the previous section, which showed that the most suitable drying temperature was 105°C, it can be concluded that the total porosity was 49.0%, 53.0% and 56.4% for GP14.5, GP17 and GP20 respectively. These values are in agreement with the values found in the literature for similar formulations (Boher, 2014). The results for porosities calculated by MIP presented in Table 7 indicate that 10% to 12% of the total pore volume of the geopolymers, against only 8% for a cement paste (Galle, 2001), had pore access diameters lower than 7nm or higher than 100 µm.

Pore microstructure

It is essential to know the cement-based material microstructure or pore size distribution if the transport mechanisms, such as diffusion or convection, are to be studied and modelled. Obtaining such information for the geopolymer, and comparing it to that for OPC, is therefore essential for their characterization.

MIP analysis performed on GP14.5 and CEM I 52.5 has shown, by the relative mercury volume introduced versus the pore access diameter presented in Figure 39 a, a great difference in the pore structure between these two materials. For the geopolymer, it was calculated that 95% of the mercury was introduced for pore diameters of 7 to 20 nm (with 83% between 10 and 20 nm), which shows a homogeneous distribution of the pore access diameter, unlike cement where 73% of the mercury was introduced in pores between 20 and 80 nm, and 21% between 7 and 20 nm. Thus, when the curve of the relative pore volume versus diameter is observed (Figure 39 b), the geopolymer has a single population of pore access centred on 15

nm diameter. These results reveal the monomodal nature of the porous network of the geopolymer, as previously observed in the literature (Rovnaník 2010, Boher 2014), while the cement shows two populations, one fine and one coarser, centred respectively on 8 and 50 nm and showing a bimodal network.

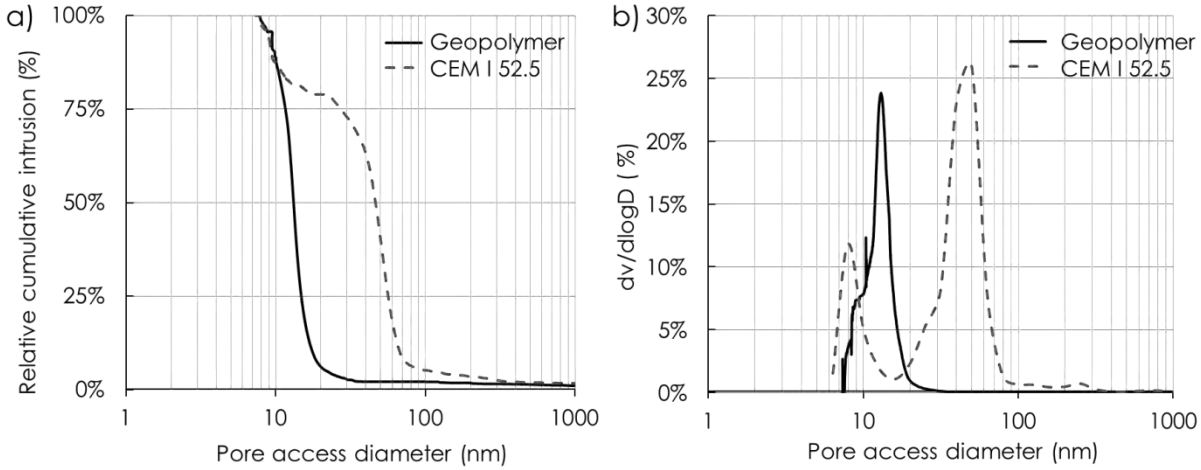

Figure 39. *Comparison of MIP cumulative intrusion (a) and pore size distribution (b) of geopolymer GP 14.5 and a CEMI cement paste.*

The literature reports (Galle, 2001) that CEM I paste pore size distributions are generally characterised by three main classes of pore access. Pore accesses located near 100 nm and above are usually associated with capillary porosity (macroporosity). A second and a third class of pore access are generally detected in the regions located around 20 nm (microporosity) and around a few nanometres (nanoporosity). This pore space domain describes the pore accesses of C-S-H and the occurrences of such pore accesses depend on the w/c ratio and on the material age and curing conditions. Comparison with the geopolymer is not obvious, partly because of their different compositions, but it seems probable that the geopolymer has one class of pore access around 15 nm, corresponding to mesoporosity formed by the volume occupied by the water during hardening, and one class of macroposity created by air occlusion (not visible by MIP).

A study of nitrogen adsorption–desorption isotherms made on the geopolymer GP14.5 provided additional information. The adsorption and desorption isotherms of Figure 40a show a distinct hysteresis loop from 0.8 to 1.0 of relative partial pressure (P/P_0). The passage of the desorption curve below the absorption curve (until P/P_0 of 0.75) was associated with degassing problems during the analysis (degassing temperature of 100°C). Nevertheless, the closeness of the hysteresis loop at $P/P_0 > 0.40$ and a type IV sorption behaviour with a

hysteresis loop of type 1 on a loop of type 2, which have already been identified on metakaolin geopolymer samples by Steins et al. (2013), indicate the absence of micropores and the formation of a well-defined mesoporous texture having interconnected pores with narrow necks and wide voids, called 'ink-bottle pores'. The BJH pore-size distribution (Figure 40b) confirms the monomodal nature of the porous network centred on 15 nm.

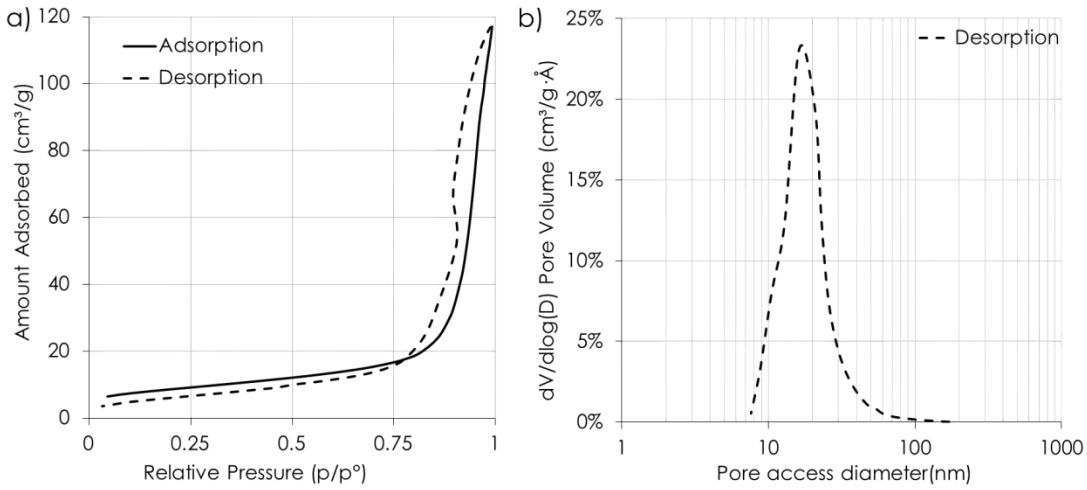

Figure 40. *a) Nitrogen adsorption–desorption isotherms and b) BJH pore-size distribution for the GP14.5 geopolymer paste.*

To visualise the impact of the amount of water initially introduced in the geopolymer on the formation of the porous network, MIP analyses of GP14.5, GP17 and GP20 (having initial water contents of 30%, 33% and 37% respectively), were performed under the same conditions. First, it was observed that all three formulations led to monomodal porous networks (Figure 41). The cumulative pore volume representation confirmed the increase in total volume measured when the initial water amount increased (Figure 41a), and its derivative revealed that the pore access diameter also increased. The median pore access diameter therefore increased from 13 nm for GP14.5 to 29 nm for GP17 and, finally, 36 nm for GP20. When the median diameter increased, the spread of the value also increased, as shown by the width of the base of the peaks for GP17 and GP20 (Figure 41 b). As an indication, 90% of the mercury was introduced between 7 and 18 nm for GP14.5, between 11and 35 nm for GP17 and between 16 and 42 nm for GP20.

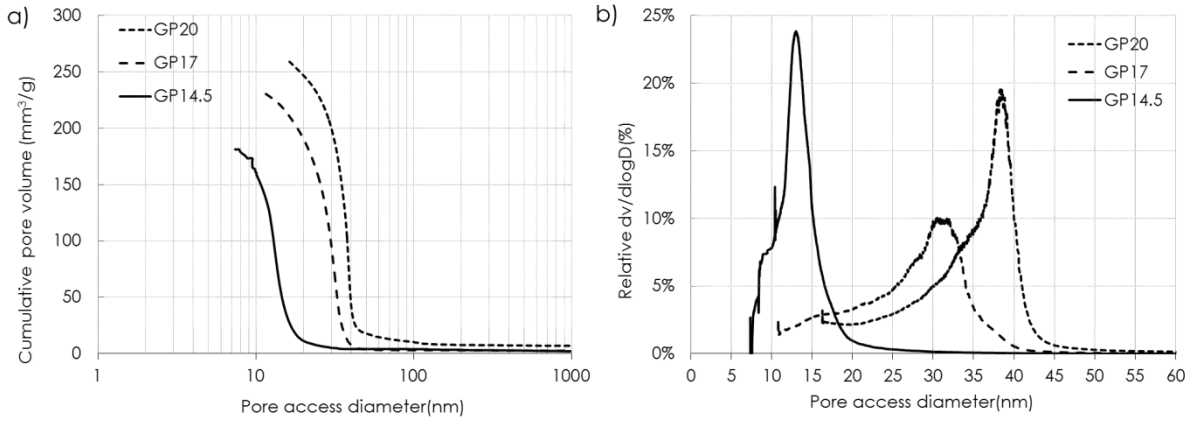

Figure 41. *Relative mercury volume introduced and relative pore volume versus pore access diameter for geopolymer pastes GP 14.5, GP 17 and GP 20.*

Exploitation of the mercury intrusion/extrusion curve is controversial because the forced intrusion of mercury into the porous network was very probably responsible for irreversible damage of the networks, resulting in an extrusion that was not representative of the initial organization of the porous system (Moro et al 2002). However, the use of this curve to compare two materials, in this case the geopolymer and cement paste, may be useful. Figure 42, which shows the volume of mercury introduced and removed depending on the pressure applied to the mercury for the cement and GP14.5 geopolymer samples, highlights incomplete hysteresis. This phenomenon can be attributed to ink-bottle-shaped pores (Moro et al., 2002), as previously observed by gas absorption. In pores of this type, intrusion cannot occur until sufficient pressure has been attained to force mercury into the smaller access pores. However, upon depressurization, the wide pore volume cannot empty until a lower pressure is reached, leaving mercury entrapped. And, as more mercury could be removed from the geopolymer (about 50%) than from cement (about 40%), this could mean that the porous network of geopolymer is probably more interconnected than that of the CEM I.

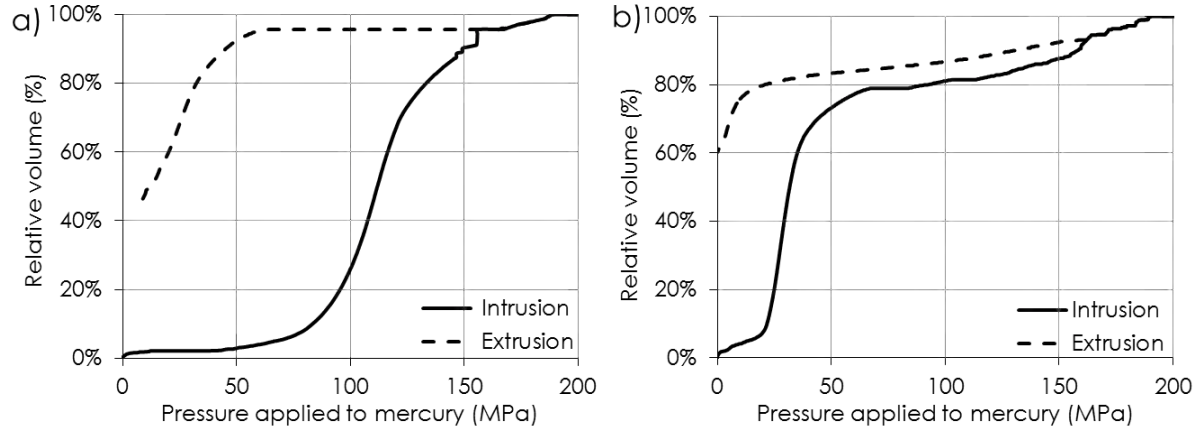

Figure 42. *Relative mercury volume depending on the pressure applied to mercury for the geopolymer GP 14.5 (a) and a CEMI cement paste (b).*

3. Stability of the geopolymer paste

No visible damage was observed over time on the surface of geopolymer stored at 20°C and 95% R.H. X-ray characterisation performed at 7, 90, 350 and 500 days indicated stability during this period, as illustrated on Figure 43, where the four patterns show no change in the amorphous or crystalline structure of geopolymer stored for 16 months at 95% R.H. This demonstrates that the structure formed during the first week was not altered or modified, at least in this curing condition.

Moreover, it was noted that crystalline phases associated with zeolite as reported in metakaolin-based geopolymer cured at high temperature by Duxson et al., (2007a), were not produced in the present study.

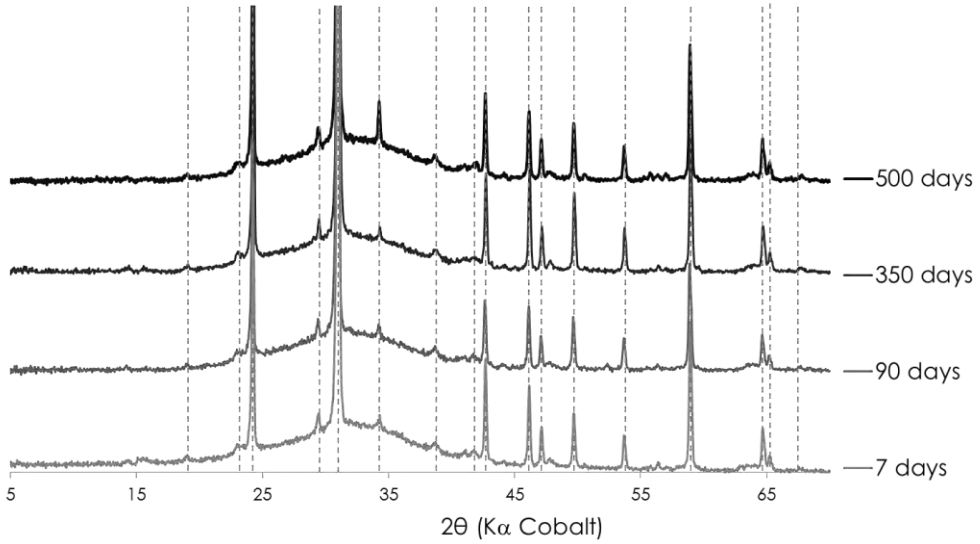

Figure 43. *XRD pattern of geopolymer paste GP14.5 cured 7, 90, 350 and 500 days at 20°C and 95% R.H.*

Similarly, the chemical characterization by microprobe also revealed the stability of the materials over time. The same analysis as the one presented previously (V.2.1) at seven days was performed on a GP14.5 paste maintained without external exchanges for 2 years. The same two parts, one taken in the centre and the other near the surface of the sample, were also quantified and led to the same composition as previously observed. The oxide mass contents measured were the same as those obtained for 7 days, to within 1%, and led to molar ratios of 4.3 for SiO_2/Al_2O_3 and 0.9 for Na_2O/Al_2O_3. The ternary diagrams by mass presented on Figure 44 highlight these similar formulations.

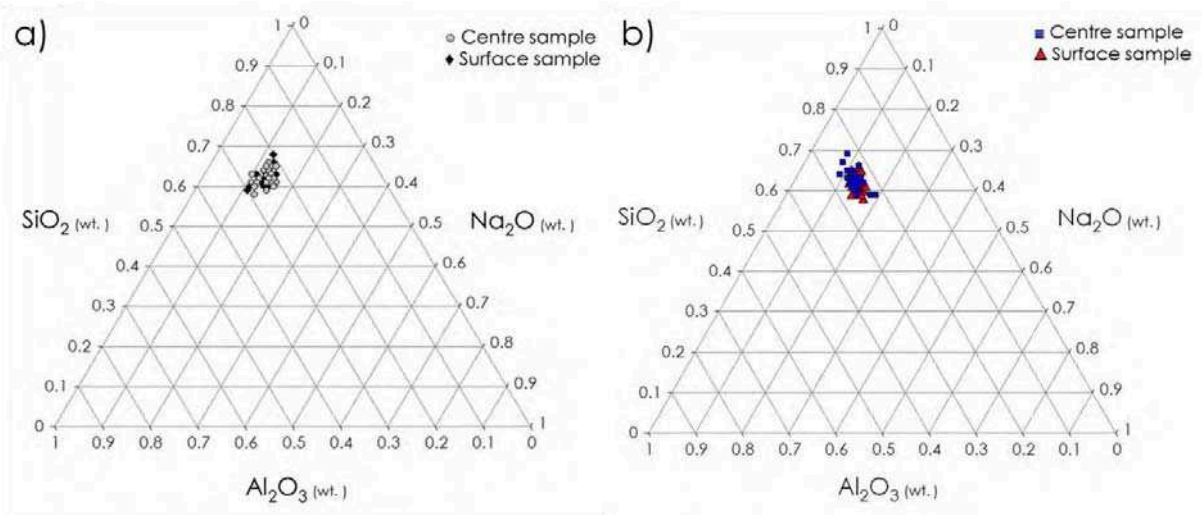

Figure 44. *Ternary diagram by mass of SiO_2, Al_2O_3 and Na_2O measured by electron microprobe on GP14.5 at a) 7 days and b) 2years (91 measurements each).*

However, regarding the stability of geopolymer, drying shrinkage was noted, which led to very large surface cracking when the specimen was exposed to a dry atmosphere, below 60% R.H., during the first few days of curing (<7 days). The pictures presented in Figure 45 show the visual aspect of 4 x 4 x 16 cm geopolymer specimens for two formulations at 48h (GP14.5 and GP17 paste and mortar) put in 50% R.H. conditions 24h after casting.

It would seem that too dry an atmosphere during the geopolymerisation (first three days) leads to excessive evaporation of water resulting in significant damage to the structure for both formulations, but it also appeared that the incorporation of aggregates minimised this phenomenon.

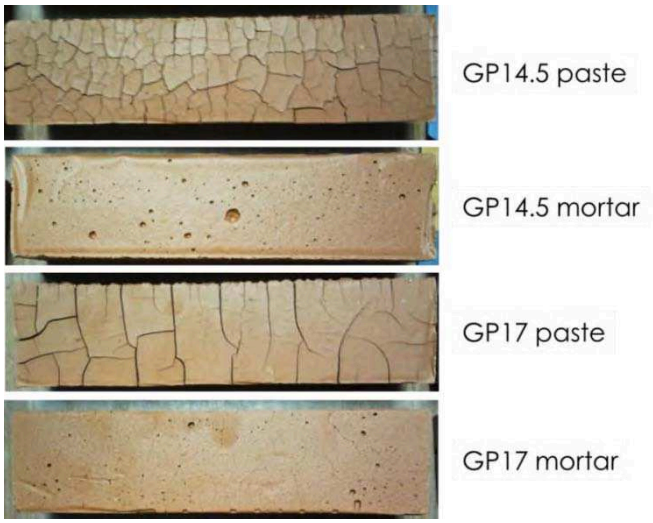

Figure 45. *Surface cracking observed on 4x4x16 geopolymer samples for GP14.5 paste and mortar and GP17 paste and mortar.*

These formulations were used for measurements of endogenous and drying shrinkage. The relative shrinkage and mass loss depending on the formulation or on the sand addition are presented on Figure 46. Exposure of geopolymer pastes to 50% R.H. 24h after casting led to very significant drying shrinkage, of 1.7% for GP14.5 and to 2.7% for GP17, in 7 days (corresponding to mass losses of 10% and 15%). After a week, the damage was judged too serious and the shrinkage measurement was not pursued. Inversely, specimens kept without external exchanges showed a variation lower than 0.01% after 28 days. The most marked endogenous shrinkage was measured for the optimal formulation GP14.5 and was 0.08% at 28 days, but the addition of sand seems to have greatly minimized this phenomenon as GP14.5 mortar experienced shrinkage of only 0.02% during the same period (Figure 46b).

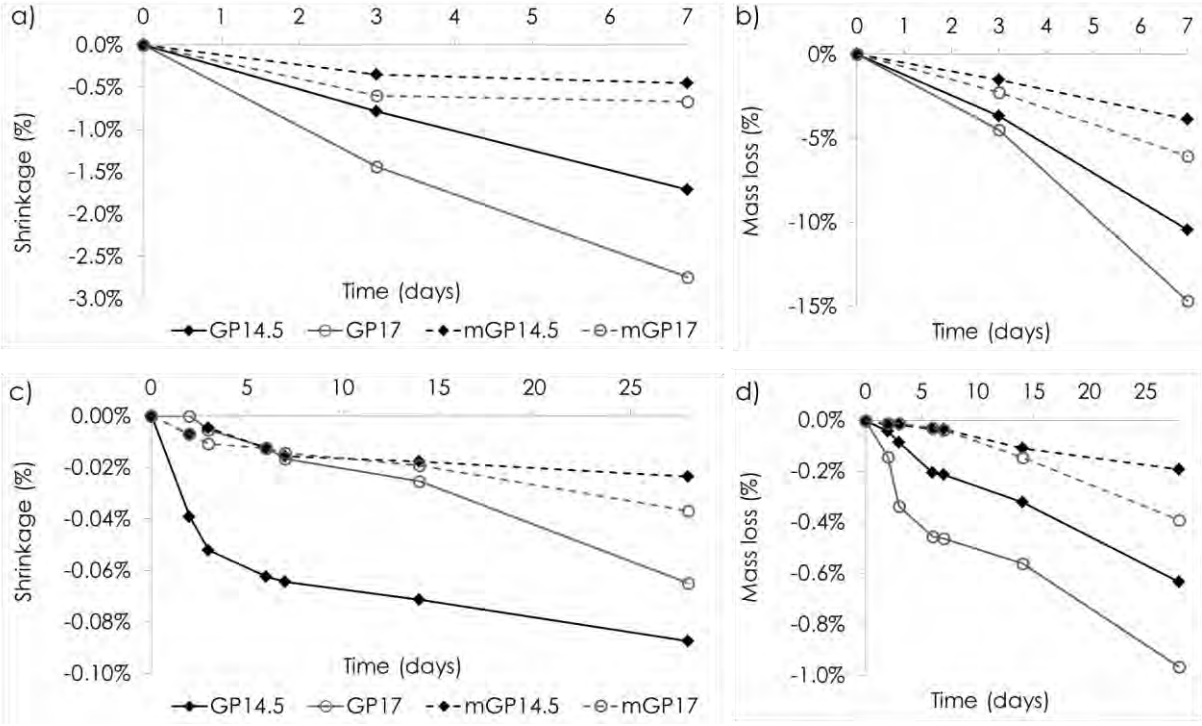

Figure 46. *a) Drying shrinkage (b) the corresponding mass loss), and c) endogenous shrinkage (d) corresponding mass loss) for the geopolymer pastes (GP14.5, GP17) and mortars (mGP14.5, mGP17).*

In short

Geopolymer morphology	Two phases: - Amorphous geopolymer - Crystalline impurities
Reactivity	Major part of the metakaolin reacted in 7 days
Chemical composition	Consistent with the formulation calculated Except for the silica difficult to analyze without quartz.
Free water	90% of the water introduced are removed at 105°C
Total porosity	2% of entrapped air bubbles 49% to 56% accessible by water 10% to 12% non accessible by Hg
Pore microstructure	Monomodal network Centered on 15nm to 36nm Presence of ink-bottle-shaped pores
Crystalline impurities	1/3 of impurities mainly quartz Impurities not altered by the reaction
Stability	Stable in moist environment Surface cracking on GP pastes cured less than 3 days in 95% R.H.

This second study provided valuable information on the four main phases of geopolymer paste, namely the amorphous part corresponding to the "pure" geopolymer, the crystalline part corresponding to impurity from the metakaolin, the water introduced, and, the porosity. Such knowledge on the geopolymer paste and its comparison with that for a cement paste will be an essential database for future studies, both for concrete applications and for durability studies.

VI. Conclusion

The performance-based study of the flexural and compressive strengths has highlighted the viability of metakaolin-based geopolymer as a binder for mortar. The importance of the formulation, widely detailed in the literature, has been verified and has led to an optimal formulation regarding the compressive strength. It corresponds to the following molar ratios: SiO_2/Al_2O_3 of 3.6, Na_2O/Al_2O_3 of 0.9 and H_2O/Na_2O of 14.5.

The reaction of geopolymerisation, known to be clearly different from cement hydration, showed faster hardening kinetics at early age than OPC, which allowed the curing time to be reduced to 7 days instead of the 28 days generally used for construction materials. It is also concluded that it is preferable to use a waterglass solution, which does not need addition of soda, and a high humidity atmosphere during the early days. Finally, the incorporation of sand in the geopolymer did not have a significant impact on the strength but proved useful to limit the surface cracking due to drying shrinkage.

It is concluded that the geopolymer binder can be compared to a CEM I 52.5 regarding the compressive strength, but has a higher flexural strength. The French standard EN 196-1 has been validated for the preparation of geopolymer mortars if the mixing water is replaced with the activating solution and the specimens are kept in a humid environment but not under water.

The study, focusing on physical, chemical and morphological characterisations of the geopolymer, allowed geopolymers and cement paste to be compared at equivalent strengths.

Morphological observations showed the presence of an amorphous phase corresponding to the "pure" geopolymer, and a crystalline phase corresponding to the impurities from the metakaolin. The amorphous phase was characterised as a unique structure having weakly bound water, unlike cement which is known to have various hydrates incorporating different water contents. The chemical composition of the geopolymer appeared to contain an excess of silica relative to the amount theoretically introduced, probably due to the large amount of nanoscale quartz particles, which were very probably analysed at the same time.

Studying the reactivity of the geopolymer reaction showed that the majority of the metakaolin reacted with the activating solution in a less exothermic reaction than cement hydration in seven days. The analysis of the crystal phase showed that the geopolymer had 1/3 by weight of impurity, provided exclusively by the metakaolin. The quantification of this phase also concluded that impurities were not altered or dissolved during the geopolymerisation.

Special attention was paid to the study of the porous network, which is known to be an essential characteristic of hydraulic binders, as an indicator of both strength and durability. It was concluded that the total pore volume of the geopolymer was higher than that of OPC, with a large difference in the organisation of the network. The geopolymers therefore predominantly presented a mesoporosity having a monomodal distribution of the pore access centred between 15 nm and 36 nm, depending on the water content. It was also determined that the GP14.5 formulation had 2% by volume of air bubbles.

Finally, the high stability of geopolymer over time was highlighted in terms of composition and structure, but with a cure condition involving a humid atmosphere during the first 7 days of curing. Over-dry curing conditions, e.g. 50% R.H., led to very high drying shrinkage resulting in harmful surface cracking. This phenomenon was, however, minimised by the addition of sand to the geopolymer.

In conclusion, the data obtained from these two studies were found to be consistent with the literature on the subject. Although they have shown a real potential for the use of geopolymer as a binder, fundamental differences with the cement matrix makes both comparisons and the application of the existing standards difficult. Thus the fabrication of geopolymer concretes will be a necessary step to provide better visibility of the possible industrial applications, and to allow durability testing, especially regarding the large amount of alkalis present in the geopolymer.

References

Barbosa, V.F.F., MacKenzie, K.J.D. and Thaumaturgo, C. (2000) Synthesis and characterisation of materials based on inorganic polymers of alumina and silica: sodium polysialate polymers. *International Journal of Inorganic Materials*, 2(4): 309-317.

Boher C. (2012). *Etude expérimentale et modélisation de la diffusion gazeuse à travers des milieux poreux partiellement saturés en eau. Application aux Verres Vycor, géopolymères et pâtes de ciment CEM V*. Université de Toulouse, Toulouse 340 (PhD (in French)).

Boher, C., Martin, I., Lorente, S., Frizon, F. (2014) Experimental investigation of gas diffusion through monomodal materials. Application to geopolymers and Vycor® glasses, *Microporous and Mesoporous Materials*, 184:28-36.

Davidovits, J. Solid-Phase Synthesis of a Mineral Blockpolymer by Low Temperature Polycondensation of Alumino-Silicate Polymers, *IUPAC Symposium on Long-Term Properties of Polymers and Polymeric Materials, Stockholm*, vol. Topic III, 1976.

Davidovits, J. PROPERTIES OF GEOPOLYMER CEMENTS, *Proceedings First International Conference on Alkaline Cements*, pp. 131-149, 1994.

Duxson P., Provis, J. L., Lukey, G. C., Mallicoat, S. W., Waltraud, M., Kriven, W., Van Deventer, J.S.J. (2005) Understanding the relationship between geopolymer composition, microstructure and mechanical properties, *Colloids and Surfaces A: Physicochemical and Engineering Aspects*, 269(1–3): 47-58 DOI: 10.1016/j.colsurfa.2005.06.060.

Duxson, P., Fernández-Jiménez, A., Provis, J. L., Lukey, G. C., Palomo, A., Deventer, J. S. J., (2007a) Geopolymer technology: the current state of the art. *Journal of Materials Science*, 42(9): 2917-2933.

Duxson P., Mallicoat, S. W., Lukey, J. L., Kriven, W., Van Deventer, J.S.J. (2007b), The effect of alkali and Si/Al ratio on the development of mechanical properties of metakaolin-based geopolymers. *Colloids and Surfaces A: Physicochemical and Engineering Aspects*. 292(1): 8-20.

Fernández-Jiménez, A., Palomo A., Criado M. (2005) Microstructure development of alkali-activated fly ash cement: a descriptive model. *Cement and Concrete Research*, 35, 1204–1209 .

Gallé, C. (2001) Effect of drying on cement-based materials pore structure as identified by mercury intrusion porosimetry: A comparative study between oven-, vacuum-, and freeze-drying, *Cement and Concrete Research*, 31(10):1467-1477. DOI: 10.1016/S0008-8846(01)00594-4.

Glukhovsky VD (1959) Soil silicates. Gosstroyizdat, Kiev,154pp

Kamalloo, A., Ganjkhanlou, Y., Aboutalebi, S. H., and Nouranian H. (2010) Modeling of compressive strength of metakaolin based geopolymers by the use of artificial neural network. *International Journal of Engineering,* 23(2):145-152.

Le Bail, A., (1995) Modelling the silica glass structure by the Rietveld method. *Journal of Non-Crystalline Solids* 183(1–2), 39-42.

Lothenbach, B., Scrivener, K., Hooton, R.D. (2011) Supplementary cementitious materials. *Cement and Concrete Research*, 41(12): 1244-1256.

Lutterotti, L., Ceccato, R., Dal Maschio, R., Pagani, E. (1998) Quantitative analysis of silicate glass in ceramic materials by the Rietveld method. *Materials Science Forum* 278–281, 87–92

Lutterotti, L., Matthies, S., Wenk, H.-R. (1999) MAUD: a friendly Java program for material analysis using diffraction. *IUCr: Newsletter of the CPD* 21, 14–15.

Mahieux, P.-Y., Aubert, J.-E., Cyr, M., Coutand, M., Husson, B. (2010) Quantitative mineralogical composition of complex mineral wastes – Contribution of the Rietveld method, *Waste Management*, 30(3):378-388. DOI:10.1016/j.wasman.2009.10.023.

MAUD Program. Available from: <http://www.ing.unitn.it/~maud/> (Consulted the 17.04.2012).

Moro, F., Böhni, H. (2002) Ink-Bottle Effect in Mercury Intrusion Porosimetry of Cement-Based Materials, *Journal of Colloid and Interface Science*, 246(1):135-149. DOI:10.1006/jcis.2001.7962.

Provis, J. L., and Van Deventer, J. S. J. (2009), Geopolymers: Structures, Processing, Properties and Industrial Applications, *Woodhead Publishing Limited*.

Rovnaník, P. (2010) Effect of curing temperature on the development of hard structure of metakaolin-based geopolymer, *Construction and Building Materials*, 24(7): 1176-1183. DOI:10.1016/j.conbuildmat.2009.12.023.

Rowles, M., et O'Connor, B. (2003) Chemical optimisation of the compressive strength of aluminosilicate geopolymers synthesised by sodium silicate activation of metakaolinite. *Journal of Materials Chemistry* 13(5): 1161-1165. DOI:10.1039/b212629j.

San Nicolas, R., (2011) Performance-based Approach for Concrete Containing Metakaolin Obtained by Flash Calcination. Université de Toulouse, Toulouse 340 (PhD (in French)).

San Nicolas, R., Cyr, M., Escadeillas G. (2013) Characteristics and applications of flash metakaolins, *Applied Clay Science*, 83–84: 253-262. DOI: 10.1016/j.clay.2013.08.036.

Shi, C., Krivenko, P. v. and Roy, D. M. (2006) *Alkali-Activated Cements and Concretes*, Abingdon, UK, Taylor and Francis.

Steins, P., Poulesquen, A., Frizon, F., Diat, O., Jestin, J., Causse, J., Lambertina, D., Rossignol, S. (2013) Effect of aging and alkali activator on the porous structure of a geopolymer, *Journal of Applied Crystallography*, 47:316-324.

UNSTATS, 2010. Greenhouse Gas Emissions by Sector (Absolute Values). United Nations Statistical Division, New York.

Van Deventer, J.S.J., Provis, J.L., Duxson, P., Lukey, G.C. (2007) Reaction mechanisms in the geopolymeric conversion of inorganic waste to useful products, *Journal of Hazardous Materials*, 139 (3): 506-513. DOI: 10.1016/j.jhazmat.2006.02.044.

Xu Hua, Van Deventer, J.S.J. (2000) The geopolymerisation of alumino-silicate minerals, *International Journal of Mineral Processing*, 59(3): 247-266. DOI: 10.1016/S0301-7516(99)00074-5.

Chapter II.

Metakaolin-based geopolymer concretes:

From fluid to dry concretes

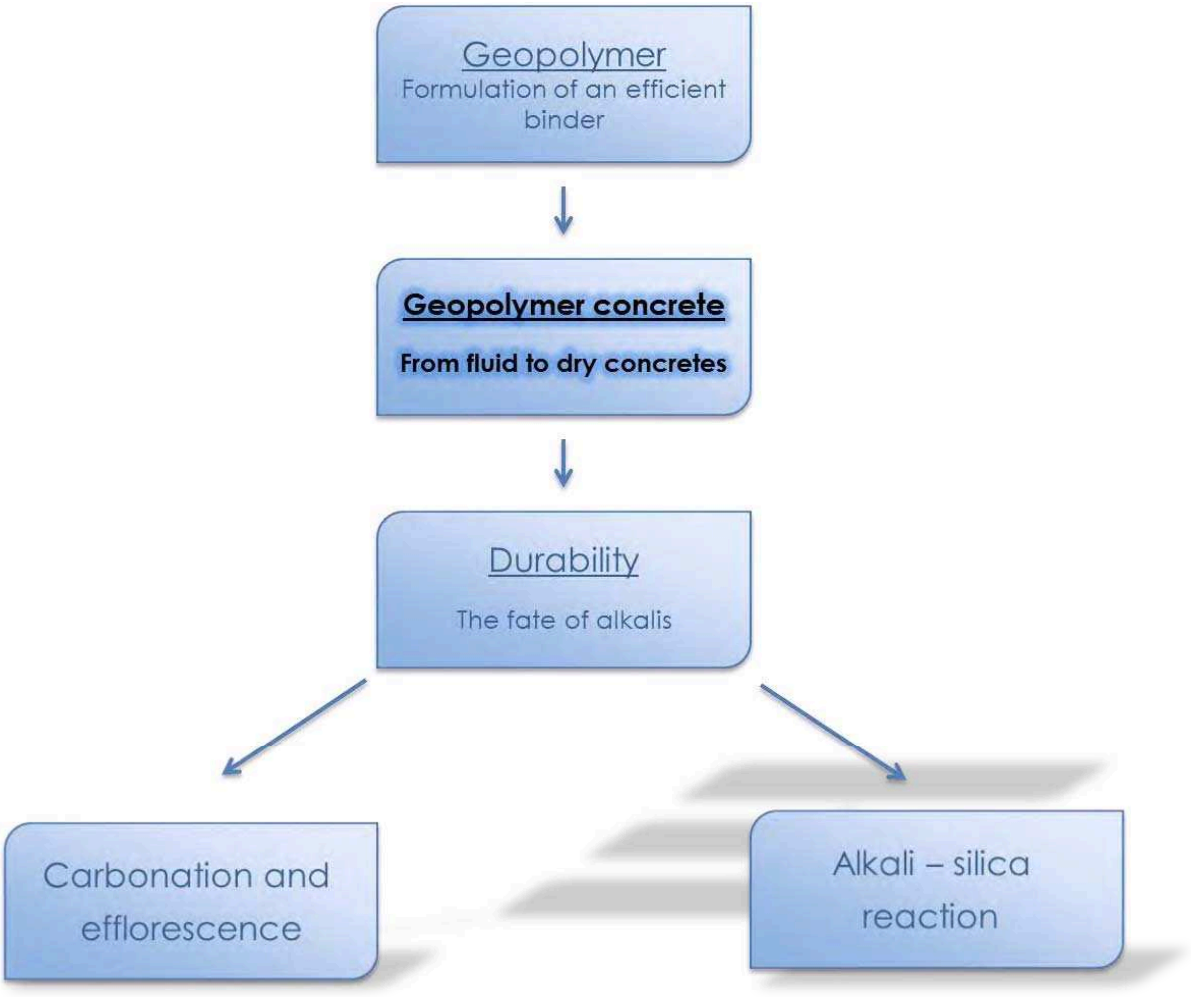

Table of contents

I. Introduction

This chapter is the direct continuation of the study conducted in the first part of this thesis, as it still focuses on the use of the metakaolin-based geopolymer as a binder, but at the scale of the concrete. The number of articles regarding geopolymer concrete is increasing and there is much evidence that large-scale constructions, as well as an industrialisation of alkali-activated materials, are possible. The purpose of this chapter is first to see what performance levels and workability could be obtained with a metakaolin-based geopolymer binder, compared to standard OPC and, in a second step, to demonstrate that the applications related to these standards are achievable.

Three formulations used previously, GP14.5, GP17 and GP20, were first chosen in order to study the density, porosity, workability and compressive strength of geopolymer concretes. The results allow us to classify the geopolymer binder with reference to standard OPC, and so to envisage possible applications of this binder. In a second step, two applications requiring opposite consistency classes were tested: fluid for making reinforced structures and dry to manufacture masonry units in a precast plant. The aim of such tests was to see if the OPC consistency classes could be applied to geopolymers and also to visualise potential scale effects.

All the results obtained, which are a first step towards industrialisation of metakaolin-based geopolymer, were needed to allow discussion of the possibilities provided by this new binder, and make recommendations for future research directions by pointing out the most appropriate applications and also some durability issues.

II. Geopolymer as a binder in civil engineering: past, present and future

The study of geopolymer in current international research is booming, particularly since the year 2010, as can be seen on the histogram of Figure 1, which indicates the number of publications per year found via the web site Sciendirect.com after searching the term "geopolymer" in the titles, abstracts and keywords. When the search was restricted to "geopolymer" and "concrete", the number of documents found was significantly lower but still growing.

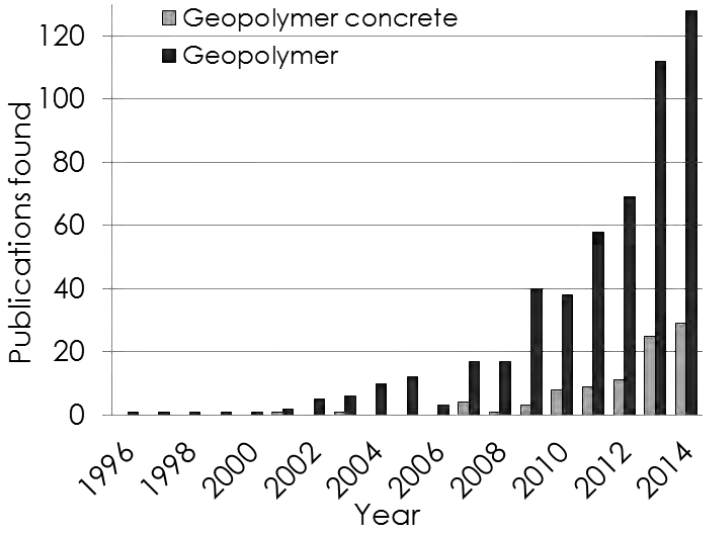

***Figure 1**. Histogram showing the number of publications per year found via the web site Sciendirect.com searching the term "geopolymer" and "geopolymer + concrete" in titles, abstracts and keywords*

Historically, the use of alkali-activated materials in the field of civil engineering dates back to the 1950s in the former USSR, where Professor Glukhovsky (Palomo et al, 2014) developed a slag and alkali waste based alternative cement to mitigate the Portland cement shortage that affected the country. Those buildings are still in place after nearly 50 years and have not encountered any significant durability problems, as can be seen in the pictures presented in Figure 2.

***Figure 2**. (a) The first residential building made of alkali-activated cement concrete without any OPC, Lipetsk, USSR, 1987–1989 (b) One of two 9-storey residential buildings, Mariupol, Ukraine, 1960 (Palomo et al, 2014).*

In the 1980s, Lone Star Industries Inc. commercialised the cement Pyrament®, a mixture of geopolymer and Portland cement that was used, among other things, to pave US military facilities. Then the Zeobond company developed the cement Ecrete® in the 2000s, based on industrial by-products such as fly ash and slag and, more recently, Bana UK Ltd began to market BanahCem®, presented as a geopolymer binder sold in two parts: a powder and a liquid solution. In 2013, the world's first public building with structural "geopolymer concrete" was built in Australia: the University of Queensland's Global Change Institute (GCI), pictures of which are presented on Figure 3. And, in November 2014, the first airport made with more than 30,000 cubic metres of a low carbon, cement-free geopolymer concrete (Wagners' Earth Friendly Concrete (EFC)) opened. The use of "geopolymer" avoided more than 6,600 tonnes of carbon emissions during the construction of the airport, which makes it the greenest airport in the world (www.geopolymer.org).

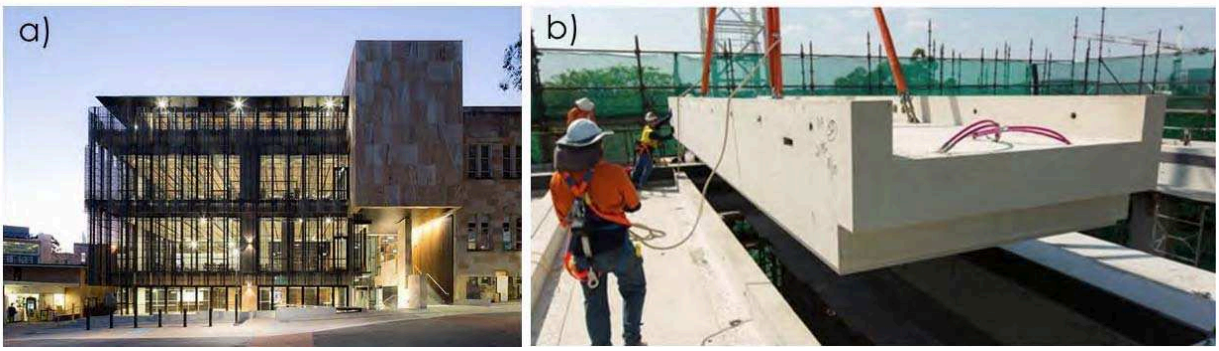

***Figure 3**. (a) Queensland University's GCI building (b) One of the 33 precast slag/fly-ash-based geopolymer concrete floor parts (www.geopolymer.org)*

The example of real constructions made with alkali-activated materials (only calcium-containing raw materials such as slags have been used) cited above shows the interest and the viability of this OPC-free binder. Nevertheless, many question remain - mainly in connection with the standardisation of these concretes and their durability, or the actual environmental impact related to their production.

Regarding standardisation, authors like Van Deventer et al. (2014) focused their studies on the conditions and test parameters needed to identify key parameters for the standardisation of these concretes. Also, a 5-year RILEM Technical Committee, 247-DTA (Durability testing of alkali-activated materials), chaired by Professor John L. Provis, was set up in 2012. The working groups are expected to deliver a set of recommendations based on round-robin tests of standardised alkali-activated material mix designs according to specific durability testing protocols.

Regarding the environmental impact, geopolymers are presented by many authors as a solution for "green" concrete regarding the raw materials used (Duxon et al, 2007b; Johnson and Gourley, 2005; Sakulich, 2011) and are sold as such by the industrials cited above. The most commonly used material in construction is concrete made with Ordinary Portland Cement (OPC), which, by its production, is the source of at least 5-7% of global CO_2 emissions (UNSTATS, 2010) and could reach nearly 10% of total CO_2 emissions in the near future (Capros et al., 2001). So geopolymer, or alkali-activated binder, which does not require any OPC to achieve the same performance, would be an interesting alternative to OPC construction. However, the environmental evaluation of geopolymer based concrete production using a Life Cycle Assessment method, e.g. that of Habert et al. (2011), while confirming this, also shows that the production of geopolymer concrete has a higher environmental impact regarding impact categories other than global warming, especially "fresh water ecotoxicity" and "marine ecotoxicity" as can be seen on Figure 4. According to these authors, this is due to the heavy effects of the production of the sodium silicate solution. As geopolymer concrete made from fly ashes or granulated blast furnace slags requires less of the sodium silicate solution to be activated, it has a lower environmental impact than geopolymer concrete made from pure metakaolin.

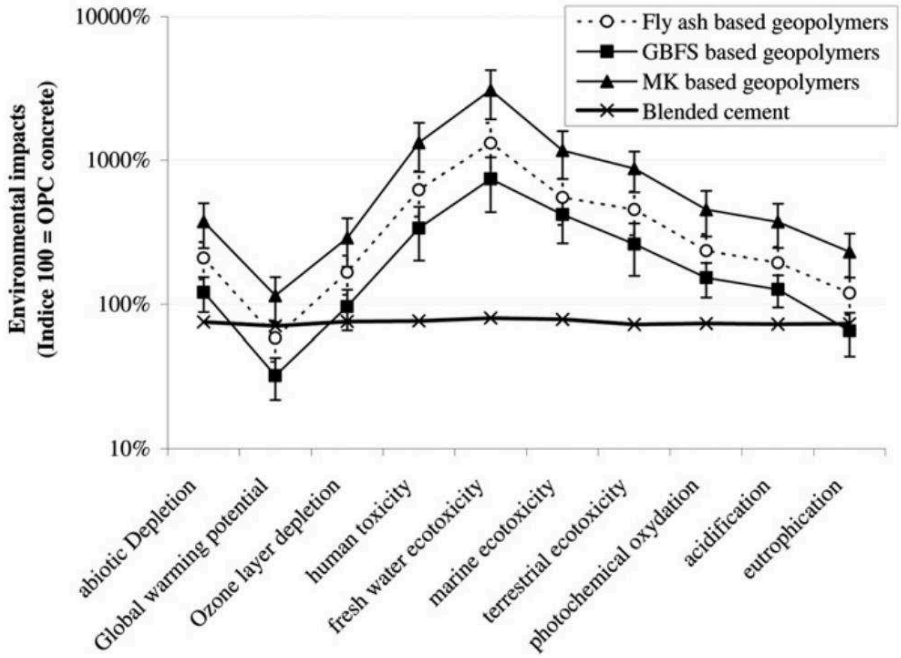

Figure 4. *Eco-profile of different type of geopolymer concrete compared to OPC based concretes (Habert et al., 2011).*

Other authors (McLellan et al., 2011) have examined the lifecycle cost and carbon impacts of OPC and geopolymers in the context of only one country (Australia). Their results show that there is a wide variation in the calculated financial and environmental "cost" of geopolymers, which can be beneficial or detrimental depending on the source location, the energy source and the mode of transport. These studies highlight the future research and development that remains to be done in the field of geopolymer concrete technology.

III. Materials, methods and equipment

1. Material

1.1 Geopolymer preparation

In this study, the materials used and the preparation method for making the binder were the same as those previously developed in Chapter I: flash metakaolin and Wg3.3 or Wg1.7 sodium silicate solutions. Three water proportions: 30%, 33% and 37% by mass of binder were chosen to make concretes and corresponded to the formulations GP14.5, GP17 and GP20 respectively (composition recalled in Table 1).

Table 1. Composition of the three geopolymer pastes using two different waterglass solutions.

	GP14.5		GP17		GP20	
	Wg3.3	**Wg1.7**	**Wg3.3**	**Wg1.7**	**Wg3.3**	**Wg1.7***
Metakaolin	52%	52%	50%	50%	47%	47%
Waterglass	43.0%	41.5%	41.0%	39.5%	38.8%	37.3%
$NaOH_{(solid)}$	4.4%	0.0%	4.2%	0.0%	3.9%	0.0%
Added water	0.6%	6.5%	5.3%	11.0%	10.4%	15.9%

* See Table 2 in Chapter 1 for the composition of the waterglass solutions.

1.2 Aggregates

Three different siliceous aggregates were used in this study:

- Non-porous silica aggregates (named aggregate P) composed mainly of well crystallised quartz, but also traces of plagioclase feldspars and muscovite, with four particle size classes: 0-0.315 mm, 1-4 mm, 4-8 mm and 8-12 mm.
- An alluvial siliceous rolled coarse aggregate from south-west France (named aggregate G) composed of quartz, plagioclase feldspars and muscovite, and having only two particle size classes: 0-4 mm and 4-10 mm.
- Rolled alluvial siliceous coarse aggregates from south-west France (named aggregate V) composed of quartz, plagioclase feldspars, and muscovite, and having three particle size classes: 0-2 mm, 0-4 mm and 2-6 mm. The water content of the aggregates on site during the factory fabrication was 4.5% for sand (0-4 mm) and 2.9% for gravel (2-6 mm).

Also, two bio-sourced aggregates were used:

- Hemp (From Hami Form): hemp shives are a co-product of the process of hemp fibre extraction from hemp stems. Hemp particles (Figure 5a) are parallelepipeds with variable shapes around 1 to 7 mm in width and 4 to 20 mm in length. They have a highly porous structure, very low bulk density and very low thermal conductivity. The hemp of this study was of French origin and was dry and untreated.
- Wood (from Agresta Technologies): wood aggregates were obtained from spruce and fir of French origin, and also came in parallelepiped-shaped particles with sizes between 4 and 10 mm (Figure 5b).

Figure 5. *Hemp a) and wood b) aggregates.*

2. Concrete preparation and laboratory equipment

2.1 Concrete preparation

The geopolymer concretes were prepared in two steps. First, the metakaolin and the aggregates were mixed, then the activating solution was introduced continuously during the mixing, until a homogeneous mixture and a dark orange colour (indicating the wetting of metakaolin) were obtained. The mixing was done in a 10 L mixer (Figure 6a, Controls®) and a 200 L mixer (Figure 6d), and vibration was used in both cases to fill the moulds. Three mould sizes were used: 100 x 100 x 100 mm cubes (Figure 6b), 110 x 220 mm cylinders and 3000 x 280 x 150 mm beams (Figure 6c).

All specimens were cured at 20°C and 95% R.H. for 24 hours and then demoulded and stored under the same conditions until testing, except for beams, which were kept at ambient temperature and relative humidity, outdoors or indoors.

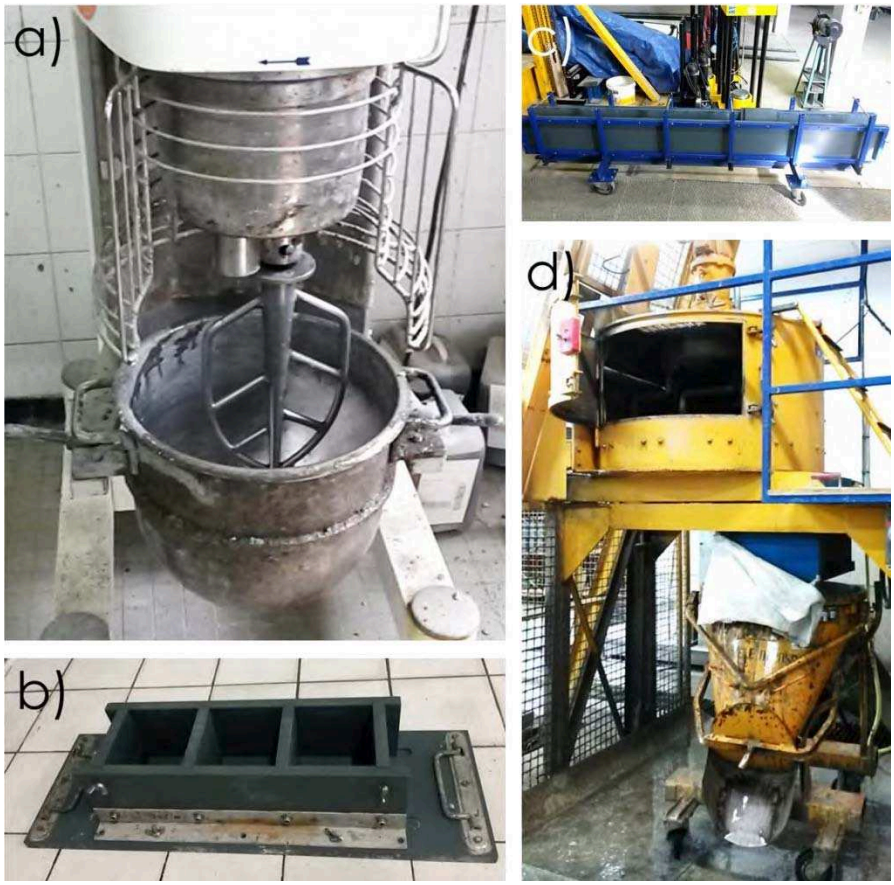

Figure 6. *a) 10 L mixer, d) 200 L mixer, b) 100 x 100 x 100 mm cubes and c) 3000 x 280 x 150 mm prism mould used to cast geopolymer concretes.*

2.2 Reinforced structure

In order to make a reinforced structure, the 3000 x 280 x 150 mm moulds were equipped with ordinary reinforcing steel (yield strength = 500 MPa). The reinforcement was composed of high adhesion armatures consisting of bars 14 mm and 6 mm in diameter, carrying one gauge in the middle as shown in the diagram of Figure 7.

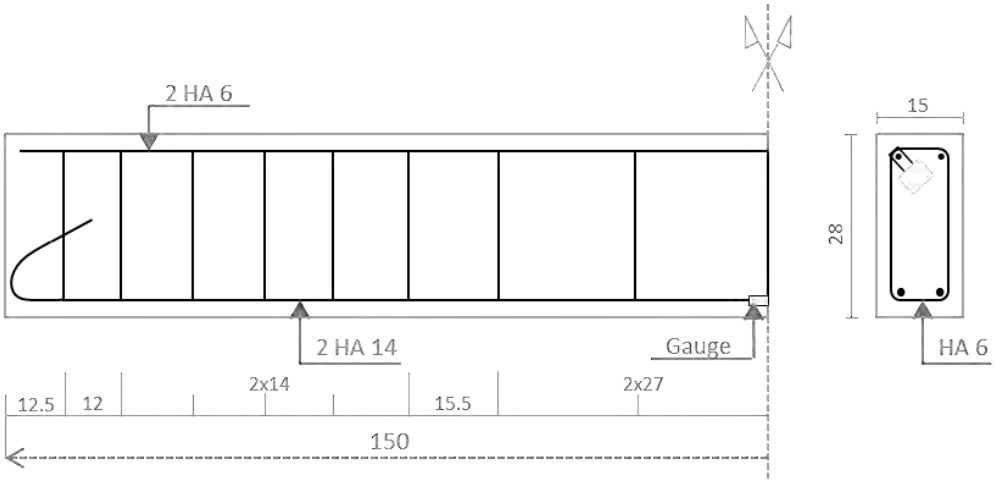

Figure 7. *Lay-out of the reinforcement (all dimensions in mm) for a half-beam.*

2.3 Vibrocompaction laboratory equipment

In order to make dry concretes in the laboratory (water content < 6% per mass of concrete), a vibro-compacting system was custom made. It comprised a PVC heightener of 40 mm height, fixed above the 100 x 100 x 100 mm moulds, and prismatic iron masses (99 x 99 x 40 mm, 3.12 kg). Placed on a vibrating table, this system (Figure 8) allowed the concrete preparation to be both vibrated and compacted and, as the moulds were removable, it was possible to replicate the immediate release of the blocks as performed in an industrial factory.

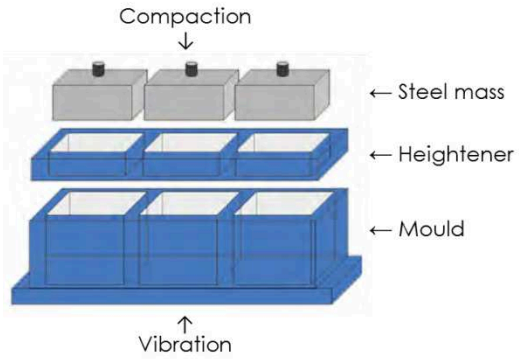

Figure 8. *Schematic representation of vibro-compaction equipment made in the laboratory.*

The preparation of the concrete remained the same as before (2.1), with, first, the mixing of aggregates and metakaolin, and then the incorporation of alkali silicate solution until a homogeneous mixture was obtained. Then the mould, extended by its heightener, was filled with a quantity of mixture previously calculated to obtain the desired final density, in one time, and the steel masses were placed above. The system was then vibrated for a few seconds until the iron masses reached the top of the mould. The mould was then disassembled and the concrete cubes were placed at 20°C and 95% R.H. for seven days.

2.4 Test method

The compressive strength measurements on concretes were carried out on 100 x 100 x 100 mm cubes using a 40 kN uniaxial press (3R®), and each value recorded was the average of 3 measurements. The total pore volume (%) was determined by measuring the porosity accessible to water via the French standard NF P18-459, as presented in Chapter I (III, 2.5), using 110 x 220 mm cylinders, from which three equal parts of 50 mm had been sawn from the central part. Each value was the average of 3 measurements performed on the cylinders. The workability of the concrete was assessed using the slump test described in the EN 206-1 standard.

3. Precast plant installation

The mixer used in the manufacturing plant was a COUVROT 1650 having a capacity of 1m^3 (Figure 9 a and b). The procedure for mixing and the fabrication of the blocks was the same as for the OPC masonry unit (MU) made in this plant, but the water normally added was replaced by the alkali silicate solution. The sodium silicate was stored in 1 m^3 containers (Figure 9c). This mixer could be opened from above during mixing, so it was possible to introduce the activating solution after mixing the aggregates and the metakaolin, during stirring. The mixing time chosen was around one minute for the dry materials, followed by a few minutes of wet mixing before the trap door at the bottom of the mixer was opened.

Figure 9. *Manufacturing plant equipment: a) 1 m^3 mixer open, b) inside of the mixer and c) the 1 m^3 sodium silicate container. SEAC "Guiraud frères" precast plant, 09120 Varilhes, France.*

Once completed, the preparation was automatically routed to the vibro-compaction device by a hopper system. The mixture was introduced into six 200 x 200 x 500 mm (external dimensions) metallic moulds, as shown in Figure 10a. The moulds were then completely filled (i.e. 240 mm, Figure 10c) and the six jacks moved down while vibrating and compacting the mixture for 16 to 20 seconds (final height of 195 mm). Then the whole system was raised to release the six geopolymer masonry units (Figure 10b). Thus the usual production rate of about 18 blocks per minute was respected.

As two types of blocks were made: full or with air blade (Figure 10d), the jacks had to be changed between castings.

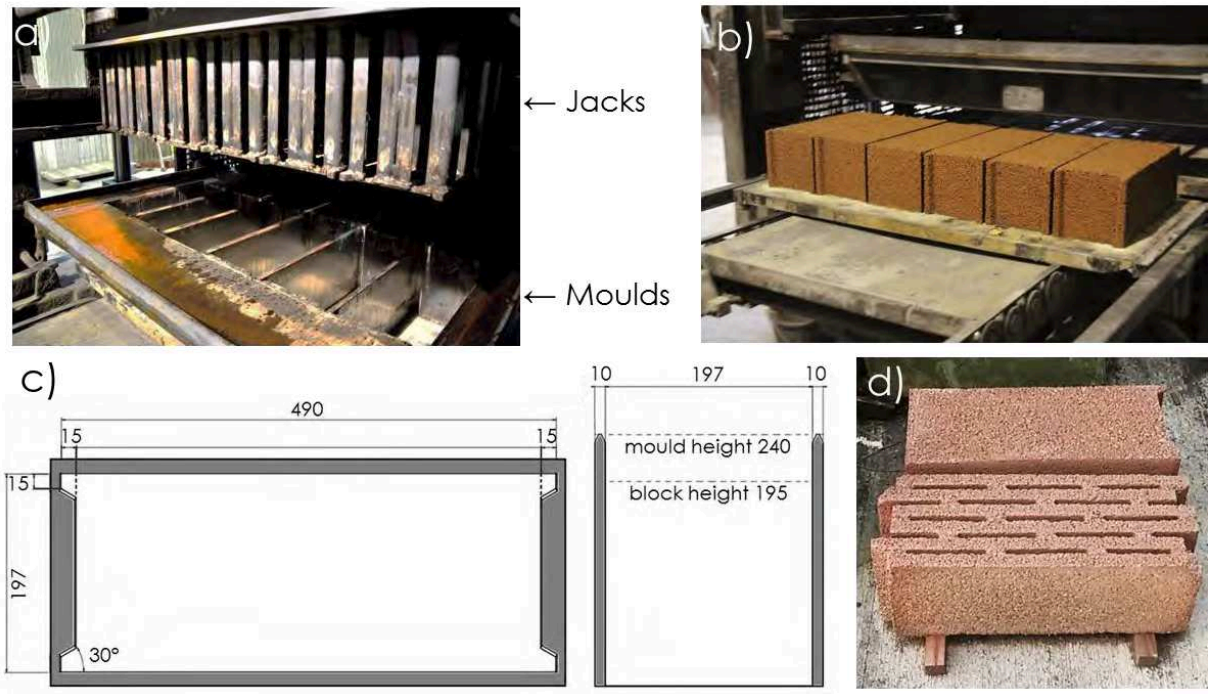

Figure 10. *a) Manufacturing plant vibro-compaction equipment with 6 moulds; b) geopolymer concrete blocks just removed from the moulds; c) schematic representation of one mould (units are mm) and d) full and air blade geopolymer blocks. SEAC "Guiraud frères" precast plant, 09120 Varilhes, France.*

The pallet of six geopolymer MU was then placed on an automatic conveyor carrying two pallets per level on 10 levels, to bring them to the storage warehouse (example for cement MU in Figure 11). The blocks were cured in a humid atmosphere for 3 days and then collected and put outdoors for the rest of the cure.

Figure 11. *Automatic conveyor in SEAC "Guiraud frères" precast plant, 09120 Varilhes, France.*

IV. Formulation of geopolymer concretes

In addition to assessing the behaviour of the geopolymer binder in the presence of aggregates, one purpose of these studies was to determine which applications would be achievable with this binder. An investigation was therefore focused on the formulation of geopolymer concretes by studying the compressive strength, the total porosity and the workability according to the water or aggregate content, and comparing them to OPC standards.

In order to envisage the possible applications of geopolymer binder, formulation studies were carried out using 3 different proportions of water (H_2O/Na_2O from 14.5 to 20) and 3 different proportions of aggregates (71% to 83% by mass) in order to observe the influence of these parameters on the fresh and hardened states of the geopolymer concrete. The aggregates chosen were non-porous silica aggregates (named P) from four particle size classes: 0-0.315 mm, 1-4 mm, 4-8 mm and 8-12 mm. For each formulation (named C1 to C9), workability, density, total porosity and compressive strength were assessed at seven days. Prisms of all formulations are presented in Figure 12 and all the results and formulations are given in Table 2.

Table 2. Geopolymer concretes: formulations and results (SiO_2/Al_2O_3 = 3.6 and Na_2O/Al_2O_3 = 0.9)

	C1	C2	C3	C4	C5	C6	C7	C8	C9
H_2O/Na_2O molar ratio	14.5	17	20	14.5	17	20	14.5	17	20
Mass % of aggregates	82.6%	82.6%	82.6%	76.9%	76.9%	76.9%	71.4%	71.4%	71.4%
Total mass % of water	5.0%	5.6%	6.2%	6.6%	7.4%	8.3%	8.2%	9.2%	10.2%
Formulation (kg/m³)									
Solid binder (Mk + $Silicate_{solid}$)	304.7	287.7	269.6	395.6	372.5	348.1	479.3	450.2	419.6
Total water	123.0	136.1	150.1	159.7	176.4	193.8	193.5	213.0	233.5
Aggregates	2036.4	2017.9	1998.3	1851.6	1829.5	1806.6	1681.4	1657.4	1632.3
Results at 7 days									
Slump (mm)	none	none	none	none	48	155	155	230	250
Bulk density (kg/m³)	2163	2244	2253	2233	2200	2143	2177	2133	2072
standard deviation	28	4	5	7	3	12	2	18	8
Porosity accessible to water	15.0%	10.5%	12.0%	11.6%	13.5%	16.2%	13.6%	15.8%	18.9%
standard deviation	1.5%	0.3%	0.3%	0.1%	0.0%	0.4%	0.2%	0.3%	0.4%
Compressive strength (MPa)	24.6	47.7	26.3	58.5	49.5	18.8	65.4	44.8	19.0
standard deviation	3.5	4.9	0.7	10.0	2.2	1.3	0.7	1.4	0.1

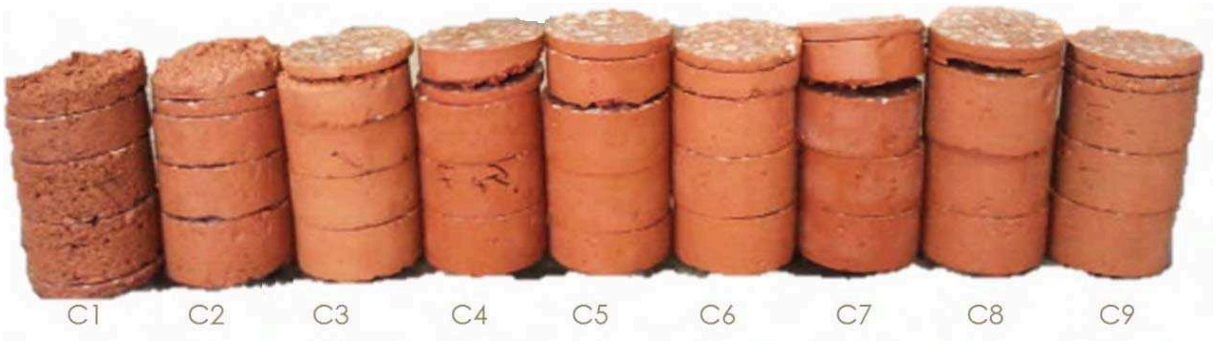

Figure 12. *Metakaolin-based geopolymer concrete prisms made with formulations C1 to C9.*

1. Workability of geopolymer concretes

Slump measurement is a test widely used to characterise the workability of concrete in the fresh state and allows formulations to be compared with one another. The nine geopolymer formulations were tested according to EN 206-1 before being introduced into the moulds. No slump was observed for the concretes having 83% by mass of aggregate, irrespective of the amount of water in the formulation. For the three concretes having 77% of aggregates (C4 to C6), the influence of water on the slump was obvious, as it increased (from none to 155 mm) as the quantity of water increased. In cases of similar water content (8.3% and 8.2% for C6 and C7) the same slump was measured (155 mm in both cases). Finally the concrete having the most water and the least aggregates (C9) showed a flat slump of 25 mm.

Observation of the slump measured versus the total amount of water in the concrete (Figure 13) highlighted the clear impact of the water content. It appeared that water content of less than 7% led to zero slump, which may be useful for immediate release concrete. Beyond 7% of water in the mixture, the workability increased quickly, passing from no slump (S1) to a maximum slump of 250 mm (S5), when only 3% of water was added.
When a concrete has S5 consistency, it becomes so fluid that it is highly susceptible to segregation. However, when an S5 concrete can flow under its own weight with adequate cohesion to resist segregation, it has the characteristics of a self-compacting concrete. So for the C9 formulation, where no particular segregation was observed, it would have been preferable to measure the slump flow to see if the concrete had the characteristics required for a self-consolidating concrete.

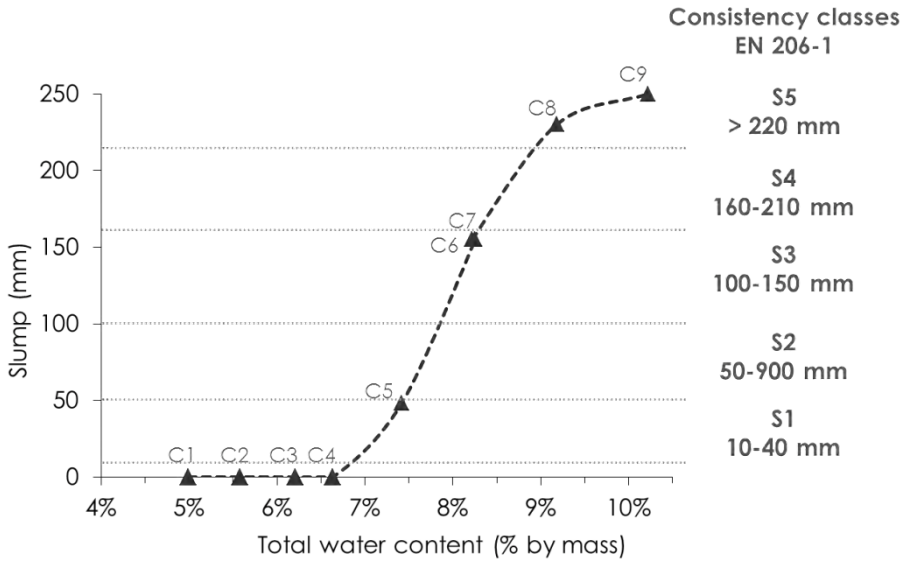

Figure 13. *Slump versus total amount of water in geopolymer concretes C1 to C9, with consistency classes according to EN206-1.*

This study on the fresh state of geopolymer concretes showed that it was possible to obtain all the consistency classes found for OPC, ranging from S1 to S5 (EN 206-1). Thus, it can be thought that a wide range of applications is possible for these materials.

2. Total porosity

The porosity studies by water intrusion, at a drying temperature of 105°C, were made at 7 days on the hardened geopolymer concretes, according to the French standard NF P18-459. The porosity measured ranged from 10.5% to 18.9% (Table 2), for an average bulk density of 2180 kg/m^3 (standard deviation 59 kg/m^3).

The first observation made on these results concerned the formulation C1, which did not seem to present coherent results. This formulation led to a very dry concrete, presenting high open porosity created by inadequate filling of the moulds by the concrete (as can be seen on the left prism in Figure 12). The results obtained for all other formulations showed the same results as those previously observed on the geopolymer paste (Chapter I), i.e. that increasing the amount of water in the geopolymer formulation increased the total porosity, whatever the aggregate proportion. Conversely, it was found that, for a given formation, increasing the amount of aggregate reduced the total pore volume. Therefore it appears that the most important parameter was the total water content in the concrete, which was controlled by both the geopolymer formulation and the amount of aggregate.

Thus, as presented in Figure 14a, the total pore volume increased almost linearly with the total amount of water in the concrete, regardless of the formulation or the aggregates content. When the porosity accessible by water intrusion, obtained in the previous chapter on pure geopolymer paste (at the same drying temperature of 105°C), was added, depending on the total water content, the linearity was still respected (Figure 14b).

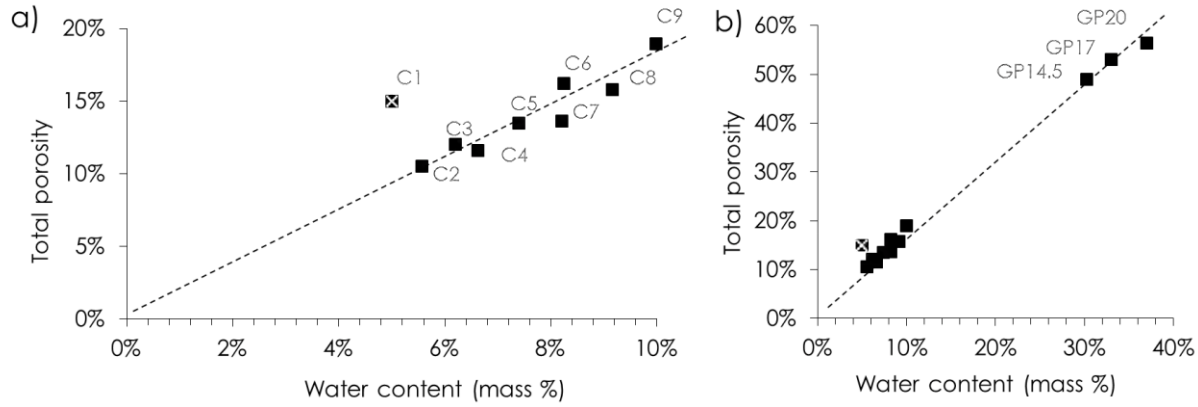

Figure 14. *Porosity accessible to water versus the total amount of water of geopolymer concretes a) without or b) with the porosities measured on geopolymer paste in Chapter I.*

The total porosity versus aggregate content presented on Figure 15a shows that increasing the quantity of aggregates decreases the total porosity with certain proportionality, whatever the formulation used. This reduction may be associated with a dilution of the geopolymer paste, leading to a decrease of the water content. But if the results previously obtained on geopolymer paste (at the same drying temperature of 105°C) are considered as 0% of aggregates, as represented in Figure 15b, the certain proportionality was still obtained for each formulation. These results suggest mainly that the total porosity of the concrete is only linked to the water content (and thus the geopolymer formulation), which would imply that the addition of aggregates does not create more porosity, at least not water-accessible porosity.

Thus these results provided information about the interfacial transition zone (ITZ) in the geopolymer concretes. In ordinary Portland cement concrete, the interface between mineral aggregates and cement binder is often described as the interfacial transition zone, and is generally perceived as the weakest region within a mortar and/or concrete structure due to its high porosity. Studies carried out on the subject with a geopolymeric matrix concluded, in general, on an absence of ITZ (Pacheco-Torgal et al., 2007, Lee and Van Deventer, 2004), or on an ITZ that was more or less dense depending on the formulation (Half et al., 2013). The total porosity results achieved in this study suggest a similar conclusion, since no porosity

seemed to be formed by the addition of aggregates. That would imply that there were no less dense or weaker areas in the paste-aggregates interface. Visual observations made after breaking a geopolymer concrete cube confirmed this absence of ITZ for these systems. As can be seen on Figure 16, only split aggregates were observed on the broken surfaces of concrete cube, proving that the interface was stronger than the grains, and therefore the ITZ did not constitute a weak area.

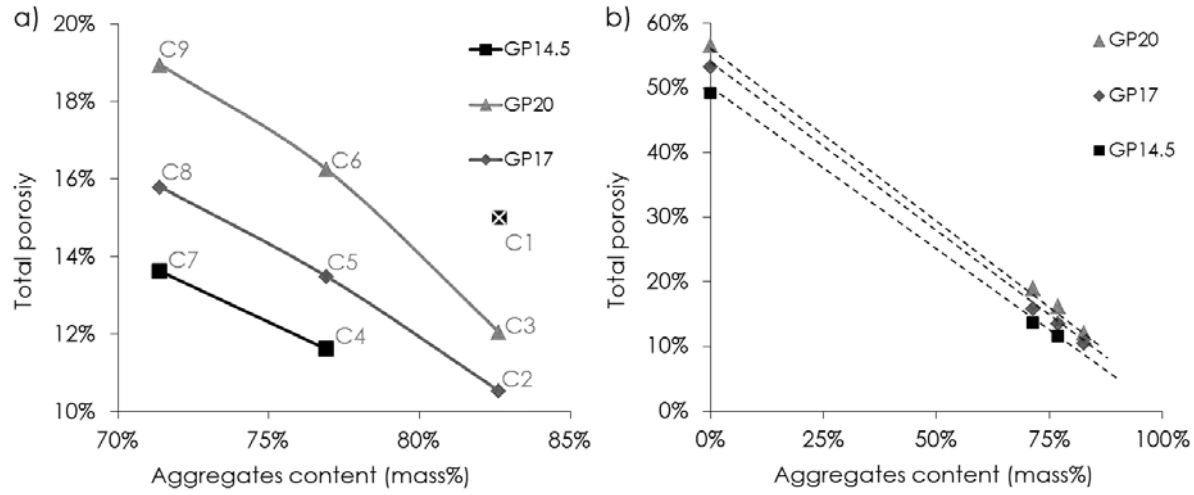

Figure 15. *a) Porosity accessible by water versus aggregate content in geopolymer concretes; b) including the previous results obtained on paste with a drying temperature of 105 ° C for the formulations GP14.5, GP17 and GP20.*

Figure 16. *100 x 100 x 100 mm geopolymer concrete prism after compressive strength breaking (Formulation GP14.5) with split aggregates (*).*

3. Mechanical properties

Two general tends emerge from the mechanical properties measured on the geopolymer concretes (Table 2):

Firstly a strong influence of the water content of the geopolymer binder was observed. As can be seen in Figure 18, the compressive strength seems similar for all formulations with a given geopolymer water content (30% for GP14.5, 33% for GP17 and 37% for GP20), with a decrease of the strength when the water content increases. Thus, for the three concretes made with formulation GP17 and all having 33% of water in their geopolymer composition (C2, C5 and C8), similar strengths of around 45 MPa were found. For the three concretes made with geopolymer GP20 (C3, C6 and C9) having 37% by mass of water in their binder, the performance was still similar but lower, around 20 MPa. The strength measured for the GP14.5 formulations seems to follow the same trend, with similar performance of around 60 MPa (C4 and C7), but with an exception for C1 due to a workability problem related to a lack of water in the system. Thus, it appeared that the concrete performance classes were determined by the paste formulations, as long as the workability was sufficient.

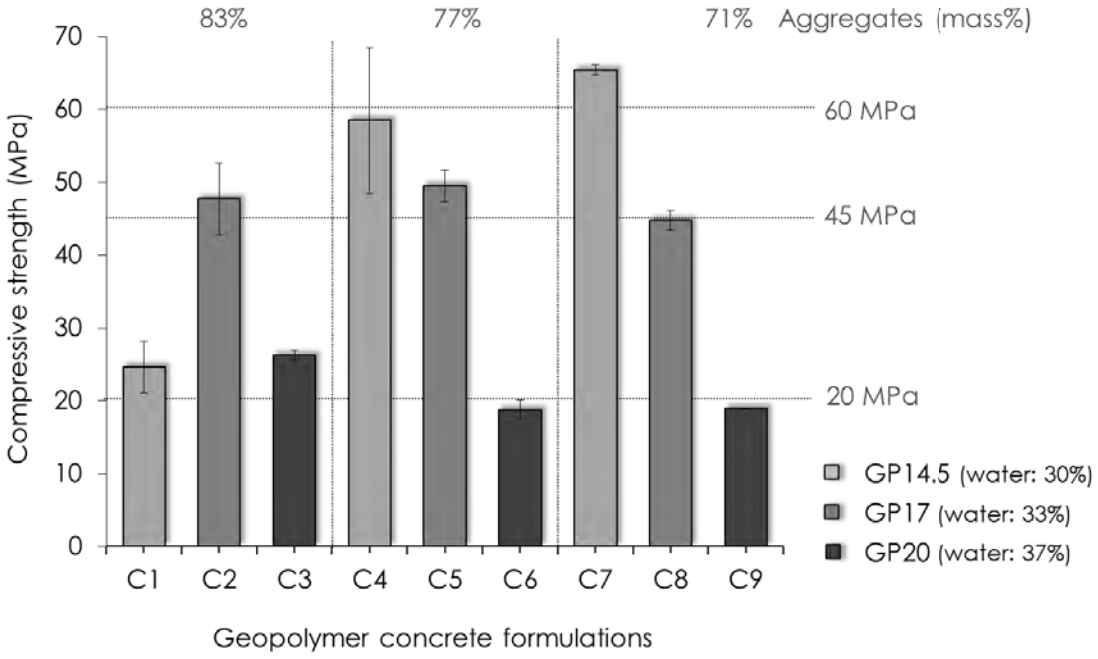

Figure 17. *Compressive strengths of geopolymer concretes.*

Secondly, the amount and particle size of the aggregates does not appear to affect the final strength of geopolymer concrete. When the compressive strength is represented versus the water content of the geopolymer paste (by the H_2O/Na_2O ratio) for four aggregate contents (Figure 18, including the previous result of Chapter I for geopolymer mortars) it appears that the strength decreases equally when the H_2O/Na_2O molar ratio increases, regardless of the amount or size of the aggregates. For example, with an H_2O/Na_2O ratio of 14.5, a compressive strength of around 60 MPa was achieved with 62% of sand, or 77% or 71% of aggregates (C4, C7, and M5). Thus, the concrete performance classes would, as stated previously, be determined by the paste formulations whatever the proportion or the size of the aggregates, as long as the workability was sufficient.

This finding could be explained by the previous observation of the absence of a weak zone between aggregate and geopolymer. If the interface between the aggregate and the binder exhibits good adhesion, in addition to the absence of weaker zones, the influence of mineral additions on the mechanical strength of the material would be negligible, the mechanical strength being completely governed by the geopolymer strength. This finding reveals a very practical aspect of the geopolymer as a binder in concrete structures, showing that it would be possible to reduce the amount of binder while maintaining the mechanical performance of the concrete.

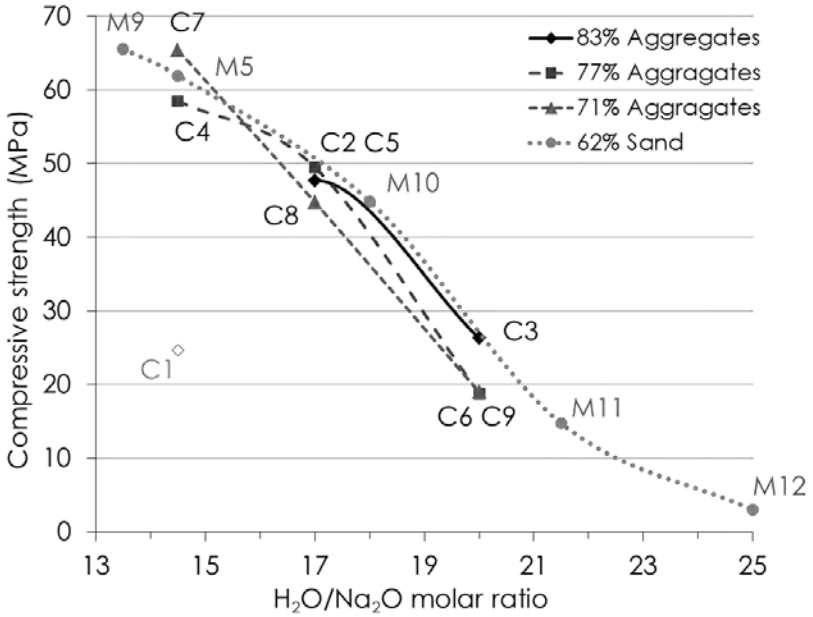

Figure 18. *Compressive strengths of geopolymer concretes depending on the H_2O/Na_2O ratio for four aggregate contents.*

Regarding the compressive strengths of the geopolymer concretes depending on their total porosities, as presented in Figure 19, it was observed that, for a given amount of aggregates, the more the porosity increased, the more the strength decreased. The fact that the porosity was found to be linked to the total water content implied that, as in OPC concrete, increasing the amount of water decreased the mechanical performance. However, as the geopolymer formulation fixed the compressive strength and not the amount of aggregates, more porous concretes (like C7) could have a higher compressive strength than a less porous formulation (like C2).

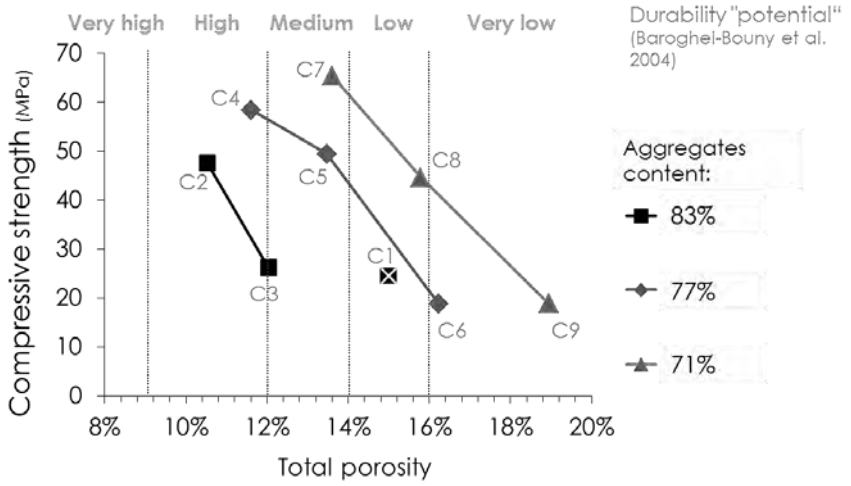

Figure 19. *Compressive strengths of geopolymer concretes depending on the total porosity and durability classes according to Baroghel-Bouny (Baroghel-Bouny et al. 2004).*

The porosity accessible to water could also be a parameter which, with the help of the AFGC AFREM 2004 manual (Baroghel-Bouny et al, 2004), would allow OPC concretes to be classified on the basis of their potential durability. In this manual, four limits, of 9%, 12%, 14%, and 16% total porosity, determine five classes of "potential" durability from very high to very low. These classes are represented in Figure 19, for discussion purposes only since these limits were defined for OPC. If they had been applied to geopolymer concrete, it would have been concluded that, of the eight formulations of geopolymer concretes analysed, none would present a very high "potential" durability ($\varepsilon < 9\%$), three would present a low or very low "potential" durability and five formulations would have a high or medium "potential" durability. However, the total porosity alone cannot predict the potential durability of geopolymer, as the porosities of these matrices are quite different from those of OPC. Moreover, the representation of Figure 19 has shown that the conclusions can vary widely depending on the aggregate content. It would therefore be risky to apply this classification to geopolymer concretes, as has been done for slag concrete (Van Deventer, 2014), because the conclusions would very probably not represent reality.

4. Economic considerations

The cost of a cubic metre of concrete is an important factor that has to be considered in addition to its compressive strength and durability. In this section, the price of geopolymer concrete (without transportation) is compared to the price of OPC, for the formulations previously presented.

Figure 20 represents the results of this economic study, according to the following hypotheses:

- The price of the cubic metre of concrete was compared "ex factory", and therefore excluded any transport rates.
- The calculated prices were presented in arbitrary units relative to a reference value of 1.0, corresponding to the price of a cubic metre of concrete made with ordinary cement (CEM I 52.5 N or R) and having a compressive strength of 20 MPa, 45 MPa or 60 MPa. The corresponding compositions selected are presented in Table 3.
- The price for the cubic metres of geopolymer concretes have been calculated from the compositions presented in Table 2 (except for the C1 formulation, judged not consistent for this study)
- The calculation considered the use of an activating solution that did not require addition of soda, and three relative prices were assumed (per tonnes): same price as cement (♦ Wgx1), twice the price of cement (● Wgx2) and three times the price of cement (▲Wgx3).
- The cost of a tonnes of metakaolin was also chosen, in relation to the price of the cement, as 0.8 times (♦ Mk0.8), equal to (♦ Mk1.0) or 1.2 (♦ Mk1.2) times the price of a tonnes of CEM I 52.5.
- Finally, the price of the cubic metres of geopolymer concrete containing 71%, 77% and 83% of aggregates were distinguished by different coloration of the markers.

Table 3. OPC concrete compositions for one cubic metre, chosen as references for the economic study.

Compressive strengths	20MPa	45MPa	60MPa
Cement (kg/m^3)	200	350	420
Water/cement	0.7	0.5	0.4
Superplasticizer	none	1%	2%

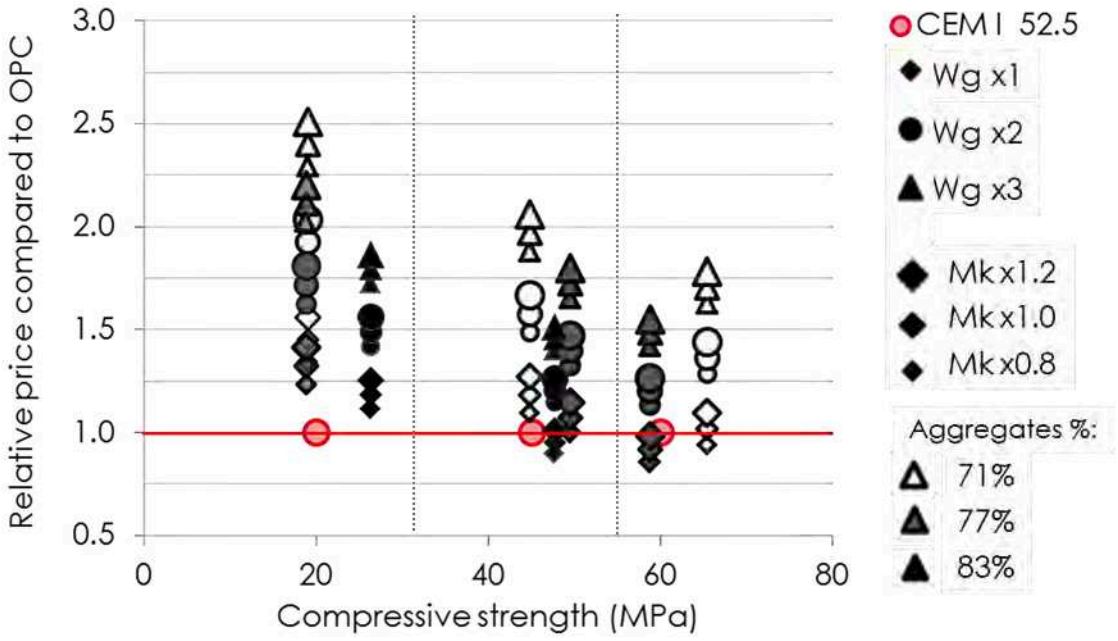

Figure 20. *Relative price of geopolymer concrete compared to OPC depending on the compressive strength, for three aggregate contents, and for three different price of metakaolin (Mk) and sodium silicate (Wg) compared to OPC price (=1).*

Several conclusions can be drawn from this economic study:

First, the influence of the desired strength on the relative price of the geopolymer concrete was considerable. It thus appeared that it would be more economical to make geopolymer concretes having high compressive strength, rather than low performance. It was calculated that, for 20 MPa, more solid binder had to be added to the geopolymer formulation than to cement for the same final compressive strength while, for 60 MPa, less solid binder was required in geopolymer formulation than that used in CEM I 52.5 formulation. Moreover, no superplasticiser had to be introduced into the mixture. So no geopolymer concretes of 20 MPa were calculated to have a price equal to or lower than that of cement, while from 45 MPa, comparable prices were obtained for both materials.

A significant influence of the price of the silicate solution on the cost of the cubic metre of geopolymer concrete was also noted, mainly due to the fact that its price could vary by a factor of one to three, compared to OPC. This choice of thrice the price of CEM I 52.5 was made realistically in view of the purity of the solutions available on the market and their rarity. The price of the waterglass solution appears to be a major issue in the economic viability of geopolymer concretes, and if it were equal to the CEM I 52.5 price (♦ on Figure 20), it would be possible to reach a similar cost for a cubic metre of concrete having a compressive strength 45MPa and beyond.

Regarding the impact of metakaolin prices, their influence on the final cost of the concrete was logically observed to be low, given the small difference of its price compared to cement. And concerning the aggregate content, the impact of its variation was also obvious: as increasing the amount of aggregates decreased the binder content, it also decreased the price of the concrete.

In conclusion, it can be said that a cubic metre of geopolymer concrete can reasonably be made at the same price as OPC concrete for equal compressive strengths, but on the following conditions:

- → The compressive strengths required must be high (45MPa or beyond).
- → The sodium silicate solution price must be equal to or lower than that of a CEM I 52.5.
- → The metakaolin cost must not exceed 1.2 times the price of cement.
- → The aggregate content in the geopolymer concrete must be higher than 71% by mass.

Some formulation optimisation studies could also allow these costs to be brought down by reducing the amount of binder in the concrete or trying to find a less expensive activation solution.

In short

Formulation	Nine formulations from dry to fluid
Workability	Viscosity higher than OPC
Slump test	Consistency classes from S1 to S5 (EN 260-1) - No slump below 7% of water by mass in the concrete formulation
Porosity	Between 10% and 20% of total porosity - Absence of ITZ supposed
Compressive strength	From 19 to 65 MPa - Negligible influence of the size or amount of aggregate - Strong effect of the GP paste formulation on the concrete strength.
Economic aspect	Price more advantageous, compared to OPC, for high performances. - Strong influence of the activating solution price.

This study on the formulation of geopolymer concrete showed that, in the presence of non-porous siliceous aggregates and for a 6 L preparation, the geopolymer was able to replace traditional Portland cement. The workability and compressive strength measured indicate a range of possible applications almost as wide as for OPC, but these theoretical results must be validated by further tests. Thus the next part of this chapter will assess the behaviour of geopolymer concretes for special applications requiring fluid to dry concretes.

V. Fluid and dry geopolymer concretes

The formulation plan has shown that all the OPC consistency classes can be achieved with a geopolymer binder according to the slump test. Further tests were undertaken to see if those classes were applicable to geopolymer concretes. On the one hand, a structural beam equipped with reinforcing steel was made in order to see if the geopolymer concrete could be fluid enough to make such structures. On the other hand, a study was conducted in which the binder/aggregate ratio was reduced, in order to assess the behaviour of dry geopolymer concretes and compare them to OPC. As this study had to be conducted using three different ranges of equipment size, from laboratory to precast plant, the scale effect was also assessed.

1. Reinforced concrete structure

The slump test showed that geopolymer concretes could be fluid. However, the high viscosity of the activating solution may lead to different behaviour of the fresh geopolymer concrete compared to OPC, especially in the particular case of reinforced structures. Making concretes incorporating steel reinforcements requires a high workability as the fresh concretes should be able to totally fill the moulds, which are often narrow, and completely coat the steel bars. As fresh geopolymer concretes have higher viscosity than cement, mainly due to the initial viscosity of sodium silicate, poor coating of the steel bars or workability problems during mixing on a larger scale (200 L) could occur.

1.1 Concrete formulation

In order to assess the feasibility of such an application, two reinforced beams were cast in the laboratory, with the same procedure as generally used for OPC. Because the consistency class suitable for the fabrication of such a structure is generally between S3 and S4, the geopolymer formulation chosen was C7, which had a slump of 155 mm (Figure 13). The activating solution used was the most concentrated one (Wg1.7), which avoided having to add a large amount of pure NaOH. The aggregates were coarse rolled alluvial siliceous aggregates from the south-west of France (aggregate G). They were characterised by two particle size classes, one of 0-4 mm and one of 4-10 mm with mass proportions of 40% and 60%, respectively.

The geopolymer formulation was the same for the two beams but the first one (B1) was cast with dry aggregates and the second one (B2) with saturated surface dry aggregates. In both cases, in addition to the 3000 x 280 x 150 mm beam, two 110 x 220 mm cylinders and three 100 x 100 x 100 mm cubes were cast, which required 143 litres of concrete. The details of the formulation and the compressive strength measured on the cubes are presented in Table 4.

Table 4. Geopolymer beam formulations and results on cubic samples (SiO_2/Al_2O_3 = 3.6 and Na_2O/Al_2O_3 = 0.9).

	B1	**B2**
H_2O/Na_2O molar ratio	14.5	14.5
Mass % of aggregates	73%	73%
Aggregates	Dry	Saturated surface dry (SSD)
Cure condition (beams and samples)	Ambient temperature and R.H. (Outside)	Ambient temperature and R.H. (Inside)
Formulation (kg/m^3)		
Solid binder (Mk + $Silicate_{solid}$)	457	
Total water	191	
Aggregates	1735	
Water/binder	0.42	
Results at 7 days on cube specimens (average of three values)		
Bulk density (kg/m^3)	2333	2350
Standard deviation	8	27
Compressive strength (MPa)	59.5	49.2
Standard deviation	0.9	1.8

The mix was prepared in a 200-L mixer following the same procedure as previously: weighed metakaolin and aggregates were mixed until a homogeneous mixture was obtained, and then the alkali silicate solution was manually introduced during mixing using buckets. The mixture was made in the same way as for an OPC, except that, shortly after the introduction of the alkali silicate solution, an increase in the viscosity of the mixture was noted, involving an increase in the shear resistance. This behaviour has already been observed on previous castings, always at the time of the waterglass solution addition, but the phenomenon was amplified by the greater quantity of mixture. However, that did not hinder the beam preparation.

1.2 Beam casting

Once the mixing had been completed, the fresh concrete was put into a bucket placed below the mixer (Figure 21 a and b). This bucket was then brought to the beam moulds by a forklift truck (Figure 21c).

Figure 21. *a) 200L mixer and the concrete bucket; b) Filling of the concrete bucket with the geopolymer concrete c) Forklift lifting the full bucket.*

The bucket was placed on top of the beam mould, which had been previously oiled and equipped with steel reinforcement (Figure 22a). Using a gutter, the mix was introduced into the mould as shown in Figure 22b. The descent of the fresh concrete by this gutter was slower than for cement concrete but was successful. The beam was cast in two layers and, to ensure proper filling of the form by the concrete, each layer was vibrated by a vibrating needle (Figure 22c).

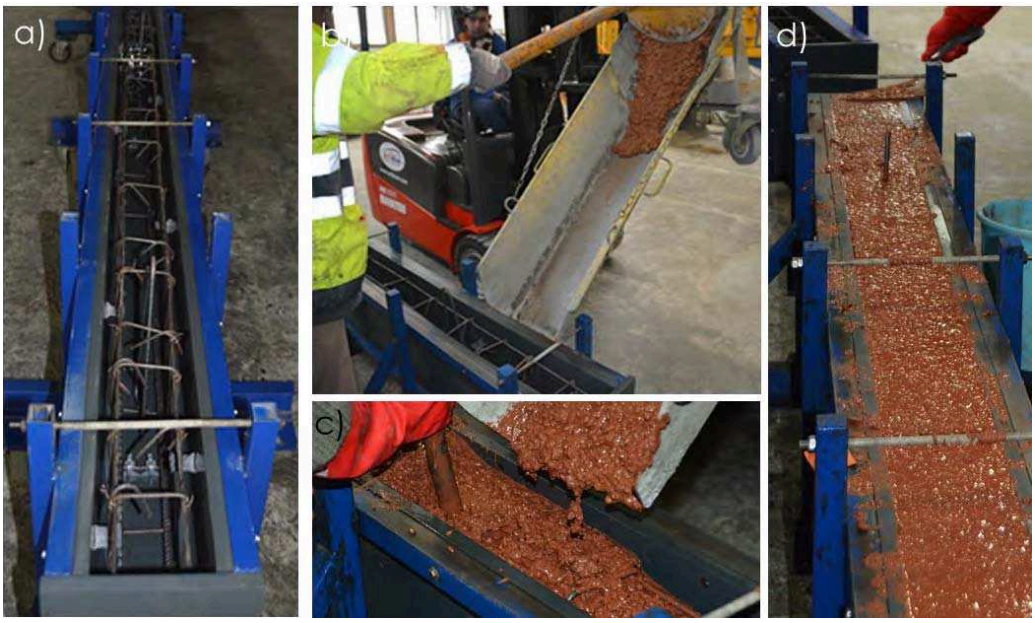

Figure 22*. a) Beam mould with the steel reinforcement; b) descent of the fresh concrete by gutter; c) vibration of the fresh geopolymer concrete using a vibrating needle and d) levelling of the beam with a trowel.*

The vibrating needle was dipped gradually into the concrete to reach the bottom of the form until there were no more surface air bubbles. The beam was finally levelled using a trowel to obtain as flat a surface as possible (Figure 22d). It was then covered with plastic for 5 days. The same operation was carried out for the casting of the second beam.

1.3 Demoulding and cure conditions

After five days, the two beams were demoulded. It was first observed that, despite the vibrations, a large number of air bubbles were trapped in the concrete, and were visible on the sides of the beams (Figure 23a). The two beams were removed from their moulds using a forklift (Figure 23b) without causing any damage or cracking. They were then stored in ambient conditions (temperature and R.H.), either outdoors (B1 Figure 23c) or indoors (B2 Figure 23d), as were the prisms and cubes made at the same time. The two beams were elevated using two wooden blocks so as to protect them from capillary rise of water. The beams were kept in these conditions and visual observations were made regularly. The beam stayed in these conditions for long-term study.

Figure 23. *a) side of B1 showing the air bubbles trapped in the fresh concrete b) beam B1 removed from its mould using a forklift; c) B1 stored outdoors and d) B2 stored indoors.*

This test showed that it was possible to make reinforced beams using the same materials and methods for mixing and casting as for OPC. This test also showed that a consistency class of between S3 and S4 was appropriate for the geopolymer concretes.

1.4 Mechanical strength

Seven days after casting, the cubes were tested in compression, and the compressive strengths shown in Table 4 are an average of three values. The first concrete (B1) had a strength of 59.5 MPa, which was in agreement with the average of 60 MPa found for this geopolymer during the formulation study. Thus, the use of coarse aggregates had only a minor impact on the concrete strength compared to the standard non-porous aggregates used in the previous section. In contrast, the use of saturated surface dry aggregate led to a significant decrease in the compressive strength, as 10 MPa less was obtained for the second concrete (B2). This observation showed the significant influence of the amount of water in the mixture, which was similar to the influence observed on OPC except that, in the case of geopolymer concrete, the decrease in water content was limited because of the large amount of water provided by the activating solution. The water content of the aggregates is thus a major issue for the formulation of geopolymer concrete.

1.5 Durability problems

After a year, surface problems were noticed on the sides of the beam (B1) and the cylinders exposed to external conditions. As shown on Figure 24 a, white crystals were observed on some parts of the beam sides, despite the protection against capillary action**.** The development of such crystals, called efflorescence, is known in OPC and is relatively well controlled. In the case of geopolymer, these patches of efflorescence appeared to be larger, probably because of the high sodium content, as they were due to the formation of alkali carbonate in the pore solution caused by carbonation with atmospheric carbon dioxide. Capillarity causes the migration of these carbonates to the surface, then their crystallisation during the evaporation of water. It was also seen that the efflorescence caused the binder surface to become detached, exposing the aggregates. In the case of the cylinder shown in Figure 24 b, the detachment was even more pronounced, probably due to the fact that the cylinder was not protected from water capillarity.

Figure 24. *Visual observation of the sides of a) the beam and b) cylinder stored outside.*

In the case of the beam kept inside, and therefore protected from rain, no surface damage or significant efflorescence was observed. Thus exposure to a moist atmosphere and to rain water resulted in a significant durability problem which would require a study of the phenomenon of carbonation of the geopolymer matrix.

The fabrication of two beams three metres long therefore showed the possibility of using the geopolymer binder like a traditional hydraulic binder for reinforced structures. The higher viscosity of the mixture in the fresh state was noted but was not a problem for the casting of the beams. In contrast, the water content of the aggregates was found to have great influence on the concrete strength. A significant efflorescence problem was also found, highlighting a damaging carbonation reaction.

2. Geopolymer concretes having low binder/aggregate ratios

2.1 Dry concrete at laboratory scale

In order to achieve dry concretes in the laboratory, a home-made vibro-compaction system was used and eight concretes were made according to the formulations of Table 5 with the aggregates V. The amount of aggregates was increased from 83% to 91% in formulations dC1 to dC6 with the same geopolymer composition. For dC7 and dC8, the amount of aggregates was fixed at 89% and the amount of water was increased. The compressive strength was measured for all the formulations at seven days and the results are presented in Table 5 as an average of three measurements. The first observation made in this study was the feasibility of demoulding the cubes immediately without damage, as shown in Figure 25 a. Regarding the

compressive strength, it was observed that, unlike the previous conclusion, increasing the amount of aggregates in the concretes markedly decreased their strengths for a given geopolymer formulation.

Table 5. Formulation of geopolymer dry concrete and compressive strengths measured on cubes (SiO_2/Al_2O_3 = 3.6 and Na_2O/Al_2O_3 = 0.9).

	dC1	dC2	dC3	dC4	dC5	dC6	dC7	dC8
H_2O/Na_2O molar ratio	14.5	14.5	14.5	14.5	14.5	14.5	**17**	**20**
Mass % of aggregates	83%	85%	86%	88%	89%	91%	89%	89%
Formulation (kg/m^3)								
Solid binder ($Mk + Silicate_{solid}$)	291.9	268.7	244.4	218.9	193.4	170.2	190.7	187.6
Total water	122.1	112.4	102.2	91.6	80.9	71.3	93.6	108.2
Aggregates	2069.9	2116.9	2166.2	2217.8	2269.6	2316.4	2238.3	2202.1
Water/binder	0.42	0.42	0.42	0.42	0.42	0.42	0.49	0.58
Results at 7 days								
Compressive strength (MPa)	11.5	8.9	7.3	4.4	3.9	1.6	0.8	0.3
standard deviation	2.0	0.5	0.1	0.3	0.6	-	-	-

To evaluate the performance of such concretes, the values obtained were compared to those of a similar formulation made with OPC. Cement concrete having similar binder/aggregate ratios is used in precast plants to make masonry units (MU). In the SEAC plant (Varilhes, France) which sells concrete MU, the blocks contain 90% by mass of aggregates, and reach strengths of around 10 MPa at 28 days. The applicable standard (EN 771-3) imposes a minimum compressive strength of 4 MPa, so that the unit can be used for load-bearing walls. The values obtained for the geopolymer dry concretes therefore show that, of eight formulations, only half had compressive strengths above 4 MPa at 7 days and only the first formulation showed a strength comparable to that of OPC, but for an aggregate content of 83% and not 90%. Thus, the geopolymer binder appears to be less efficient than OPC for making dry concrete.

However, a problem of homogeneity was observed visually in all cubes of concrete. As can be seen in Figure 25 b and c, only the superficial part of the cubes presented a consolidated binder having the right rigidity and colour. Below a few millimetres depth, the geopolymer resembled a light pink powder, as if it was the initial metakaolin that had not reacted. This was the first time in this study that such a phenomenon was observed and it could not be formally explained. It was possibly due to a lack of binder in the mixture resulting in the geopolymerisation reaction not taking place or due to the vibration, which would encourage the geopolymer paste to move towards the exterior of the cube.

Figure 25. *a) Geopolymer dry concrete cubes; b) during c) and after breaking.*

This suggests that it was not possible to make a proper geopolymer concrete with more than 82% of aggregates. However as the precast plant infrastructures allowed much higher vibration and compaction, further tests were conducted before definitely concluding that geopolymer could not be used as a binder in dry concrete.

2.2 Dry concrete at industrial scale

To determine if geopolymer could be used as a binder for dry concretes, large scale testing was needed. As previously mentioned, the precast plant installation allowed the fabrication of cement masonry units having 90% by mass of aggregates thanks to high vibration and compaction. This equipment was used to make geopolymer dry concretes.

The geopolymer concrete formulations were designed to be as close as possible to the formulation of blocks made in the factory:

Binder 10% *Water/cement ratio 0.8*	*- 126 kg/m^3 of cement* *- 100 kg/m^3 of water* *- 0.25L of admixture* *(not used in the case of geopolymer concretes)*
Aggregates 90% *1950 kg/m^3*	*- 450 kg/m^3 of 0-2 aggregates* *- 300 kg/m^3 of 0-4 aggregates* *- 1250 kg/m^3 of 2-6 aggregates*

Four batches of 540 L were made in the precast plant with geopolymer GP14.5 and 87.7% to 90.1% by mass of aggregates V. The formulations and mechanical strength obtained at 8 days are shown in Table 6. These formulations correspond to the formulations C4 to C6 performed in the laboratory which gave compressive strengths between 1.6 and 4.4 MPa.

Table 6. Formulations and mechanical strengths of geopolymer full MU made in SEAC "Guiraud frères" precast plant, 09120 Varilhes, France.

	$GP_{MU}1$	$GP_{MU}2$	$GP_{MU}3$	$GP_{MU}4$
H_2O/Na_2O molar ratio	14.5	14.5	14.5	14.5
Mass % of aggregates	87.7%	88.5%	89.3%	90.1%
Mass % of water	3.6%	3.4%	3.2%	2.9%
Formulation (kg/m^3)				
Solid binder ($Mk + Silicate_{solid}$)	218.9	205.7	192.2	178.4
Total water	91.6	86.3	80.6	74.8
Aggregates	2217.8	2244.0	2271.4	2299.5
Water/binder	0.42	0.42	0.42	0.42
Results at 8 days				
Compressive strength (MPa)	>11.5	>11.5	≈ 11	≈ 9

The preparation was carried out as presented previously by mixing first the aggregates and the metakaolin for one minute, and then adding the silicate solution during stirring. As the aggregates were stored outside, their water content had to be considered. Fortunately, the amount of water brought by the aggregates never exceeded the 6.5% of water required in the formulation of the geopolymer GP14.5 (see Table 1), thus the amount of excess water needed for GP14.5 was not added in the mixer. The preparation of 540 L of geopolymer concrete presented no problems (Figure 26 a). The final consistency was similar to that obtained for an OPC formulation (Figure 26 b).

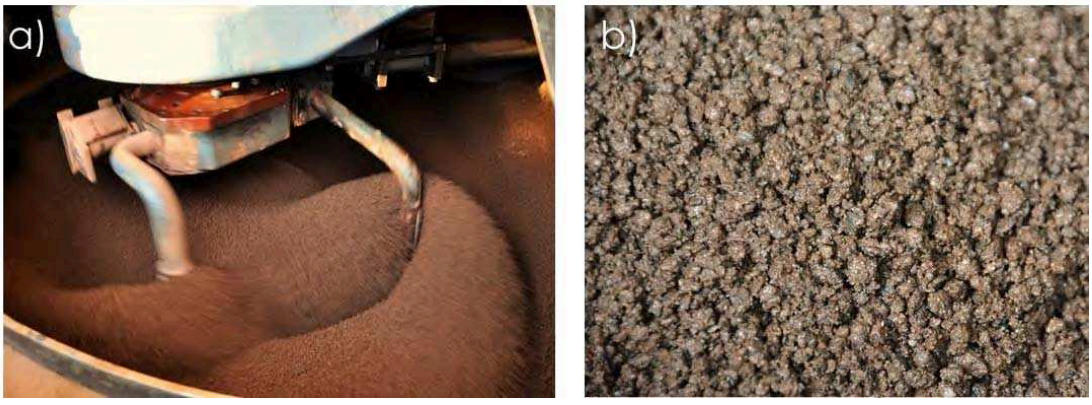

Figure 26. *a) Mixing of the $GP_{MU}1$ formulation; b) $GP_{MU}1$ after mixing.*

The vibro-compaction did not exceed the 20 seconds generally used in the plant and the immediate release was performed, for full and air blade units, without any damage, as can be seen on the pictures of Figure 27 a and b.

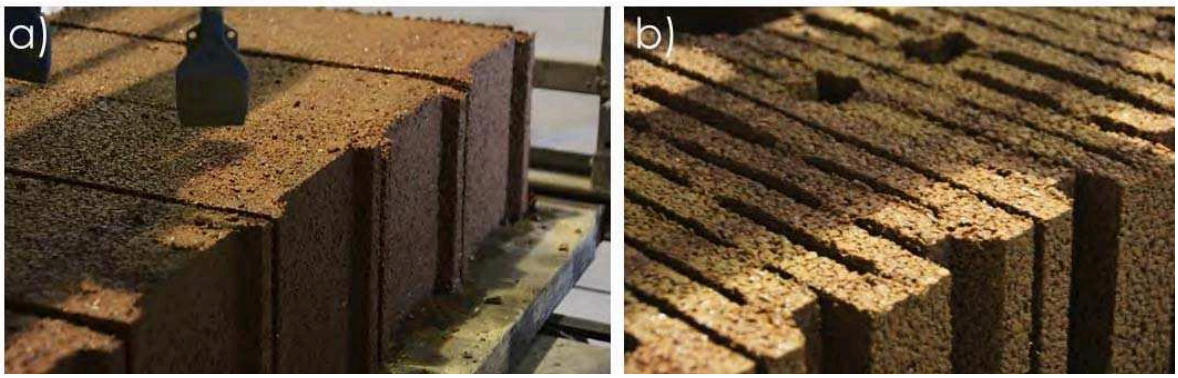

Figure 27. *Geopolymer MU after immediate release for a) full and b) air blade units.*

After being stored in the warehouse for three days (maintained in wet conditions) the geopolymer units were manipulated without undergoing damage and were placed in ambient conditions until the strength test at 8 days. Concerning the compressive strength measured, it was observed that, for the two first formulations, $GP_{MU}1$ and $GP_{MU}2$, the exact compressive strength could not be measured as it exceeded the maximum load of the plant press of 11.5 MPa. A compressive strength of 11MPa was obtained for the third formulation having nearly 90% of aggregates, which was similar to that of an OPC masonry unit incorporating the same amount of aggregates. The last formulation showed a lower strength of 9 MPa, which was nevertheless well above the 4 MPa stipulated in the standard. In addition to the compressive strength tests, all the specimens were broken in order to assess the homogeneity of the binder in the middle of the block. It can be verified on the pictures of Figure 28 (a and b) that the distribution and rigidity of the geopolymer binder were perfect throughout the concrete, unlike what was observed in the previous laboratory tests.

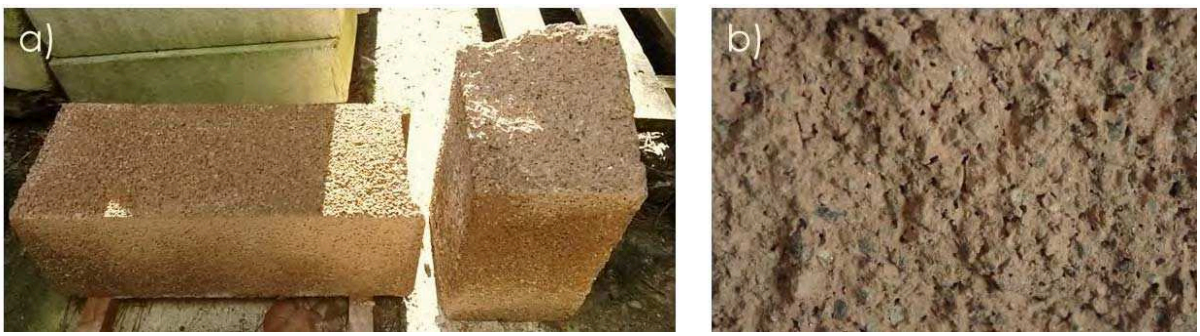

Figure 28. *a) $GP_{MU}1$ full unit and after breaking b) observation of the inside of the unit after breaking.*

It should be noted that the first formulation, $GP_{MU}1$, was also used to make air blade units. In this case, although the immediate release occurred without problems, some blocks were damaged during the transport to the storage warehouse. Intact units were tested in compression and a strength of 4.5MPa was measured at 8 days. For these blocks, a very dry appearance was observed inside the concrete, like the previous observation made in the laboratory. This geopolymer formulation does not give air blade masonry units as efficient as the full MUs, and so would require an optimisation study.

Moreover, two significant aesthetic problems were also noticed on the geopolymer masonry unit. First, a large amount of efflorescence was observed on the block surfaces shortly after the outside storage. This time, the efflorescence appeared faster and was larger that on the beam, almost completely covering the surface of the block with white crystals (Figure 29 a). This crystallisation appeared on all the MU and laboratory blocks as soon as the specimens were moistened (rainwater). These observations recall the importance of evaluating the carbonation reaction in a geopolymer matrix, which will be treated in Chapter III.

Figure 29. *GP_{MU} full unit presenting a) efflorescences and b) surface scaling.*

The exposure of geopolymer dry concrete to rain water also caused surface scaling. This phenomenon was noticed after a few months, when there was an increase in precipitation. Lateral walls of some MU lost their superficial layers of binder thus resulting, as seen on Figure 29 b, in walls on which the aggregates were exposed. This phenomenon, resembling scaling or leaching, was not anticipated, especially as the beam made with the same binder and also stored outdoors did not show these symptoms. This would imply that the geopolymer binder was weaker, especially with respect to water, when present in too small a quantity.

However, the use of industrial porous aggregates could also be responsible for the poorer adhesion with the binder, resulting in the observed leaching. In fact, the results found earlier, highlighting the good adhesion between the binder and the aggregates, were obtained using well-crystallised, non-porous siliceous aggregates. So the nature of the aggregates may have had a detrimental impact on the binder-aggregate interface.

Thus this study on the manufacture of dry concrete has shown that, with appropriate equipment, it is possible to make masonry units similar to those made with OPC. Only the air blade blocks failed to achieve the desired performance and would require an optimisation study. The efflorescence and scaling problems highlighted the necessity to study the carbonation reaction and the influence of the nature of the aggregates on the durability of the geopolymer.

2.3 Concrete incorporating bio-sourced aggregates

The plant in which the geopolymer concrete blocks were made has diversified its product range by manufacturing concrete incorporating bio-sourced aggregates for the production of masonry units with high insulating potential. To make the most environmentally friendly products, they use a formulation based on a lime-metakaolin binder mixture (Magniont, 2010) without any Portland cement. However, the use of this binder only allows the manufacture of filling masonry units because the 4 MPa required for load bearing units cannot be achieved without incorporating some CEM I. Tests were therefore performed to assess whether the geopolymer could increase the performance of these bio-sourced concretes without the need to add cement. Two concretes incorporating bio-sourced aggregates, hemp and wood, were designed according to the formulation made in the plant (Table 7).

The masonry units were manufactured in the same way as with mineral aggregate, and led to proper full blocs incorporating hemp or wood (Figure 30), but the high viscosity of the binder did not allow air blade blocks to be made. The compressive strength of full masonry units was tested at 8 days, and the resulting value presented in Table 7 shows that they failed to increase the performance to 4 MPa.

Table 7. Formulations and mechanical strengths of geopolymer MU made with bio-sourced aggregates in SEAC "Guiraud frères" precast plant, 09120 Varilhes, France.

	GP_{MU}Hemp	GP_{MU}Wood
H_2O/Na_2O molar ratio	14.5	14.5
Mass % of aggregates	16%	30%
Mass % of water	25%	20%
Formulation (kg/m^3)		
Solid binder (Mk + $Silicate_{solid}$)	283.1	283.5
Total water	118.7	119.0
Aggregates	78.4	174.7
Results at 8 days		
Compressive strength (MPa)	≈ 1.5	≈ 0.5

Visual observations of the inside of the blocks after breaking showed very different behaviour of the binder according to the nature of the bio-sourced aggregates. Hemp concretes showed a homogeneous distribution of hardened geopolymer binder, as for mineral aggregates but, in contrast, wood concrete did not present such good consolidation of the binder. The blocks made with wood aggregates all presented the same texture and appeared to be made up of very friable red-orange powder agglomerates. It would seem that the geopolymerisation reaction did not take place properly. No literature could be found on the subject but the problem may have come from a detrimental interaction of the sugar provided by the wood during the geopolymer gel phase. In addition, very large efflorescence was observed in the hemp and wood units, probably due to the large amount of binder in these concretes.

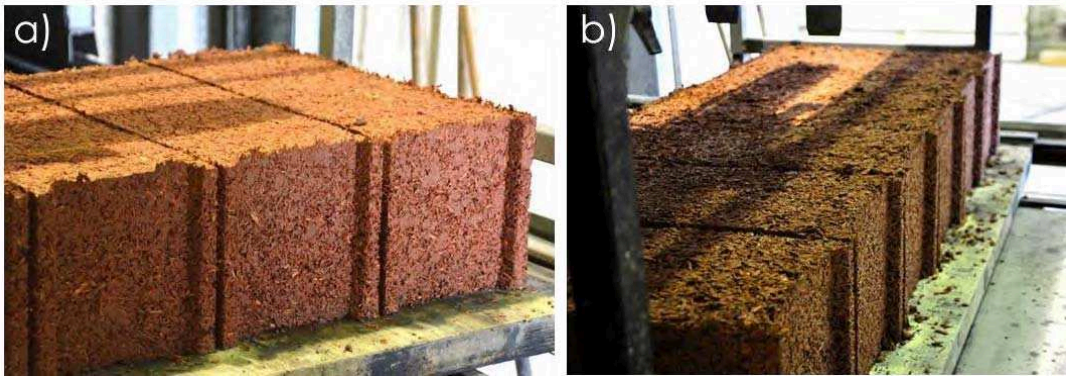

Figure 30. *GP_{MU} full unit incorporating a) hemp and b) wood aggregates.*

Despite these results, the use of geopolymer as a binder for bio-sourced concrete could be an interesting application, but would require further studies on the raw materials and the formulations.

In short

Fluid concrete	As OPC, consistency class between S3 and S4 allows the coating of the reinforcing steels
Dry concrete	Formulation and performance similar to OPC with the right vibro-compaction system
Scale effect	Similar behavior for mixture of 6L, 200L or 540L
Durability issues	• Carbonation causing efflorescences • Binder-aggregates adhesion problems
Bio-sourced concretes	Possible application of geopolymer binder which would require optimization studies
Industrialisation	Not problems noted using geopolymer in precast plant installation

The second part of this chapter has shown that the consistency classes used to determine the possible applications of traditional Portland cement are applicable to geopolymers, at least in the case of classical reinforced concrete structures and dry concrete for masonry units. No significant scale effects were observed and the use of geopolymer in an industrial environment was validated. Two issues related to the durability of geopolymer concrete structures were raised and will be the subject of studies in the next two chapters.

VII. Conclusion

The current literature tends to show that, despite a lack of standards, the fabrication and industrialisation of geopolymer concrete are possible for a wide range of applications. The results obtained and presented in this chapter have led to similar conclusions.

The formulation study of geopolymer concretes showed that, in the presence of non-porous siliceous aggregates, the metakaolin-based geopolymer activated by a sodium silicate solution was able to replace a traditional Portland cement. The range of possible applications was found to be almost as wide as for the OPC according to the slump test. Despite the results on the total porosity, which appears to be larger than in OPC concrete, the compressive strength could reach more than 60 MPa in 7 days. It was also highlighted that, unlike cement, geopolymer concrete would not present ITZs at their binder-aggregate interfaces, and that the size and amount of aggregate would have a negligible effect on the performance of the concrete.

Further tests showed that making reinforced beams using the same consistency classes as used with OPC validated the use of geopolymer binder for this application despite the higher viscosity of the mixture. Using a precast plant installation allowed geopolymer masonry units to be made, showing that, even with a high binder/aggregate mass ratio, geopolymer binder can lead to the same performance levels as cement. Geopolymer concrete mixed in batches of 10 L, 200 L, or 1 m^3 showed similar behaviour, demonstrating an absence of scale effect for these matrices, and the feasibility of using them in an industrial plant.

Finally, these studies have emphasised the importance of assessing the durability of these new materials because even the non-aggressive conditions found in an ordinary outside environment were revealed to be detrimental for the appearance of the geopolymer concretes. Thus the needs to study the mechanisms of carbonation leading to efflorescence, and the influence of the nature of the aggregates used at the binder/aggregate interface, have been noted.

References

Baroghel-Bouny V. et al., (2004) Conception des bétons pour une durée de vie donnée des ouvrages, Maîtrise de la durabilité vis-à-vis de la corrosion des armatures et de l'alcali réaction. *Etat de l'art et Guide pour la mise en œuvre d'une approche performantielle et prédictive sur la base d'indicateurs de durabilité.* Association Française de Génie Civil.

Capros, P., Kouvaritakis, N., Mantzos, L. (2001) Economic Evaluation of Sectoral Emission Reduction Objectives for Climate Change: Top-down Analysis of Greenhouse Gas Emission Possibilities in the E.U., *Contribution to a Study for DG Environment*. European Commission

Demie, S., Nuruddin, M.F. and Shafiq, N. (2013) Effects of micro-structure characteristics of interfacial transition zone on the compressive strength of self-compacting geopolymer concrete. *Construction and Building Materials.* 41: 91-98. DOI: 10.1016/j.conbuildmat.2012.11.067.

Duxson P., Provis, J. L., Lukey, G. C., Van Deventer, J.S.J. (2007b), The role of inorganic polymer technology in the development of 'green concrete'. *Cement and Concrete Research*, 37(12): 1590-1597. DOI: 10.1016/j.cemconres.2007.08.018.

Habert, G., d'Espinose de Lacaillerie, J.B., Roussel, N. (2011) An environmental evaluation of geopolymer based concrete production: reviewing current research trends. *Journal of Cleaner Production*, 19(11): 1229-1238. DOI: 10.1016/j.jclepro.2011.03.012.

Johnson, G., Gourley, G. (2005) Developments in geopolymer precast concrete. *Geopolymer, Green Chemistry and Sustainable Developpement Solution*, G. Institue, pp. 139-143.

Lee, W.K.W. and Van Deventer J.S.J. (2004) The interface between natural siliceous aggregates and geopolymers. *Cement and Concrete Research*. 34(2): 195-206. DOI: 10.1016/S0008-8846(03)00250-3.

Magniont, C., (2010) Contribution à la formulation et à la caractérisation d'un écomatériau de construction à base d'agroressources. Université de Toulouse, Toulouse 340 (PhD (in French)).

McLellan, B. C., Williams, R. P., Lay, J., Van Riessen, A., Corder, G. D. (2011) Costs and carbon emissions for geopolymer pastes in comparison to ordinary portland cement. *Journal of Cleaner Production*, 19(9–10):1080-1090

Pacheco-Torgal, F., Castro-Gomes J. and Jalali, S. (2007) Investigations about the effect of aggregates on strength and microstructure of geopolymeric mine waste mud binders. *Cement and Concrete Research*. 37(6): 933-941.

Palomo, A., Krivenko, P., Garcia-Lodeiro, I., Kavalerova, E., Maltseva, O., Fernández-Jiménez, A. (2014) A review on alkaline activation: new analytical perspectives. *Materiales de Construcción*, 64(315). DOI: 10.3989/mc.2014.00314

Sakulich, A. R. (2011) Reinforced geopolymer composites for enhanced material greenness and durability, *Sustainable Cities and Society*, 1(4): 195-210.

Van Deventer, J.S.J., San Nicolas, R., Ismail, I., Bernal, A. S., Brice, D. G., Provis, J. L. (2014) Microstructure and durability of alkali-activated materials as key parameters for standardization, *Journal of Sustainable Cement-Based Materials*, DOI: 10.1080/21650373.2014.979265

Chapter III.

Carbonation of metakaolin-based geopolymer

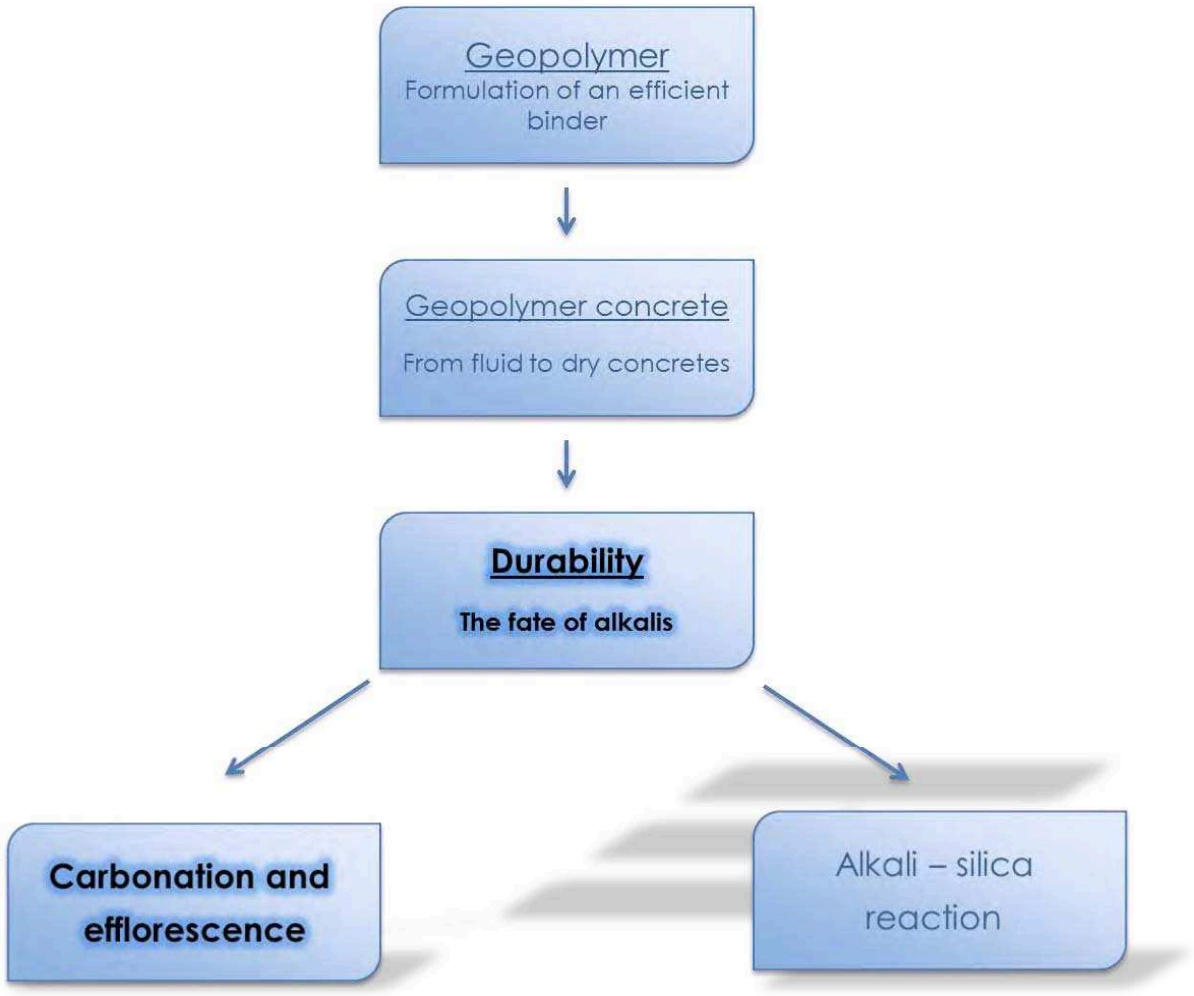

Table of contents

I. Introduction

The carbonation of Portland cement pastes is known to be a slow reaction leading to the formation of insoluble calcium carbonate deeper and deeper in the structure. The consequence of this carbonation is a gradual decrease in the pH of the pore solution. The pH can reach a value lower than 9, which is the limit value for the depassivation of steel in concrete, and can thus cause corrosion by carbonation. In addition, the dissolution of CO_2 in the pore solution could lead to carbonates formation and cause efflorescence (white crystals appearing on the surface). Studies of carbonation are usually performed in accelerated conditions (atmosphere with a higher concentration of CO_2) and the carbonation front is followed by means of a coloured indicator (phenolphthalein). In geopolymer based on metakaolin having a very low calcium content, dissolved CO_2 reacts with the abundant alkalis in the pore solution to form alkali-carbonates. For geopolymer activated by sodium silicate, it has been shown (Bakharev et al., 2001; Bernal et al., 2010; Criado et al., 2005; Bernal et al., 2012) that sodium carbonates are formed but the high solubility of these carbonates and their pH greater than 10 may make the use of existing standard tests unsuitable. In addition, it has been suggested that accelerated tests are not representative of the reaction taking place in natural conditions, and may result in the formation of sodium bicarbonate (Bernal et al, 2012).

This study aims to evaluate the behaviour of metakaolin-based geopolymer pastes activated by sodium silicate in the presence of CO_2 (natural and accelerated conditions) to assess the potential risks of durability associated with this reaction. A first part was therefore dedicated to the study of the pore solution in order to identify the products of the reaction, determine the impact of this reaction on the pH, and assess the resulting risk of this reaction by using infrared spectroscopy and chemical titrations. In this section, the relevance of the existing tests standardised for cementitious matrices will also be assessed. Then a study of sodium carbonate in the form of crystals (efflorescence), carried out in order to characterise the compounds formed and to determine the parameters influencing their growth, will be described.

Parts of the results obtained in this study have led to a publication and an oral communication in an international Congress: *Pouhet, R., and Cyr, M. (2014). Studies of Natural and Accelerated Carbonation in Metakaolin-Based Geopolymer. In Advances in Science and Technology (Vol. 92, pp. 38-43).*

II. Carbonation of alkali-activated materials

The reaction occurring between carbon dioxide from the air and the cement matrix is called carbonation. It is one of the most harmful degradation processes and can drastically affect the long-term durability of civil infrastructures (Hobbs, 2001, Glasser et al., 2008). The reaction mechanisms and the consequences of this reaction on cement structures are widely known and many standardised tests exist to assess the kinetics and the impact of this reaction. After a description of the carbonation phenomena in the cement matrix, a review of existing literature on the carbonation reaction and consequences occurring in alkali-activated materials will be presented.

1. Carbonation in OPC

1.1 Carbonation reactions

The carbon dioxide (CO_2) of the air, in gaseous form, can penetrate concrete through the porous network or cracks. In the presence of water, this gas is diluted and forms carbonate in solution, according to the following reaction (Ollivier and Vichot, 2008):

$$CO_2 + H_2O \leftrightarrow H_2CO_3 \quad (1)$$

$$H_2CO_3 + H_2O \leftrightarrow HCO_3^- + H_3O^+ \quad (2)$$

$$HCO_3^- + H_2O \leftrightarrow CO_3^{2-} + H_3O^+ \quad (3)$$

The main reaction occurring in cement pore solution after this carbonate formation is the conversion of the cement hydration products, particularly calcium hydroxide $Ca(OH)_2$, into insoluble calcium carbonate (Equation 4) (Usdowski, 1982 and Cowie et Glasser, 1992). However, it should be noted that the alkalis (NaOH, KOH) present in small amounts in the cement pore solution may also be carbonated (Equations 5 and 6).

$$H_2CO_3 + Ca(OH)_2 \leftrightarrow CaCO_3 + 2H_2O \quad (4)$$

$$H_2CO_3 + 2KOH \rightarrow K_2CO_3 + 2H_2O \quad (5)$$

$$H_2CO_3 + 2NaOH \rightarrow Na_2CO_3 + 2H_2O \quad (6)$$

The presence of alkali carbonate in solution is known to increase the solubility of calcium hydroxide, as presented in Equations 7 and 8, which may then be carbonated in larger quantities:

$$K_2CO_3 + Ca(OH)_2 \rightarrow CaCO_3 + 2KOH \quad (7)$$

$$Na_2CO_3 + Ca(OH)_2 \rightarrow CaCO_3 + 2KOH \quad (8)$$

1.2 Consequences of carbonation for OPC

The most damaging consequence of the carbonation of concrete is due to the reaction presented in Equation 4 and corresponds to the dissolution of the portlandite. Portlandite constitutes the most significant hydroxide (OH^-) supply of the cement paste, maintaining a high pH of 12.5, so the consumption of this hydrate will lead to a reduction of the pH of the pore solution, possibly to a value under 9. This low pH will have a major impact in the case of reinforced structures because, at this basicity (pH < 9), the reinforcement steel loses its passivation layer (Pourbaix, 74), and can then corrode. Once the corrosion of the reinforcement has started, localised (Figure 1) or generalised bursting may result.

Figure 1. *Example of carbonation on a building facade (from http://www.cement.org)*

Carbonation in the cementitious system may also be responsible for the appearance of efflorescence. Efflorescence is the growth of salt crystals on a surface, caused by the evaporation of salt-laden water. In building materials, efflorescence refers to a deposit, usually white, that occasionally develops on the surface of the materials (Figure 2). This phenomenon is generally harmless and may only be an aesthetic problem but, in some cases, excessive efflorescence can cause expansion in regions close to the surface and may finally disrupt the material surface (Allahverdi et al., 2014).

The mechanism of efflorescence formation can be described by chemical and physical processes involving: presence of dissolved calcium and carbonate, presence of water, capillary action, hydrostatic pressure, and evaporation. In Portland-cement-based materials, it mainly consists of calcium carbonate formed as shown in Equation 4. In fact, the soluble calcium hydroxide of the pore solution migrates to the concrete surface, either after having already been dissolved in the mixing water of the fresh concretes or when the hardened concrete is exposed to the effect of rain or dew. Once the concrete surface is reached, the calcium hydroxide reacts with carbon dioxide in the air to form water-insoluble calcium carbonate (Kresse, 1989; Bensted 2000; Norsuzailina et al, 2013).

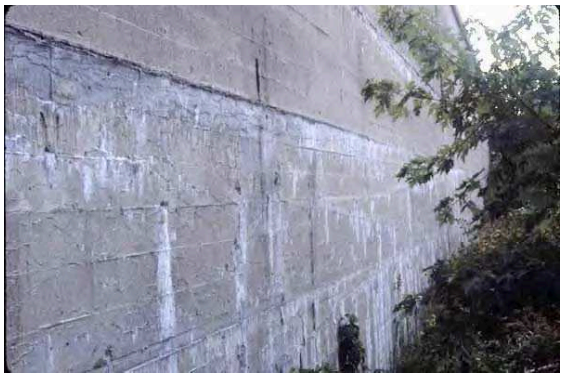

Figure 2. *Illustration of efflorescence on concrete wall (from http://www.concrete.org)*

1.3 Standards and test methods for control and prevention of carbonation

The relatively low concentration of CO_2 in the atmosphere (0.03 – 0.04%) makes carbonation a slow process in dense, chemically stable cementitious materials. This has led to the development of accelerated testing methods exposing the material to high CO_2 concentrations, from 0.1% to 50% to induce faster carbonation. As carbonation in a cementitious matrix leads to a decrease in pH, the propagation of the reaction is observed in the concrete using a coloured indicator, phenolphthalein, which is pink under basic conditions (pH > 9) and is colourless below this value. Thus, when the concrete is exposed to this indicator the carbonated zone (<9) and the non-carbonated zone (>9) can be easily distinguished, as shown in Figure 3. The limit between these two colours is called the carbonation front and its measurement over time provides a kinetics of carbonation often used in the study of the resistance of concrete to CO_2.

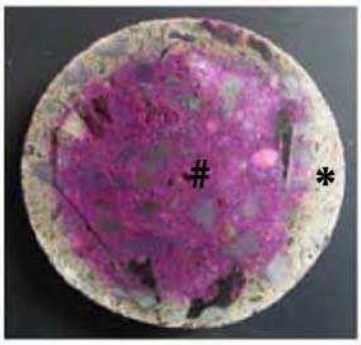

Figure 3. *Example of phenolphthalein test showing the carbonated (#) and non-carbonated (*) zones of the concrete (From Bernal et al., 2011)*

The summary of accelerated test methods presented on Table 1 was made by Bernal (2014). In these tests, the atmosphere is always artificially concentrated in carbon dioxide (from 0.1% to 50%) and the indicator used is always phenolphthalein, but the reproducibility and the repeatability of the results obtained by following different accelerated carbonation protocols has been strongly questioned (Sanjuan et al., 2003). Nevertheless, these tests assessing the kinetics of carbonation are used to compare and optimise concrete formulations.

Table 1. Summary of accelerated test methods (from Bernal, 2014)

Test	Sample preconditioning required	Indicator	Exposure conditions
BS EN 13295:2004	Specimens covered with a plastic film for 24h, then demoulded and sealed again with a plastic film for 48h. After this, the samples are aged and preconditioned for 25 days under the same temperature and humidity conditions specified for the carbonation testing.	1g of phenolphthalein dissolved in 70 mL of ethanol, diluted to 100 mL with distilled or deionised water	$[CO_2]$ -1%, T- 21 ± 2ºC RH- 60 ± 10%
RILEM CPC-18	Not specified	solution of 1% phenolphthalein in 70% ethanol	$[CO_2]$ – Not specified T- 20ºC RH - 65%
NORDTEST METHOD: NT Build 357	Specimens are stripped 1 day after casting, and cured in water at 20 ± 2ºC for 14 days, then cured in air at 50 ± 5% RH, 20 ± 2ºC until reaching a total of 28 days of curing	1g phenolphthalein dissolved in 500 mL of distilled/ion exchanged water, and 500 mL ethanol	$[CO_2]$ -3%, T- not specified RH – 55-65 %
Portuguese Standard LNEC E391	Samples cured submerged in water for 14 days at 20 ± 2ºC, and stored in an enclosed environment at 50 ± 5% RH and 20 ± 2ºC until 28 days	0.1% of phenolphthalein in an alcoholic solution	$[CO_2]$-5 ± 0.1% T- 23 ± 3ºC RH – 55-65 %
French test method AFPC-AFREM. (AFPC-AFREM, 1997).	Specimens after 28 days of curing (immersed in water) are storage in controlled climatic conditions of 50% RH and 20°C until constant weight	0.1% of phenolphthalein in an alcoholic solution	$[CO_2]$ -50%, T- 20°C RH – 65 %

Regarding the efflorescence phenomenon, it is not possible to totally eliminate efflorescence formation in cement-based materials but long-term experiments on calcium-based hydrated products have led to recommendations for reducing its appearance (Allahverdi et al, 2014):

- Minimise free soluble salts from raw materials
- Minimise concrete permeability
- Avoid the exposure of concrete to uneven moisture conditions

Many efflorescence control admixtures have also been developed for cement concrete systems. They close the pores to prevent efflorescence migration to the surface or just to limit its appearance.

2. Carbonation of geopolymer

There are a limited number of published studies evaluating carbonation of alkali-activated materials, and far fewer were found on low calcium content systems. In a first step, our survey focused on the reaction product obtained by natural and accelerated carbonation in an alkali-activated system. A review of the articles found that discuss the carbonation of a geopolymer system is presented below. Finally, studies addressing the problems of efflorescence in geopolymer are investigated.

2.1 Product of carbonation reaction in AAM systems

In the carbonation of slag activated by sodium hydroxide or silicate, the reaction product obtained is mainly calcium and sodium carbonates, formed according to Equations 4 and 6 (Palacios and Puertas, 2006; Bernal et al., 2010). Palacios and Puertas (2006) identified calcium carbonate polymorphs, calcite, vaterite and aragonite, as the main crystalline accelerated carbonation products of these silicate-activated slag binders. Bernal et al. (2010) only found calcite as the calcium carbonate polymorph formed by carbonation. The differences in the carbonation products formed in these materials are mainly attributable to the exposure conditions used in each study: R.H. maintained at 43.2% in a K_2CO_3 solution for Palacios and Puertas, and 3% of CO_2 at 20°C and 65% R.H. for Bernal et al.

These differences in the accelerated conditions also led to the formation of different reaction products, as the first study found sodium carbonate in the form of natron ($Na_2CO_3 \cdot 10H_2O$), while Bernal et al. identified trona ($Na_3(CO_3)(HCO_3) \cdot {}_2H_2O$). Concerning these two sodium carbonates, Bernal et al. (2012, 2013) found that, under atmospheric CO_2 concentrations, the formation of natron ($Na_2CO3 \cdot 10H_2O$) was favoured while, under accelerated carbonation testing conditions (CO_2 concentrations between 1% and 100%), the formation of nahcolite ($NaHCO_3$) prevailed (Figure 4). These authors also showed that the formation of trona was favoured over natron when the temperature of exposure increased slightly, whatever the CO_2 concentration.

The authors also stated that modifications of the carbonate(natron)/bicarbonate(trona) phase equilibrium favouring the formation of bicarbonates would lead to a more notable decrease in pH, by as much as 2 pH units (Bernal et al., 2012).

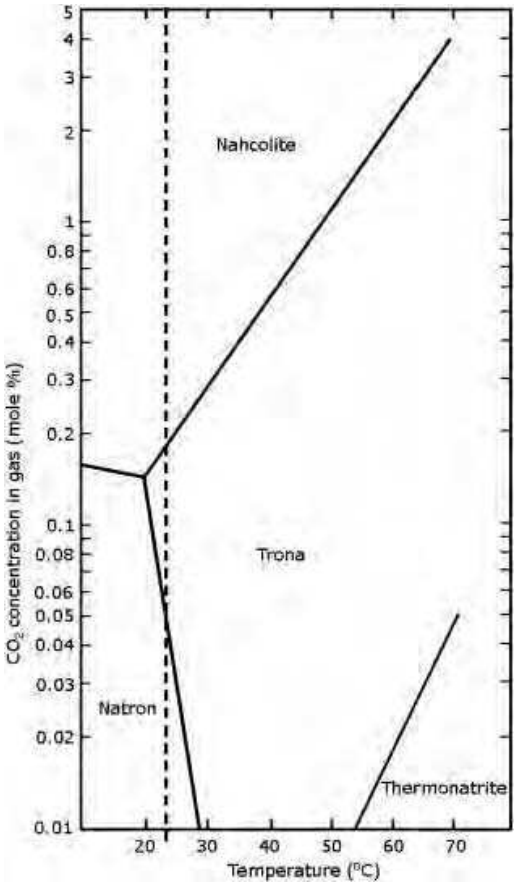

Figure 4. *Phase diagram as a function of temperature and gas phase CO_2 concentration for the Na_2CO_3—$NaHCO_3$—CO_2—H_2O system in an air atmosphere at ambient pressure. (From Bernal et al., 2012)*

In a recent study (Bernal et al., 2013), huntite ($Mg_3Ca(CO_3)_4$) was also observed as an accelerated carbonation product derived from the degradation of hydrotalcite (one of the secondary products in alkali-activated slag binder) in the presence of high CO_2 concentrations.

2.2 Carbonation of geopolymer

The largest number of published studies on the carbonation of alkali-activated systems concern slags, and they seem to be in general agreement that these materials are more susceptible to carbonation than conventional Portland cements (Bernal, 2014). No references were found on the carbonation of pure metakaolin-based geopolymer but two recent studies (2005 and 2014) focusing on fly ash based geopolymer having a low calcium content gave information on the carbonation of these systems.

First, in 2005, Criado et al. (2005) assessed the effect of the curing conditions on the carbonation products of class F fly ash geopolymer (calcium content 2.44%). The geopolymers formulated in this study were made with sodium hydroxide or silicate, and a "solution/ash" ratio of 0.4, and all the specimens were then heated at 85°C for variable lengths of time. Two tests methods were tried, one exposing the specimens to carbonation at early age and the other preventing their carbonation. XRD and IRTF were used for mineralogical characterisation in this study, and ion chromatography was used to determine the soluble sodium content. For this measurement, the sodium was previously extracted from the materials by immersion in deionised water after having undergone vacuum drying. The degree of reaction was also measured according to the procedure published by Granizo et al. (2002).

Using XRD, they identified that, when the fly ash was activated with sodium hydroxide, herschelite (form of zeolite having $NaAlSi_2O_6$, $3H_2O$ formulation) was formed, but when a sodium silicate was used, sodium bicarbonate appeared without any herschelite. Moreover, for the whole duration of thermal treatment (5, 12, 20 h or 7 days) and whatever the type of alkali activating solution used (hydroxide or silicate), all the IFTR spectra showed an intense band in the 1450 cm^{-1} region, characteristic of alkali carbonates. It should be noted that the presence of sodium bicarbonate and not sodium carbonate was in agreement with the Na_2CO_3 - $NaHCO_3$ - CO_2 - H_2O diagram (Figure 4) presented by Bernal et al. (2012) and would be due to the heat treatment.

According to the authors, carbonation occurred very rapidly during the early stages of the process when the material was in contact with the atmosphere. This fast carbonation, inducing the formation of sodium bicarbonate, would lead to a decrease of pH and therefore a less efficient activation of the ashes. This initial carbonation process can be avoided by simply controlling the environmental curing regime (high relative humidity).

More recently, Badar et al. (2014) have studied the corrosion of steel bars induced by accelerated carbonation in low and high calcium fly ash geopolymer concretes. In this study, three fly ashes, all class F according to ASTM C 618, were used as main precursors for the production of geopolymer concretes. These fly ashes contained 1.97%, 5% and 12.93% of calcium. The fly ash systems were activated with a blend of commercial sodium silicate and 14 M of sodium hydroxide. Cylindrical reinforced concrete specimens 15 cm in height by 7 cm in diameter, were cast and cured at 80°C for 72 h. A single carbon steel deformed rebar, 300 mm in length and 6 mm in diameter, was sand blasted and placed at the centre of each cylindrical mould prior to casting of the concrete. The concretes were then placed in accelerated carbonation conditions at 24°C, 65% R.H. and 5% of CO_2. Control samples were also made and stored under the same temperature and humidity conditions but with atmospheric CO_2 content. These samples were used as "non-carbonated" references despite the possible natural carbonation. The carbonation depth of the geopolymer concretes after 450 days of CO_2 exposure was evaluated using two pH indicators: phenolphthalein (purple/pink to colourless at pH 10 to 8.3) and alizarin yellow R (red to yellow at pH 12 to 10.1). Indirect tensile strength measurement (ASTM C 496-96), pore structure characterisation (by mercury intrusion porosimetry), XRD analysis and measurement of corrosion potential (ASTM C876) were also performed on the samples and control.

It was found that, for all the concrete formulations, accelerated carbonation led to a remarkable decrease in the pH, a reduction in the mechanical strength properties, and an increase in the total porosity. The drop in pH, in both low-Ca and higher-Ca fly ash geopolymers (Figure 5), was associated with the carbonation of the pore solution, as sodium carbonates were observed as the main reaction products formed in specimens exposed to 5% of CO_2.

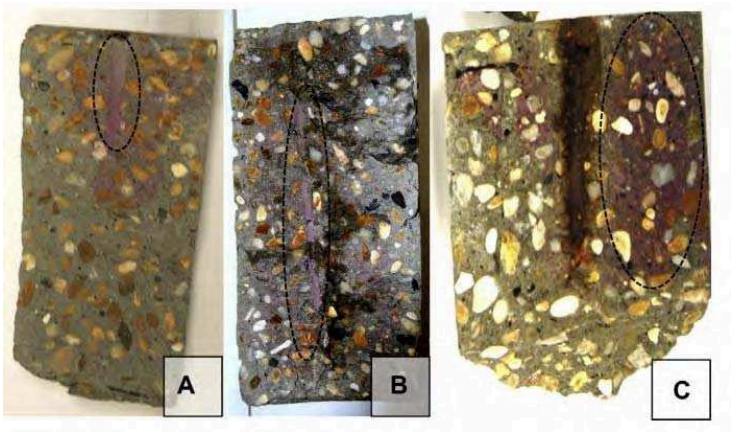

Figure 5. *Photographs of geopolymer concrete produced with fly ashes having (A) 1.97%, (B) 5% and (C) 12.93% of CaO, sprayed with the phenolphthalein indicator after 450 days of CO_2 exposure (From Bardar et al., 2014).*

Electrochemical testing showed that, up to 200 days, the high alkalinity of the system promoted the passivation of the steel rebar under natural CO_2 content but seemed to lead to a corrosion process after that. The results in accelerated conditions were inconclusive. A much better resistance to corrosion for the geopolymer made with low-calcium content was also noted.

The authors concluded this study by stating that low-Ca class F fly ashes were more suitable than those containing higher levels of Ca for the production of steel-reinforced geopolymer concrete from a durability point of view, as the chemical and physical properties of these materials seemed to reduce the risk of corrosion in the steel reinforcement.

2.3 Efflorescence in geopolymer

Like those on carbonation, published studies assessing efflorescence problems in geopolymer are limited, although these materials have shown a higher tendency to efflorescence formation than OPC, mainly due to the following characteristics (Allahverdi et al., 2014):

- Open microstructure resulting in higher permeability (Škvára et al., 2009).
- High alkali concentration in the pore solution (Lloyd et al., 2010).
- Weak binding property of sodium cations in the aluminosilicate framework (Szklorzová et al., 2008; Bortnovsky et al., 2008; Škvára et al., 2012).

Allahverdi et al. have studied and compared the efflorescence in alkali-activated natural pozzolan and slag systems (2008, 2010, and 2011). In all their studies, they conducted the same test in order to compare the efflorescence formed: after 28 days of curing, a 2x2x2 cm cube was placed in 50 mL of water and kept in an open-air atmosphere at 25°C until complete evaporation of the water. Regarding the natural pozzolan geopolymers and based on qualitative comparison (e.g. Figure 6), they showed that the amount of efflorescence formed did not depend on the Na_2O concentration alone, although it was the most notable factor, but that the silica modulus of the alkali activator and the water/binder ratio also had an influence on the efflorescence (Allahverdi et al., 2008). They also concluded in this study that the high compressive strength achievable with high Na_2O concentration did not necessarily indicate soundness and durability.

Pacheco-Torgal and Jalali reached the same conclusion in their study concerning the influence of sodium carbonate addition on the thermal reactivity of tungsten mine-waste mud-based

binders. They found that the samples that presented the highest compressive strength were also those that led to much greater efflorescence. This means that even an early high compressive strength does not always indicate a stable structure formation (Pacheco-Torgal and Jalali, 2010). The same procedure applied to alkali-activated slags led to the conclusion that, below 3% of sodium oxide by weight of slag, specimens showed a slight to moderate tendency to efflorescence but, above 4.5%; a severe risk of efflorescence was expected (Allahverdi et al., 2010). They finally studied the influence of the incorporation of slag in a geopolymer based on natural pozzolans and showed that, in the optimal amount, this incorporation could reduce the formation of efflorescence, without necessarily improving the compressive strength (Allahverdi et al., 2011). They thus reached an optimal formulation in terms of efflorescence and compressive strength (36 MPa) by mixing 5 wt.% of blast-furnace slags and 8 wt.% of Na_2O with a w/c ratio of 0.3.

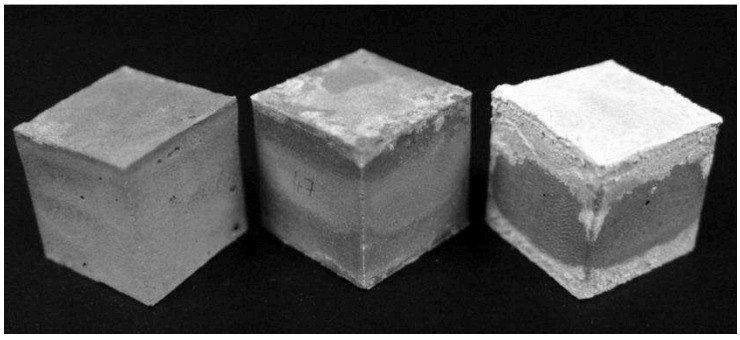

Figure 6. *Natural pozzolan geopolymers exhibiting (from left): no, slight, and severe efflorescence (from Allahverdi et al., 2008).*

Škvára et al. have focused their work on the bond between alkali and geopolymer framework based on low-calcium brown coal fly ash or metakaolin (Škvára et al. 2009, 2012). In their first study, they assessed the impact of temperature, from 20°C to 1000°C, on the binder susceptibility to exhibit efflorescence, and found that the tendency for efflorescence formation declined substantially when the material was fired at temperatures higher than 600°C (Škvára et al., 2009). Based on ^{23}Na NMR MAS spectral analysis, they explained this phenomenon by saying that in geopolymer, the alkalis are bonded to Al in an Si-O-Al chain structure in the form of $Na,K(H_2O)_n^+$ rather than as Na^+ and K^+. In this form, the bond with the aluminium is weaker than the direct bond of Na^+, which would explain the ease with which alkali is leached out of the alkali-activated binder and thus the formation of efflorescence. So a heat treatment at more than 600°C would allow the elimination of the residual water around the alkali, and would promote the formation of alkali metal bonds.

In their most recent study published in 2012, they carried out a series of long-term leaching experiments on alkali-activated fly ash and metakaolin in deionised water (Škvára et al., 2012). By comparing the results obtained (compressive strength, NMR MAS, SEM and leaching modelling) for leached and unleached specimens, they concluded that the alkali could be simply removed from the material without affecting the gel structure and without any significant loss in strength. According to the author, the main role of the alkalis is to create a strongly basic environment for the dissolution of the aluminosilicate precursors and, after gel formation, they remain in the nanostructure of (Na,K)-A-S-H as unnecessary load-bearing remnants from the activating solution. Using the model of Barbosa et al. (Barbosa et al., 2000) they explained their results by saying that cavities of sufficient size to accommodate the charge-balancing hydrated alkali in the form $Na,K(H_2O)_n^+$, provided by the randomly oriented Al and Si polymeric chains, might as well be occupied by H_3O^+ (Figure 7 a and b). This would explain the negligible loss of strength observed despite the alkaline leaching.

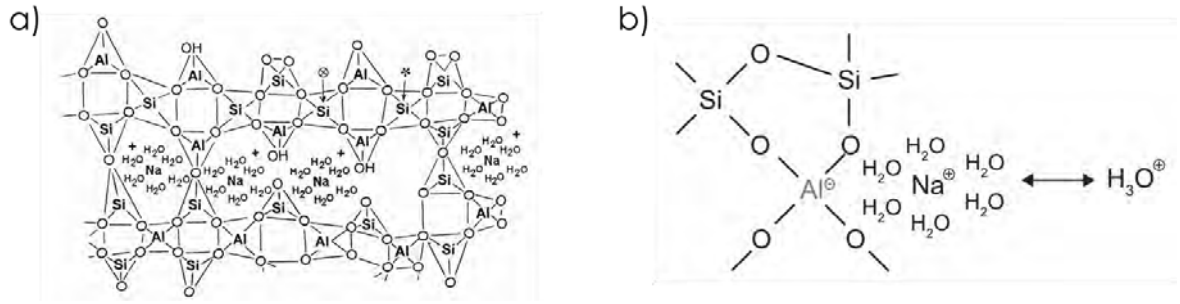

Figure 7. *(A) Semi-schematic structure for Na–polysialate polymer (from Barbosa et al. 2000) and (B) bond according to Barbosa et al. and its replacement with an H_3O^+ cation during leaching (from Škvára et al., 2012).*

Finally, Kani et al. (2012) and Suchý et al. (2014) focused their work on controlling the formation of efflorescence in alkali-activated systems. First, it was published that the efflorescence in geopolymeric binders derived from natural pozzolanic precursors could be reduced either by the addition of alumina-rich admixtures or by hydrothermal curing (Kani et al., 2012). According to these authors, each of these techniques provides benefits by enhancing the binder structure formation process.

Then, in 2014, Suchý et al. showed that a considerable amount of efflorescence in alkali activated blast furnace slag could be avoided with an addition of $AlF_3{\cdot}3H2O$ (Suchý et al. 2014). This chemical compound would react with sodium cations in solution to form insoluble $2Na_3[AlF_6]$, thus greatly limiting their leaching and the formation of efflorescence. However, since the dose of $AlF_3{\cdot}3H_2O$ in alkali activated slag had a negative effect on the compressive strength, a compromise between the mechanical properties and the efflorescence must be found.

In short	
Resistance to carbonation for AAM	- High-calcium content: appears lower than OPC - Low-calcium content: inconclusive
Product of carbonation in geopolymer	Alkali carbonate or bicarbonate
Risk of corrosion by carbonation	Possible
Risk of efflorescence formation	High
Effect on the pH	Unquantified reduction
Necessity of accelerated test	unproven and seems to lead to unrepresentative reaction product
Control of the efflorescences	Some thoughts but nothing definite

This review of the literature clearly shows a lack of information on the carbonation of geopolymer and its consequences. It appears that efflorescence is a major issue in these systems, but the risk of corrosion by carbonation and the need for an accelerated test as used for OPC still remains to be evaluated. The risk of efflorescence also needs to be studied in only metakaolin-based systems.

III. Materials and Methods

1. Preparation of samples and cure conditions

The raw materials used for the studies of geopolymer carbonation were the same as previously: flash metakaolin and sodium silicate (Wg1.7). Pure (>99%) sodium carbonate and bicarbonate (VWR®) were also used in this study to make reference samples.

All the pastes for the study of the pore solution were prepared by mixing the components in the following mass percentages: 52% MK, 41.5% Wg1.7, and 6.5% water (corresponding to GP14.5 formulation), until a homogeneous mixture was obtained. Then, the pastes were cast in 91 x 62 x 40 mm plastic moulds, hermetically sealed, and stored at 20°C. After 24 h, the three different curing conditions presented in Table 2 were applied. For cure condition 1, the prisms were not removed from the plastic moulds, in order to prevent any external exchanges. The second condition of cure was achieved by placing the prism in a conditioned room at 20°C and 95% R.H. Finally, a part of the sample was placed in a chamber connected to an inlet for carbon dioxide in order to maintain an atmosphere containing 50% of CO_2 and a relative humidity of 50%.

Table 2. Cure conditions used in the carbonation studies

Cure conditions	Name	Temperature	Relative humidity	CO_2 content
1	Endogenous	20°C	None	None
2	Natural	20°C	95%	Atmospheric
3	Accelerated	20°C	50%	50%

The geopolymer pastes prepared for the study of efflorescence were cast in plastic moulds 33 mm in diameter and 50 mm high. In this part, the formulation GP14.5 is used together with various other additives that will be described specifically in the section concerned.

2. Test methods

2.1 Extraction of the pore solution

A high-pressure device for extracting fluid from porous materials was used to obtain the pore solution of the geopolymer paste (Cyr et al., 2008). At various times, the geopolymer prisms were removed from their cure conditions and crushed to obtain pieces around 20 mm. The

apparatus used (Figure 8) was composed of two thick cylinders ((1) and (2)), fitted into each other and standing on a base plate (3) that contained a solution collector (4). The crushed sample (≈ 300 g) was then placed in the device and compressed by an axial load generated by a 3000 kN hydraulic press on a set of pistons ((5), (6), (7)). As the porous material was compressed, pore fluid was forced into a circular channel and then passed through one of the three holes drilled in the solution collector (4). The solution was collected in a small polypropylene recipient (8), which could be removed through a drawer system (9). The extraction was carried out on a 3000 kN Amsler compression testing machine, using a loading rate of 1 MPa/s up to 1500 kN.

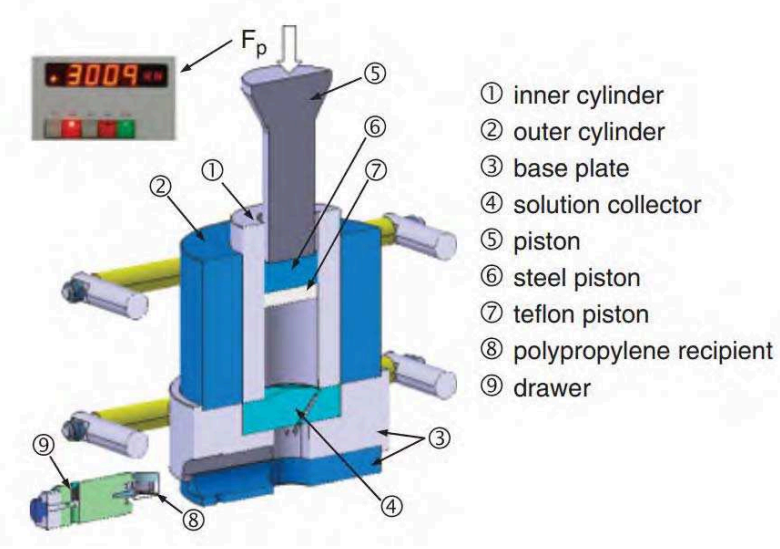

Figure 8. *High-pressure device for extracting fluid from porous materials (From Cyr et al., 2008).*

2.2 Chemical analysis

Directly after the extraction, three consecutive analyses were conducted on the pore solution:

- First, the pH of the solution was measured using a standard pH meter (HACH PH31) previously calibrated between pH 11 and 13.
- Then, a drop of this solution was analysed by Fourier transform infrared spectroscopy (FTIR, Perkin-Elmer Spectrum). The analysis was made by deposition of a drop of pore solution directly on the diamond cell after measurement of the background in the air. The spectrum obtained was an accumulation of 12 measurements made between 4000 cm^{-1} and 800 cm^{-1}.
- Finally, depending on the volume of pore solution collected by extraction (between 2 mL and 10 mL), it was diluted with deionised water so as to obtain a known volume of

solution, named V_b, for pH metric titration with hydrochloric acid. The principle of this titration was to measure the pH of the pore solution depending on the HCl volume (V_a) added. The experimental device used for the titration is schematically represented in Figure 9a.

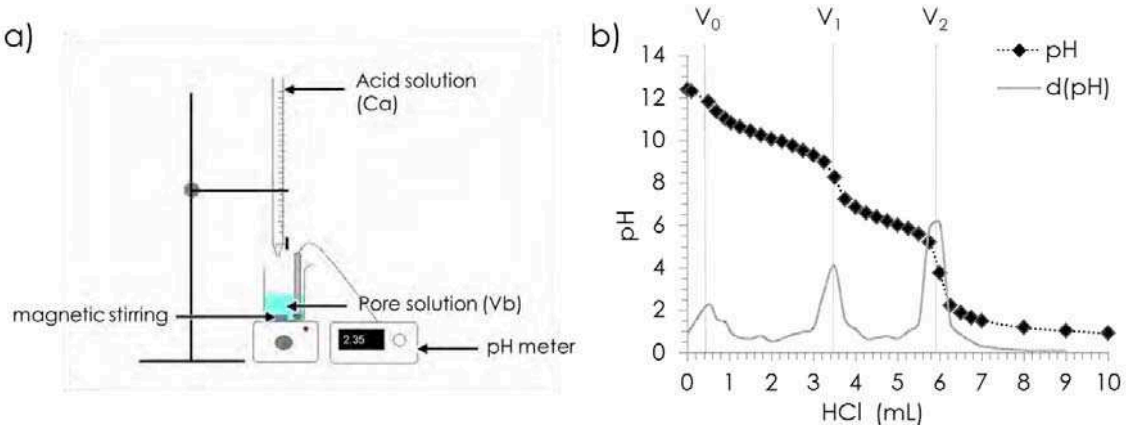

Figure 9. *Diagram of a) a pH metric titration and b) theoretical titration curve.*

The pH of the solution was then recorded for each volume of acid added, and the titration curve was plotted (Figure 9b). The equivalent volumes were obtained by using the derivative of curve. The three equivalent volumes measured ($V_{0, 1, 2}$) are associated to the following three successive reactions:

$$OH^- + H_3O^+ \rightarrow 2H_2O \qquad K_0=10^{14} \qquad (9)$$

$$CO_3^{2-} + H_3O^+ \rightarrow HCO_3^- + H_2O \qquad K_1=10^{10.3} \qquad (10)$$

$$HCO_3^- + H_3O^+ \rightarrow CO_{2aq} + 2H_2O \qquad K_2=10^{6.4} \qquad (11)$$

The unknown concentrations of bases (OH^-, CO_3^{2-} and HCO_3^-) were then calculated using the law of conservation of matter, described by Equations 12, 13 and 14.

$$n_{acid} = n_{base} \qquad (12)$$

$$C_{acid} \times V_{acid} = C_{base} \times V_{base} \qquad (13)$$

$$C_{base} = (C_{acid} \times V_{acid}) / V_{base} \qquad (14)$$

Hydroxide quantification The first equivalent volume V_o measured corresponded to the volume of acid required to react with all the OH^- in the solution, according to Equation (9). The hydroxide concentration could then be calculated by using Equation (15):

$$[OH^-] = (C_A \times V_0) / V_B \qquad (15)$$

Carbonate quantification When there was no more hydroxide in solution, the strong acid reacted with the stronger remaining base in solution (CO_3^{2-}), according to Equation (10). The carbonate concentration was calculated (Equation 16) using the volume of acid required for this reaction (V_1-V_0).

$$[CO_3^{2-}] = (C_A \times (V_1 - V_0))/ V_B \quad (16)$$

Bicarbonate quantification The reaction between carbonate and hydrochloric acid led to the formation of bicarbonate in solution (Equation 13). Being a basic compound, HCO_3^- also reacted with the addition of HCl, according to Equation (11). Its concentration was calculated with the volume of acid required for this reaction (V_2-V_1) using Equation (17):

$$[HCO_3^-] = (C_A \times (V_2 - V_1))/ V_B \quad (17)$$

After removing the dilution factor, the real hydroxide and carbonate concentrations were obtained and other information could be calculated:

Calculation of the carbonation degree The general equation of carbonation taking place in solution is presented in Equation (18). The degree of carbonation, corresponding to the molar amount of hydroxide transformed by carbonation over the molar amount of hydroxide before carbonation, could then be calculated using Equation (19).

$$2OH^-_{\text{aqueous}} + CO_{2\ \text{dissolved gases}} \rightarrow CO_3^{2-} + H_2O \quad (18)$$

$$\%\text{carbonation} = 2[CO_3^{2-}] / ([OH^-] + 2[CO_3^{2-}]) \quad (19)$$

Determination of bicarbonate rate in solution In theory, the bicarbonate present in solution originated from the reaction of the CO_3^{2-} with the acid (Equation 10). Thus, the volumes V_2 - V_1 and V_1-V_0 should be equivalent. However, if some bicarbonate was present before the titration, it was possible to calculated their initial concentration (Equation 20), and so the bicarbonate rate in solution (Equation 21)

$$[HCO_3^-]_{\text{initial}} = [HCO_3^-]_{\text{measured}} - [CO_3^{2-}]_{\text{measured}} \quad (20)$$

$$\%HCO_{3\ \text{in solution}}^- = ([HCO_3^-] - [CO_3^{2-}]) / [HCO_3^-] \quad (21)$$

2.3 Capillary rise test

After seven days of cure at 20°C and 95% R.H., the geopolymer cylinders were placed in a support containing sand submerged by deionised water. The cylinders were submerged from the bottom up in 2 or 3 mm of deionised water, and the support was placed in an air-conditioned room at 20°C at around 60% R.H., protected from draughts. By capillary action, the deionised water rose in the cylinder, becoming loaded with free alkali metal salt, and, once in contact with the air, the water evaporated causing the salt to crystallise on the surface (Figure 10).

Figure 10. *Capillary rise test on geopolymer cylinder showing efflorescence.*

In order to follow the crystallisation, a monitoring camera was set up (Figure 11) in a climatic chamber set at 20°C and 50% R.H. A camera (HV-F22, HITACHI) and a flash were programmed to take a picture every 5 minutes of the surface of the geopolymer cylinder (33 mm diameter and 50 mm height) semi-immersed in deionised water.

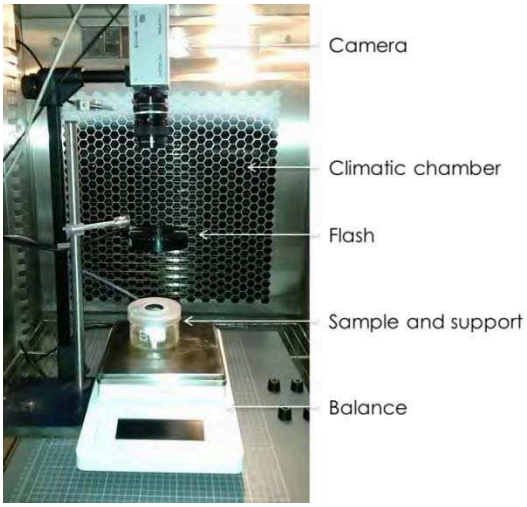

Figure 11. *Device for efflorescence formation followed by camera.*

The mineralogical characterisation of the efflorescence formed was performed by IR spectroscopy and XRD, using the same apparatus and procedure as described in Chapter I.

IV. Carbonation of the pore solution

1. Choice of the experimental approach

As previously stated, the information provided by the literature on the subject does not allow conclusions to be drawn on the resistance of metakaolin-based geopolymer to carbonation. Thus, the main purposes of this part of the study were:

→ to highlight the reaction between the metakaolin-based geopolymer and the atmospheric CO_2, and its kinetics.
→ to determine the impact of this reaction on the geopolymer paste, especially on the pH of the pore solution.
→ to assess the relevance of the existing tests standardised for a cementitious matrix.
→ to identify the potential durability risks of this reaction.

To the author's knowledge, no standards or existing procedures make it possible to achieve these objectives. Thus, an experimental approach focused on the analysis of pore solution was developed for this study. The choices that were made for this experimental approach are presented below.

Choices for the study of the pore solution

Because of the insolubility of calcium carbonate, the methods developed to assess the carbonation of OPC all focus on the measurement of the carbonation front, mainly with the phenolphthalein indicator. In the case of the geopolymer, although the pH variation induced by carbonation could be visible via a colour indicator, a distinct carbonation front is difficult to determine given the high solubility and mobility of the sodium carbonate (Criado et al., 2005; Škvára et al., 2012). It was thus decided to develop a method for the study of carbonation through the pore solution. This method could provide precise pH values, which are not yet referenced in the literature for metakaolin-based geopolymer.

This choice was confirmed by preliminary tests, which showed the difficulty of obtaining clear coloration of the phenolphthalein on the geopolymer surfaces without drying (Figure 12).

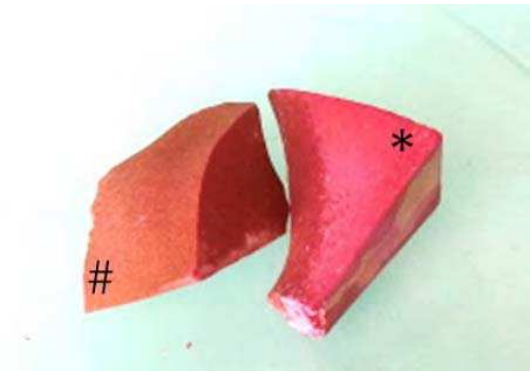

Figure 12. *Geopolymer paste samples cured for seven days at 95% R.H. and 20°C, exposed to phenolphthalein without drying (#) and after drying (*).*

Choice of the specimens studied

In order to simplify the study, it was chosen to evaluate the impact of the carbonation reaction on pure geopolymer pastes, to assess the reaction at the binder level, and avoid possible reaction alterations due to the contribution of other chemical elements provided by aggregates. The geopolymer formulation that was the best characterised in Chapter I was thus selected for this study: GP14.5.

Choice of the relative humidity of the test

Studying the formation of carbonates in solution requires working at a repeatable volume of water to have comparable concentrations and the volume of water extracted from the geopolymer must be high enough to allow the measurements to be achieved. Thus, the impact of relative humidity during the test, linked to the water saturation of the geopolymer, is of major importance.

This R.H. value was chosen by studying the results of Boher et al. (2014) obtained on metakaolin-based geopolymer having similar porous organisation (monomodal network centred at 15 nm with 49% of total porosity). In their works, the authors determined the degree of saturation depending on the relative humidity in a metakaolin-based system (Figure 13). They showed that, for relative humidities between 10% and 80%, the water saturation of the network was only around 20%, while it reached almost 70% at 95% R.H. In view of these elements, it was decided to fix the relative humidity of the study of carbonation at 95% R.H. in order to ensure that a sufficient quantity of extracting solution was obtained to perform the analysis, even after 1 year of cure.

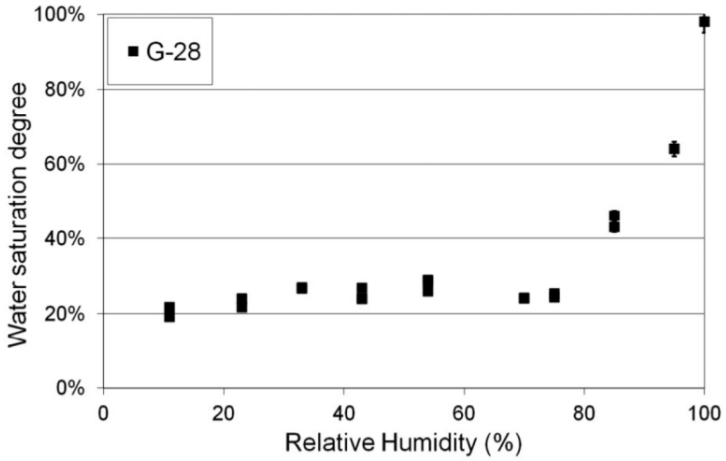

Figure 13. *Water saturation degree versus relative humidity for metakaolin-based geopolymer (from Boher et al., 2014)*

2. Influence of the carbonation on the pore solution pH

2.1. pH evolution in endogenous condition

To be able to evaluate the influence of carbonation on the pH of the pore solution, a study had to be made in endogenous conditions. The pHs of pore solutions of 91 x 62 x 40 mm GP14.5 geopolymer prisms kept in endogenous conditions were measured directly after their extraction at different times up to one year. The values obtained are plotted on the graph shown in Figures 14a, up to 365 days and with a logarithmic scale for better visibility on Figure 14b. It was first observed that the evolution of the pH showed a logarithmic trend, with a rapid decrease of the values in the first days followed by stabilisation over time. Without external exchanges, the high initial value of pH of 13.9, obtained just after preparation, decreased rapidly to reach 13 at three days, 12.8 at seven days, finally stabilising at a value slightly above 12.

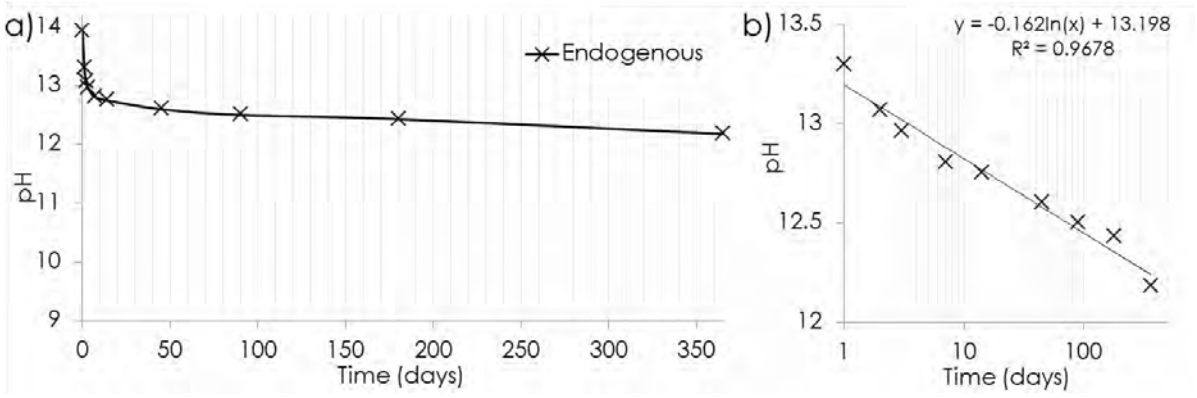

Figure 14. *pH evolution of the geopolymer pore solution kept in endogenous conditions up to 365 days. a) linear scale and b) logarithmic scale.*

This very fast decrease in the basicity of the pore solution is reminiscent of the very rapid increase in the geopolymer strength at early age, presented in Chapter I as the time required for the geopolymerisation reaction to take place. In fact, when those values are plotted together, as presented in Figure 15, it can be seen that the rapid decrease in pH during the first days of curing was almost inversely proportional to the rapid increase in compressive strength. So this decrease in pH would be involved in the reaction of geopolymerisation.

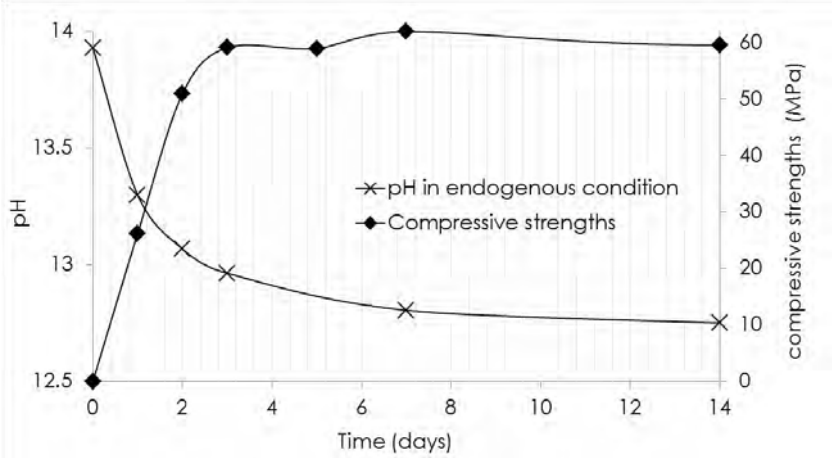

Figure 15. *pH evolution of the pore solution kept in endogenous condition and compressive strength (data from chapter I) of metakaolin-based geopolymer.*

Observations of the semi-schematic structure of Na–polysialate polymer by Barbosa (2000) could explain this pH evolution at early age. This semi-schematic structure, presented on Figure 16, shows the presence of hydroxide bound to the matrix (circled in red in Figure 16). It is thus possible to imagine that the OH^- provided by the activation solution being initially in solution imposes a very high pH, close to 14, and then the binding of some OH^- within the structure will rapidly decrease the pH, until equilibrium is obtained. So when the structure is stabilised, at nearly 14 days, the hydroxide ions that have not bonded remain in the pore solution and maintain a high pH.

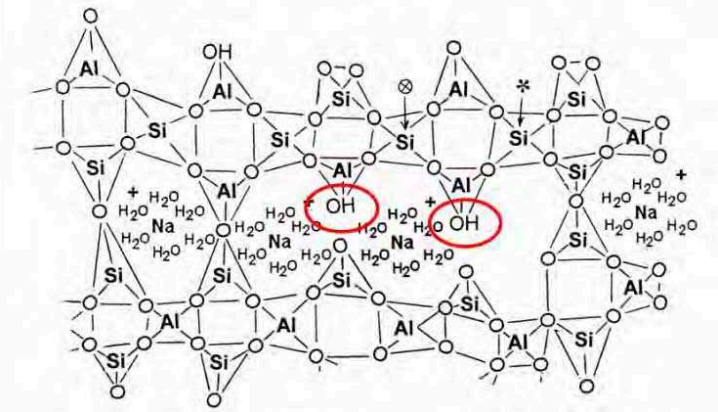

Figure 16. *Semi-schematic structure for Na–polysialate polymer (from Barbosa et al., 2000) where the hydroxides bonded to the structure have been circled in red.*

2.2. pH evolution in natural conditions

Regarding the evolution of the pH inside the geopolymer pore solution for samples kept at 20°C and 95% R.H., i.e. in contact with the atmosphere, a similar trend was shown but with a greater decrease: after only 14 days, the pH of this solution exposed to atmospheric CO_2 was nearly 12 and reached 10.5 after one year (figure 17 a and b). This lower value of pH of the pore solution exposed to external exchanges was associated with the carbonation of the solution, by reaction of the hydroxide with the dissolved carbonic acid to form carbonates CO_3^{2-} in solution (Equation 15).

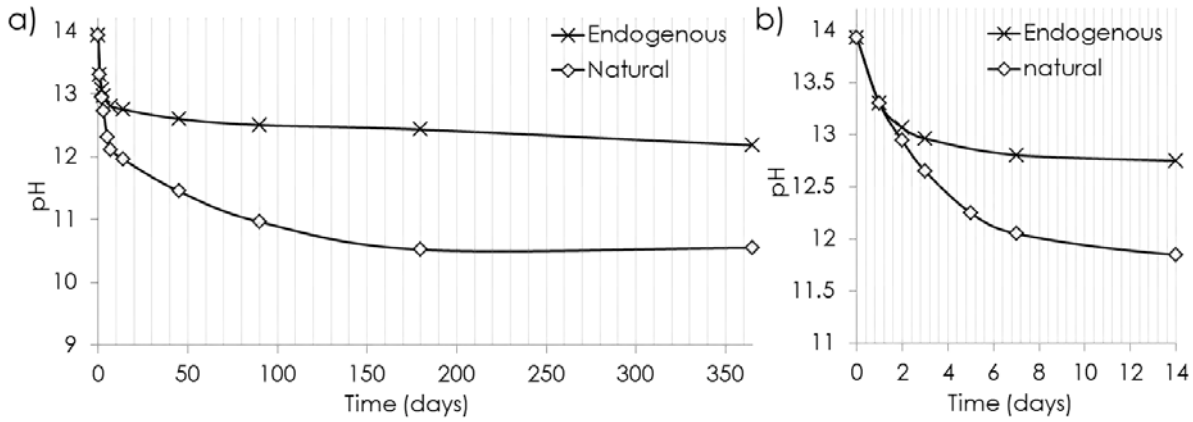

Figure 17. *pH evolution of the geopolymer pore solution cured in natural and endogenous conditions up to a) 365 days and b) 14 days.*

Figure 17b clearly shows that the difference in pH between endogenous and natural condition began from the second day of cure (day 2: endogenous 13.1 and natural 12.9) and increased over time, highlighting a, probably very fast, carbonation of the pore solution. Thus, the continuation of the study of carbonation was concentrated on the evolution of the carbonates in solution during the first fourteen days of curing. Nevertheless, the decrease of the solution basicity between 14 and 180 days, although lower, also demonstrates a phenomenon that may be associated with a continuity of the carbonation reaction.

3. Analysis of carbonates of the pore solutions

3.1. FTIR analysis of the carbonates formed under natural condition

In order to identify and quantify the carbonate within the pore solution using FTIR spectroscopy, a preliminary analysis was carried out using a pure sodium carbonate solution as a reference. Thus five solutions with mass concentrations ranging from 10 to 200g.L^{-1} were made and analysed by FTIR. The spectra obtained between 2000 cm^{-1} and 800 cm^{-1} for these five references are shown in Figure 18a. On these spectra, two major vibrations bands were identified:

- *1640cm^{-1}* associated with bonding vibrations of H–OH bonds, related to water.
- *1378-1390cm^{-1}* corresponding to the stretching vibration of O–C–O bonds in the carbonate group (CO_3^{2-}) (Bernal et al., 2010)

The superposition of these spectra highlighted the quantitative aspect of this analysis, as the area of the vibration was proportional to the carbonate concentration. A calibration curve was thus made by plotting the area under the vibration mode associated with the carbonate (between 1500 and 1200cm^{-1}) versus the concentration of Na_2CO_3 (Figure 18b). The linear equation obtained thus permitted the carbonates in the geopolymer pore solution to be quantified, assuming there were no superpositions or matrix effects around this band of vibration.

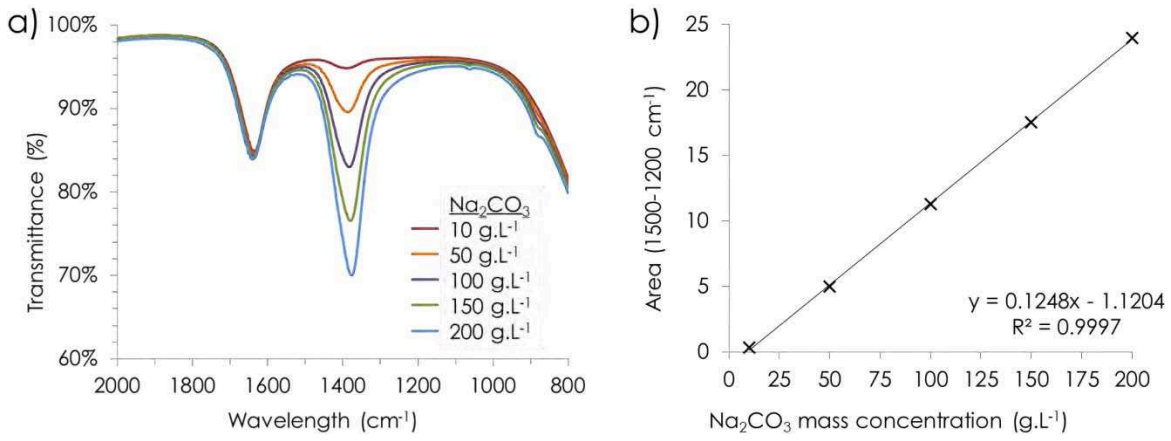

Figure 18. *a) FTIR spectra of pure Na_2CO_3 solutions having mass concentrations of 10, 50, 100, 150, and 200 g.L-1 between 2000 cm^{-1} and 800 cm^{-1} and b) Calibration curve of the area of the carbonate vibrations between 1500 and 1200 cm^{-1}, plotted versus the mass concentration of the references.*

Figure 19 shows the infrared spectrum between 2000 and 800 cm^{-1} for the pore solutions extracted after 1, 3, 5, 7 and 14 days from the geopolymer paste kept at 20°C, 95% R.H. and at atmospheric CO_2 content. As previously seen on the reference spectra, all spectra exhibited infrared vibration around 1640 cm^{-1} related to water, and also the mode associated with the stretching vibration of O–C–O bonds in the carbonate group between 1382 and 1394cm^{-1}. An increase in the intensity of this vibration mode was observed, showing an increase in the carbonate concentration and signifying a larger carbonation of the pore solution.

Another vibration mode at 1008 cm^{-1}, only found in the spectrum of the pore solution extracted at 1 day, was assigned to the asymmetric stretching vibration of Si–O–T bonds, where T is tetrahedral silicon or aluminium (Bernal et al., 2010; Criado et al., 2005). This vibration mode was explained by the presence of geopolymer particles in solution, probably due to the fact that, at 24h, the matrix was too fragile for the strength applied during the extraction. This resulted in the extraction of some of the solid portion at the same time as the pore solution.

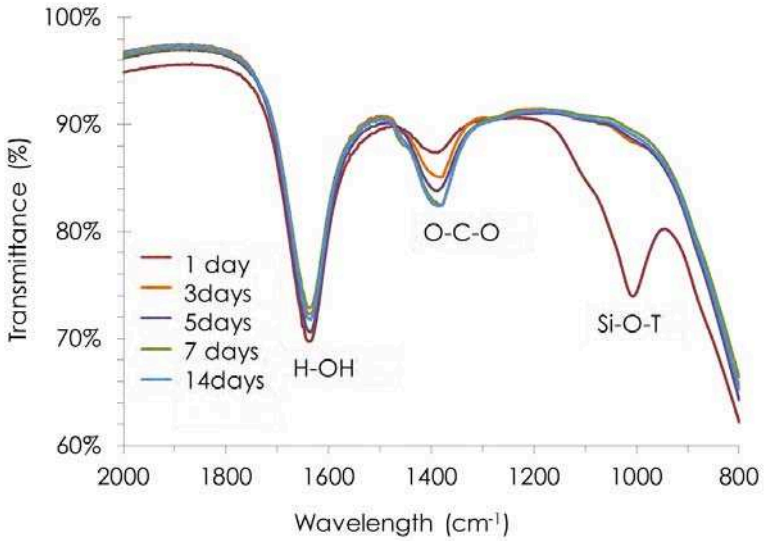

Figure 19. *FTIR spectra of pore solutions of geopolymer paste cured at 20°C, 95% R.H. and atmospheric CO_2%, extracted after 1, 3, 5, 7 and 14 days between 2000 cm^{-1} and 800 cm^{-1}.*

The areas under the vibration bands associated with carbonates were, as for the reference samples, calculated between 1500 and 1200 cm^{-1}, allowing the determination of the carbonate concentration presented in Table 3, by means of the linear equation (Figure 18b). These results show very fast carbonation as the mass concentration of carbonates increased from 16.1 $g.L^{-1}$ at 24 h to 30.7 $g.L^{-1}$ in only 3 days. This concentration continued to increase during the first week and then stabilised at a concentration near to 40 $g.L^{-1}$, since this value was calculated for both 7 and 14 days.

Table 3. pH, area of the vibration band, and mass concentration of Na_2CO_3 ($g.L^{-1}$) in the geopolymer pore solutions (calculated from the calibration equation) at 1, 3, 5, 7 and 14 days.

Time	pH	Area (1500-1200cm^{-1})	Na_2CO_3 mass concentration ($g.L^{-1}$)
1 days	13.3	0.89	16.1
3 days	12.8	2.71	30.6
5 days	12.4	2.86	31.9
7 days	12.1	3.85	39.9
14 days	12.0	3.85	39.9

These infrared analyses of the pore solution of metakaolin-based geopolymer thus highlighted the carbonation reaction between the carbon dioxide from the air and the geopolymer pore solution. Unlike the reaction occurring in Portland cement, the reaction appears to be very fast with early stabilisation at only seven days of exposure to atmospheric CO_2. From the position of the carbonate vibration band, similar to that of the reference, the carbonates could be identified as sodium carbonates but other tests were performed to confirm this conclusion.

3.2. Titration of carbonates with hydrochloric acid

A titration with hydrochloric acid (HCl) at 0.5 M was performed on the pore solutions of the geopolymer extracted after 3, 5, 7, and 14 days of cure at 20°C, 95% R.H. and natural CO_2%. For each titration, a curve such as that presented for the 3-day analysis in Figure 20 was obtained.

As presented earlier, this curve shows three falls of the pH value and highlights the three successive reactions that took place in the solution during the titration. First, the H_3O^+ provided by HCl reacted with the OH^- of the solution (**(1)** in Figure 20). A volume V_0 = 1.15mL of HCl was necessary to consume all the OH^-, leading to a first drop of pH. This first step demonstrated that the solution was not completely carbonated at this time. The second drop showed the amount of acid (V_1-V_0 = 2.35 mL) necessary to transform all the CO_3^{2-} in solution into HCO_3^- (**(2)** in Figure 20). The third drop marked the end of the reaction between the H_3O^+ and the HCO_3^- formed during the previous reaction (V_2-V_1 = 2.35 mL, **(3)** in Figure 20). The fact that the volumes V_1-V_0 and V_2-V_1 were identical means that no HCO_3^- was initially present in the pore solution (since all HCO_3^- came from the second reaction during the titration) and the same conclusion was reached for the other titrations made to quantify the carbonate formed under natural conditions.

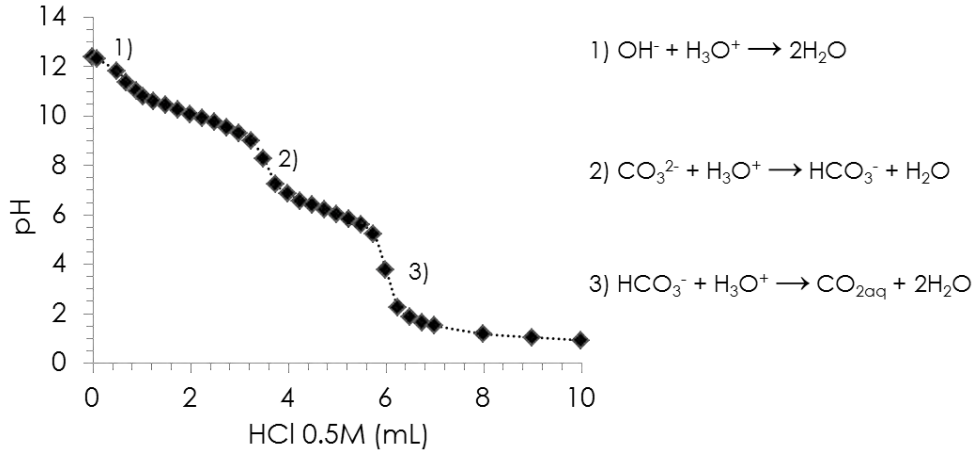

Figure 20. *Titration curve of geopolymer pore solution extracted after 3 days cured at 20°C, 95% R.H. and natural CO_2% by a 0.5M HCl solution followed by pH.*

These titrations carried out on the pore solution at 3, 5, 7 and 14 days allowed the OH^-, CO_3^{2-} and HCO_3^- present in solution to be quantified using Equations 12 to 14 as presented in part I. 2.2 and so the sodium carbonate concentration and the degree of carbonation to be determined (presented in Table 4). The carbonate concentrations obtained show the same evolution as previously found by infrared analysis, with a rapid increase of the concentration during the first seven days followed by a stabilisation between 7 and 14 days. The values obtained were also very similar to that found previously with a concentration at 14 days of 37.1 $g.L^{-1}$ instead of 39.9 $g.L^{-1}$. In addition, the calculation of the degree of carbonation showed that the pore solution was 80% carbonated in just 3 days, and reached 97% of solution carbonated at the end of the first week. The increase in the rate of carbonation was consistent with the measured decrease in pH.

Table 4. Mass concentration of Na_2CO_3 ($g.L^{-1}$) and degree of carbonation (%) of the geopolymer pore solutions at 3, 5, 7 ,14 and 180 days.

Time	3 days	5 days	7 days	14 days	180 days
pH	12.8	12.4	12.1	12.0	10.9
Na_2CO_3 mass concentration	24.9 $g.L^{-1}$	28.6 $g.L^{-1}$	37.1 $g.L^{-1}$	37.1 $g.L^{-1}$	11.9$g.L^{-1}$
Degree of carbonation	80%	89%	97%	97%	100%

The same titration by the hydrochloric acid was made with the pore solution extracted after 180 days of cure at 20°C, 95% R.H. and natural CO_2%. A sodium carbonate mass concentration of nearly 12 $g.L^{-1}$ was calculated, with a 100% carbonation of the solution. The associated pH found was also lower than previously, with a value of 10.5, explained by the presence of 10% of bicarbonate in solution (using Equations 20 and 21).

3.3. Influence of accelerated test conditions

As mentioned in the first part (I.1.3), the methods designed for the study of carbonation in a cement matrix always use accelerated conditions, i.e. an atmosphere with an artificially increased CO_2 concentration (from 0.1 to 50% instead of 0.03-0.04%). These tests are widely reported in the literature studying the carbonation of alkali-activated materials, mainly based on slags (Bakharev et al., 2001; Palacios and Puertas, 2006; Bernal et al., 2010, 2012). However, as reported by Bernal et al. (2012), increasing the CO_2 content in the atmosphere changes the carbonate (Na_2CO_3)/bicarbonate ($NaHCO_3$) phase equilibrium and leads to a more notable decrease in pH. Thus, to evaluate the influence of these accelerated tests on the carbonation product of metakaolin-based geopolymer, the same titration measurements were performed on pore solutions extracted from geopolymer cured under 50% of CO_2 at 3, 5, 7 and 14 days. However, the chamber used to create this concentrated carbon dioxide atmosphere had a relative humidity of 50%, so the calculated concentrations could not be compared to the results obtained in natural conditions at 95% R.H. due to the impossibility of estimating the dilution ratio.

On the titration curve of the solution extracted at 3 days (Figure 21), and also at 5, 7, and 14 days, the drop in pH corresponding to the OH^- was no longer visible, demonstrating total carbonation of the pore solutions. The observation of the titration curves also showed that the volume required to react with the CO_3^{2-} (V_1 = 9.5 mL) was lower than the acid volume required for the HCO_3^- (V_2-V_1 = 12 mL). Based on these results, it was concluded that, like the previous solutions extracted at 180 days, these pore solutions contained HCO_3^- in solution before titration began.

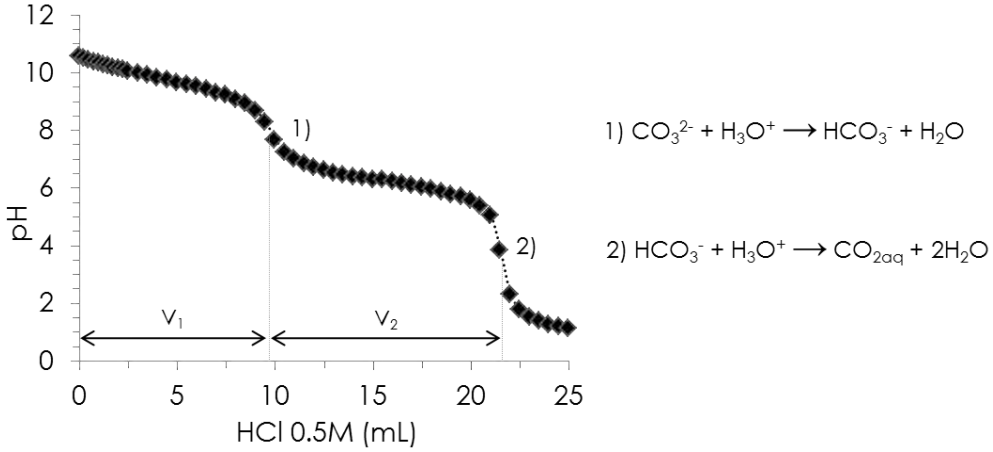

Figure 21. *Titration curve of geopolymer pore solution extracted after 3 days cured at 20°C, 50% R.H. and 50% of CO_2 by a 0.5M HCl solution followed by pH.*

This finding was in agreement with the fact that the pH values measured for these pore solutions were all below 10.5, while they were around 12 in natural conditions for the same period. Thus, the presence of sodium bicarbonate in solution has a non-negligible influence on the pH, as reported by Bernal et al. (2012). The quantification of this bicarbonate rate in solution shows an increase in the $HCO3^-$ concentration depending on the time of cure. It was thus calculated, as shown in Figure 22, that the HCO_3^- concentration in solution was 21% from the third day of cure and reached 38% at 14 days.

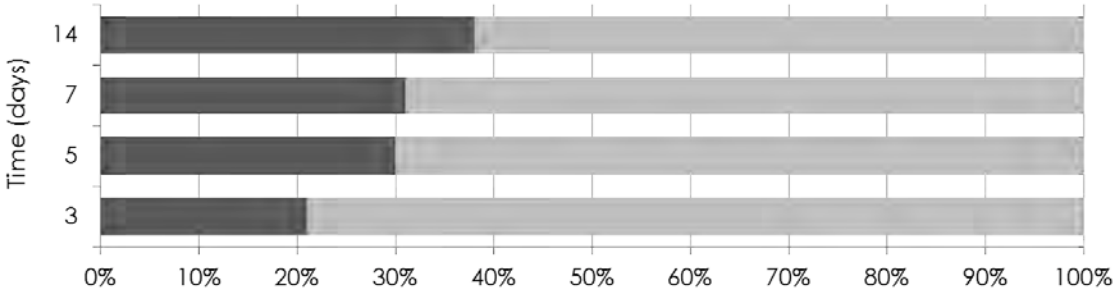

	3	5	7	14
Bicarbonate	21%	30%	31%	38%
Carbonate	79%	70%	69%	62%

Figure 22. *Na_2CO_3 and $NaHCO_3$ relative concentrations found in the pore solution of geopolymer cured in accelerated conditions (20°C, 50% R.H. and 50% of CO_2) extracted at 3, 5, 7 and 14 days .*

4. Impact of carbonation on the durability of geopolymer

4.1. On the mechanical strength

Carbonation is known to increase the mechanical strength in the cement matrix over time (Lea, 1970; Young et al., 1974) mainly due to the formation of calcium carbonate in the porous network. In geopolymer, the carbonates formed are very mobile, thus the question of the influence of carbonation on the mechanical behaviour arises. As the compressive strengths obtained in Chapter I for the mortar had the same geopolymer formulation and were cured in the same conditions (20°C, 95% R.H.) as in the natural carbonation study, the values were compared in order to visualise the influence of carbonation on the mechanical properties (Figure 23). The rapid decrease in pH during the first few days of curing was observed to be almost inversely proportional to the rapid increase in compressive strength, as it was for the carbonation in endogenous conditions.

To be able to conclude on the influence of carbonation on the mechanical performance of geopolymer, measurements of compressive strength in endogenous conditions should have been made. However, the observation of Figure 23 shows that carbonation does not seem to have a harmful effect over time as the compressive strength also increases when the carbonate concentration increases.

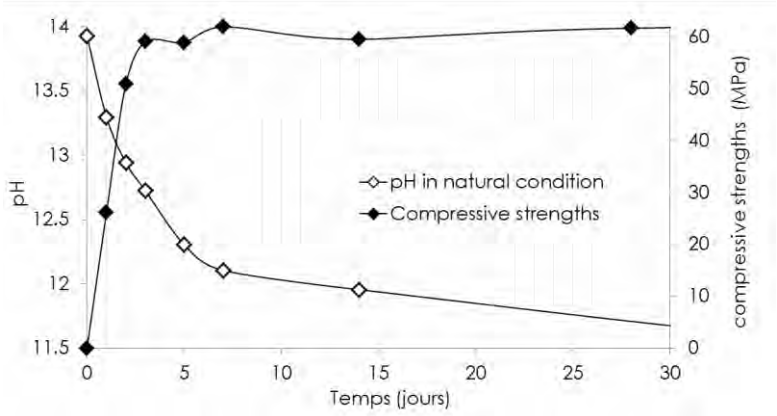

Figure 23. *pH evolution of the pore solution and compressive strength (data from chapter I) of metakaolin-based geopolymer.*

4.2. Risk of corrosion by carbonation

As in OPC reinforced structures, if the pH of the pore solution of geopolymer falls below 9, the steel reinforcements will no longer be passivated and will therefore subject to corrosion. The assessment of the evolution of the pH in the geopolymer pore solution over time in endogenous conditions showed that, without any external exchanges, the pore solution stabilised at a basicity similar to that of OPC, i.e. above 12. This value preserves the passivation layer of steel and presents no risk of corrosion.

Regarding the pH evolution when the geopolymer pore solutions were subjected to natural carbonation, a long-term stabilisation at 10.5 was observed over a year. This value would also maintain the passivation layer on the reinforcing steel. Under these conditions, with this formulation and up to one year, it would be possible to state that there is no risk of corrosion by carbonation in metakaolin-based geopolymer.

The titrations performed and the pH evolution over time showed that the carbonation reaction in the geopolymer pore solution with natural CO_2 content would occur in two separate phases (schematic representation on Figure 24) followed by a stabilisation of the pH:

- *Phase 1* nearly total carbonation of the pore solution during the first two weeks of exposure to atmospheric CO_2 leading to the formation of Na_2CO_3, and a pH value of around 12.
- *Phase 2* evolution of the carbonate/bicarbonate phase equilibrium resulting in the formation of bicarbonate (10% at 180 days) stabilising the pH at around 10.5, with no visible changes between six months and a year.

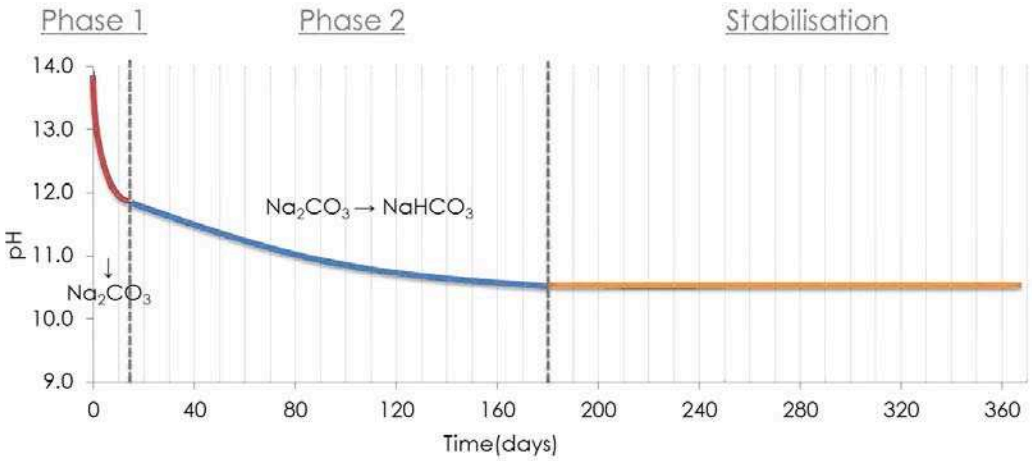

Figure 24. *Schematic representation of the two phases of the carbonation of the geopolymer pore solution.*

Many parameters can influence the resulting pH of these two carbonation phases, the main ones being the geopolymer formulation related to the amount of alkalis provided and the organisation of the porous network; the relative humidity, related to the water saturation of the porous network; and the temperature and the carbon dioxide content of the air, related to the carbonate/bicarbonate equilibrium phases. The following sections will provide some hypotheses about the impact of these parameters on the risk of corrosion by carbonation of geopolymer.

- *Influence of the geopolymer formulation*

The analysis of the GP14.5 pore solution showed the formation of 40 $g.L^{-1}$ of sodium carbonate in 14 days, corresponding to 10% of the initial amount of sodium introduced. If the formulation of the geopolymer had had a different sodium content, lower or higher, it is very

probable that carbonation would still have taken place but the final concentration of sodium carbonate would have been different. Thus, it is the influence of the carbonate concentration that needs to be evaluated regarding the risk of corrosion by carbonation. To assess the impact of this concentration on the pH of the pore solution, five solutions made from industrial sodium carbonate, having concentrations of 10, 50, 100, 150 and 200 $g.L^{-1}$, were made and their pH was measured. The values obtained, presented in Figure 25, showed that this pH increased linearly, from 11.46 to 11.78, with the mass concentration of carbonate. These results demonstrate that the alkali concentration, and thus the initial formulation of the geopolymer, had an influence on the pH of the pore solution, but it appears that it would not lead to a risk of corrosion by carbonation as the pH value remained well above 9.

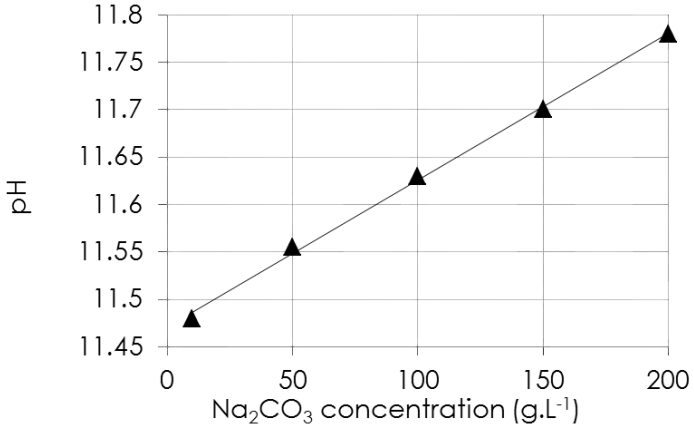

Figure 25. *pH versus mass concentration of industrial Na_2CO_3 solution measured at 20°C.*

The total volume and the organisation of the porous network, strongly related to the geopolymer formation, could also have a significant influence on carbonation. As the entire reaction studied took place in the liquid phase, the interconnectivity of the network played a major role and, given the rapidity of carbonation observed, large network connectivity can be assumed, as already shown in Chapter I for this formulation.

We recall that the analyses carried out on a GP14.5 geopolymer paste showed a monomodal organisation of the porous network, centred on a single access pore size around 15 nm, for a total volume of 49%. Thus the modification of one of these parameters could affect the carbonation reaction within the network. However, if only the access size or total volume varies (as observed for the GP17 and GP20 formulation), then the effect will be the same as previously, and just the carbonate concentration or the reaction kinetics will be impacted without significant influence on the pH. Only the reduction of network interconnectivity could have an influence on the pH value, by isolating portions of the porosity from the exterior. But

this influence would not be detrimental since the isolated portion would no longer be subjected to carbonation, so the pH would remain high enough to maintain a steel passivation layer.

- *Influence of the relative humidity*

The relative humidity during the carbonation test is a major parameter since it determines the total amount of water present in the porous network of the geopolymer. The total amount of water influences the carbonate concentration as well as the pH of the solution. However, as its impact on the pH value is only related to the variation of the carbonate concentration, the same conclusions as previously (for the formulation and the porous network influences) can be drawn, i.e. that the relative humidity variation should not lead to a pH sufficiently low to depassivate the reinforcing steel.

Thus in relative humidity closer to actual environmental levels (between 50% and 70%), the total amount of water in the geopolymer porous network would decrease from 65% to 20% (according to Boher et al., 2014). This reduction of the total amount of water would result in an increase of the carbonate concentration from 40 to 130 $g.L^{-1}$ (if it is considered that the same quantity of carbonate was formed). This concentration would remain well below the solubility limit of sodium carbonate of 300 $g.L^{-1}$ and the resulting pH for this concentration would be around 11.65 (according to Figure 25).

- *Carbon dioxide content and temperature*

In natural conditions, it was found that the carbon dioxide content mainly influences phase 2 of the carbonation. The two titrations made at 14 and 180 days revealed that, between these two times, formation of HCO_3^- took place in the solution in addition to the CO_3^{2-}, showing an evolution of the carbonate/bicarbonate phase equilibrium.

This equilibrium phase between carbonate (natron) and bicarbonate (nahcolite) was studied by Bernal et al. in 2012 (Bernal et al., 2012), who showed that the bicarbonate formed was strongly dependent on the CO_2 content of the air. According to their calculations (Figure 26), at the ambient carbon dioxide level (0.03-0.04%) and at 25°C, the equilibrium would be nearly 30% of bicarbonate in a system formed when 1 mol/kg NaOH solution was exposed to pseudo-open system gas environments with CO_2. In addition, as mentioned in the first part of this chapter (Figure 4), the same study also pointed out the importance of temperature on the equilibrium phases of carbonates. It was shown that an increase in temperature to above 25°C

resulted in the formation of trona ($Na_3H(CO_3)_2$) instead of natron (Na_2CO_3) at natural CO_2 content. This would lead to the presence of HCO_3^- in solution, affecting the pH value.

Thus the value of 10% of HCO_3^- found in the pore solution extracted at 180 days (20°C and natural CO_2 content) seems in agreement with the literature, since the 30% of HCO_3^- found in Bernal's article can reasonably be attributed to the higher temperature of 25°C.

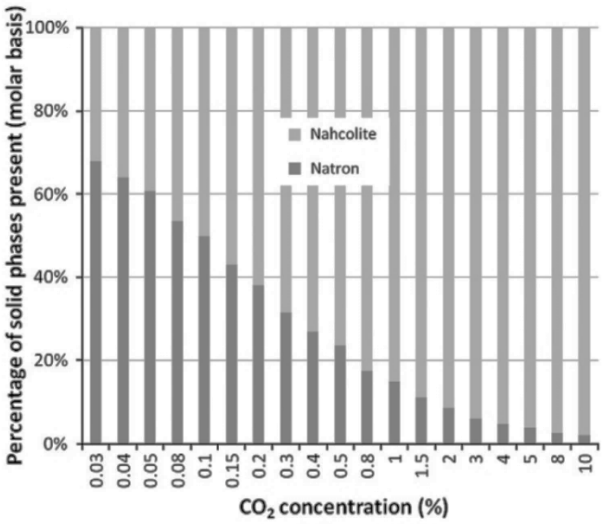

Figure 26. *Phases (and relative concentrations) calculated to be formed when 1 mol/kg NaOH solution is exposed to pseudo-open system gas environments with CO_2 present at different concentrations in dry air, at 25°C (From Bernal et a.l, 2012).*

Furthermore, in order to estimate the impact of this phase equilibrium evolution on the pH of the pore solution, pH measurements were performed on reference solutions made from industrial sodium carbonate and bicarbonates. Ten solutions at 10 $g.L^{-1}$ of sodium carbonate were made, with variable sodium bicarbonate substitutions ranging from 0% to 100%, every 10%. The pH values measured at 20°C versus the bicarbonate substitution rate are presented in Figure 27.

Observation of the pH values versus bicarbonate substitution rate clearly highlights the influence of the bicarbonate concentration on the basicity of the solution. The higher pH corresponds to the solution containing only sodium carbonate (same value as in Figure 25 for the solution at 10 $g.L^{-1}$) and the more the bicarbonate content increases, the more the pH value decreases, reaching 8.5 for the solution made only with sodium bicarbonate. It was particularly observed that, for a sodium bicarbonate content of 10%, a pH similar to the 10.5 measured for the pore solution extracted at 180 days was obtained.

Thus the balance between the carbonate and bicarbonate appears to have taken six months to stabilise. As a pH of 10.5 was also measured at one year, it is highly probable that no evolution took place in the carbonate phase equilibrium between 6 months and a year, which would imply that this pH will be maintained over time. So there would be no risk of corrosion by carbonation in the metakaolin-based geopolymer structure at natural CO_2 content and 20°C.

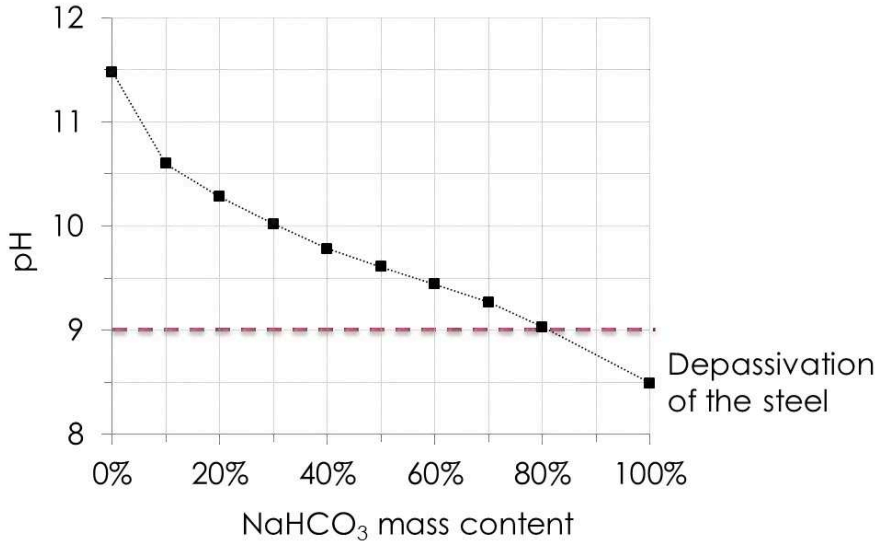

Figure 27. *pH of carbonate/bicarbonate mixture (10g.L^{-1}) prepared from pure product depending on the bicarbonate content (at 20°C).*

In contrast, exposure to an atmosphere with an artificially raised carbon dioxide concentration led to higher bicarbonate rates, so different conclusions about corrosion may be found under accelerated testing. The exposure to 50% of CO_2 in the air formed 38% of sodium bicarbonate in the pore solution in 14 days, a concentration which would correspond to a pH lower than 10 according to Figure 27. The use of accelerated tests therefore changes the carbonates phase equilibrium completely, as found by Bernal et al., leading to abnormally low pH that is not representative of the reaction under natural conditions. Due to the dry atmosphere (50% R.H.) in the 50% CO_2 chamber, no extraction could be achieved beyond 14 days. It can nevertheless be imagined that, if the accelerated testing had been continued over a year, as is the case for OPC, it could have led to a sufficiently low pH to depassivate the reinforcement steel ($NaHCO_3$ content > 80%).

The same conclusion can be drawn regarding the curing temperature. Increasing the temperature would also increase the bicarbonate content, which would imply a decrease in the pH value. If the data obtained in this study are compared with those of the calculation by Bernal et al., a temperature increase from 20°C to 25°C would results in an increase of the bicarbonate content from 10% to 30%, leading to a pH of about 10 instead of 10.5. The exposure to even higher temperature could result, in the worst case, in a pH allowing corrosion by carbonation. For further investigations, a study on the actual impact of temperature on the pH of the pore solution would be necessary, in order to determine the temperature from which the risk of corrosion due to carbonation would appear.

4.3. Fate of the alkali carbonates formed

In addition to providing information about the bicarbonate content, the titrations performed at 14 and 180 days showed a significant decrease in the concentration of sodium carbonate, from 40 $g.L^{-1}$ to 12 $g.L^{-1}$. The chemical analysis carried out in chapter I had shown no change in the geopolymer composition over time, so this decrease cannot be attributed to an incorporation of carbonate in the structure during those six months. The phenomenon that appears most likely to explain this decrease in alkaline content would be leaching. The tests being carried out in a humid atmosphere, it is possible that, once the solution is fully carbonated, the alkalis are brought to the surface by a concentration gradient, attracted by the water on the sample surface. This would cause a leaching of alkali carbonates.

As for the mechanical strength, this leaching does not damage the geopolymer structure, but might be a source of potential problems, such as crystallisation of the carbonates in the form of efflorescence.

In short

Carbonation reaction product	Sodium carbonate and bicarbonate
Reaction kinetic	Pore solution carbonated at 97% in 7 days
pH of the pore solution	At one years: - 12.5 in endogenous condition - 10.5 in natural condition (95% R.H., 20°C)
carbonate/bicarbonate phase equilibrium	10% of bicarbonate at 6 months in natural condition (95% R.H., 20°C)
Impact of carbonation on the durability of GP	Not detrimental influence on the mechanical strengths No risk of corrosion by carbonation except for: - higher temperature - higher CO_2 content in the air Potential problem due to leaching of alkaline carbonates
Relevance of accelerated tests	Leads to unrepresentative results

This study of geopolymer pore solution over time, in different conditions, has highlighted the different stages of carbonation in the metakaolin-based geopolymer. It has thus been shown that the solution in the pores of the geopolymer is almost completely carbonated in only two weeks, followed by an evolution in the phase equilibrium of sodium carbonate and then a stabilisation after the first six months of curing. It was concluded that the carbonation reaction had an important influence on the pH of the pore solution, which, in standard conservation conditions, does not result in the depassivation of reinforcing steel. It was finally determined that the only parameters that could cause corrosion by carbonation would be an increase of the CO_2 content in the air or a significant increase of the temperature. However, the risk of efflorescence related to the very high alkali content needs to be assessed.

V. Efflorescence of metakaolin-based geopolymer

Efflorescence does not constitute a real durability problem for OPC concrete structures. However, it causes serious aesthetic problems, which are now well controlled thanks to the use of anti-efflorescence agents. As shown in Chapter II, the metakaolin-based geopolymer system is also subject to these problems, which in some cases (beams) can even lead to surface damage. Although the study of the carbonation of the pore solution can explain the phenomenon responsible for this efflorescence, an investigation of how these crystals grow is needed.

In this section of the geopolymer carbonation study, the aims were to identify the efflorescence formed and determine their formation kinetics and the parameters influencing this growth. The crystals formed under natural conditions and a concentrated CO_2 atmosphere were thus characterised by XRD and IR spectroscopy. Different curing conditions, formulations and anti-efflorescence agents for OPC were also tested in semi-immersion to visually compare their effects on the efflorescence. This non-exhaustive study, based on visual observations, provided further information on the carbonation of geopolymer and recommendations are given for reducing the problems associated with efflorescence as much as possible.

1. Characterisation of efflorescence

1.1. In natural CO_2 environment

In order to induce the crystal growth of efflorescence and furnish a sufficient quantity for analysis, a geopolymer paste prism of the same size as previously was placed in semi-immersion (principle presented in the next section). This test was performed on geopolymer kept in natural carbonation conditions (at 20°C and 95 % R.H.) for 7 days, since it had been shown that a week was sufficient to almost completely carbonate the pore solution. After a week of semi-immersion test in a conditioning room at 20°C and 50% R.H., a sufficient quantity of crystals was collected to perform the analysis. The characteristics of the efflorescence formed were determined by XRD and IR spectroscopy after crushing the crystals recovered on the surface of the geopolymer to less than 40µm. The XRD pattern obtained is presented in Figure 28 and IR spectrum in Figure 29.

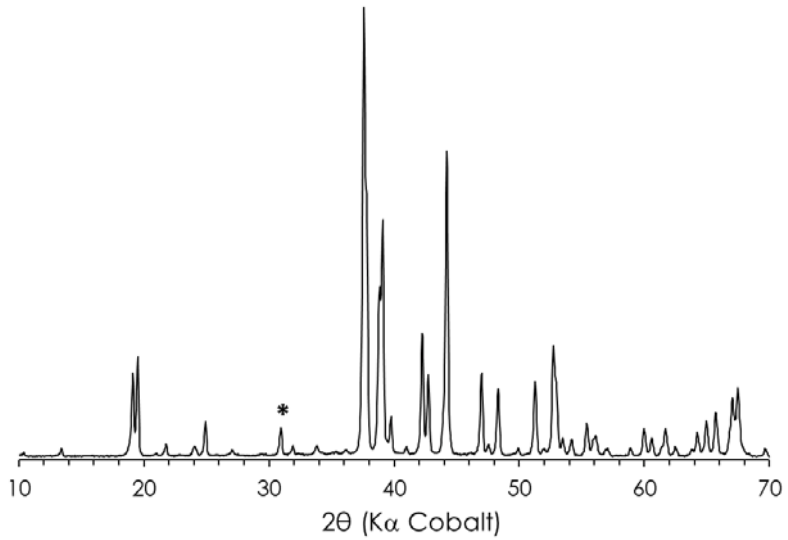

Figure 28. *XRD pattern of efflorescence formed under natural CO_2 environment at 20°C and 50% R.H. All the peaks were identified as $Na_2CO_3.H_2O$ (PDF # 08-0448) except for a quartz peak noted (*).*

The results of the mineralogical analysis showed the almost exclusive presence of sodium carbonate monohydrate ($Na_2CO_3.H_2O$, Powder Diffraction File (PDF) # 08-0448). Just one peak characteristic of quartz (* in Figure 28) was also found on this pattern, probably originating from an impurity included during the recovery of the crystals. The infrared spectrum was compared with the spectrum of pure crystals of sodium carbonate (industrial product) obtained with the same apparatus, in order to identify the efflorescence formed. This comparison, presented in Figure 29, confirms the formation of sodium carbonate in the natural CO_2 environment, as the two spectra appear to be very similar. A slight shift toward the lower wavelength for the transmissions measured for the efflorescences, and the presence of a vibration band around 1650 cm^{-1} were, however, noted. This phenomenon can be explained by the fact that, unlike the pure product, the Na_2CO_3 crystals formed were hydrated (confirmed by the monohydrate structure found by XRD).

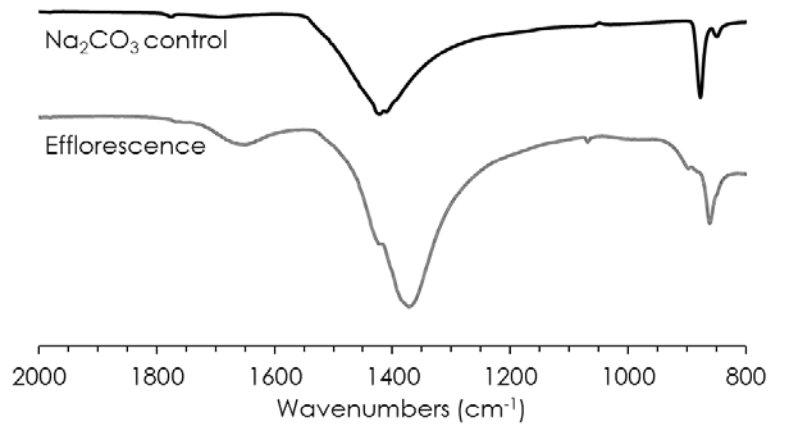

Figure 29. *Infrared spectra of pure Na_2CO_3 crystals and efflorescence residues collected on geopolymer paste cured at natural CO_2 concentration (20°C and 95% R.H.).*

1.2. In high CO_2 environment

Exactly the same test procedure was carried out here, except that the cure for 7 days and the semi-immersion test were conducted under a high CO_2 concentration of 50%. The crystals formed were visually similar to those found in a natural atmosphere, and present in an equivalent amount. They were also crushed to less than 40µm and analysed by XRD and IR spectroscopy. The XRD pattern obtained is presented in Figure 30. Only one compound was identified on this pattern corresponding to nahcolite ($NaHCO_3$, (PDF) # 15-0700). However, although all the observed peaks were found at the diffraction angle corresponding to nahcolite, the intensity of the peaks did not correspond to the PDF file. Thus the peak marked with the * on Figure 30 shows an abnormally high intensity. This phenomenon could indicate that the aggressive condition of this environment led to crystallisation with a different orientation organisation.

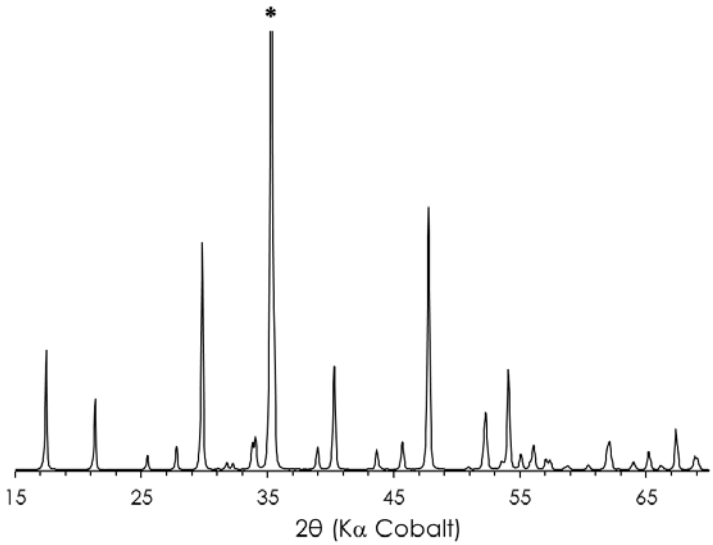

Figure 30. *XRD pattern of efflorescence formed under an atmosphere at 50% of CO_2, 20°C and 50% R.H, where all the peaks were identified as $NaHCO_3$ (PDF # 15-0700). (*) identifies the peak at 100% at 2θ of 35.3.*

In order to confirm the formation of bicarbonate in accelerated conditions, the infrared spectrum recorded for the collected efflorescence was compared to that of pure industrial crystals of $NaHCO_3$. The two spectra presented in Figure 31 show vibration bands at the same wavelength for both compounds. Only the measured intensities vary, those for the experimental efflorescence being higher than for the commercial product. This analysis thus confirms the results obtained by XRD by demonstrating that, under an atmosphere with 50% of carbon dioxide, the efflorescence formed is composed of sodium bicarbonates.

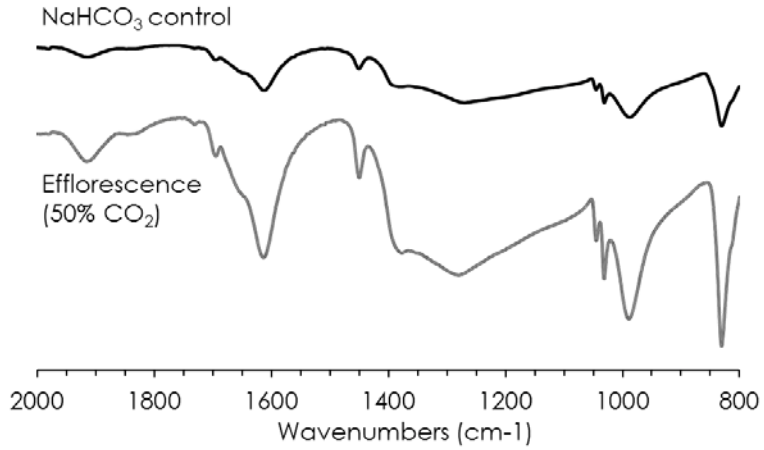

Figure 31. *Infrared spectra of pure $NaHCO_3$ crystals and efflorescence residues collected on geopolymer paste cured at 50% of CO_2 (20°C and 50% R.H.).*

The characterisation of the crystals formed in natural and accelerated conditions therefore confirms the results of the previous section, showing that the increased CO_2 content in the air leads to a different carbonation reaction product. However, no significant effect was observed on the growth of efflorescence between these two conditions.

2. Observation of the efflorescence growth

2.1. Principle of capillary rise test

In order to provoke efflorescence, capillary rise tests were carried out. The principle of this test is schematically represented in Figure 32. At time t = 0 (a in Figure 32) the carbonated geopolymer paste, having its pore solution concentrated in CO_3^{2-} and Na^+ species, is placed in ultrapure water. By capillary action via the porous network of the geopolymer, the alkali carbonates migrated to the top of the sample (b), and then gradually move to the external surface (c). Once in contact with the air, the water of the pore solution evaporates and the alkali carbonates crystallise locally (d).

In order to obtain comparable observations of the efflorescences formed, the same protocol was used in all the study: geopolymer pastes were cast into cylindrical moulds of 33 mm diameter and 50 mm height. After 24h, all samples were demoulded and placed under natural carbonation at 20°C and 95% R.H. for seven days, then tested.

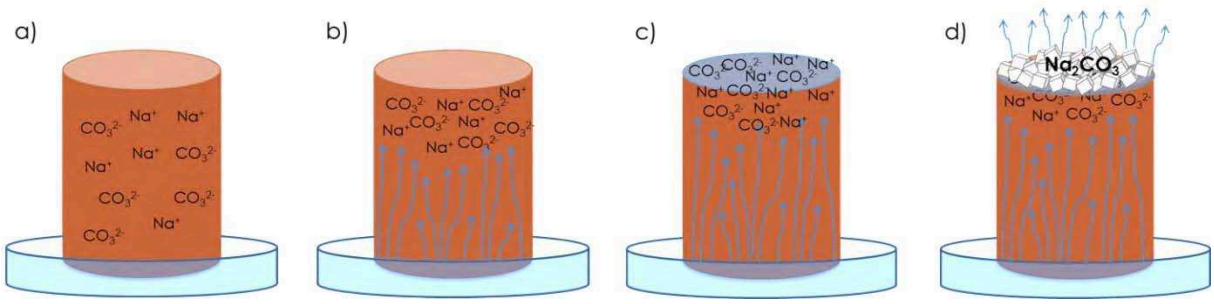

Figure 32. *Schematic representation of the principle of the capillary rise test.*

2.2. Efflorescence kinetics

To follow the formation of efflorescence, a monitoring camera (Figure 11) was programmed to photograph the surface of a geopolymer sample, placed in semi-immersion, every 5 minutes. This geopolymer paste, having the formulation GP14.5, was cast into a cylindrical mould of 33 mm diameter and 50 mm height and was kept in natural carbonation conditions (20°C and 95% R.H.) for seven days before being placed in the device. The semi-immersion was carried out with ultrapure water and the climatic chamber was set at a temperature of 20°C and a relative humidity of 50%.

The photographs obtained showed no change in the surface of the sample during the first 24 hours of semi-immersion, as can be seen in the first image of Figure 33. It was observed that the first crystals appeared after 31 hours of semi-immersion (second image), followed by a fast increase of this crystallisation. As can be seen on the third, fourth and fifth images, taken at 32, 34 and 40 hours of semi-immersion, these crystals developed very fast, almost completely covering the surface in less than 9 hours after the first appearance. Finally, it was observed that, after 48 hours of testing, the crystals began to deteriorate the sample surface by peeling a portion of the sample centre (sixth image on Figure 33).

It appeared that the crystal growth did not occur in a specific location but rather uniformly over the sample surface, suggesting a homogeneous distribution of the porous network, except for the central area. It was observed that crystals in this area formed later, around 40 h after the beginning of the immersion, while all other crystals appeared after only 31 h. Moreover, it was in this same area that the peeling was observed after 48h of testing (sixth picture in Figure 33). This could indicate a lower or more closed porosity in this area, which would provoke subflorescence (efflorescence under the surface) causing the deterioration.

These results suggest that, under favourable conditions, the appearance of efflorescence on the surface of a metakaolin-based geopolymer paste would be fast and uniformly distributed, and that the surface condition would affect the appearance of damage.

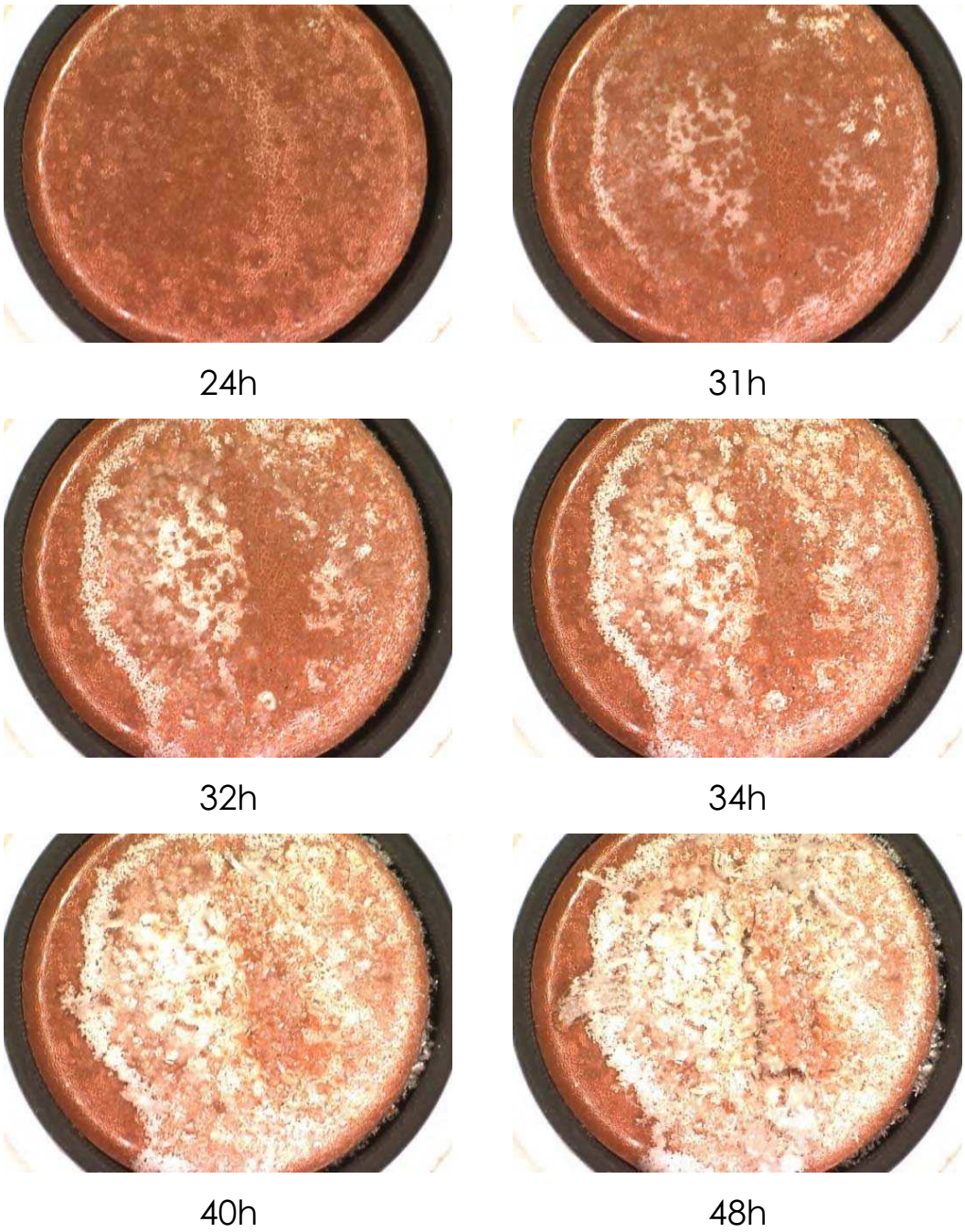

Figure 33. *Photographs of the surface of a GP14.5 geopolymer paste placed in semi-immersion in ultrapure water at 20°C and 50% R.H. after 24h, 31h, 32h, 34h, 40h, and 48h.*

2.3. Parameters influencing efflorescence growth

In the work reported in this section, several parameters that could influence the growth of the efflorescence crystals were studied, using the capillary rise test. The influence of the surface condition, curing temperature and the geopolymer formulation were evaluated by visual observation of the efflorescence after seven days of natural carbonation followed by seven days of semi-immersion. The aim of these tests was to improve the knowledge of this growth to better anticipate its development. In addition, several product additions, known to slow growth in alkali-activated materials or in OPC, were tested to evaluate their action on metakaolin-based geopolymer.

Surface influence

To assess the effect of the surface on the growth of efflorescence, three specimens of the same size and same formulation were made, and only the surface condition of the top of the cylinder was modified. The first (a on Figure 34) had its upper surface dried in the open air during the first 24 hours of curing, while the second was protected from any exchanges during the same period (b on Figure 34). The last specimen had half of its upper surface dried in open air and the other half dried without exchanges (c on Figure 34).

Figure 34. *Efflorescence observation on the surface of a GP14.5 geopolymer paste when the surface was dried during the first 24 hours: a) in the open air, b) under protection or c) 50% in the open air (#) and 50% under protection (*).*

In the first case, the same observation as previously made was obtained, i.e. uniform crystallisation throughout the open-air-dried surface. Concerning the surface cured under protection, the efflorescence was observed to be located on the outer parts. Finally, the third specimen revealed significantly higher crystallisation on the surface dried in the open air than on the surface kept without exchanges during the first 24h of cure.

These results therefore suggested that the surface dried under protection would have a more closed porosity which would not allow the migration of alkali outwards, contrary to the surface dried in the open air.

These results suggest that, unlike the surface dried in the open air, the surface dried under protection would have more closed porosity which would reduce the alkali migration outwards. The surface of the geopolymer dried in the open air would therefore be the most sensitive to efflorescence growth. However, in the light of these results and those of the previous section, it would also be the surface least likely to suffer surface deterioration due to subflorescence.

Curing temperature

The study of the pore solution showed that temperature had a significant impact on the carbonate equilibrium phases. Thus the influence of heat treatment on efflorescence needed to be studied. The photographs presented in Figure 35 show two geopolymer cylinders of the same size and same formulation cured at two different temperatures: **a)** was cured at 20°C for the first 24 hours while **b)** was cured at 40°C during the same period. Visual observations of the efflorescences developed by these two specimens highlighted a strong influence of the curing temperature on the growth of the sodium carbonate crystals, and demonstrated that a thermal treatment resulted in a larger, more compact efflorescence.

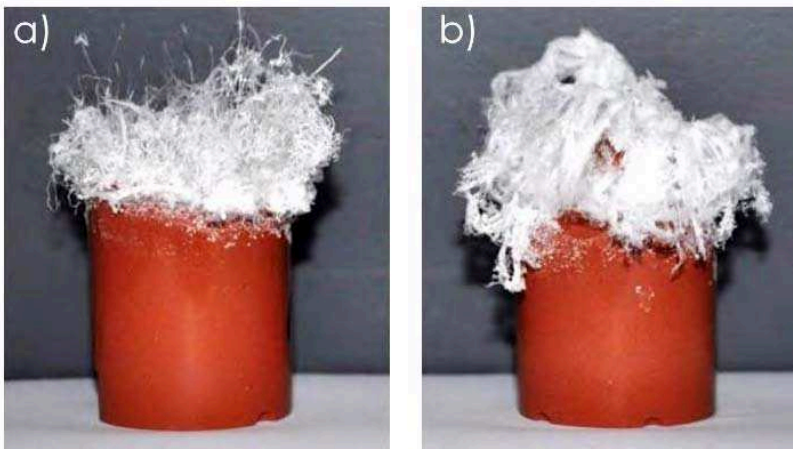

Figure 35. *Efflorescence on GP14.5 geopolymer paste cured at 20°C a) and 40°C b) during the first 24h.*

Sand additions

The efflorescence of four geopolymer mortars incorporating 40%, 50%, 60% and 70% of sand by mass were compared to the efflorescence obtained for a pure geopolymer paste having the

same formulation, to evaluate the impact of the addition of sand on their growth (Figure 36). It was thus shown that the addition of sand decreased the amount of crystals formed during the semi-immersion test. This result is consistent with the fact that the addition of sand reduces the quantity of binder and thus of the alkali responsible for efflorescence.

Figure 36. *Efflorescence observations on GP14.5 geopolymer having from left to right: 0%, 40%, 50%, 60% and 70% of sand by mass at 7 days.*

Geopolymer formulation

Finally, probably the most important parameter, namely the nature of the alkali, was also evaluated in this study. For this, three other waterglass solutions based on potassium or sodium-potassium mixtures were used to formulate geopolymers. Using the dry matter content of these industrial solutions (Table 5), three new geopolymer formulations (**b**, **c**, and **d** on Table 5 and Figure 37) were calculated so as to have the same molar ratios as the GP14. 5 formulation (**a** on Table 5 and Figure 37), i.e. SiO_2/Al_2O_3 of 3.6, Na_2O/Al_2O_3 of 0.9 and H_2O/ Na_2O of 14.5.

Table 5. Identification, silicate/alkali molar ratio and dry content composition of the waterglass solutions used.

Samples on Figure 37	Waterglass solutions ID	SiO_2/Me_2O molar ratio M = Na or K	Dry content composition (mass%)
a)	Wg1.7Na	1.7	SiO_2: 27.8%; Na_2O: 16.9%
b)	Wg1.7NaK	1.7	SiO_2: 25.3%; Na_2O: 13.7%; K_2O: 2.7%
c)	Wg1.5K	1.5	SiO_2: 21.9%; K_2O: 22.8%
d)	Wg1.0K	1.0	SiO_2: 20.5%; K_2O: 31.5%

The results of the semi-immersion tests revealed a significant influence of the nature of the alkali on the crystal growth. Compared with the formulation based only on sodium (a on Figure 37), the mixture of sodium and potassium (b on Figure 37) reduced, though not significantly, the amount of crystals formed. In the case of only potassium-based waterglass, it was even observed that no growth occurred during the seven-day test in semi-immersion (c and d on Figure 37).

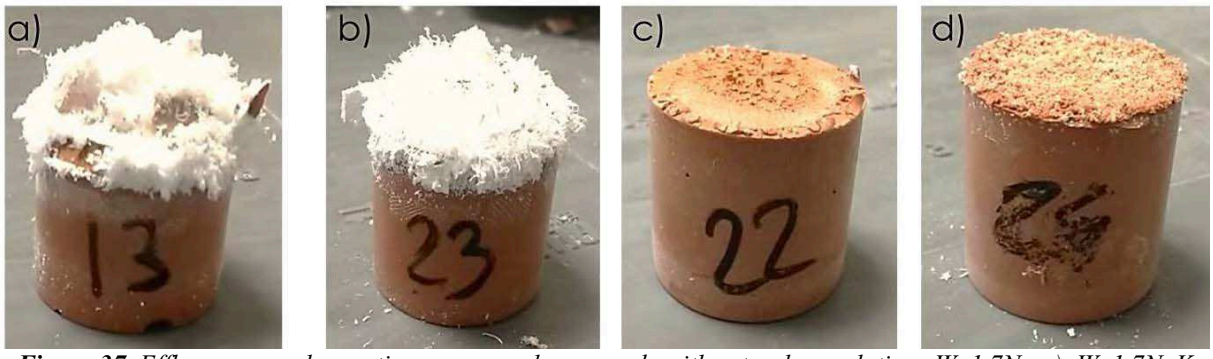

Figure 37. *Efflorescence observations on geopolymer made with saterglass solutions Wg1.7Na a), Wg1.7NaK b), Wg1.5K c), and Wg1.0K d) (composition in Table 5) after 7 days of semi-immersion.*

These observations thus show that the use of potassium-based waterglass solutions would significantly reduce, or totally remove, the efflorescence growth on metakaolin-based-geopolymer surfaces. The use of this kind of solutions will be so strongly recommended for structures in an environment favourable for efflorescence. Nevertheless, these results do not allow us to rule on whether it would be possible to reduce the efflorescence growth as significantly in the case of sodium-based geopolymer having another formulation. For this, a more extensive study of the geopolymer formulation would be necessary in order to find the right proportion of sodium to both dissolve the metakaolin and reduce the efflorescence risks.

2.4. Test of efflorescence reducing agents (ERA)

As presented in the first part of this chapter, in 2014, a study by Suchý et al. showed that $AlF_3 \cdot 3H2O$ could reduce efflorescence in alkali-activated blast furnace slag (Suchý et al. 2014). To assess whether this result might be applicable to the system based on metakaolin, two samples of geopolymer GP14.5 were prepared with an addition of aluminium fluoride, in an amount similar to that mentioned in the article. It was first observed that the addition of this compound to the mixture led to a strong thixotropic effect of the preparation. Then, during demoulding at 24 h, very marked shrinkage was observed for the geopolymer having the most significant addition of AlF_3.

Then, after a week of semi-immersion testing, a large amount of efflorescence was found, with significant surface damage, as presented in the two photographs of Figure 38. This test thus demonstrated that the incorporation of this compound did not reduce efflorescence growth in metakaolin-based geopolymer as it would in the case of the alkali-activated slags.

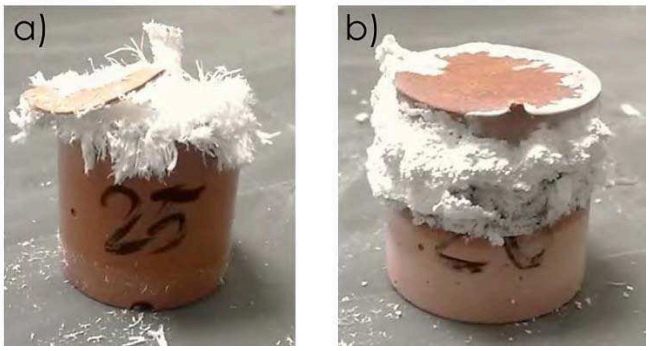

Figure 38. *Efflorescence observation on GP14.5 geopolymer with addition of $AlF_3.3H_2O$ by mass relative to the Mk of a 1: 6) and b) 1: 7*

Finally, six commercial anti-efflorescence agents used in concrete structures were tested. These six products from different suppliers, presented in Table 6, all had a water-repellent action that reduced the apparition of efflorescence in OPC. Two were in solid form and were added, at 1% by mass, to a GP14.5 formulation during the mixing. Three others were in liquid form and were also added during mixing and in the same proportion. The last ERA was a surface water repellent, to be applied on the surface after 24 h. It was designed to avoid water exchanges with the outside.

Table 6. Identification, actions and mass contents of the industrial efflorescence reducing agents (ERA) used in the geopolymer GP14.5.

Samples on Figure 36	ID of ERA	Action	Content (% by mass)
a)	ERA1	Solid water repellent	1%
b)	ERA2	Solid water repellent	1%
c)	ERA3	Liquid water repellent	1%
d)	ERA4	Liquid water repellent	1%
e)	ERA5	Surface water repellent	application on the surface after 24h
f)	ERA6	Liquid water repellent	1%

After a week of semi-immersion testing, all the specimens presented non-negligible amounts of efflorescence, together with significant surface damage (Figure 39). In the five cases where an ERA (liquid or solid) was added, there was detachment of the upper part of the geopolymer cylinders (Figure 39 a, b, c, d, and f). In the case of the surface ERA, entire pieces were seen to have become detached from the top of the cylinder (Figure 39 e). The addition of a product having a water-repellent action thus had a detrimental influence on metakaolin-based geopolymer, by promoting subflorescence leading to surface damage.

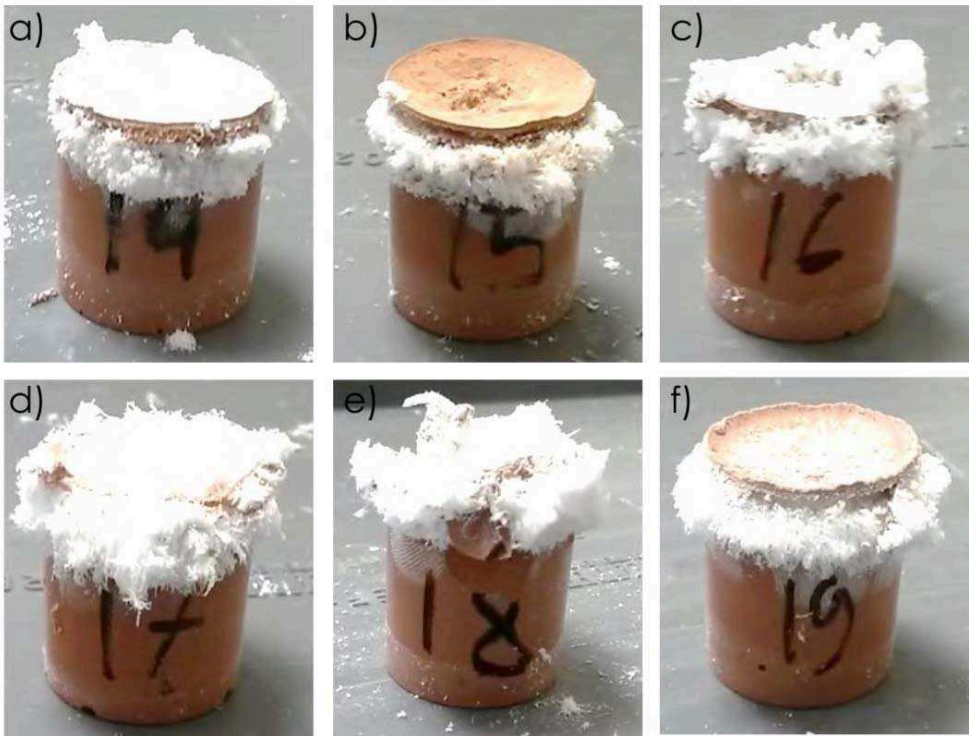

Figure 39. *Efflorescence on GP14.5 geopolymer with addition of industrial efflorescence reducing agents (ERA) made for OPC, presented in Table 6.*

However, as pointed out previously, this study was not exhaustive, and many other tests would be required to conclude on the impact of the ERA on metakaolin-based geopolymer. Even though these results suggest that they do not prevent efflorescence, the influence of the composition or the amount added remains to be assessed.

Nevertheless, these observations showed that, regardless of their forms or compositions, water repellents did not appear to be an effective solution for reducing efflorescence in geopolymer, as they seemed to encourage subflorescence. An extensive study of the formulation of the geopolymer to reduce the amount of alkalis would probably be a better approach to avoid this durability issue.

In short

Efflorescence risk in Mk-based geopolymer	High
Characterization of the crystals formed	- In natural condition: sodium carbonate - In accelerated condition (50% of CO_2): sodium bicarbonate
Crystal growth speed	Fast and in large quantities
Durability issues due to efflorescence	Significant surface damage due to subflorescence
<u>Parameters influencing growth</u>	
The surface condition:	- largest growth on surfaces cured in open air - largest surface damages on the surfaces cured under protection (subflorescence)
Curing temperature	Efflorescence larger and more dense in the case of heat treatment
Nature of the alkali	The sodium substitution by the potassium led to a significant reduction of the efflorescences.
ERA	None of the ERA tested had a positive impact in metakaolin-based GP.

This study highlighted the importance of efflorescence in sodium-based geopolymers and has revealed potential risks concerning their durability. Factors influencing the growth of efflorescence crystals have been shown, allowing their behaviour to be better understood. It was thus shown that the use of potassium would reduce the appearance of efflorescence but, on the other hand, the products used for this purpose in OPC would have no impact in the case of geopolymer. It therefore appears that a study dedicated to this efflorescence phenomenon in metakaolin-based geopolymer and to the possible ways of avoiding it would be highly desirable. A sodium-based geopolymer formulation study would be very appropriate and should aim to find the right proportion of sodium to ensure good mechanical performances while making less alkali available for the growth of efflorescence.

VI. Conclusion

The experimental work performed in this study was intended to assess the durability risks due to the carbonation reaction in metakaolin-based geopolymer activated by sodium silicate. Regarding the risks of corrosion by carbonation, which is the greatest risk in OPC structures, the evaluation of the impact of this reaction within the pore solution, using FTIR analysis and pH-meter titration, led to the following conclusions.

- After 365 days, the pH of the pore solution of geopolymer paste cured in a natural carbon dioxide atmosphere presented no risk of corrosion by carbonation, since the pH value of the pore solution was higher than the steel depassivation limit of 9.

- It has been shown that the carbonation reaction in the pore solution would occur in two steps, with first the carbonation of the sodium to form sodium carbonate, followed by an evolution in the carbonate/ bicarbonate phase equilibrium.

- The carbonate/ bicarbonate phase equilibrium emerged as the determining factor of the pH of the pore solution over time. And it was shown to be highly dependent on the temperature and the CO_2 content of the air.

- The rapidity of the carbonation reaction in these systems (pore solution carbonated at 97% in 14 days) revealed that the accelerated tests performed for OPC were useless for the geopolymer formulation studied. Moreover, it was also concluded that these tests changed the carbonate phase equilibrium, resulting in a reaction product that was not representative of the natural reaction and even led to false conclusions.

- It was concluded that the risk of corrosion by carbonation in metakaolin-based geopolymer activated by sodium silicate was negligible and that only an increase in the CO_2 content of the air, or a significant increase in temperature would lead to durability issues due to carbonation.

In contrast, the efflorescence observation revealed non-negligible durability issues for geopolymer activated by sodium silicate. A significant growth of sodium carbonate crystals was found on the surface of the geopolymer, leading to notable aesthetic problems. It was also shown that this growth could be responsible for serious surface damage (as previously observed on beam surfaces). In this study the following conclusions were drawn:

- Efflorescence growth was found to be very fast and dense, with favoured emergence on surfaces that had been cured in the open air.

- Surfaces cured under protection, such as those in contact with the mould walls, seem to have a more closed porosity, preserving them from significant efflorescence growth. However, this is thought to induce a subflorescence that would be responsible for the surface damage.

- In this work context, the addition of commercial efflorescence reducing agents did not enable this efflorescence growth to be reduced, and only the use of potassium silicate would greatly minimise its appearance.

Due to their very high alkali content compared to OPC, geopolymers are open to many questions, especially regarding their durability. The results of this study provide some answers concerning carbonation, showing that it would not be detrimental to steel reinforcement but that the risks of efflorescence are significant and need to be further evaluated in order to be prevented.

References

Allahverdi, A., Mehrpour, K., Kani, E. N. (2008) Investigating the possibility of utilizing pumice-type natural pozzonal in production of geopolymer cement. *CERAMICS SILIKATY*, 52(1): 16.

Allahverdi, A., Shaverdi, B., Kani, E. N. (2010) Influence of sodium oxide on properties of fresh and hardened paste of alkali-activated blast-furnace slag. *International Journal of Civil Engineering*, 8: 304-314.

Allahverdi, A., Kani, E. N., Yazdanipour, M. (2011) Effects of blast-furnace slag on natural pozzolan-based geopolymer cement. *Ceramics-Silikaty*, 55(1): 68-78.

Allahverdi, A. Kani, E.N., Hossain K.M.A., and Lachemi, M. (2014) Methods to control efflorescence in alkali-activated cement-based materials. *In: Handbook of Alkali-activated Cements, Mortars and Concretes*, Editors: F. Pacheco-Torgal, J. Labrincha, C. Leonelli, A. Palomo, P. Chindaprasit, Woodhead Publishing Limited, Cambridge (UK), in press

Badar, M. S., Kupwade-Patil, K., Bernal, S. A., Provis, J. L., Allouche, E. N. (2014). Corrosion of steel bars induced by accelerated carbonation in low and high calcium fly ash geopolymer concretes. *Construction and Building Materials*, 61: 79-89.

Bakharev, T., Sanjayan, J. G., Cheng, Y. B. (2001) Resistance of alkali-activated slag concrete to carbonation. *Cement and Concrete Research*, 31(9), 1277-1283.

Barbosa, V. F., MacKenzie, K. J., Thaumaturgo, C. (2000) Synthesis and characterisation of materials based on inorganic polymers of alumina and silica: sodium polysialate polymers. *International Journal of Inorganic Materials*, 2(4): 309-317.

Bensted, J. (2000) Efflorescence-prevention is better than cure. *Concrete*. 34(8): 40-1.

Bernal, S. A., de Gutierrez, R. M., Provis, J. L., Rose, V. (2010) Effect of silicate modulus and metakaolin incorporation on the carbonation of alkali silicate-activated slags. *Cement and Concrete Research*, 40(6): 898-907.

Bernal, S. A., de Gutiérrez, R. M., Pedraza, A. L., Provis, J. L., Rodriguez, E. D., Delvasto, S. (2011) Effect of binder content on the performance of alkali-activated slag concretes. *Cement and Concrete Research*, 41(1): 1-8.

Bernal, S. A., Provis, J. L., Brice, D. G., Kilcullen, A., Duxson, P., Van Deventer, J. S. (2012) Accelerated carbonation testing of alkali-activated binders significantly underestimates

service life: the role of pore solution chemistry. *Cement and Concrete Research*, 42(10): 1317-1326.

Bernal, S. A., Provis, J. L., Walkley, B., San Nicolas, R., Gehman, J. D., Brice, D. G., Van Deventer, J. S. (2013) Gel nanostructure in alkali-activated binders based on slag and fly ash, and effects of accelerated carbonation. *Cement and Concrete Research*, 53: 127-144.

Bernal, S.A. (2014) The resistance of alkali-activated cement-based binders to carbonation. *In: Handbook of Alkali-activated Cements, Mortars and Concretes*, Editors: F. Pacheco-Torgal, J. Labrincha, C. Leonelli, A. Palomo, P. Chindaprasit, Woodhead Publishing Limited, Cambridge (UK), in press

Bensted, J. (2000) Efflorescence-prevention is better than cure. *Concrete*, 34(8): 40-1.

Boher, C., Martin, I., Lorente, S., Frizon, F. (2014). Experimental investigation of gas diffusion through monomodal materials. Application to geopolymers and Vycor® glasses. *Microporous and Mesoporous Materials*, 184: 28-36.

Bortnovsky, O., Dědeček, J., Tvarůžková, Z., Sobalík, Z., Šubrt, J. (2008) Metal ions as probes for characterization of geopolymer materials. *Journal of the American Ceramic Society*, 91(9): 3052-3057.

Cowie, J., and Glasser, F. P. (1992) The reaction between cement and natural waters containing dissolved carbon dioxide. *Advances in cement research*, 4(15): 119-134.

Criado, M., Palomo, A., Fernández-Jiménez, A. (2005) Alkali activation of fly ashes. Part 1: Effect of curing conditions on the carbonation of the reaction products. *Fuel*, 84(16): 2048-2054.

Cyr, M., Rivard, P., Labrecque, F., Daidie, A. (2008) High-Pressure Device for Fluid Extraction from Porous Materials: Application to Cement-Based Materials. *Journal of the American Ceramic Society*, 91(8): 2653-2658.

Galan, I., Andrade, C., Castellote, M. (2013) Natural and accelerated CO 2 binding kinetics in cement paste at different relative humidities. *Cement and Concrete Research*, 49: 21-28.

Glasser, F. P., Marchand, J., Samson, E. (2008) Durability of concrete - degradation phenomena involving detrimental chemical reactions. *Cement and Concrete Research,* 38(2): 226-246.

Granizo, M. L., Alonso, S., Blanco-Varela, M. T., Palomo, A. (2002) Alkaline activation of metakaolin: effect of calcium hydroxide in the products of reaction. *Journal of the American Ceramic Society*, 85(1), 225-231.

Hobbs, D. W. (2001) Concrete deterioration: causes, diagnosis, and minimising risk. *International Materials Reviews*, 46(3): 117-144.

Houst, Y. F. (1996) The role of moisture in the carbonation of cementitious materials. *Internationale Zeitschrift für Bauinstandsetzen und Baudenkmalpflege*, 2(LTP-ARTICLE-1996-029), 49-66.

Kresse, P. (1989) Coloured concrete and its enemy: efflorescence. *Chemistry and Industry*. 93-5.

Lea, F. M. (1970) *The chemistry of cement and concrete*. Edward Arnold.

Lloyd, R. R., Provis, J. L., Van Deventer, J. S. (2010) Pore solution composition and alkali diffusion in inorganic polymer cement. *Cement and Concrete Research.* 40(9): 1386-1392.

Kani, E. N., Allahverdi, A., Provis, J. L. (2012) Efflorescence control in geopolymer binders based on natural pozzolan. *Cement and Concrete Composites*, 34(1): 25-33.

Norsuzailina, M. S., and Sinin, H. (2013) Efflorescence Phenomenon on Concrete Structures. *Advanced Materials Research* 626: 747-750.

Ollivier, J.P. and Vichot, A. (2008) La durabilité des bétons : Bases scientifiques pour la formulation de bétons durables dans leur environnement, Presses de l'École nationale des ponts et chaussées (In French).

Pacheco-Torgal, F., and Jalali, S. (2010) Influence of sodium carbonate addition on the thermal reactivity of tungsten mine waste mud based binders. *Construction and Building Materia*ls, 24(1): 56-60.

Palacios, M., and Puertas, F. (2006) Effect of carbonation on alkali-activated slag paste. *Journal of the American Ceramic Society*, 89(10): 3211-3221.

Papadakis, V. G., Vayenas, C. G., Fardis, M. N. (1991) Experimental investigation and mathematical modeling of the concrete carbonation problem. *Chemical Engineering Science*, 46(5): 1333-1338.

Pouhet, R., and Cyr, M. (2014) Studies of Natural and Accelerated Carbonation in Metakaolin-Based Geopolymer. *In Advances in Science and Technology*. (Vol. 92, pp.38-43).

Pourbaix, M. (1974) Atlas of electrochemical equilibria in aqueous solutions.

Sanjuan, M. A., Andrade, C., and Cheyrezy, M. (2003) Concrete carbonation tests in natural and accelerated conditions. *Advances in Cement Research*, 15(4): 171-180.

Škvára, F., Kopecký, L., Šmilauer, V., Bittnar, Z. (2009) Material and structural characterization of alkali activated low-calcium brown coal fly ash. *Journal of Hazardous Materials.* 168(2): 711-720.

Škvára, F., Šmilauer, V., Hlaváček, P., Kopecký, L., Cilova, Z. (2012) A weak alkali bond in (N, K)–A–S–H gels: evidence from leaching and modeling. *Ceramics–Silikáty*, 56(4): 374-382.

Suchý, R., Pořízka, J., Wasserbauer, J., & Kalina, L. (2014) Reduction of Efflorescence in the Alkali Activated Systems. *Advanced Materials Research*. 1000: 318-321.

Szklorzová, H., Bílek, V. (2008) Influence of alkali ions in the activator on the performance of alkali-activated mortars. In *Proceedings of the 3rd International Symposium on Non-Traditional Cement and Concrete*. 777-784.

Usdowski, E. (1982) Reactions and Equilibria in the Systems CO_2-H_2O and CaCO3-CO_2-H_2O (0°-50° C). *A Review. Neues Jahrbuch für Mineralogie-Abhandlungen*, 148-171.

Young, J. F., Berger, R. L., Breese, J. (1974) Accelerated curing of compacted calcium silicate mortars on exposure to CO2. *Journal of the American ceramic society*, 57(9): 394-397.

Chapter IV.

Alkali–silica reaction in metakaolin-based geopolymer mortar

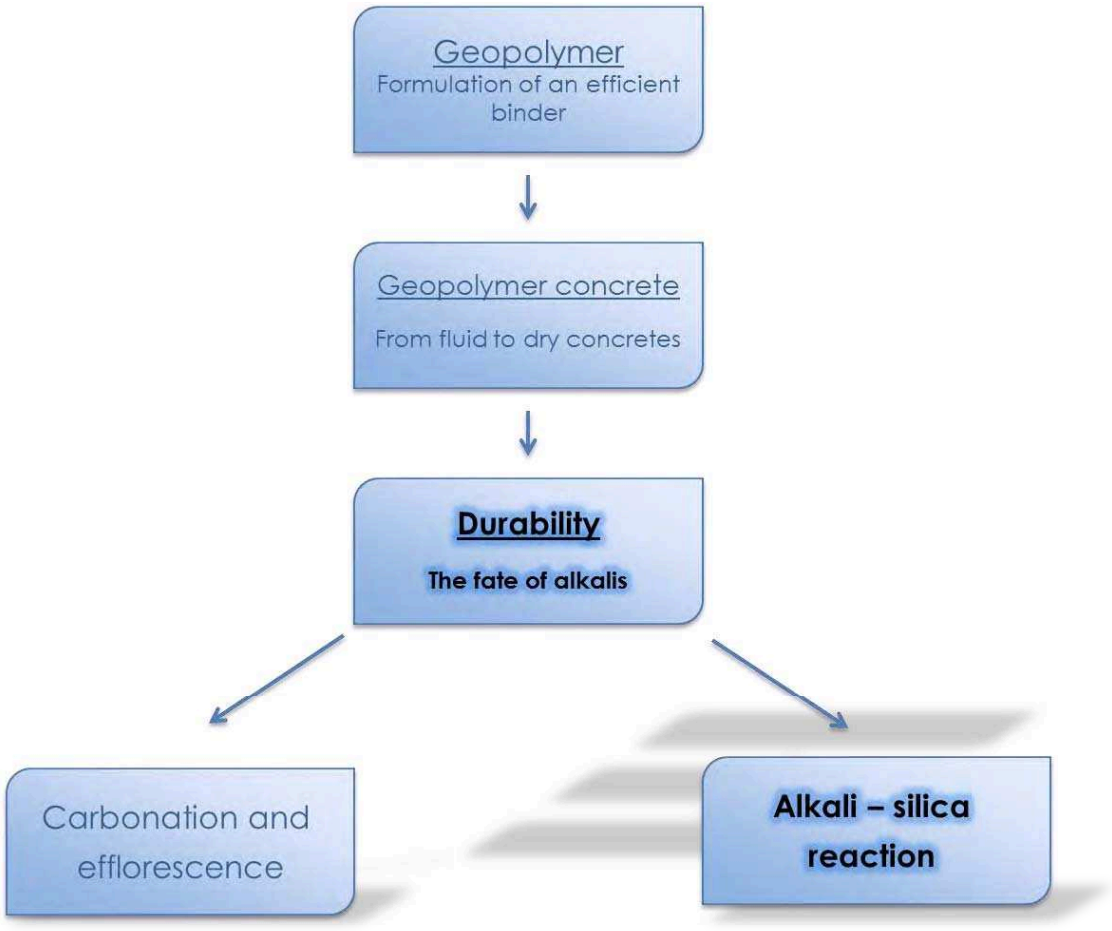

Table of content

I. Introduction

The previous chapters have shown that metakaolin-based geopolymer could potentially offer an efficient alternative to ordinary Portland cement (OPC) for the formulation of concrete. However, many concerns can be expressed with regard to alkali-silica reaction (ASR) since the activation solution used involves high alkali content. This widely studied reaction involving, in Portland cement concrete, the presence of soluble alkalis, a moist environment and the presence of alkali-reactive aggregates, causes significant and irreversible damage in structures due to swelling of the concrete. The current literature on ASR in alkali-activated materials does not allow their behaviour towards this reaction to be predicted, although some tendencies have emerged from these studies. The largest number of studies performed on alkali-activated materials (AAM) concerns alkali-activated slag (AAS), but does not allow us to conclude on their resistance against ASR. Studies of aluminosilicate systems (based on fly ash or metakaolin) show that they seem to resist ASR better than AAS or OPC. But the limited number of existing articles, in which the accelerated tests, the formulation and the aggregates used are different most of the time, show that no conclusion can actually be drawn regarding ASR resistance of geopolymers. The subject of metakaolin-based geopolymer and ASR remains to be investigated.

This study had thus two purposes. First an investigation was made on the ASR behaviour of metakaolin-based geopolymer mortars in presence of six different sands, having various levels of ASR reactivity. The tests carried out involved dimensional changes, mechanical characteristics, and SEM-EDX analysis, in order to determine if the geopolymers are actually more resistant to ASR than OPC. A comparison with OPC mortars was systematically carried out to reveal the reactivity of the sands used and also to bring out differences in the behaviour of these two systems. In a second time, a study was performed on the various accelerated test conditions, based on OPC standards, by varying some parameters that could affect the results to ensure the viability of the stated conclusions. A test in natural conditions also verified these claims.

This chapter is based on three published studies: a detailed review of the literature (Cyr and Pouhet 2014), an article in Materials and Structures (Pouhet and Cyr 2015) and a conference proceeding of the International Conference on Non-Traditional Cement and Concrete (Pouhet and Cyr 2014).

II. Resistance of alkali-activated binders to alkali-aggregate reaction

This part presents the bibliographic data on the susceptibility of alkali-activated binders to be affected by alkali-aggregate reaction (AAR). As this reaction usually occurs in Portland cement concretes, the macro- and microscopic manifestations of alkali-silica reaction (ASR), as well as their mechanisms in Portland cement-based materials is first explained. Then a synthesis of the results found in the literature regarding ASR in alkali-activated binders based on fly ash and metakaolin is presented.

1. AAR in Portland cement concrete

Alkali-aggregate reaction is an endogenous reaction which usually occurs in Portland cement concretes. It is generated from the internal components of the initial concrete mixture, without the need for exterior aggressive agents. The reaction products are expansive compounds which induce stresses, and hence cracking, in concrete. Many international congresses have been dedicated to this concrete pathology (ICAAR1 to ICAAR14). The two principal types of AAR are the alkali-silica reaction (ASR) and the alkali-carbonate reaction (ACR), the former being much more frequent than the latter.

Alkali-silica reaction (ASR) was first identified in the 1940's (Stanton, 1940) and occurs when the amorphous or poorly crystallised silica phase in an aggregate (e.g. chert, flint, chalcedony or opaline sandstone) is attacked and dissolved by the alkali hydroxides in the concrete pore solution. The formation of an alkali-silica gel leads to concrete swelling and cracking. ASR will develop only if the following conditions are found: sufficient amount of alkalis in concrete pore solution, sufficient moisture level in concrete and reactive aggregate.

Alkali-carbonate reaction (ACR) involves the de-dolomitisation (decomposition of dolomite to brucite and calcite) of carbonate rocks by strongly alkaline solutions, to form expansive products (Swenson, 1957, Swenson and Gillot, 1964). The expansion often occurs within the aggregate particle causing cracks and, therefore, deleterious expansion of the mass. Some authors report that the dissolution of dolomite could expose silicate minerals initially enclosed in the limestone, to produce alkali-silica or -silicate gels (Gillott, 1964, Hudec, 1990).

1.1 Visual and microscopic manifestations of ASR

Alkali-silica reaction in Portland cement concretes can be found in different kinds of structures. Figure 1 shows a hydraulic dam in which ASR was detected (Sellier et al., 2009). Map-cracking pattern is a typical indicator of ASR, and the network of cracks appears when the pressure exerted by the gel exceeds the tensile strength of the concrete, which is generally about 10% of its compressive strength. The expansion could also lead to relative displacements of different portions of the structure, which can cause serviceability problems. However, the risk of catastrophic failure is low due to the slow kinetics of ASR-deterioration, since the reaction could take many years to develop. It can be noted that surface deposits (efflorescence) of ASR gel or calcium carbonate can be found along cracks in concrete (Figure 1). Popouts caused by a fragment breaking out of the surface of the concrete can also be seen. They leave a hole that is usually 25 to 50 mm large.

Figure 1. *View of an ASR map-cracking pattern in a dam*

At a macroscopic scale, the observation of ASR-affected concretes reveals traces of gel in pores and at the interface between paste and aggregates (circles on Figure 2). Reaction rims are also seen around reactive aggregates (arrows on Figure 2).

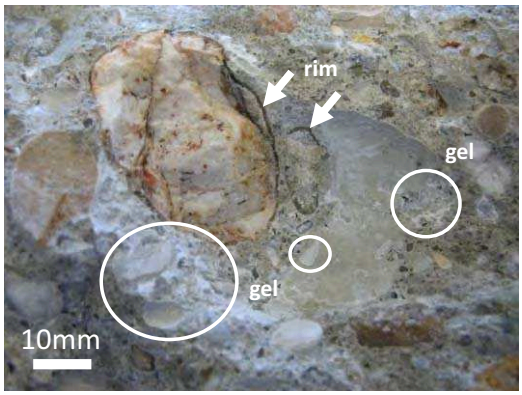

Figure 2. *Visual observation of a dam-concrete affected by ASR. Circles show traces of gel in pores and aggregate-prints (Sellier et al., 2009).*

At a microscopic scale (Figure 3a-b), the reaction products of ASR have a typical morphology and composition that can easily be identified using scanning electron microscopy (SEM) and energy dispersive X-ray spectrometry (EDX). Smooth textures are usually characteristic of young gels (Figure 3c), while older gels often crystallise as rosette-types morphologies (Figure 3d).

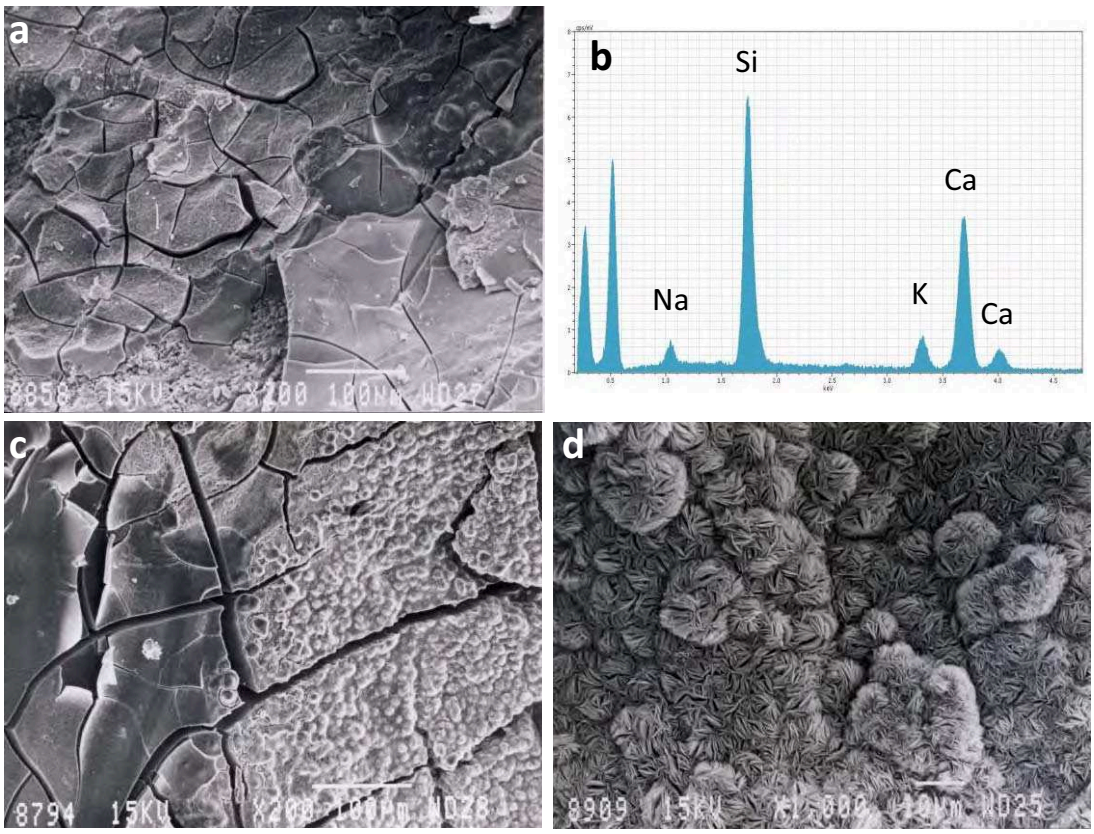

Figure 3. *Typical morphologies and composition of ASR-reaction products obtained with scanning electron microscopy (SEM) and energy dispersive X-ray spectrometry (EDX). (a,b,c) SEM micrographs and EDX spectrum of ASR-gel (cracks were provoked by the drying in the microscope chamber), (d) Rosette-type morphology of crystallised gel.*

In the laboratory, the main tests to identify reactive aggregates or reactive concrete formulations are based on expansion measurements, although other kind of tests can be performed, such as petrographic examination, chemical tests, etc. Due to the long time needed for the development of ASR, these tests need to be accelerated most of the time for laboratory testing. The main problem is thus to make sure that the accelerated tests do not lead to a denaturation of the phenomenon and so provide misleading information. This is a key point that was studied and discussed for several years in the case of Portland cement concretes, and it must be expected that it will be the same for alkali-activated materials (AAM).

1.2 Mechanisms of ASR

The presence of alkalis and reactive silica are necessary conditions for ASR to occur. In Portland cement concretes, alkalis come mainly from the cement, but aggregates, mineral additives and organic admixtures can bring some and are usually taken into account. It is often recognised that concrete is free of abnormal expansion due to ASR if the alkali content in the mixture does not exceed 3-5 kg of Na_2O_{eq} per m^3 of concrete (Rogers and Hooton, 1991, Hobbs, 1993, Thomas et al., 1996, Shehata and Thomas, 2000). It should be noted that in the case of AAM, the alkali content could reach values of more than 40 kg per m^3.

The different forms of SiO_2 that have been reported to be alkali-reactive include opal or opaline silica, chancedony, cristobalite, tridymite, microcrystalline, cryptocrystalline and highly-strained quartz, and amorphous silica found in volcanic or artificial glasses (Sims and Nixon, 2003). Many aggregates in the world can be totally or partly composed of one or many of these forms of reactive silica. Most of them were listed by RILEM TC 191-ARP (Sims and Nixon, 2003), the main ones being: andesite, chert, granite, gneiss, greywacke, siliceous limestone, quartzite, rhyolite, sandstone and tuff. The silica in aggregates is composed of siloxane bridges (Si-O-Si), and surfaces, both external and internal, are covered with silanol groups (Si-OH).

ASR in concrete is initiated by the dissolution of the different forms of active silicates present in the aggregate. Dent Glasser and Kataoka (1981a, 1981b) identified two mechanisms leading to the dissolution of silica in the concrete environment: hydroxyl ion attack of siloxane bridges (equation 1) and reaction of hydroxide ions with silanol groups (equation 2)

$$\equiv Si - O - Si \equiv + 2OH^- \rightarrow \equiv Si - O^- + {}^-O - Si \equiv + H_2O \quad (1)$$

$$\equiv Si - OH + OH^- \rightarrow \equiv Si - O^- + H_2O \quad (2)$$

The negatively charged Si–O– species attracts positive charges such as Na^+, K^+ and Ca^{2+}, which diffuse into the reaction product in sufficient numbers to balance the charge on the negatively charged groups. The approximate stoichiometry of the reaction product, when considering sodium, would be Na0.38SiO2.19 (Dent Glasser and Kataoka, 1981a).

The reaction product is usually identified as a gel-like structure which has a higher specific volume than that of the replaced SiO_2. According to Glasser (1992), this creates swelling pressure, expansion and cracking which are characteristic of the alkali-silica reaction. The gel could also permeate through a part of the connected porous volume between aggregate and cement paste and fills a part of the connected porosity (Jones, 1988). Then the gel would exert a pressure on the cement paste, which might cause cracking and expansion of the concrete.

Other hypotheses were made to explain the expansion behaviour related or not to the production of the gel: osmotic pressure (Dent-Glasser, 1979, Diamond, 1989), double layer theory (Prezzi et al., 1997), crystallisation pressure theory (Dron and al., 1997), aggregate swelling theory (Garcia-Diaz et al., 2006).

2. AAR in alkali-activated binders

A few studies exist about the assessment of alkali-aggregate reaction of alkali-activated binders, most of them regarding the alkali-activated slag. Many of them were carried out by using tests such as ASTM C1260, which consists in accelerating the reaction by conserving mortar samples at 80°C in 1M NaOH solution for 14 days. This test is quite rapid, since the results are available in two weeks, but the conditions of the tests are relatively harsh and it can be wondered if this test is really representative of what could be found in real structures. To the author's knowledge, no in-situ tests are reported in the literature for AAR of alkali-activated binders, except maybe the long term construction made in Russia and China and reported by Shi et al. (2005), but without knowing if the aggregates were potentially reactive or not.

AAM can be separated into two categories regarding their vulnerability to AAR, alkali-activated slag and alkali-alumino-silicate, since the composition of the raw materials are very different for the two types of AAM, the former having high amounts of calcium while the later usually have much less of this element. The presence of calcium could have a significant influence on the swelling of cement-based materials containing alkali-reactive aggregates (Diamond, 1989).

In the context of this study, only reviews referring to the aluminosilicate systems having low calcium content are presented and, as no ACR references have been found, only ASR is treated. Regarding the alkali-activated slag systems, which are more extensively detailed in the literature, they have been treated in a detailed review of the literature (Cyr and Pouhet 2014).

2.1 ASR in alkali-activated fly ash systems

Two studies partly or totally dedicated to ASR of activated fly ash (AAFA) systems were carried out by Fernández-Jiménez, Palomo and García-Lodeiro (Fernandez-Jimenez et al., 2007, García- Lodeiro et al., 2007). The authors used a standardised test (ASTM C1260) to evaluate the ASR of AAFA systems compared to those containing Portland cement, by measuring the dimensional variation of samples of size 2.5x2.5x28.5 cm immersed in a 1M solution of sodium hydroxide at 85°C (instead of 80°C as specified in the standard). In OPC systems, the expansion must be below 0.1% after 16 days of immersion to be indicative of innocuous behaviour in most cases. In the work of Fernandez-Jimenez et al. (2007), the expansion tests were carried out with a siliceous sand composed of quartz and calcite, commonly used to make concrete in Spain and regarded as non-reactive. García- Lodeiro et al. (2007) studied the behaviour of three different types of mortar for both systems (OPC and AAFA): one containing the non-reactive siliceous sand, one made of opal sand, and, finally, one which was a mixture of 90 % non-reactive sand and 10% of opal sand. The binder in the Portland cement references was a CEM I with low alkali content (Na_2O_{eq} of 0.46%). AAFA mortars were made with two similar Spanish type F fly ashes, with low calcium content (CaO =3.21% and 2.44%) and a SiO_2/Al_2O_3 ratio around 2.1. The activating solution was composed of an 8M NaOH solution or a mixture of 85% 12.5M NaOH + 15% sodium silicate (SiO_2/Na_2O = 0.16). The sand/binder mass ratio of the mortars was 2.25 and the liquid/solid ratio was 0.47. The mortars were initially cured for 20 h at 85°C and a relative humidity of 99%.

The expansion results for immersion ages up to 16 days are given on Figure 4. The tests were prolonged to 90 days (García- Lodeiro et al., 2007 – B on the Figures) and 180 days (Fernandez-Jimenez et al., 2007 – A on the Figures), as shown on Figure 4. It was seen that all reference mortars with Portland cement showed very high expansions, the value of 0.1% being exceeded before the ninth day. The expansions of more than 0.20 % at 16 days after casting were indicative of potentially deleterious expansion, according to ASTM C1260. The maximum expansion was obtained for the OPC3, which contained 10% of opal (pessimum effect of this aggregate (Hobbs, 1988)). It is noteworthy that the siliceous sand, considered by the authors as non-reactive, presented much higher expansion values than the limit imposed by the test. This could have been due to the presence of cryptocrystalline quartz in its structure.

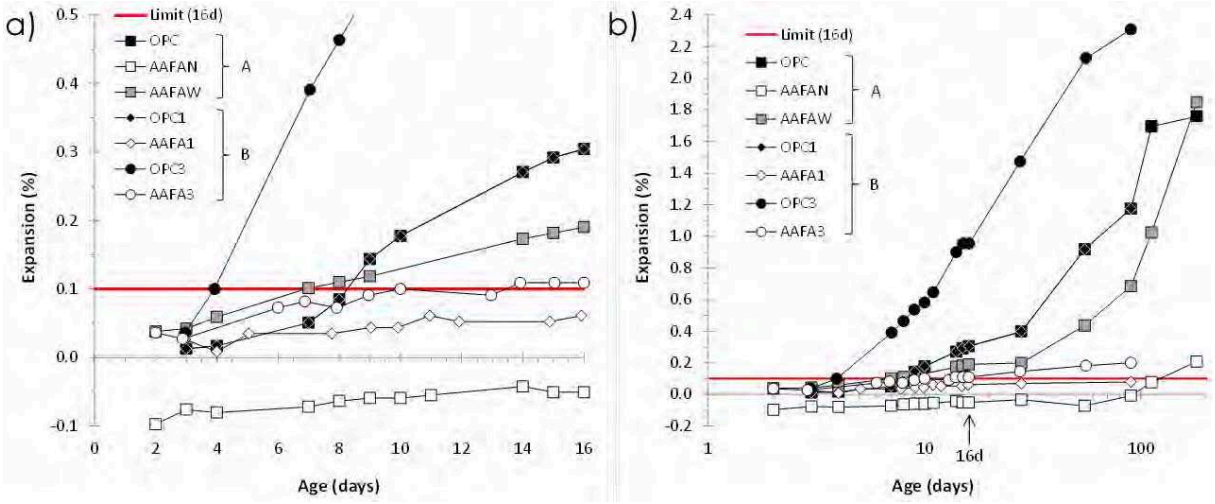

Figure 4. *Expansion of mortars made of Portland cement (OPC) and activated fly ash (AAFA) up to 16 days (a) and 180 days (b), according to ASTM C1260 (85°C in 1M NaOH). Data from Fernandez-Jimenez et al.(2007)(A) and García- Lodeiro et al. (2007)(B).*

Generally speaking, the alkali-activated fly ash mortars presented much lower expansions than their OPC replicate. However it cannot be said that AAFA systems were completely safe regarding ASR swelling. On the one hand, some results were indicative of innocuous behaviour (expansion < 0.1% at 16d), for instance AAFA mixtures with siliceous sand as the sole aggregate and NaOH as the sole activator. But on the other hand, a few AAFA mortars showed disturbing behaviour:

- AAFAW, containing a siliceous sand and an activator made of 15% of sodium silicate and 85% of 12.5M NaOH, showed a significant expansion in the first days of the test, and followed a similar trend as that of OPC. However, no surface cracking was seen after 16d. According to the authors, the conditions of the accelerated test may have caused the

formation of ASR-expansive products and/or zeolites that was believed to be the cause of a certain amount of stress, which would contribute to the expansion detected.

- AFAN, composed of a siliceous sand and activated by a 8M NaOH solution, presented an increase in its kinetics of expansion after 100 d, leading to the question of whether the ASR was only delayed. However, it should be said that 100 d at 85°C in 1M NaOH solution could represent a very long time when compared to in situ conservation.
- AAFA3, made of 10% opal sand, had an expansion slightly higher than the limit of 0.1% at 16 d.
- The expansion results of AAFA2, containing 100% opal sand and activated by an 8M NaOH solution, were not presented in the paper due to the early deterioration of the specimens. This was probably caused by an almost immediate dissolution of the highly reactive silica from opal, as proved by the disappearance of the characteristic XRD peak of this mineral.

In both papers, studies were also made with SEM / EDX and XRD to better understand the mechanisms of ASR in OPC and AAFA matrices. OPC systems (García- Lodeiro et al., 2007) showed the presence of gel with high sodium concentration at 16 days and gel morphology such as "rosette ", "pseudo-rosette" or "rod" at 90 days. A drop of portlandite content characterised by a decrease of XRD-peak intensities was found between 16 and 90 days. This was interpreted as an incorporation of calcium in the ASR gels.

In AAFAN, SEM observations at 16 days did not reveal the formation of typical gel structure of ASR, but crystalline phases of zeolites were found: hydroxysodalite, herschelite and zeolite P (Fernandez- Jimenez and al. 2007). The presence of zeolite P was explained by the very aggressive conditions to which the specimens were subjected. At 180 days SEM observation showed small amounts of alkali-silicate gel containing calcium (Ca/Si = 0.15 and Na/Si = 0.72) with pseudo-rosettes morphology, and a supplementary zeolite phase: analcime (Si/Al = 2.40 and Na/Al = 1.26) (Fernandez- Jimenez and al., 2007). This might explain the increase in the kinetic of expansion of this mortar after 100 d.

For AAFA1, García- Lodeiro et al. (2007) found mainly an amorphous phase without calcium at 16 days (P4 on Figure 5a). At 90 days, in addition to this amorphous phase, they found the presence of zeolites P (P5 on Figure 5b), but also very few alkali -aggregate reaction products with a pseudo-rosette type morphology (P4 on Figure 5b). The same observations were made for AAFA3, with a greater amount of zeolite probably due to the 10% of highly reactive silica introduced by the opal (Figure 5c).

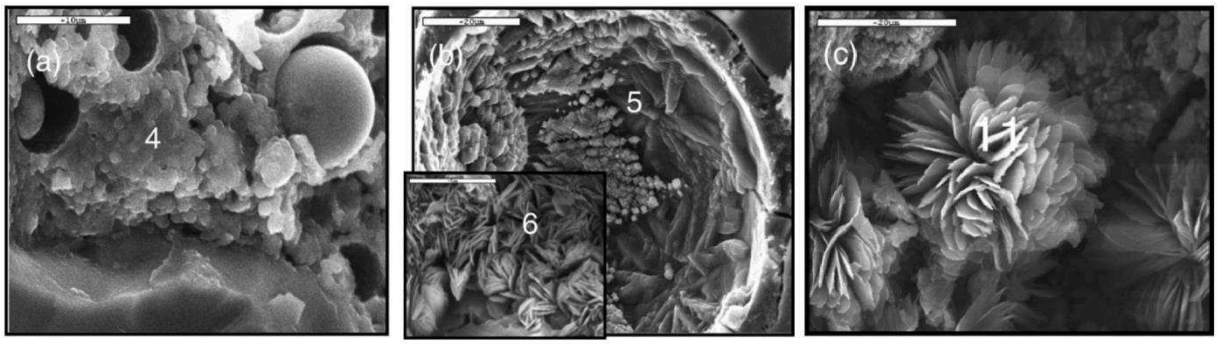

Figure 5. *Photomicrograph of AAFA1 mortar (a) at 16 days. (P4) product of alkaline activation; (b) At 90 days, zeolitic crystalline compounds in the matrix (P5); ASR product with a "rosette-type" morphology (P6). And of FA3 mortar (c) at 90 days. (P11) ASR product with a "pseudo rosette-type" morphology. Pictures from García-Lodeiro et al. (2007).*

Although some evidence of an attack of the aggregates was found in the case of AAFA, reduced expansions compared to that of OPC systems were obtained. According to the authors of these papers, this could be due to different factors:

- A deficiency in calcium, which has an essential role in ASR, as already stated in different studies (Dent Glasser and Kataoka, 1982, Chatterji, 1979, Thomas, 1998). Several authors (Bleszynski and Thomas, 1998, Shehata and Thomas, 2000) proved that the addition of $Ca(OH)_2$ promoted ASR-induced expansion and others (Hou et al., 2004) showed that there was a direct relationship between portlandite uptake and the formation of ASR gels.

- Alkali-silicate gel with pseudo-rosettes morphology would be sufficiently fluid to seep through cracks and partially or completely fill the gaps in the matrix, thereby attenuating expansion.

- The increase in zeolite concentration due to the ASR would not be harmful, because they are normally formed as a precipitate in the preexisting pores in the matrix, thereby their growth would not cause stress which could lead to the formation of cracks.
However it must be kept in mind that more realistic conditions of conservation (than 85°C in 1M NaOH solution) still need to be tested to confirm the possible innocuous behaviour of alkali-activated fly ash systems.

2.3 ASR in alkali-activated metakaolin

The results on metakaolin-based geopolymers are rare. Li et al. (2005, 2006) compared the ASR-behaviour of cement-based binders (Portland cement and slag, fly ash and silica fume) to one geopolymer composed of metakaolin, fly ash, silica fume and alkali-activator. The alkali content in the geopolymer reached 12.1%. The reactive aggregate was a crushed quartz glass with an amorphous silica content of more than 90%. The ASR test was based on ASTM C441, itself based on ASTM C227 (38°C). The results showed that the higher expansions were obtained for mortars containing Portland cement only, followed by mixtures with pozzolans (65 to 82% reduction of expansion). The geopolymer mortar, which contained a much higher alkali content than OPC-based mortars (12.1% vs. less than 1%), led to negligible length variations (0.01% at 14 days and -0.03% at 90 days). According to the authors, "geopolymers do not generate any dangerous alkali-silica reaction", since there would be not enough free alkalis to react with the reactive aggregate and thus produce alkali-silica gel, as Na^+ and K^+ are fixed in the framework cavities of SiO_4 and AlO_4 to balance the negative charge of Al^{3+}.

Literature on fly ash and metakaolin based systems are therefore not conclusive regarding the susceptibility of these materials to ASR. Those studies generally provide results on only a few different aggregates, and use a single accelerated test to assess the impact of the ASR on the geopolymer. The purpose of this study is therefore to evaluate as thoroughly as possible the behaviour of metakaolin-based geopolymer against ASR, by using seven sand aggregates having variable reactivity but also by comparing the influence of the different conditions of accelerated and natural testing.

III. Materials and Methods

1. Material

1.1 Binders

The materials used in this study were:

- Calcined flash metakaolin (Table 1)
- Cement: CEM I 52.5 N CE CP2 NF (0.48% Na_2O equivalent), according to NF EN 197-1 (Table 1)
- Waterglass solution, molar ratio SiO_2/Na_2O = 3.3 (Wg3.3)
- Pure-grade NaOH and KOH

All the geopolymers were made using the "flash" metakaolin studied previously. The activating solution was an industrial waterglass solution (Bétol 49T, Woellner) containing 8% Na_2O by mass and having an SiO_2/Na_2O molar ratio of 3.3. Pure NaOH was added to this commercial solution 24 hours before mixing to obtain the desired amount of alkalis in the final formulation. The comparison was made with a CEM I 52.5 mortar in which were added pure KOH to boost the alkali amount of the OPC mortars.

Table 1. Chemical composition of the raw materials (% by mass)

	SiO_2	Al_2O_3	Fe_2O_3	CaO	MgO	Na_2O	K_2O	SO_3
Cement	19.75	5.27	2.39	63.97	1.93	0.17	0.48	2.95
Metakaolin	68.10	24.10	3.73	0.91	0.22	0.08	0.35	0.03

1.2 Sand aggregates

Seven sands were selected in order to cover a wide range of types and geological origins, from low to high kinetics of silica dissolution. Their type and mineralogy are listed in Table 2 and their XRD patterns are shown in Figure 6. For each aggregate, particle size was controlled by sieving between 0.16 mm and 2 mm.

Table 2. Types and mineralogy of the reactive used.

I.D.	Name	Type	Mineralogy	Theoretical ASR reactivity
a	Marble sand	-	Calcite	none
b	Quartz	-	Quartz	very low
c	Quartzite	Metamorphic	Quartz, micas (tr), amorphous material (tr)	medium
d	Siliceous limestone	Sedimentary sand	Calcite, quartz, micas (tr), feldspars (tr)	medium
e	Sand with opal	Alluvial sand	Quartz, feldspars, opal	high
f	Soda-glass	Crushed glass	Amorphous material	high
g	Opal	Igneous	Amorphous material, tridymite, quartz (tr)	high

o Sand **a** was a marble sand composed entirely of calcite, and thus having no silica to be dissolved. This sand was chosen as a reference for non-reactive aggregate as it usually presents no trace of ASR (Gao et al. 2011).

o Sand **b** was a siliceous sand used in standard mortars in accordance with EN 196-1. This quartz sand is usually considered as non-reactive regarding ASR, although it can expand slightly in accelerated test conditions (Gao et al. 2013).

o Sand **c** was a quartzite sand of metamorphic origin and it was selected for its low kinetics of silica dissolution (Carles-Gibergues et al. 2013). It contained mainly quartz, phyllosilicate minerals (mica-type such as muscovite) and amorphous silica (around 7.6% by mass) (Gao et al. 2013).

o Sand **d** was a sedimentary siliceous limestone composed of calcite and dolomite, with significant amounts of impurities including quartz, plagioclase feldspars, micas, kaolinite and pyrite. It contained around 7% by mass of amorphous SiO_2 (Gao et al. 2013) and was considered to have a low kinetics of silica dissolution in ASR tests (Carles-Gibergues et al. 2008).

o Sand **e** was an alluvial sand containing opal (around 10% by mass), well crystallised quartz and plagioclase feldspars (Cyr et al. 2009). This sand was chosen for its high alkali-silica reactivity and its high kinetics of silica dissolution due to the presence of opal (Cyr et al. 2009).

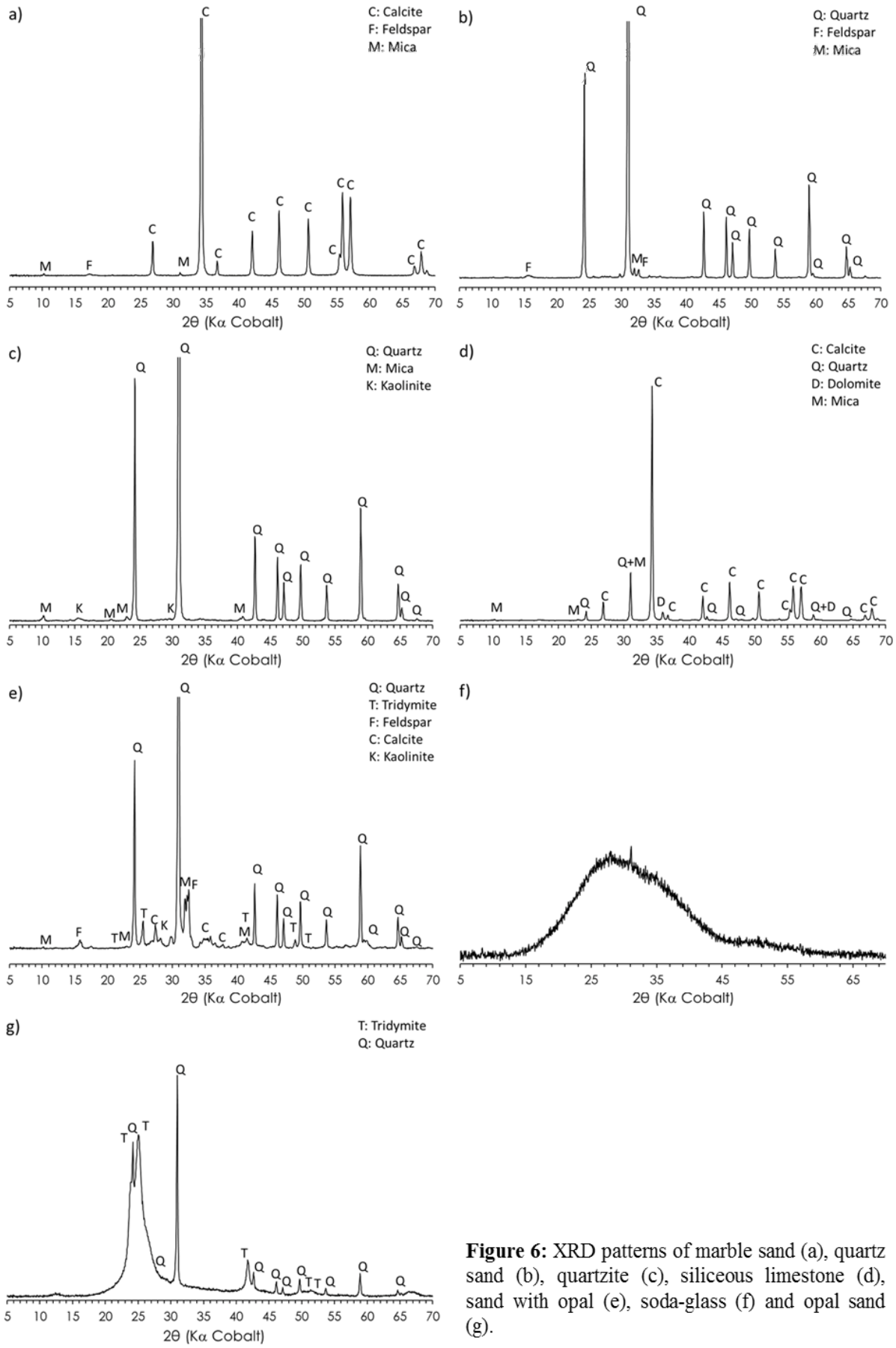

Figure 6: XRD patterns of marble sand (a), quartz sand (b), quartzite (c), siliceous limestone (d), sand with opal (e), soda-glass (f) and opal sand (g).

o Sand **f** was a glass resulting from the crushing of glass bottles. It was chosen for its amorphous structure and thus the large amount of silica available to be dissolved (around 68% by mass), leading to high ASR-expansion (Carles-Gibergues et al. 2008; Idir et al. 2010).This kind of aggregate is often used as the modelled aggregate in ASR studies (e.g. (Carles-Gibergues et al. 2008)).

o Sand **g** was an opal corresponding to igneous rock having a predominant glassy phase. It is very deleterious and is commonly reported in laboratory experiments as a reference mineral for the study of ASR (Gao et al. 2011).

2. Sample preparation and test methods

2.1 Sample preparation

All mortars were prepared with one part of metakaolin or cement for three parts of sand (by mass). The solid/liquid ratio for geopolymer mortars and the w/c ratio for OPC was set to 0.5 and KOH tablets were added to the OPC water to reach 8 kg/m^3 of Na_2O_{eq} (including alkalis of the cement) in order to provide a sufficient amount of alkali for the reaction. The sands used were all of controlled size, fixed at 0.16 mm – 2 mm. The geopolymer mortar was prepared in two steps. First, the pure NaOH and water were added to the industrial waterglass solution to reach a final H_2O/Na_2O molar ratio of 17 (composition in Table 3). After the total dissolution of the sodium hydroxide, the solution was cooled to 20°C for 24 h and then introduced into the metakaolin-sand mix until a homogeneous mixture was obtained. Thus the geopolymer paste had the following molar ratios: SiO_2/Al_2O_3=3.6; Na_2O/Al_2O_3=0.9 and H_2O/Na_2O=17 (corresponding to the formulation GP17).

Table 3. Mass composition of GP17.

	Metakaolin	Waterglass Wg3.3	$NaOH_{(solid)}$	Water
GP17	50.0%	41.0%	4.2%	5.3%

Mortars were prepared according to European standard EN 196-1 (AFNOR 2006). This standard describes the procedure (mixing and casting) used for the preparation of mortars, and has been validated for the preparation of geopolymer mortars in the first chapter. They were

cast in 4x4x16 cm and 2x2x16 cm prisms (expansion measurements) and 2x2x2 cm cubes (other tests). The samples were demoulded after a cure of 24h at 20°C and 95% RH.
Immediately after demoulding, all the prisms were measured using the scale micrometer method (specimens had stainless steel shrinkage bolts at both ends, as can be seen in Figure 7). Each measurement was the mean of three values from three replicate specimens. After these measurements, some prisms were covered with waterproof paper to protect the specimens from exterior exchanges, particularly for the carbonation. It was decided to allow 28 days for the cement hydration and geopolymerisation reactions before starting the accelerated tests. The specimens were therefore stored at 20°C in sealed plastic bags during this period. Only specimens made with the mixture of opal-marble (10%-90% by mass) sand were placed directly in non-accelerated test conditions at 20°C and 95% R.H.

Figure 7. *2x2x16 cm geopolymer (left) and cement (right) mortar prisms showing stainless steel shrinkage bolts.*

2.2 Test methods

After 28 days without external exchange, the prisms were stored at 20°C, 38°C or 60°C, after being placed either on grids in watertight containers containing 20 mm of water (mortar bars were not in contact with the water) or immersed in solutions (water, saturated CaO or 1M NaOH) depending on the test. Expansion and mass measurements were performed every seven days after the containers and the prisms had been cooled for 24h at 20°C. This test was based on the standard NF P 18-454 (AFNOR 2004) and was designed for concrete, but it has also been validated on mortars and 2x2x16 cm specimens (Idir et al. 2010). In order to follow the evolution of the mechanical characteristics of each specimen, dynamic Young's moduli were calculated from the speed of a sound wave measured in the mortar (Pundit). These tests were carried out at the same time as the expansion measurements.
Observations using a scanning electron microscope (JEOL JSM-6700F and JEOL JSM-6380 equipped with a RONTEC EDX system and JEOL JSM-6700F) were carried out on some mortar cubes (after platinum or carbon metallisation) at 170 days to observe the presence or absence of gel and to obtain information on their morphology and composition.

IV. Alkali–silica reaction in metakaolin-based geopolymer mortar

The aim of this first study was to investigate the ASR behaviour of geopolymer mortars in the presence of six different sands having various levels of ASR reactivity, using the measurement of the dimensions, the mechanical characteristics, and SEM– EDX observations. For this part of the ASR study we chose to apply only one accelerated test condition based on NF P 18-454 (AFNOR 2004), test conditions being sufficiently aggressive to accelerate the ASR in the cementitious system, but less aggressive than immersion in a sodium hydroxide solution. A comparison with OPC mortars was systematically carried out in order to evaluate the reactivity of the sands and to bring out differences in the behaviour of these two systems, to try to determine whether metakaolin-based geopolymer can actually resist ASR better than OPC does.

1. Mortar prism expansion

Expansion measurements were performed every seven days, up to 250 days, on each 2x2x16 cm OPC and GP specimen, all kept under the same accelerated conditions (in watertight containers containing 20 mm of water at 60°C). The evolution of these expansions over time is presented in Figures 8 and 9.

1.1 OPC specimens

As expected and illustrated on Figure 8, three swelling trends were observed for OPC: low, moderate (<0.10%) and high expansions (> 0.10%). Low expansion was observed on the mortars containing marble sand (OPC-a), but slow, moderate swelling was measured for the mortar made with the standardised quartz sand (OPC-b: 0.05% at 30 days). This swelling was unexpected because sand b usually does not lead to any ASR-expansion in normal conditions. This sand was composed of quartz without undulatory extinction, known to be stable and weakly reactive to alkalis (Gao et al. 2013). This behaviour confirms that even a non-reactive siliceous sand can still supply silica for the alkali-silica reaction when it is kept in aggressive conditions, such as 60°C and high alkali concentration (8 kg/m^3 here).

Quartzite (OPC-c) and siliceous limestone (OPC-d) sands showed moderate swelling kinetics leading to a non-negligible expansion at 90 days: 0.06% and 0.09%, respectively. It was noted that the expansions measured for sands b (quartz) and c (quartzite) were similar (0.05% vs. 0.06%).

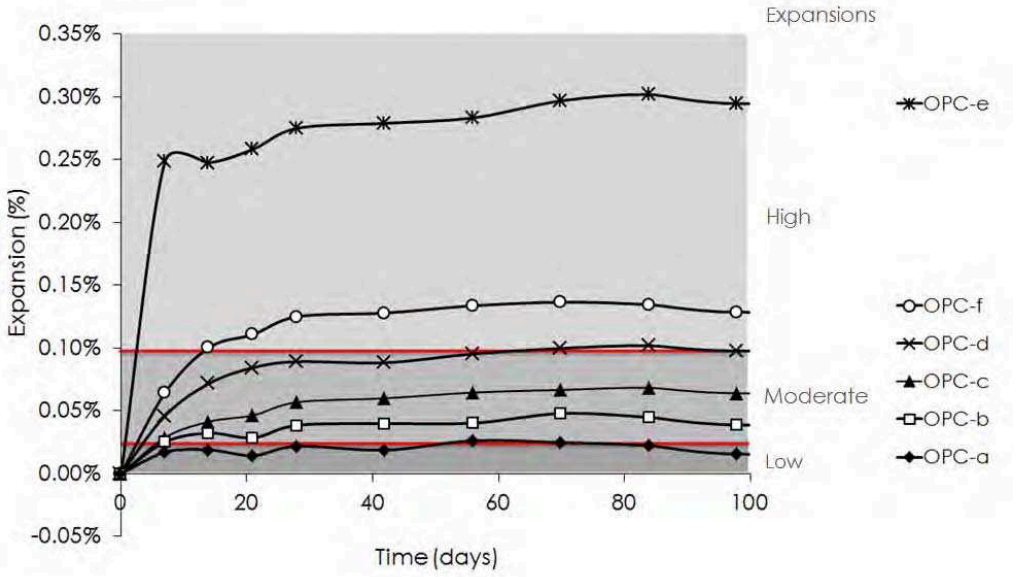

Figure 8. *Expansion curves with time for OPC mortars made with six different sands marble (OPC-a), quartz (OPC-b), quartzite (OPC-c), siliceous limestone (OPC-d), alluvial sand with opal (OPC-e) and crushed soda-glass (OPC-f) (error bars less than 0.03%) up to 100 days.*

Finally it was found that sands e (alluvial with opal) and f (crushed glass), both chosen for their theoretically fast reactivity, did not show the same type of swelling. The alluvial sand led to significant, fast expansion (0.25% at 7 days) while the crushed glass gave slower swelling kinetics, comparable to sands c and d, but with a higher final expansion (0.15% at 90 days). The much higher expansion obtained with sand e compared with the mortar made of crushed glass sand (providing more than 7 times more available silica) might be explained by the concept of pessimum proportion, which suggests that, when a mortar contains a certain proportion of reactive aggregates such as opal combined with a given amount of inert aggregates, its expansion is maximum (Hobbs 1988).

1.2 GP specimens

The curves involving geopolymer binder (Figure 9) showed similar behaviour regardless of the sand used, since no change in dimensions was measured over time for any mortar, even in the presence of very reactive aggregates. The only difference in behaviour that was noted in this study was for the GP mortar made with crushed glass sand, which showed a very slight

shrinkage, constant over a hundred days (approximately -0.008%) with a stabilisation at 0.005% after 250 days.

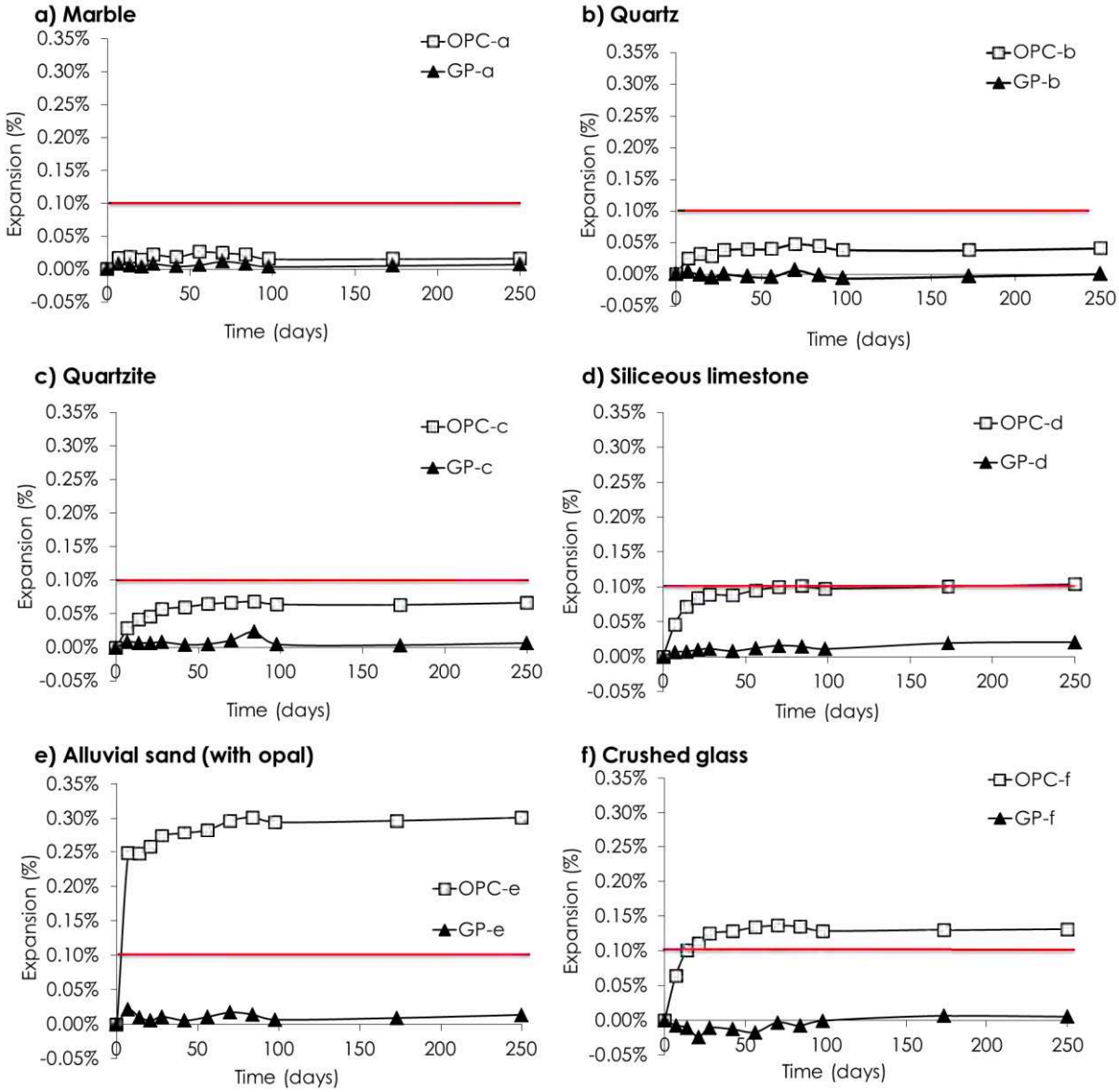

Figure 9. *Expansion curves with time for OPC and GP mortar made with six different sands marble (a), quartz (b), quartzite (c), siliceous limestone (d), alluvial sand with opal (e) and crushed soda-glass (f) (error bars less than 0.03% for OPC and 0.01% for GP).*

Since expansion was measured for OPC in presence of the sands b, c, d, e and f, confirming a certain reactivity of these materials, while no expansion seemed to occur for the geopolymer mortars with the same sand, geopolymer appears to be more efficient than the cement in this field of durability.

2. Mechanical performance studies

Figure 10 shows the mean variations (interval 21-90 days) of the dynamic Young's modulus (relative to the initial values) of the cement and geopolymer mortars for the six sands studied. The values, directly related to the rigidity of the mortars, allowed us to see the impact of the accelerated tests on their ASR-induced damage.

It was found that the rigidity of OPC mortar with marble (sand a) increased, while no significant variation appeared for the same mortar with geopolymer binder. The quartz and quartzite sands (b and c), which had almost the same ASR final expansion, again showed a similar trend with a slight decrease in modulus for the OPC mortars and a slight increase for the geopolymer mortars (mainly sand b). However, this test seemed to have no impact on the two mortars made with siliceous limestone (sand d).

The mortars containing the most reactive aggregates (sands e and f), and having led to significant ASR swelling, presented different behaviours in terms of Young's modulus variations. In the case of the alluvial sand bound by an OPC matrix, a significant decrease was observed (mean value of -18.5 %) and was probably linked to some damage produced by the ASR-expansion (> 0.25%). In contrast, the same sand used with a geopolymer binder showed an increase in its rigidity. Glass aggregate followed a different trend. Although the OPC mortar exhibited a slight decrease in rigidity, the modulus of geopolymer dropped sharply, by more than 50%, even without any long-term expansion. In that case, and as will be seen in the next section (Figure 12b), it was very likely that the detrimental effect on the rigidity of the mortar was caused by the formation of gel. Indeed, a gel layer was found around the glass aggregates, which led to dissociation and weakening of the bond between the aggregate and the paste.

To sum up, the overall general trends for the rigidity studies of the mortars containing alkali-reactive aggregates were:

- a negligible (-0.7%) to significant (-18.5%) decrease in the rigidity of OPC mixtures (except for marble).
- a slight (-1.1%) decrease to moderate (+7.2%) increase in the rigidity of geopolymer mixtures. Only the geopolymer mortar containing crushed glass particles did not follow this trend, probably due to the formation of a gel layer between the aggregate and the paste.

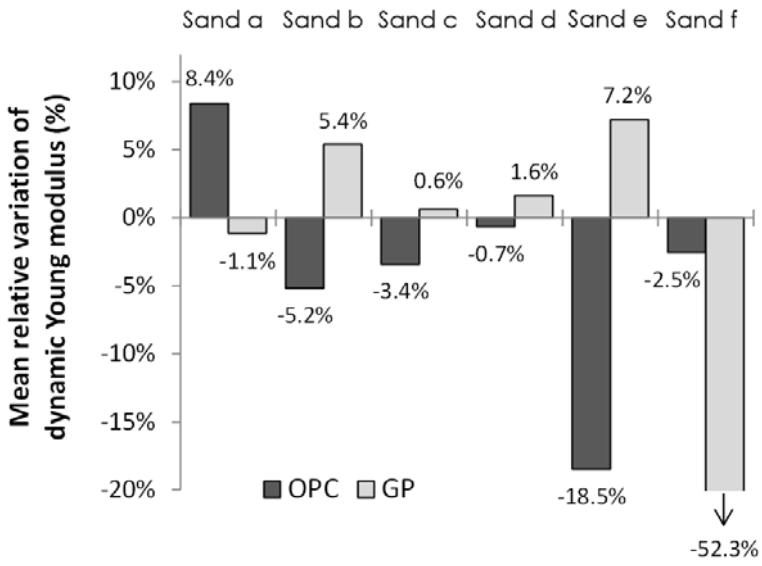

Figure 10. *Variations of the dynamic Young's modulus (mean values in the interval 21-90 days, in % relative to the initial values) for OPC and GP17 mortars.*

3. SEM/EDX studies

No expansions were measured on the geopolymer prisms but this did not mean that no ASR occurred. A scanning electron microscopy study was carried out at 170 days on the 2x2x2 cm specimens cured under the same conditions as the prisms to verify the presence or absence of alkali-silica gel in these matrices when the two most reactive sands (e and f) were used. Observations were first carried out on the OPC mortar that had shown the most significant expansion (OPC-e) to study the morphology of the gels formed (Figure 11). It was noted that, after 170 days at 60°C and 95% RH, the ASR products were in the form of a cracked gel, typical of this kind of reaction.

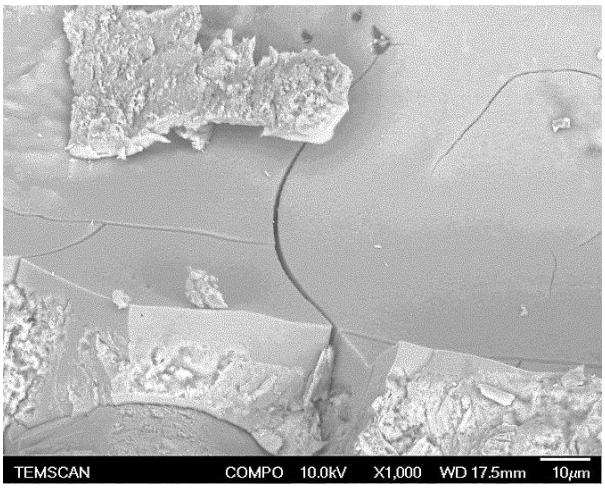

Figure 11. *Photomicrograph of OPC-e mortar (alluvial sand with opal) at 170 days with typical ASR gel.*

Observations were then made on the geopolymer mortars in presence of the alluvial sand (Figure 12a) and the soda-glass sand (Figure 12b). Despite the absence of expansion of these two specimens, reaction products were seen in both cases. For the alluvial sand (GP-e), cracked gel morphology, similar to ASR gels observed for OPC-e, was found within cavities (Figure 12a: P2). However, very little gel was observed on the entire sample. On the other hand, many spots of reaction products were observed inside cavities or interfaces between geopolymer and sand on GP-f mortar, which was made of crushed glass (Figure 12b).

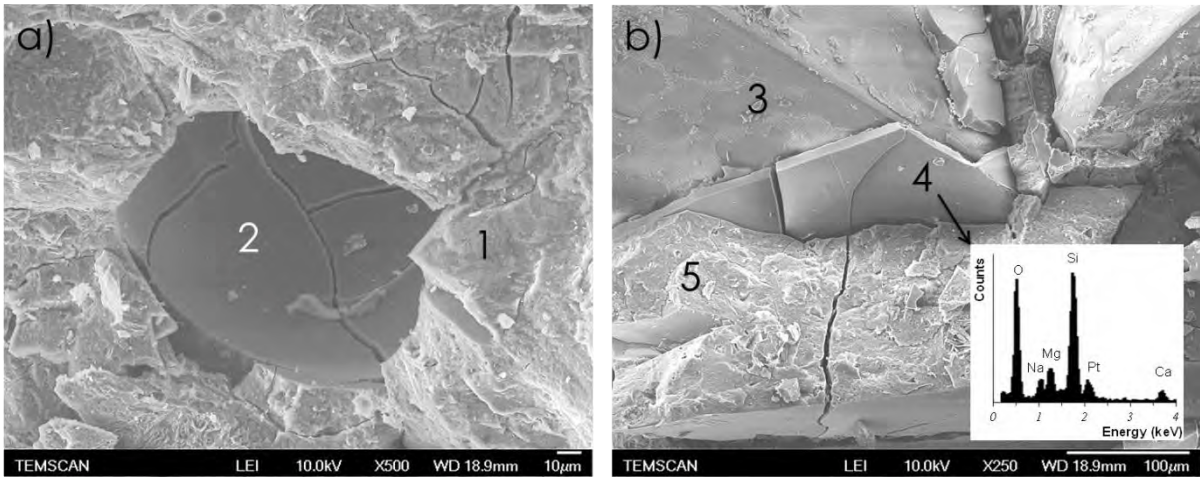

Figure 12. *(a) Photomicrograph of GP-e mortar at 170 days (P1: geopolymer; P2: gel-like ASR product) and (b) Photomicrograph of GP-f mortar at 170 days (P3: glass aggregate; P4: gel-like ASR product with EDX analyses and P5: geopolymer).*

Figure 12b gives a good illustration of the morphology of the sample analysed, where it was possible to clearly distinguish the presence of a newly formed product that looked like a gel layer (P4) around 10 μm thick at the interface between the glass grain (P3) and the geopolymer paste (P5). EDX analysis showed the presence not only of elements typically found in ASR-gels (Si, Na, Ca) but also of a significant quantity of Mg, an element that was initially in the glass aggregates. The question arises as to whether this new compound was an ASR-gel, or just a product due to the reaction of the external glass layer with the surrounding environment rich in hydroxide and alkalis. Nonetheless, this layer was probably responsible for the marked decrease in the rigidity of the mortar, as seen on Figure 10. It should be noted that the presence of gel layers around glass aggregates had already been seen by Idir et al. (2011; 2013). These authors found that glass particles attacked by alkaline solutions in model systems formed reaction rings around the grains, which were regarded as alkali–silica gels containing small amounts of calcium. Several other EDX analyses were performed on GP-f mortar in order to obtain the semi-quantitative chemical composition of the different phases

and particularly of the gel formed. It should be noted that the analysis was not performed on sand **e** due to the difficulty of performing EDX analyses in the cavity where the gel was situated. Figures 13a and b show a photomicrograph of glass aggregate covered by a cracked layer of newly formed product. The mass compositions of the compounds determined by EDX analyses are illustrated in a ternary diagram of SiO_2-CaO-Na_2O. Figure 13a was taken at the interface between the aggregate and the geopolymer, and an absence of continuity can be seen between the two phases, as if the gel layer formed had broken the adherence. Compared to the sound aggregate, the new-formed products had a lower alkali content and a small increase in their calcium content. They were also significantly different in composition when compared to the geopolymer matrix.

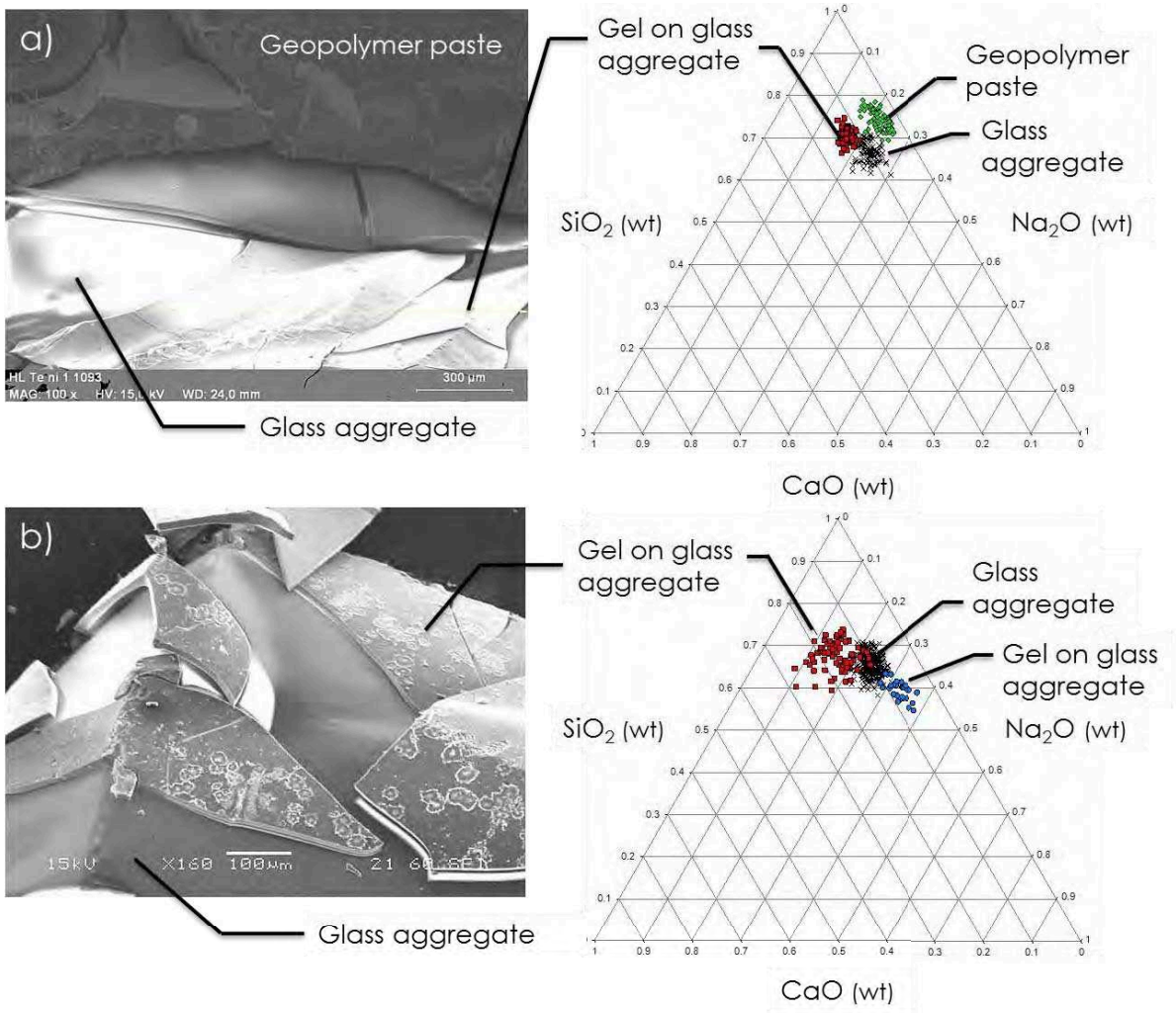

Figure 13. *Photomicrograph and Energy Dispersive X-ray spectrometry (ternary diagram SiO_2-CaO-Na_2O in % weight) for (a) paste-aggregate interface of GP-f mortar and (b) glass aggregate detached from GP-f mortar.*

Figure 13b was taken on a glass aggregate that was easily detached from the geopolymer paste. The attacked glass particles were covered by a thin layer of product having compositions differing from that of the raw glass. The alkali contents of the new-formed products was sometimes increased (circles on ternary diagram of Figure 13b), but could also show a decrease (squares on the same diagram). In the latter case, the calcium content increased significantly. It should be noted that the calcium came mainly from the original glass. As seen on Figure 14, the Ca/Si molar ratio of these products was in the range 0.1-0.4, while the Na/Si ratio reached more than 1 in certain zones (range 0.3-1.4), often much higher than is typical for ASR-gels (>0.5) (Idir et al. 2011; Idir et al. 2013).

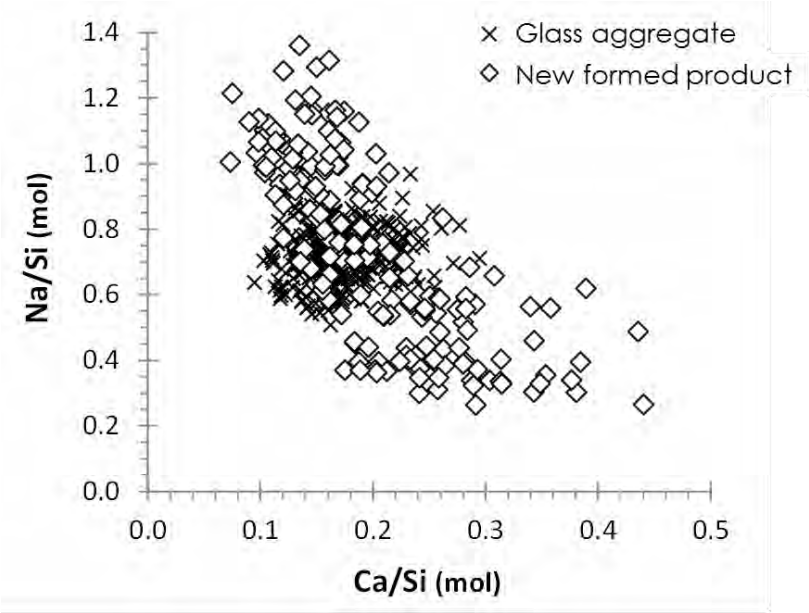

Figure 14. *Composition of new-formed products around glass particles in geopolymer mortar.*

4. Discussion of ASR in geopolymer matrices

ASR and damage caused by this reaction on Portland cement concrete are now well known in the literature and, even if there is no simple solution, many studies on the subject have helped to achieve effective recommendations for preventing these effects when reactive aggregates need to be employed: use OPC with very low alkali content, lithium salts, or pozzolans (Thomas 2011; Feng et al. 2005).

In a geopolymer matrix, it is not easy to achieve all of these measures and some are just impossible, e.g. the control of the alkaline content that is necessary to attack the metakaolin but also the reactivity of the aggregates used, which may differ with the aggressiveness of the activating solution used (pH, alkalinity, ...). These questions justify the topic of study of this third chapter, which was conducted to determine whether the alkali-silica reaction could occur in geopolymer matrices, and mainly if it could be as damaging as in OPC.

The study of dimensional variation using different reactivity rates of aggregates showed significant expansion in OPC mortars, while no expansion at all was detected in the geopolymer systems, although SEM observations revealed the formation of reaction products in alluvial-opal and glass aggregates. These products had a morphology similar to those usually found in OPC systems, especially for the alluvial aggregate. To attempt to explain this difference in the gel behaviour between these two matrices, it is necessary to trace the damage mechanisms of the ASR on OPC, to try to understand which differences could lead to an absence of expansion. Schematically, the occurrence of internal stresses due to ASR and causing damage in OPC are the result of three consecutive steps:

- Dissolution of the reactive silica
- Expansion of the gel formed
- Propagation of the gel into the porous network

These three steps lead to the saturation of the porous volume and thus to the occurrence of internal tensions causing damage to the specimen. Thus, if one of these steps does not take place as in the OPC structure, that could explain the absence of damage to the geopolymer specimens.

4.1 Dissolution of the reactive silica - pH of the pore solution

Alkalinity and pH of the pore solution are known to have a major impact on the attack of silica in reactive aggregates, since they control the breakdown of the amorphous phase, according to the mechanisms described by Dent Glasser and Kataoka (1981; 1982). The pH is partly driven by the alkali concentration in the pore solution, which itself depends on the soluble alkali of the cement in OPC systems. Alkali contents in OPC concretes are typically in the range 2-6 kg/m^3. In the case of geopolymers, the activator usually involves very high alkali concentration which reaches around 150 kg/m^3 for the formulation GP17. The solubility of amorphous or not well crystallised silica is strongly dependent on the pH values, especially in high-pH ranges. A variation of one pH unit can modify the solubility of silica by several orders of magnitude (Iller, 1979).

In order to evaluate the medium surrounding the aggregates in a geopolymer-based matrix, a study of the pore solution pH was made on a geopolymer paste having the same formulation as the mortars of this study. For this, a high-pressure device for extracting fluid from porous materials (Cyr et al. 2008) was used on the geopolymer at various times (technique presented more specifically in chapter III). Figure 15 reports the evolution of the pH inside the geopolymer pores up to 180 days, for a sample kept at 20°C and 95% R.H., i.e. in contact with the atmosphere, and for a sample kept in a sealed bag without any external exchanges.

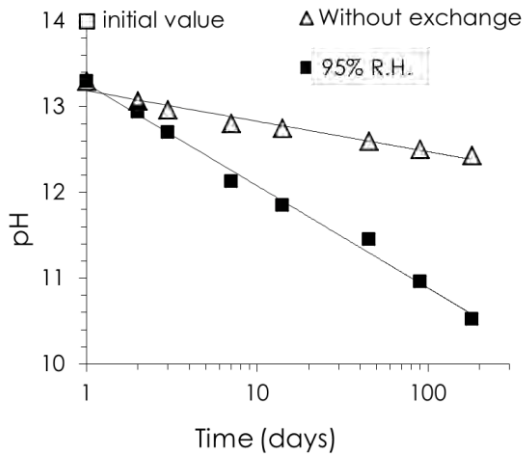

Figure 15. *pH evolution of the geopolymer pore solution for a paste kept in a moist room (95% R.H.) and in a sealed bag.*

It can be seen that, although there was a strong initial pH of 14 which was imposed by the activating solution, the pH dropped rapidly in the following days, at a rate proportional to the logarithm of time. After 14 days in a moist atmosphere (same conditions as ASR accelerated

testing), the pH was lower than 12 and reached 10.5 at 6 months, while it stabilised at around 12.5 in endogenous conditions. This rapid decrease of the pH was probably due to the carbonation of the pore solution, which led to the consumption of alkalis to form alkali-carbonate compounds (as presented in Chapter III). According to this study and assuming a similar evolution of the pH for the specimens used for the ASR study in view of their relatively small size (2x2x16 cm), at least two main hypotheses can be put forward to explain the absence of ASR in geopolymers:

- The first one is related to the very high initial pH in the mixture, which can lead to a very rapid reaction of the amorphous silica within the aggregates and the hydroxides present in the solution. This phenomenon, already described by Gifford and Gillott (1996) in their work on alkali-activated slag, would occur during the early period of hardening.
- The second hypothesis is that the fairly rapid drop in the pH would not leave enough time for hydroxides to break the silica network within the aggregates, thus reducing the formation of alkali-silica gels and so limiting the harmful effect of ASR. Since the amount of reaction products is an important parameter, less ASR gel (for a given gel composition) implies less probability of expansion. Results from the literature (Pietersen 1993; Fraay et al. 1989) tend to show that this hypothesis is plausible, as a pH decrease of 0.3 (e.g. 13.7 to 13.4) could lead to 50-75% less silica being dissolved (Figure 16). At pH below 13, the reduction is even more significant, which means that the attack on the reactive aggregates can perhaps be strongly reduced.

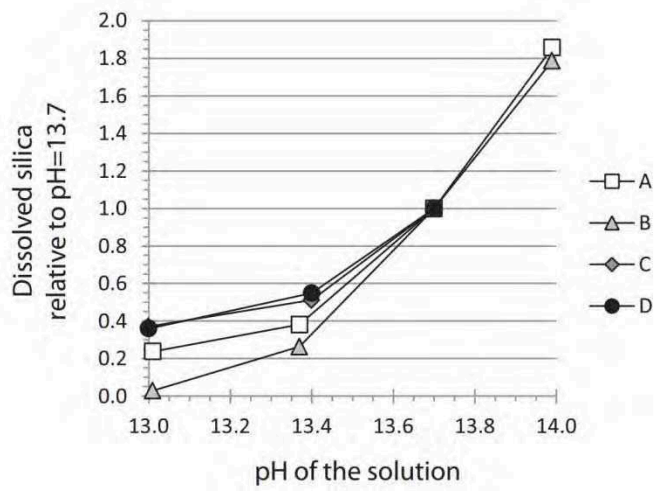

Figure 16. *Dissolved silica relative to pH = 13.7, measured from dissolution experiments of fly ash in NaOH solutions at pH = 13.0, 13.4, 13.7 and 14.0. Data from Fraay et al, 1989 (A: 20 °C; B: 40 °C), and Pietersen 1993 (C and D: 40 °C). Figure from Cyr et al. 2014.*

But regarding the evolution of the pH of the geopolymer kept in a sealed sag, it was noticed that, at only 14 days, a difference of pH of 1 between the two storage conditions was observed. Knowing this and in order to visualise the influence of the pH on the development of ASR in the geopolymer system, the same accelerated test was performed in endogenous condition. So 2x2x16cm OPC and GP specimens were made using the most reactive sand (alluvial sand with opal), and were protected from any external exchange immediately after demoulding with adhesive waterproof paper. They were then placed at 60°C and their dimensional changes were measured every seven days. These results were then compared to those obtained previously with the same sand (Figure 17).

It was first noted that even without a water supply the highly reactive sand resulted in swelling for the OPC. This expansion was smaller than during storage in moist conditions but still well above 0.10%. In contrast the geopolymer mortar presented a slight shrinkage of 0.03% reached in 14 days, without further variation up to 100 days. The shrinkage observed is reminiscent of the previous results (Chapter I) reporting tests in endogenous conditions, showing similar behaviour of the materials at 20°C or 60°C, and whatever the composition of the sand used.

According to the results in endogenous conditions, i.e. equivalent long term pH for both OPC and GP (around 12.5), the absence of swelling in the GP mortar could mean that pH would not be the only factor involved.

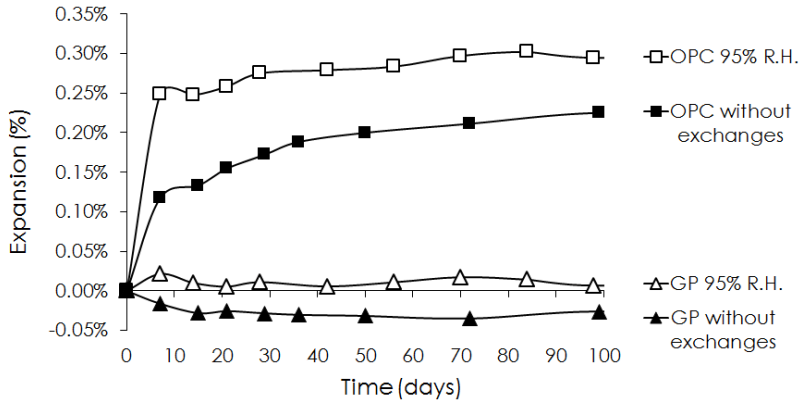

Figure 17. *Expansion curves with time for OPC and GP mortars made with the alluvial sand with opal (e) and kept at 60°C with or without external exchanges (error bars less than 0.03% for OPC and 0.01% for GP).*

4.2 Expansion of the gel formed - Role of calcium

It is generally assumed that calcium plays an important role regarding ASR expansion in Portland-cement-based materials. On the one hand, silica-based reaction products with high calcium contents are usually associated with C-S-H formed by cement and pozzolan hydration, with Ca/Si ratios of approximately 1.7-1.0 for typical and pozzolanic C-S-H, respectively. These products are responsible for the strength increase and do not involve any abnormal swelling behaviour. But, on the other hand, many authors have stated that a calcium deficiency in alkali-silica reaction products would lead to an absence of swelling (Dent Glasser and Kataoka, 1982). In diluted modelled systems, the portlandite content would be one of the main factors determining the amount of dissolved silica: in the presence of calcium, more silica would be dissolved (Leemann et al. 2011).Without added portlandite, the reaction initially produces alkali-silica compounds, but the reaction would stop as soon as the solution became saturated with respect to silica. In OPC alkali-reactive systems, it is expected that the potential of the reaction products for an expansion may be highest at a Ca/Si ratio between 0.20 and 0.30 (Leemann et al. 2011).

In the case of fly ash-based geopolymers, García-Lodeiro et al. (García-Lodeiro et al, 2007) and Fernandez-Jiménez et al. (Fernandez-Jiménez et al, 2007) suggested that the deficiency of calcium in their systems could partly explain the lower expansion observed, although there was some evidence of an attack of the reactive aggregates. In the current work, the only calcium in metakaolin-based geopolymer is provided by the metakaolin, which contains less than 2% by mass of CaO. The calcium deficiency could thus be a factor influencing the difference in behaviour of ASR gels, most likely in their expansion phase. The only mixture that led to higher calcium gels was the one made of crushed glass in the geopolymer matrix, but the newly formed product might not have been ASR gel in the strictest meaning of the term.

To see if calcium may have a role on the ASR gel development in the geopolymer, additional tests were performed. As the addition of calcium during the preparation of geopolymer would automatically lead to a different formulation (probably production of C-S-H), it was chosen to introduce calcium into the pore solution of the hardened geopolymer in order to see the influence that it could have on the expansion of the mortar (still with the alluvial sand with opal).

Identical 2x2x16 cm specimens to those previously made in geopolymer with the sand **e** were made and saturated with lime solution during 24 h, after 28 days (i.e. at the beginning of the accelerated tests), and seven days after the start of the accelerated tests. The expansion curves obtained are presented on Figure 18 with expansion measured for the GP17 mortar with sand **e**.

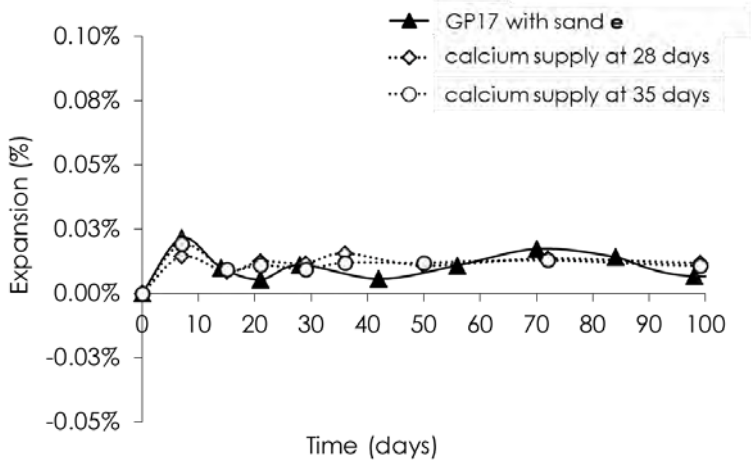

Figure 18. *Expansion curves of GP mortars made with the alluvial sand with opal (sand e) showing the influence of the addition of calcium in the matrix (error bars less than 0.01%).*

Once again, no swelling was measured, and this time the same negligible expansions that had previously been seen were obtained, indicating either a zero influence of the addition of calcium or that it was not added at the right time. Finally to try to verify this second hypothesis one last test was conducted. To provide continuous calcium in the system, the same specimens of geopolymer were this time immersed in a lime saturated solution from the beginning of the accelerated test (60°C). To remove the influence of an immersion on the dimension variations, controls were also immersed in an ultrapure water solution.

This time slight swelling was observed on geopolymer specimens during the seven first days of immersion with stabilisation over time at around 0.04% (Figure 19). However, the exact same expansion was measured for the geopolymer immersed in lime or in water. This slight expansion was probably caused by the immersion and not by the addition of calcium, which again did not seem to produce any reaction with the hardened geopolymer.

Adding calcium did not lead to expansion of geopolymer mortars, either because calcium had no effect or due to an incorrect incorporation of this element in the system. So it remains difficult to rule on the effect on calcium on ASR in geopolymer matrices.

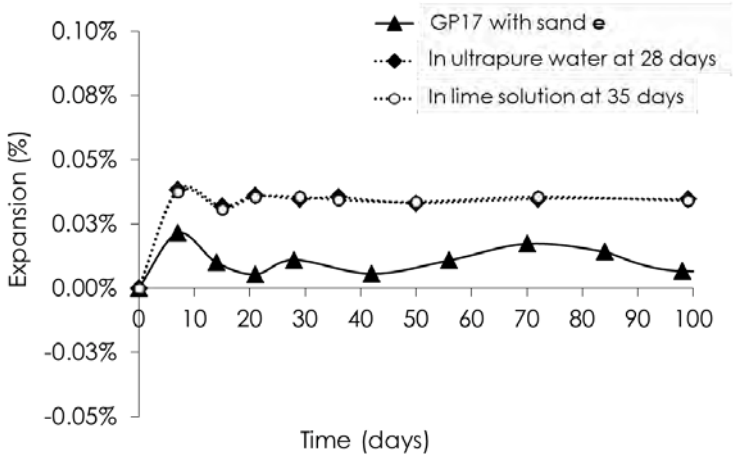

Figure 19. *Expansion curves of GP mortars made with the alluvial sand with opal (sand e) showing the influence of the immersion in lime solution and in water during the accelerated test (error bars less than 0.01%).*

4.3 Propagation of the gel into the porous network - accommodation of the gel

The SEM observations made on the different samples did not find as much gel as in OPC systems (except maybe for glass aggregate mixtures, but some doubts can be voiced as to whether the reaction rims were ASR gels or not). However, the presence of gel is not necessarily associated with swelling, whatever its nature. The accommodation of the gel by the porosity of the paste is the basis of several numerical models. It has been shown (Multon et al. 2009) that, depending on the size of reactive grains, the gels might not induce ASR-swelling. The porosity of the paste is sufficient to give the gel enough space to diffuse into the paste without exerting excessive stress on the solid skeleton and so without causing swelling.

Gifford and Gillott (1996) already supposed that the viscous alkali silica gel produced in alkali-activated slag (AAS) systems could be more easily accommodated in the porosity of AAS systems than in OPC concrete. Geopolymers are known to have a porous network different from that of OPC mixtures (Shi 1996, Boher 2012). The result of the previous study on the geopolymer porous networks and its differences with OPC system (Chapter I) could explain the differences in gel accommodation between those two materials, as shown in Table 4 where the previous results are summarised.

The total pore volume (accessible by water) was much higher for the geopolymer GP17 than for OPC (w/c = 0.5). It was also found that the geopolymer had a monomodal porous network centred around 25 nm when the cement presented a bi-or tri-modal network and the differences between the median pore access diameters of these two matrices show the

regularity of the geopolymer networks compared to OPC. Moreover it has been seen in chapters I and III that the porosity of geopolymer was probably strongly connected. Thus the volume accessible to the gels was larger and more accessible than in OPC, so it could be imagined that this would greatly reduce the appearance of internal tension, and thus the damage caused by ASR.

Table 4. Data on the porous networks of GP17 and CEMI 52.5 pastes from chapter I.

	GP17	**OPC**
Porosity accessible by water (%)	53%	43%
Access pore organisation	monomodal	Bi or tri modal
Average pore diameter (nm)	25,2	26.6
Median pore diameter (nm)	28,6	46.4

In short

Expansion	No characteristic ASR swelling on geopolymer
Mechanical performance	- No change, or a moderate increase in rigidity of geopolymer mortar - Drop of rigidity for GP with crushed glass
Morphologies observation	- Presence of gels similar to ASR gels for mortar made with reactive sand containing opal, but in smaller content - Formation of a reaction product on the surface of the crushed glass resulting in a significant decrease in adhesion with the paste.
Explication possible de la non expansion de mortiers GP	- pH of the pore solution causing a very quick or slow dissolution of the reactive silica of the aggregates. - Non- expansive gels due to an absence of calcium - Geopolymer porous network allowing the accommodation of the gel reduced the appearance of internal tension

This study has shown that the incorporation of reactive sands in metakaolin-based geopolymer mortars activated by sodium silicate does not lead to the ASR swelling characteristic of OPC mortars. This could be due to various phenomena: fast decrease in the pH, lack of calcium in the new-formed products, or accommodation of the gels in the porous network. None of these hypotheses can actually be excluded. The results of this chapter allowed us to conclude that, under the same condition and in spite of their very high concentration of sodium, geopolymers have a higher durability than OPC regarding the alkali-silica reaction. The second part of this study on the ASR in geopolymer systems will therefore aim to verify this conclusion for other accelerated test parameters, but also for natural conditions.

V. Influence of the test conditions on ASR in geopolymer

It was shown in the previous section that the alkali-silica reaction would not be damaging for metakaolin-based geopolymer mortars made with reactive sand. Nevertheless accelerated tests were all conducted under the same conditions, namely 60°C in a moist environment. Thus, it was decided to study the ASR-behaviour of the same geopolymer mortar in the presence of the most reactive sand previously used (sand e – alluvial sand with opal) using other tests found in the literature. Table 5 shows the different test conditions generally used in the literature for the study of ASR in alkali-activated materials (AAM) systems and based on OPC standards. From there, it was decided to study the influence of the principal parameters changing in these standards, namely the temperature, the cure conditions, and the dimension of specimens, on the expansion results.

Table 5. Accelerated ASR tests reported in the literature on AAM systems.

Stabdards	T (°C)	Age of test	Cure condition	Specimens dimensions (cm)	References
ASTM C1293	38	1 year	moist conditions	7.5 x 7.5 x 28.5	Bakharev et al, 2000
CSA A23.2-14A-94	38	1 year		7.5 x 7.5 x 30.5	Gifford et al, 1996
based on ASTM C227	38	180 days		1 x 1 x 6	Chen et al, 2002
BSI Draft DD218 (1995)	60	1 year		7.5 x 7.5 x 28	Al-Otaibi, 2007
ASTM C1260-94	80	16 days	1M NaOH solution	2.5 x 2.5 x 23	Fernández-Jiménez et a, 2002
	80	14 days		2.5 x 2.5 x 28.7	Puertas et al, 2009

A test under natural conditions was also carried out on the same geopolymer formulation and the results compared to those for an OPC mortar. In order to obtain swelling within a reasonable time, a mixture of sand containing only 10% of reactive sand (opal) and 90% of sand having no silica (marble) was chosen. These proportions were chosen for their pessimum effect, theoretically leading to maximum expansions (Hobbs, 1988). The specimens were placed at 20°C and 95% R.H. and the dimensions were followed every 7 days.

1. Influence of the accelerated testing conditions

1.1 Influence of the temperature

The same procedure as before, based on the NF P 18-454 standard, was applied to GP and OPC specimens with dimensions 2x2x16 cm and containing the sand e. Only the storage temperature was changed. Thus the samples were placed at 38°C after their 28 days of curing and the results of the expansion measurements were compared to those performed at 60°C. It was observed (Figure 20) that the reduction of the test temperature (60°C to 38°C) decreased the total expansion of the OPC (0.17% instead of 0.3%). A reduction of the reaction kinetics was also noted as, under those conditions, the OPC reached the limit value of 0.1% at 28 days instead of within 7 days when kept at 60°C.

Concerning the geopolymer mortar, the expansion measured at 38°C was slight in the first 14 days, with a stabilisation at 0.03%. However, the total dimensional variations were of the same order of magnitude as those obtained at 60°C, showing a negligible influence of the temperature on the expansion of geopolymer mortar in presence of highly reactive sand.

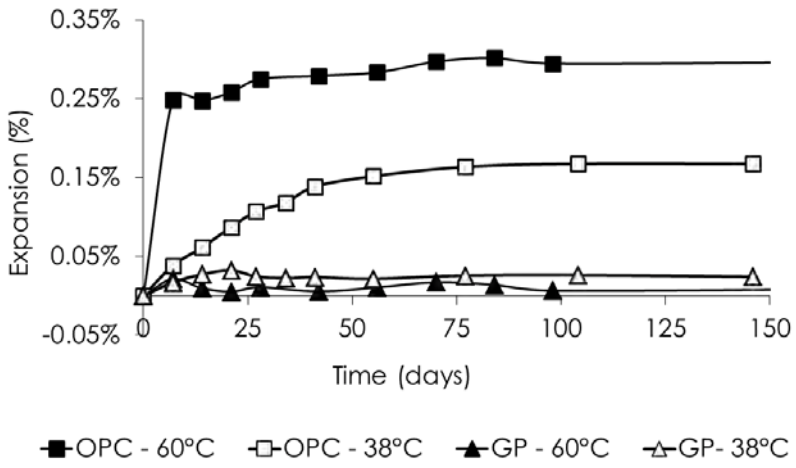

Figure 20. *Expansion curves of OPC and GP mortars made with the alluvial sand with opal (sand e) showing the influence of the temperature of the accelerated testing (error bars less than 0.03% for OPC and 0.01% for GP).*

1.2 Scale effect

To overcome the problem caused by the scale effect, the same procedure was performed, still in moist conditions and at 60°C, but with a volume of specimen four times larger. Thus the dimensions of 4x4x16 cm mortar specimens made with GP and OPC were followed and compared to the results obtained for the 2x2x16cm specimens. Increasing the volume logically increased the linear expansion measured for the OPC mortars with an augmentation of almost 0.1% (i.e. a quarter of the total expansion)(Figure 21). In contrast, the geopolymer mortar showed nearly zero expansion (<0.001%) up to 150 days. In this case, the increase by four of the volume of the specimens once again showed this absence of ASR expansions in the geopolymer.

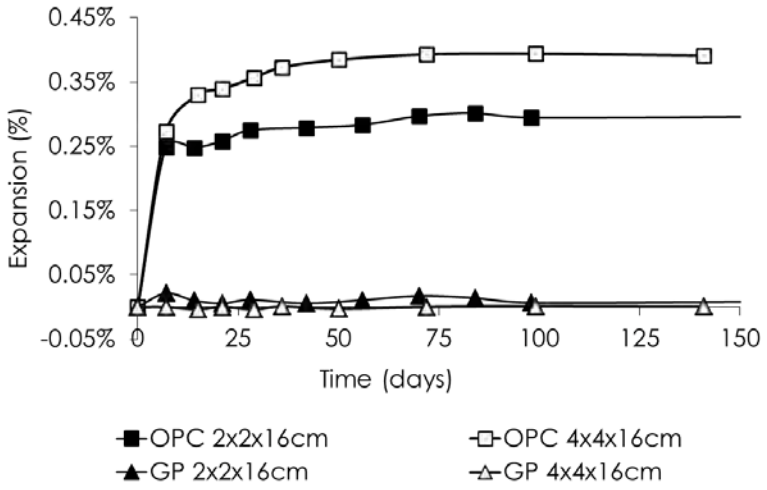

Figure 21. *Expansion curves of OPC and GP mortars made with the alluvial sand with opal (sand e) showing the influence of the dimension of the specimens (error bars less than 0.03% for OPC and 0.01% for GP).*

1.3 Influence on the curing condition

To try to reproduce ASTM C1260-94, the standard most used in the literature for ASR studies on geopolymer systems (Fernandez-Jimenez et al, 2007 and García- Lodeiro et al, 2007) but also the standard imposing the harshest cure conditions, 2x2x16 cm GP and OPC specimens were prepared and placed in a 1M NaOH solution (after 28 days of curing at 20°C in sealed bags). In order to study only the influence of the curing conditions, a temperature of 60°C was nevertheless chosen and not 80°C as recommended in the standard.

It was found that immersion in a 1M NaOH solution at 60°C resulted in the highest expansions for both OPC and geopolymer, which reached respectively 0.65% and 0.12% at 470 days (Figure 22). The fact that the maximum expansions of the OPC more than doubled (from 0.3% to 0.65%) for the same specimen dimensions, incorporating the same sand and at the same temperature, clearly showed the aggressiveness of this curing condition.

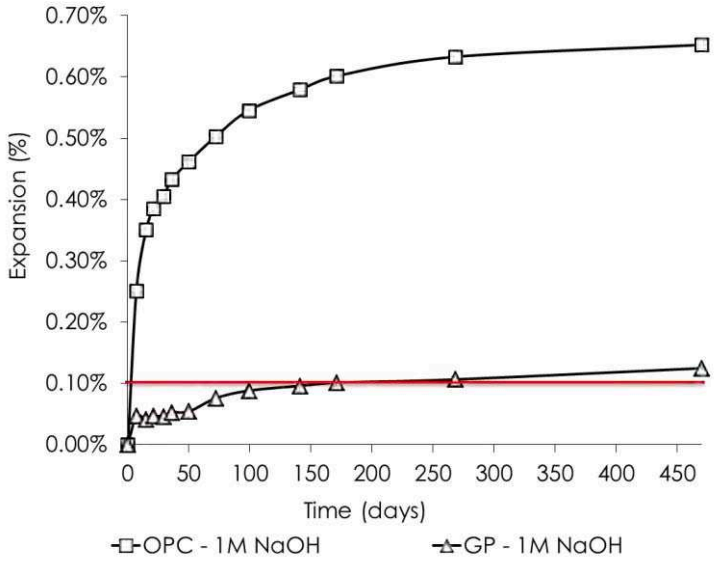

Figure 22. *Expansion curves of OPC and GP mortars made with the alluvial sand with opal (sand e) cured in 1M NaOH solution up to 470 days (error bars less 0.01% for GP and 0.04% for OPC).*

At 150 days of testing, GP mortars reached the upper expansion limit value of 0.1% (Figure 8) while, in all other cases, a value of 0.04% was never exceeded. Moreover the evolution of the expansions between 150 and 470 days showed the continuity of the swelling. This result also confirms the aggressiveness of this test (usually performed at 80°C) and questions its ability to reflect the reality of the reaction. This aggressiveness was also highlighted by superficial degradations observed on the geopolymer specimens at 28 days, as illustrated by the porous surface obtained, visible on Figure 23.

Figure 23. *2x2x16cm geopolymer mortar made with the alluvial sand with opal (sand e) cured at 60°C immersed in a1M NaOH solution for 28 days.*

However, compared to the OPC, which exceeded the limit during the first week, metakaolin-based geopolymers showed a much better resistance to ASR, by reaching this value at more than 100 days.

2. Non-accelerated ASR testing

2.1 Expansion measurement

In order to observe the phenomenon without altering the chemical reaction taking place in these matrices, a non-accelerated test was performed on OPC and GP mortars with a mixture of opal-marble sand, of 10%-90% by mass corresponding to the "pessimum" proportion. 2x2x16 cm specimens were cured at 20°C and 95% R.H. from their preparation, and the expansions measured are presented on Figure 24.

These results show that, even at room temperature, if favourable conditions for development of ASR-gels are met, significant expansions are obtained in systems made of Portland cement, which exceeded 0.1% in only 10 days and reached 0.25% at 50 days. On the other hand, no clear change in dimensions was observed for the geopolymer system, which stabilised at 0.003% up to 175 days, after a slight shrinkage of 0.02% maximum during the first 50 days.

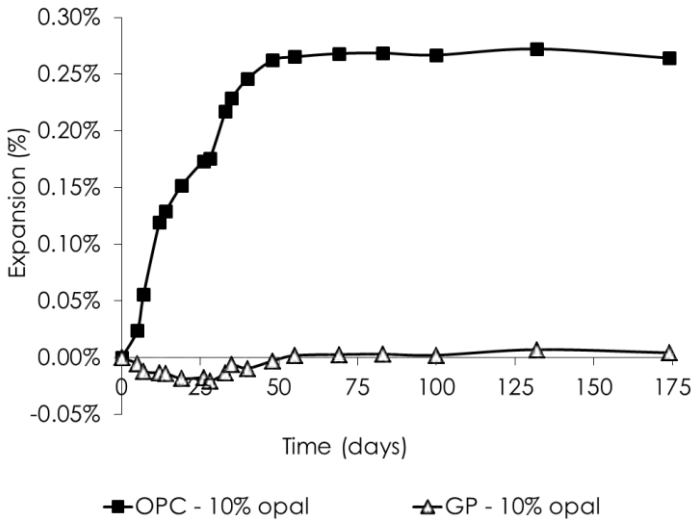

Figure 24. *Expansion curves of OPC and GP mortars made with 10% of opal and 90% of marble, cured at 20°C and 95% R.H. (error bars less 0.01% for GP and 0.02% for OPC).*

The visual observations of the surface of these two mortars at 100 days, illustrated on Figure 25, revealed a slightly cracked surface with release of gel from the pores for the OPC (with * in Figure 25a), whereas the surface of the geopolymer had the same appearance as at the first day.

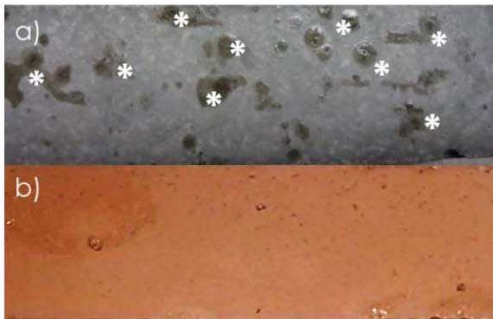

Figure 25. *Surfaces, at 100 days, of 2x2x2cm OPC (a) and GP (b) mortar made with 10% of opal and 90% of marble, cured at 20°C and 95% R.H..*

2.2 SEM observations

Since the absence of swelling does not mean the absence of gel formation, a study using a scanning electron microscope was carried out on GP mortar in the presence of opal-marble sand mixture after 170 days at 20°C and 95% R.H. It can be seen (Figure 26) that gel was present at the interface between the geopolymer paste and the opal aggregates. These gels (with a thickness around 10 µm) found in large quantities in the analysed sample had a morphology similar to that of ASR gels commonly observed in Portland cement - reactive aggregate mixtures, but was also similar to the gel previously observed on the glass aggregates.

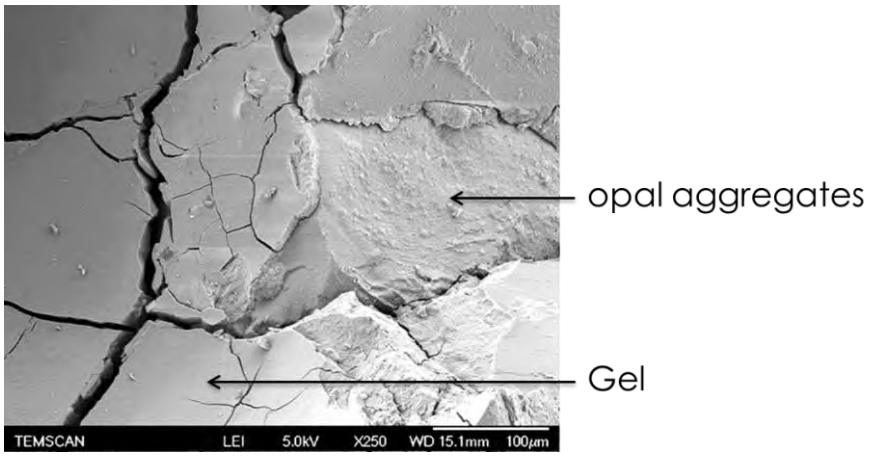

Figure 26. *Photomicrograph of GP mortar at 170 days showing ASR product with cracking morphology of gel.*

A complex siliceous structure was also observed on these specimens: it looked like ASR-gel with "rosette" morphology (Figure 27). This structure could also be identified as zeolites, crystalline products formed in geopolymer and often observed in the literature (Fernandez-Jimenez et al., 2007, García- Lodeiro et al., 2007, Duxon et al 2006). However, zeolites are not usually formed at room temperature, so the observed products rather suggest crystallised ASR-product, formed by the dissolution of the opal in the sand.

The formation of this product therefore indicates that there was, as in the OPC, dissolution of the reactive silica of the opal, but without causing any expansion.

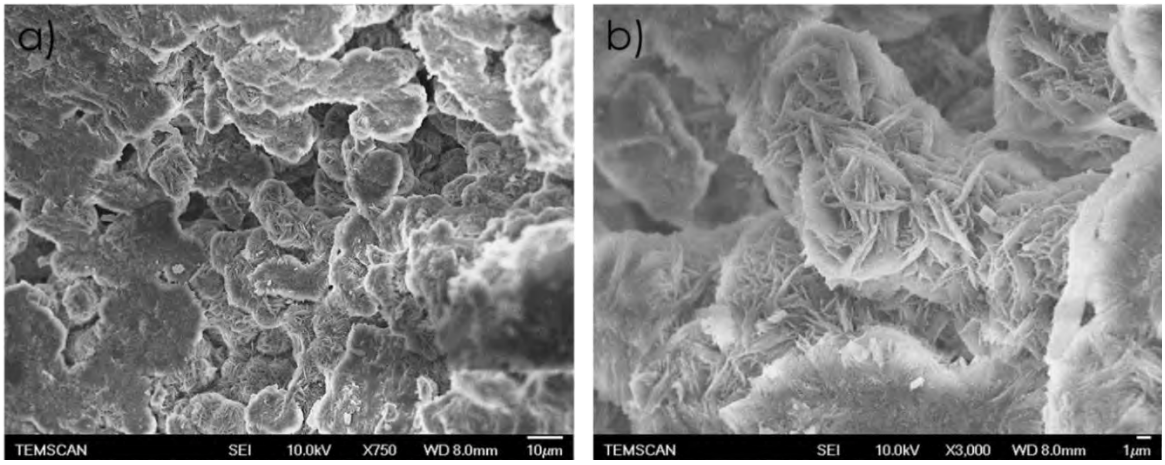

Figure 27. *Photomicrographs of GP mortar at 170 days. ASR product with a "rosette-type" morphology at two scales x750 (a) and x3,000(b).*

In short

Accelerated test conditions:

Test temperature	No expansion observed at 20°C, 38°C and 60°C
Dimension	Multiply the volume of the mortar by 4 showed no scale effect
Cure condition	Only immersion in a 1M NaOH solution has led to an expansion of the geopolymer superior at 0.1% after 150 days.

Non-accelerated ASR testing:

Expansion	Unlike OPC, zero-expansion of the geopolymer mortar with 10% of opal at 20°C and 95% R.H.
SEM observations	Formation of at least two types of reaction products: cracked gels and "rosette-type" crystals

This study showed that no expansion was obtained for geopolymer mortars with very reactive aggregates (opal), even by varying the temperature of the test or the size of the specimens. Only aggressive conditions, like immersion in a 1M NaOH solution, led to a non-negligible expansion of geopolymer mortars, but with very slow reaction kinetics compared to OPC. The non-accelerated test confirmed the conclusion drawn earlier that the geopolymer seemed to develop no harmful reaction in presence of reactive aggregates and optimal conditions for ASR, even though reaction products could be seen at the ITZ.

VI. Conclusion

The experimental studies performed in this chapter were intended to assess the ASR-behaviour of geopolymer mortars in the presence of reactive sands. The work was carried out on geopolymer and OPC mortars incorporating seven different alkali-reactive sands, each having a different level of reactivity, and used different test conditions, accelerated or not. The morphology and compositions of the products of reaction formed were analysed using SEM and EDX after 170 days of cure. Regarding the experimental results obtained in this study, the following conclusions can be drawn:

- The incorporation of reactive sands in metakaolin-based geopolymer mortars activated by sodium silicate does not lead to the ASR swelling characteristic of OPC mortars. This could be due to various phenomena: fast decrease of the pH, lack of calcium in the new-formed products, or accommodation of the gels in the porous network.

- No change, or a moderate increase, was observed in the rigidity of geopolymer specimens. Only the geopolymer mortar containing crushed glass particles did not follow this trend, probably due to the formation of a gel layer between the aggregate and the paste.

- Some gels with morphologies similar to those of ASR gels were observed at paste-aggregate interfaces or in cavities in mortars made with the reactive sands containing opal.

- The formation of a reaction product, covering the entire surface of the glass grains in the sand and resulting in a significant decrease in adhesion between the sand and the geopolymer, was observed. The question arises as to whether this new compound was an ASR gel or just a product due to the reaction of the external glass layer with the surrounding environment rich in alkalis.

- The results of the different accelerated test conditions used in this study allow it to be stated that, whatever the parameters studied and whether they were favourable or unfavourable to the development of ASR swelling gel, no characteristic swelling was

observed in geopolymer mortars in presence of reactive sand, except for the immersion in 1M NaOH solution.

- The results provided by the non-accelerated test also showed the absence of expansion of GP mortars when all favourable conditions (for OPC expansion) were combined, and highlighted the formation of reaction products in the GP with morphologies close to the ASR products found in OPC. However, the results of this study tend to show that these reaction products do not lead to expansion, whatever the conditions.

Due to their very high alkali content compared to OPC, geopolymers give rise to many questions, especially regarding their durability. The results of this study provide some answers concerning the alkali-aggregate reaction, by showing that the durability of the geopolymer against ASR could be higher than that of OPC under the same test conditions.

References

1st ICAAR, Aalborg Portland R and D seminar on alkali-silica reaction, Karlstrup, Denmark, 1974.

2nd ICAAR, Symposium on AAR, preventative measures, Reykjavik, Iceland, 1975.

3rd ICAAR, The effects of alkalis on the properties of concrete, Wexham Springs, London 1976.

4th ICAAR, The effects of alkalis in cement and concrete, Purdue University, Indiana, USA, 1978.

5th ICAAR, The effects of alkalis in cement and concrete, Cape Town, South Africa, 1981.

6th ICAAR, Alkalis in concrete, research and practice, Copenhagen, Denmark, 1983.

7th ICAAR, Concrete alkali-aggregate reactions, Ottawa, Canada 1987.

8th ICAAR, Alkali-aggregate reaction, Kyoto, Japan, 1989.

9th ICAAR, Alkali-aggregate reaction in concrete, London, UK 1992.

10th ICAAR, Alkali-aggregate reaction in concrete, Melbourne, Australia, 1996.

11th ICAAR, Alkali-aggregate reaction in concrete, Quebec City, Canada, 2000.

12th ICAAR, Alkali-aggregate reaction in concrete, Beijing, China, 2004.

13th ICAAR, Alkali-aggregate reaction in concrete, Trondheim, Norway, 2008.

14th ICAAR, Alkali-aggregate reaction in concrete, Austin, Texas, USA, 2012.

AFNOR. NF P18-454 (2004) Béton – Réactivité d'une formule de béton vis-à-vis de l'alcali-réaction – Essai de performance

AFNOR. NF EN 196-1 (2006) Methods of testing cement – part 1: determination of strength.

ASTM C 227 – 03, Standard test method for potential alkali reactivity of cement-aggregate combinations (mortar-bar method), 2003

ASTM C 441 – 02a, Standard test method for effectiveness of pozzolans or ground blast-furnace slag in preventing excessive expansion of concrete due to the alkali-silica reaction, 2002.

Bleszynski, R. F. and Thomas. M. D. A. (1998) Microstructural Studies of Alkali-Silica Reaction in Fly Ash Concrete Immersed in Alkaline Solutions, *Advanced Cement Based Materials*, 7: 66–78.

Boher, C., (2012) Experimental study and modeling of gas diffusion through porous partially water saturated environments. Application to Vycor glasses, geopolymer and CEM V cement paste. Université de Toulouse, Toulouse (PhD thesis (in French)).

Carles-Gibergues, A., Cyr, M., Moisson, M., Ringot, E. (2008) A simple way to mitigate alkali-silica reaction. *Materials and Structures.* 41:173-83

Chatterji, S. (1979) The role of $Ca(OH)_2$ in the breakdown of Portland cement concrete due to alkali-silica reaction, *Cement and Concrete Research*, 9: 185-188.

Cyr, M., Rivard, P., Labrecque, F., Daidié, A. (2008) High-pressure device for fluid extraction from porous materials: application to cement-based materials. *Journal of the American Ceramic Society* 91: 2653-2658

Cyr, M., Rivard, P., Labrecque, F. (2009) Reduction of ASR-expansion using powders ground from various sources of reactive aggregates. *Cement and Concrete Composites.* 31:438-446

Cyr, M., and Pouhet, R. (2014). Resistance to alkali-aggregate reaction (AAR) of alkali-activated cement-based binders. Handbook of Alkali-Activated Cements, Mortars and Concretes, 397.

Cyr, M., Trinh, M., Husson, B., Casaux-Ginestet, G. (2014). Effect of cement type on metakaolin efficiency. *Cement and Concrete Research.* 64: 63-72.

Dent Glasser, L. S. (1979) Osmotic pressure and the swelling of gels. *Cement and Concrete Research*, 9: 515–517

Dent Glasser, L. S., and Kataoka, N. (1981a) The chemistry of alkali-aggregate reactions. Proceedings of *the Fifth International conference on Alkali-Aggregate Reactions*, Cape Town, South Africa, paper S252/23, 66.

Dent Glasser, L. S. and Kataoka, N. (1981b) The chemistry of alkali-aggregate reactions. *Cement and Concrete Research.* 11(1): 1-9.

Dent Glasser, L. S. and Kataoka, N. (1982) The role of calcium in the alkali–aggregate reaction. *Cement and Concrete Research*. 12: 321-331.

Diamond, S. (1989) ASR - Another look at mechanisms, *in 8th International Conference on Alkali-Aggregate Reaction in Concrete*, 83-94.

Dron, R., Brivot, F., Chaussadent, T. (1997) Mechanism of the alkali-silica reaction', Proceedings of *the 10th International Congress on the Chemistry of Cement*, Gothenburg, vol. 4: Performance and durability of Cementitious materials, 8.

Duxson, P., Fernández-Jiménez, A., Provis, J.L., Lukey, G.C., Palomo, A., Van Deventer, J.S. (2006) Geopolymer technology: the current state of the art. *Journal of Materials Science.* 42: 2917-2933.

Feng, X., Thomas, M.D.A., Bremner, T.W., Balcom, B.J., Folliard, K.J. (2005) Studies on lithium salts to mitigate ASR-induced expansion in new concrete - a critical review. *Cement and Concrete Research.* 35: 1789-1796.

Fernandez-Jimenez, A., García-Lodeiro, I. and Palomo, A. (2007) Durability of alkali-activated fly ash cementitious materials. *Journal of Materials Science.* 42: 3055–3065.

Fraay, A.L.A., Bijen, J.M., De Haan, Y.M. (1989) The reaction of fly ash in concrete: a critical examination. *Cement and Concrete Research.* 19: 235-246.

Gao, X., Multon, S., Cyr, M., Sellier, A. (2011) Optimising an expansion test for the assessment of alkali-silica reaction in concrete structures. *Materials and Structures*. 44: 1641-1653.

Gao X., Cyr M., Multon S., Sellier A. (2013) A comparison of methods for chemical assessment of reactive silica in concrete aggregates by selective dissolution. *Cement and Concrete Composites*. 37: 82-94.

Garcia-Diaz, E., Riche, J., Bulteel, D., Vernet, C. (2006) Mechanism of damage for the alkali–silica reaction. *Cement and Concrete Research.* 36(2): 395-400.

García-Lodeiro I, Palomo A and Fernández-Jiménez A (2007), 'Alkali–aggregate reaction in activated fly ash systems', *Cement and Concrete Research*, *37*(2), 175–183.

Gifford, P.M. and Gillott, J.E. (1996) Alkali-silica reaction (ASR) and alkali-carbonate reaction (ACR) in activated blast furnace slag cement (ABFSC) concrete. *Cement and Concrete Research. 26*(1): 21–26.

Gillott, J.E. (1964) Mechanisms and kinetics of expansion in the alkali-carbonate rock reaction. *Canadian Journal of Earth Science.* 1: 121–45.

Glasser, F.P. (1992) Chemistry of alkali-aggregate reaction, in Swamy, R. N. (Ed.). *The Alkali-Silica Reaction in Concrete*. London, Blackie and Son Ltd.

Hudec, P.P. (1990) Common factors affecting alkali reactivity and frost durability of aggregates, in Durability of Building Materials and Components. Proceedings *Fifth International Conference Brighton.* UK, J.M. Baker et al. (Eds), E & FN Spon, London.

Hobbs, D.W. (1988) Alkali-silica reaction in concrete, *Thomas Telford*, London.

Hobbs, D.W. (1993) Deleterious alkali–silica reactivity in the laboratory and under field conditions. *Magazine of Concrete Research.* 45 (163): 103-112.

Hou, X., Stuble, L.J. and Kirkpatrick, R. J. (2004) Formation of ASR gel and the role of CSH and portlandite. *Cement and Concrete Research.* 34: 1683-1696.

Idir, R., Cyr, M., Tagnit-Hamou, A. (2010) Use of fine glass as ASR inhibitor in glass aggregate mortars. *Construction and Building Materials.* 24: 1309-1312.

Idir, R., Cyr, M., Tagnit-Hamou, A. (2011) Pozzolanic properties of fine and coarse color-mixed glass cullet. *Cement and Concrete Composites.* 33: 19-29.

Idir, R., Cyr, M., Tagnit-Hamou, A. (2013) Role of the nature of reaction products in the differing behaviours of fine glass powders and coarse glass aggregates used in concrete. *Materials and Structures.* 46: 233-243

Iler, R. K. (1979) The Chemistry of Silica: Solubility, Polymerization, Colloid and Surface Properties, and Biochemistry. *John Wiley and Sons*, New York.

Jones, T. N. (1988) A new interpretation of alkali-silica reaction and expansion mechanisms in concrete. *Chemistry and Industry*. 40–44.

Leemann, A., Le Saout, G., Winnefeld, F., Rentsch D., Lothenbach, B. (2011) Alkali-silica reaction: the influence of calcium on silica dissolution and the formation of reaction products. *Journal of the American Ceramic Society.* 94: 1243-1249.

Li, K-L., Huang, G-H., Chen, J., Wang, D., Nanjing, X.T. and Co, H.T. (2005) Early Mechanical Property and Durability of Geopolymer. *Geopolymer: green chemistry and sustainable development solutions.* 117–120.

Li, K., Huang, G., Jiang, L-H., Cai, Y-B., Chen, J. and Ding, J-T. (2006) Study on Abilities of Mineral Admixtures and Geopolymer to Restrain ASR. *Key Engineering Materials.* 302-303, 248-254.

Multon, S., Sellier, A., Cyr, M. (2009) Chemo-mechanical modelling for prediction of alkali silica reaction (ASR) expansion. *Cement and Concrete Research.* 39: 490-500.

Pietersen, H.S. (1993) Reactivity of fly ash and slag in cement, *PhD thesis*, Delft University of Technology

Pouhet, R., Cyr, M. (2014) Influence of test conditions on alkali-aggregate reaction in metakaolin-based geopolymer mortar. in *the 5th International Conference Non-Traditional Cement & Concrete*. 173-176.

Pouhet, R. and Cyr, M. (2015) Alkali–silica reaction in metakaolin-based geopolymer mortar. *Materials and Structures.*

Prezzin, M., Monteiron, J.M., Spositon, G. (1997) The alkali-silica reaction. Part I: Use of the double layer theory to explain the behaviour of reaction-products gels. *ACI Materials Journal*. Technical paper.

Rogers, C.A., Hooton, R.D. (1991) Reduction in mortar and concrete expansion with reactive aggregates due to alkali leaching. *Cement, Concrete and Aggregates.* 13(1): 42-49.

Sellier, A., Bourdarot, E., Multon, S., Cyr, M., Grimal, E. (2009) Combination of structural monitoring and laboratory tests for the assessment of AAR-swelling - Application to a gate structure dam. *ACI Materials Journal.* 106 (3): 281-290.

Shi, C. (1996) Strength, pore structure and permeability of alkali-activated slag mortars. *Cement and Concrete Research.* 26: 1789-1799.

Shi, C., Pavel., V.K. and Della, R. (2005) *Alkali-Activated Cements and Concretes*, USA, Taylor & Francis.

Shehata, M.H., Thomas, M.D.A (2000) The effect of fl y ash composition on the expansion of concrete due to alkali–silica reaction. *Cement and Concrete Research.* 30(7): 1063-1072.

Sims, I. and Nixon, P. (2003) RILEM TC 191-ARP: Alkali-reactivity and prevention - Assessment, specification and diagnosis of alkali-reactivity, RILEM Recommended Test Method AAR-I: Detection of potential alkali-reactivity of aggregates- Petrographic method, *Materials and Structures*, 36: 480-496.

Stanton, T. E. (1940) Expansion of Concrete Through Reaction Between Cement and Aggregate. *Proceedings of the American Society of Civil Engineers.* 66: 1781-1811. (also published with discussions in 1942 *ASCE Transactions*, 107, 54–126).

Swenson, E.G. and Gillot, J.E. (1964) Alkali-carbonate rock reaction. *Highway Research Board Bulletin.* 275: 18-31.

Swenson, E.G. (1957) A Canadian reactive aggregate undetected by ASTM tests. *ASTM Bulletin.* 226: 48-51.

Thomas, M.D.A, Blackwell, B.Q. and Nixon, P.J. (1996) Estimating the alkali contribution from fly ash to expansion due to alkali-aggregate reaction in concrete. *Magazine of Concrete Research.* 48(177): 251–264.

Thomas, M.D.A. and Innis, F.A. 1998) Effect of slag on expansion due to alkali-aggregate reaction in concrete. *ACI Materials Journal*. 95(6): 716-724.

Thomas, M.D.A. (1998) The role of calcium in alkali–silica reaction. *Materials Science of Concrete* (Sidney Diamond Symposium). 325-337.

Thomas, M.D.A. (2011) The effect of supplementary cementing materials on alkali-silica reaction: A review. *Cement and Concrete Research.* 41: 1224-1231

General conclusion and Perspectives

The literature reviews presented in each section show the interest that carries the scientific international community on geopolymer as building materials, but also highlights a lack of general knowledge on materials based only on metakaolin, mainly about civil engineering standards, industrial applications, and durability issues.

The diversity of the raw materials and the geopolymerisation, which is not yet fully understood, wondered about the reproducibility and the possible comparison of the results presented in the literature. In addition, as the reaction and the formulation of geopolymer are very different from those of cement, interrogations appeared about the civil engineering codes and standards. The observation of the "cement free" building constructions currently performed worldwide demonstrated the potential of alkali-activated materials but shows a very low utilisation of the metakaolin. Furthermore, literatures on metakaolin-based systems are not conclusive concerning some durability issues of these materials, especially when alkalis are involved like in carbonation or alkali-silica reaction (ASR). Regarding the carbonation reaction, it appears that the risk of efflorescence is real, however there is no information about the evolution of the pH of the pore solution over time, and thus on the risk of corrosion of reinforcement by carbonation. Finally, the results found on the behaviour of geopolymer in presence of reactive aggregates to ASR do not allow to rule about their ability to resist against this reaction.

The objective of this thesis was therefore to assess the ability of metakaolin-based geopolymer to substitute traditional Portland cement for the production of durable concrete structures. Thus, three aspects have been treated:

- *Geopolymer, formulation of an efficient binder (Chapter I)*
- *Geopolymer concrete, from fluid to dry concretes (Chapter II)*
- *Durability, the fate of alkalis (Chapter III and IV)*

Chapter I was devoted to the formulation and characterisation of metakaolin-based geopolymer.

Based on the literature, the importance of the proportions of the four main components of this material, SiO_2, Al_2O_3, Na_2O and H_2O on the final strength obtained was shown and has led to an optimal formulation. It was noted that the compressive strength obtained with this formulation was at least equal to that of a CEM I 52.5 and other characteristics, such as hardening kinetics or flexural strength, revealed clear advantages. At the same time, this study has shown that the standard used for the manufacture of OPC mortar was applicable to geopolymer, and provided some recommendations for improvements.
In a second time, physical, chemical and morphological characterisations of the geopolymer were used to make comparisons, at equivalent strengths, between geopolymers and cement. Thus the studies addressing the reactivity, the composition and the free water in these systems showed nearly total geopolymerisation that was less exothermic than cement hydration, leading to the formation of a structure having a uniform, stable amorphous phase corresponding to the "pure" geopolymer, and a crystalline phase corresponding to the impurities from the metakaolin. Particular importance was given to the study of the porous network, the essential characteristic of a binder, which showed a volume and a pore organisation very different from those in OPC, despite the similar compressive strength.

This study allowed to conclude that metakaolin-based geopolymers could actually be an effective solution for the formulation of cement-free, strong mortars. The use of impure metakaolin obtained by flash calcination revealed interesting properties, in agreement with the literature, but further studies on dissolution/reaction mechanisms of this metakaolin would be needed to obtain a full characterisation.

Chapter II was focused on the study of geopolymer concretes based on metakaolin, to determine what applications would be achievable, and to see whether some cement standards could be applied to these matrices.

First, a study was conducted on the formulation of these concretes to assess their workability, porosity and compressive strength. The study of both fresh and hardened states of geopolymer concretes revealed a wide range of applications, from fluid concrete suitable for the production of reinforced structures, to very dry concrete used to produce masonry units. It was also shown that geopolymer concretes could have similar mechanical properties to cementitious concretes, despite a larger porosity.

The range of theoretically feasible applications was the main subject of the second part of this study, with the fabrication of fluid and dry concretes. It was thus shown that the consistency classes of cement standards could be applied to metakaolin-based geopolymer concrete activated by sodium silicate, for the manufacture of reinforced structures and masonry units with proper equipment.

This works have demonstrated that a wide range of applications were achievable with geopolymer based metakaolin and have also highlighted that it was quite possible to use them in precast plant made for OPC.

Chapter III had assessed the potential risk of durability linked to the presence of carbon dioxide from the air on metakaolin-based geopolymer.

A pH study of the geopolymer pore solution showed its very fast decrease compared to OPC, with almost total carbonation after only 14 days. In natural atmospheric CO_2 conditions (20°C and 95% R.H.), it was found that the formation of sodium carbonate did not lead to a decrease of the pH below a value of 10.5 at one year, thus limiting the risk of corrosion by depassivation of the reinforcement. A study of accelerated carbonation performed under an atmosphere at 50% of CO_2 highlighted a different equilibrium of the sodium carbonate phases, resulting in the formation of large amounts of sodium bicarbonate responsible for a lower pH of the pore solution, and a potential risk of corrosion by carbonation. That result demonstrated that the accelerated carbonation test had very limited usefulness for the mixtures studied, given the rapidity of the natural reaction and the fact that it led to different reaction products, not representative of the natural reaction.
Secondly, the study of efflorescence carried out by semi-immersion tests in natural or accelerated conditions confirmed the different nature of the crystals formed (sodium carbonate or bicarbonate), but showed no significant difference on the amount of efflorescence formed. The study of parameters that can influence the growth of sodium carbonate, in natural conditions, revealed that the nature of the alkali used to make the geopolymer is a major issue, as the use of potassium instead of sodium eliminated the formation of efflorescence. Furthermore the state of the surface of the geopolymer was shown to have a strong influence on the efflorescence, as was a heat treatment, but none of the efflorescence reducing agents (ERA) tested reduced the appearance of crystals in a sodium-based system.

This study therefore allowed to conclude that, unlike the cement matrix, carbonation would not represent a durability issue in geopolymer concretes, regarding corrosion of reinforcement. Conversely, it appeared that the efflorescence, in addition to an aesthetic problem, could lead to severe surface damages in these systems. This study also provided an innovative experimental approach to assess the impact of carbonation in the metakaolin-based geopolymer matrix, which would be interesting to pursue and expand to other alkali-activated materials.

Chapter IV was devoted to the risk assessment that could be induced by the alkali-silica reaction (ASR) in metakaolin-based geopolymers.

The behaviour of geopolymer in presence of reactive aggregates was first investigated by monitoring the dimension changes and the dynamic modulus of the specimens placed in accelerated conditions at 60°C and 95% R.H. for up to 250 days. SEM and EDX analyses were also performed at 170 days to visualise the newly formed products. A comparison with an ordinary Portland cement (OPC) was made for all aggregates to ensure their alkali-silica reactivity and compare how the ASR had affected these two systems. Results showed that geopolymers, although they contained high concentrations of alkalis, were more able to resist ASR than OPC was, and no characteristic swelling or any significant loss of rigidity was observed for the geopolymer specimens. An exception was nevertheless noted for the mortar made with crushed glass sand, where a significant drop in rigidity was found with the presence of a gel layer at the surface of the glass grains but without any swelling.

In a second part, dimensional change measurements on geopolymer mortar specimens containing highly reactive sand (opal, known as one of the most reactive aggregates regarding ASR) in various accelerated test conditions (curing, temperature, dimensions of specimens) ensured the reliability of the previous results by showing that, whatever the conditions of the accelerated test, no swelling appeared. Nonetheless, it was noted that a non-negligible expansion (> 0.1%) appeared when the specimens were immersed in a 1M NaOH solution, but this swelling occurred after 150 days of immersion against less than 7 days for OPC. This confirmed again a better resistance of geopolymer matrices to ASR. Finally, non-accelerated testing allowed us to conclude that, despite the greater or lesser severity of the tests used, geopolymers resist ASR better than OPC does.

This last chapter demonstrated that, unlike cement, alkali-silica reaction is not harmful to geopolymer based on metakaolin. This study highlighted a potential application of geopolymer by showing that it could be used with reactive aggregates without causing damage. However, the several hypotheses submitted to try to explain the absence of damage due to ASR in this geopolymer system would require to be validated by further studies.

Perspectives

The contribution of the knowledge of the metakaolin-based geopolymer provided by this thesis leads to various perspectives for future studies, focused on the scientific understanding of this material, or on specific industrial issues. Among them:

Scientific purpose

- Given that this study has mainly been achieved using one source of metakaolin and a single composition of activation solution, it would be interesting to consider other metakaolin, e.g. most pure or with different finesses, or other sources of activation, like potassium, in order to see the influence on the properties studied. The main purpose would be to predict the final properties of the geopolymer whatever the raw materials used.
- A study would also be required in order to better understand the role and the fate of alkalis in the hardened system, mainly for the study of efflorescence, which remains a major durability issue for these materials.

Industrial purpose

- Given the real advantage than represents a binder that does not react with aggregates reactive to ASR, further study on massive structures might reveal very interesting applications in the construction areas affected by this reaction. The same conclusion could be made for structures impacted by the corrosion by carbonation.
- Regarding the price of the geopolymer concrete calculated in this study, it would be interesting to develop products for specific applications where the cement is not efficient, e.g. concretes resistant to high temperatures.

List of Figures

Chapter I.

Formulation and Characterisation of Metakaolin based-geopolymer

Chapter II.

Metakaolin-based geopolymer concretes: From fluid to dry concretes

Chapter III.

Carbonation of metakaolin-based geopolymer

Chapter IV.

Alkali–silica reaction in metakaolin-based geopolymer mortar

List of Tables

Chapter I.

Formulation and Characterisation of Metakaolin based-geopolymer

Chapter II.

Metakaolin-based geopolymer concretes: From fluid to dry concretes

Chapter III.

Carbonation of metakaolin-based geopolymer

Chapter IV.

Alkali–silica reaction in metakaolin-based geopolymer mortar

Titre : Formulation et durabilité des géopolymères à base de métakaolin

Résumé :
Les principaux objectifs de cette thèse étaient d'évaluer la formulation et la durabilité des géopolymères à base de métakaolin utilisés comme liants dans des matériaux de construction. Les géopolymères sont des matériaux à activation alcaline faisant l'objet d'études de plus en plus nombreuses de la communauté internationale car ils représentent une alternative aux ciments Portland traditionnels. La première partie de cette étude a donc été dédiée à la formulation de ces matériaux réalisés exclusivement à partir de métakaolin flash et de silicate de sodium et a permis de mettre en évidence des performances comparables à un CEM I 52.5. Une caractérisation physico-chimique ainsi qu'une étude du réseau poreux a souligné les différences entre ces deux matériaux et a permis l'élaboration d'une base de donnée sur les caractéristiques du matériau. La réalisation de béton, allant jusqu'à la fabrication en usine de préfabrication, a montré la capacité des géopolymères à remplacer totalement les liants hydrauliques connus, en terme de mise en œuvre et de performances mécaniques. Les questions de durabilité liées au fort taux d'alcalins dans cette matrice ont été traitées par des études sur la réaction alcali-silice et sur la carbonatation. Les résultats obtenus ont permis de conclure que la réaction alcali-silice ne serait pas préjudiciable dans une matrice de métakaolin activé par du silicate de sodium, et que la réaction très rapide des alcalins de la solution interstitielle des pâtes de géopolymère avec le CO_2 atmosphérique ne conduirait pas à une chute de pH significative, préjudiciable dans les matrices cimentaires, mais faciliterait l'apparition d'efflorescences.

Mots clés : Géopolymère ; Métakaolin ; Durabilité ; Réaction alcali-silice ; Carbonatation

Title : Formulation and durability of metakaolin-based geopolymers

Abstract :
The main objectives of this thesis were to assess the formulation and durability of metakaolin-based geopolymers as a binder for civil engineering materials. Geopolymers are alkali-activated materials; they are increasingly studied by the international community as they represent an alternative to traditional Portland cement. The first part of this study has been dedicated to the formulation of these materials, exclusively made from flash metakaolin and sodium silicate, which has shown performances comparable to a CEM I 52.5. A physicochemical characterization and a study of the porous network have highlighted differences between these two materials and allowed developing a database on the characteristics of the material. The achievement of concrete, up to precast plant, showed their ability to completely substitute known hydraulic binders, in terms of workability and compressive strength. Durability issues related to the high alkali content in this matrix were assessed by studies on alkali-silica reaction and carbonation. The results obtained have concluded that the alkali-silica reaction would not be detrimental in a matrix of metakaolin activated by sodium silicate, and that the very rapid reaction of the alkalis in the geopolymer pastes pore solution with atmospheric CO_2 do not lead to a significant drop of the concrete pH, which could be detrimental in cement matrix, but could lead to the appearance of efflorescence on the surfaces of geopolymer.

Key-words : Geopolymer ; Metakaolin ; Durability; Alkali-silica reaction ; Carbonation